eman ta zabal zazu

Universidad del País Vasco
Euskal Herriko Unibertsitatea

Departamento de Ingeniería Química

MICROENCAPSULATION AND MICROWAVE DRYING TECHNOLOGIES FOR STABILIZATION OF NATURAL INGREDIENTS IN THE FOOD INDUSTRY

TECNOLOGIÁS DE MICROENCAPSULACIÓN Y SECADO POR MICROONDAS PARA LA ESTABILIZACIÓN DE INGREDIENTES NATURALES EN LA INDUSTRIA ALIMENTARIA

TESIS DOCTORAL

Janire Mardaras Urrutia

Tesis Doctoral dirigida por

Dr. J.I. Lombraña Alonso y Dra. Mª Carmen Villarán Velasco

Septiembre 2016

Agradecimientos

Debo agradecerle a mi director de tesis José Ignacio Lombraña de manera especial la dedicación, el esfuerzo y el apoyo que ha sido para mí a lo largo de este proceso. También a María Carmen Villarán, mi directora de tesis por darme la oportunidad de trabajar junto a ella en Tecnalia y permitirme conocer más de cerca el trabajo de investigación que se realiza desde los centros tecnológicos.

A la Universidad de Wroclaw por acogerme y permitirme realizar la estancia en Polonia, a Adam Figiel por su disposición y ayuda. A Marta Pasławska por hacerme sentir como en casa y por su gran generosidad. I should also like to thanks to the University of Wroclaw for my 3 months stay. Especially to Adam Figiel because of his help and willingness and to Marta Pasławska who made me feel at home, dziękuję bardzo.

A los profesores del Departamento de Ingeniería química por acogerme aún viniendo de otra rama de conocimiento y por cada uno de los momentos que me han dedicado. En especial a Federico Mijangos y Fernando Varona con los que he tenido la ocasión de tener una relación más cercana. A Monika Ortueta por todo su apoyo, comprensión y dedicación.

Al personal de la universidad tanto a los chicos de mantenimiento como al personal de servicios de la universidad en general, por cada duda y problema resuelto, gracias.

Esta tesis es un cúmulo de casualidades y decisiones que me han traído hasta aquí. Todo esto comenzó mucho antes de lo que yo misma soy capaz de admitir, cuando mi carácter aún estaba por forjar allá por los años que iba al Colegio tuve una profesora de Química, Pilar Ortega, que me hizo sentir que la Química era mi camino. Comencé la carrera con compañeros increíbles con sueños inalcanzables que creíamos posibles. Esta tesis se la dedico en especial a mi amiga, Laura con la que comencé el camino y que yo continúo por las dos. A Alberto, que como siempre le digo que gracias a él o a veces por su culpa me encuentro en esta tesitura.

A los compañeros de laboratorio por tantos momentos especiales, Soraya, Leire, Maite, Héctor. A Igor y a Saray que a pesar de realizar el proyecto con mi ayuda siguen queriendo mantener la relación. A las chicas de las quedadas del café por cada uno de esos momentos. A Arrate y Arritxu por las charlas de despacho compartidas. De manera especial a Oihane, todo un descubrimiento para mí en este último año eskerrik asko. A Lourdes que la considero mucho más que una compañera, por su apoyo férreo, por su comprensión, vamos que por todo y más mil gracias. A Elena por todos los viajes piso arriba piso abajo para darnos ánimos, por ser un gran apoyo para mí y por compartir tantos momentos de desesperación que se arreglaban con un ratito juntas.

A mi cuadrilla, Jani, Aina, Cortina e Izu por comprender lo importante que es para mí esta tesis.

A Ainhoa y Nerea por seguir ahí a pesar de los años, y por ese viajecito en barco que me ayudó a despejarme y coger con más ganas la tesis.

A mi familia, a aita y ama por inculcarme los valores del esfuerzo y la superación, por estar ahí para mí siempre y por darme alas. A Leire, por ser tan diferente a mí y por venir a revolucionarlo todo. A Jorge, mi compañero por ser como eres, por que sigamos cumpliendo sueños y alcanzando nuevos retos.

SUMMARY

In the context of the growing interest of the population regarding health and wellness, functional foods play a key role in the diet. The concept of functional food (emerged in the 80s in Japan), expressed implicitly that foods and food components can exert a beneficial influence on physiological functions to improve the state of health and welfare. This trend makes the production of functional ingredients, with activity demonstrated, and stabilized to permit their incorporation into a larger number of food matrices. It is a study area of great interest and very demanded by the food industry in which this thesis is framed, oriented to the development of protection systems and drying technologies that allow to obtain probiotics ingredients in stable conditions for the use in the design of new elaborated foods.

Dehydration is commonly used to stabilize probiotics and bioactive compounds for storage, handling, transport and subsequent use in functional food applications. Freeze-drying is a widespread technique for dehydration of probiotics, dairy cultures and bioactive compounds, while spray-drying has been applied to the dehydration of a limited number of probiotic cultures and bioactive compounds. It has been shown that cellular inactivation occurs mostly at the freezing step along freeze drying process. On the other hand, the spray drying is a significantly shorter process but leads cells to a high thermal stress due to the high temperatures required during the process (100 - 200°C).

These two have been selected as a reference for the analysis of the process Near Fluidizing Microwave Drying (NFMD) proposed as an alternative to the previously mentioned technologies. The proposed process reduces heat stress of the samples due to the moderate temperatures employed (5-45°C). The technology proposed combines the technology of microencapsulation for the protection of natural ingredients with the process of drying, applying the heating by microwave on a fixed-fluidized bed of particles. For the study of the process NFMD has needed a systematic experimental work of the proposed method to select the processing conditions. After the analysis of the obtained results exposed throughout this thesis can be concluded that in general, they have been established the operational parameters of the combined process of microencapsulation and the NFMD process. This minimizes the problems that are originated in the reference drying technologies. The mathematical model applied

successfully describes the process and permit to analyze the interrelationship between variables for the most favorable design of the drying process, taking into account aspects of quality and energy efficiency.

Finally, the NFMD process has been assessed quantitatively as an alternative to freeze drying and spray drying. Related to aspects of consumption energy and quality it was found that while freeze-drying presents a higher consumption comparing with NFMD, the experienced thermal stress is considerably higher in spray drying, being both not recommended comparing with the proposed process. Consequently, the NFMD process more equilibrated in the analyzed aspects was proposed as economically viable alternative for the elaboration of functional foods through microencapsulated ingredients.

RESUMEN

En el contexto del creciente interés de la población referente a la salud y el bienestar, los alimentos funcionales juegan un papel clave en la dieta. El concepto de alimento funcional (años 80, en Japón), implícitamente expresa que alimentos y componentes alimentarios pueden ejercer una influencia beneficiosa sobre las funciones fisiológicas para mejorar el estado de salud y bienestar. Esta tendencia hace que la producción de ingredientes funcionales, con actividad demostrada y estabilizada para su incorporación a un mayor número de matrices de alimentos, es una área de estudio de gran interés y muy demandado por la industria de alimentaria. En este sentido se ha enmarcado esta tesis, orientada al desarrollo de sistemas de protección y secado que permiten obtener ingredientes probióticos y antioxidantes en condiciones estables para el uso en la elaboración de nuevos alimentos.

La deshidratación es utilizada para estabilizar los probióticos y compuestos bioactivos para su almacenamiento y posterior uso en la elaboración de alimentos funcionales. La liofilización es una técnica muy extendida en la deshidratación de probióticos, cultivos lácteos y compuestos bioactivos, mientras que el secado por aspersión se ha aplicado a la deshidratación de un número limitado de cultivos probióticos y compuestos bioactivos. Se ha observado que la inactivación de las células probióticas ocurre mayoritariamente durante la etapa de congelación en el proceso de liofilización. El proceso de secado por aspersión o spray drying, en cambio, es un proceso significativamente más corto pero lleva a las células a un elevado estrés térmico debido a las altas temperaturas requeridas durante el proceso (100-200ºC).

Se han tomado estas dos tecnologías de secado como referencia a la hora de analizar el proceso *Near Fluidizing Microwave Drying* (NFMD) propuesto como tecnología alternativa a las previamente mencionadas. El proceso propuesto consigue disminuir el estrés térmico de las muestras debido al empleo temperaturas moderadas (5-45ºC). La tecnología propuesta combina el empleo de la tecnología de microencapsulación para la protección de los ingredientes naturales con el proceso de secado, aplicando el calentamiento por microondas sobre un lecho fijo-fluidizado de material particulado. Para el estudio del proceso NFMD se ha necesitado un trabajo experimental sistemático del método propuesto a fin de seleccionar las condiciones del

proceso. Tras el análisis de los resultados obtenidos y expuestos a lo largo de esta tesis se puede concluir de manera general que se ha conseguido establecer los parámetros operacionales del proceso de elaboración combinando la tecnología de microencapsulación junto con el proceso NFMD. Esto ha sido posible al minimizar los problemas que se originan en las tecnologías de secado de referencia. Se ha aplicado un modelo matemático que describe satisfactoriamente el proceso y con el que a su vez se ha podido analizar la interrelación de las variables intrínsecas del proceso a la hora de diseñar el proceso de secado que sea más favorable teniendo en cuenta aspectos de calidad y eficiencia energética.

Finalmente, el proceso NFMD se ha valorado cuantitativamente como alternativa de secado frente a la liofilización y *spray-drying*. Al analizar los aspectos de consumo energético y de calidad, se encuentra que mientras la liofilización presenta un consumo superior al proceso NFMD, en el caso del spray drying, es el estrés térmico experimentado el que es considerablemente superior, por lo que ambos resultan desaconsejables respecto al proceso NFMD En consecuencia, el proceso NFMD más equilibrado en los aspectos analizados, se propone como alternativa económicamente viable para la elaboración de alimentos funcionales a través de ingredientes microencapsulados.

Chapter 1

INTRODUCTION AND OBJECTIVES

1 INTRODUCTION AND OBJECTIVES

In recent decades, there has been a change in food trends in developed countries, and the concept of balanced diet has come to mean maintaining a proper diet based on foods that promote health and improve the welfare (Ashwell, 2004). In this sense, a growing number of consumers are aware that foods are not only necessary for nutrition and sustenance, but also play an important role in improving the quality of life and the prevention of chronic diseases prevalent in today's society. On the other hand, the level of health is directly associated with health spending, so the frequent incidence of these diseases, the increase in life expectancy and the aging of the population have had impact on the increase in the cost of health care, encouraging public policies aimed at improving practices and eating habits of the population (Beristain and Bustinduy, 2005, Innobasque, 2011).

1.1 Functional foods

In this context of health and wellness, functional foods play a key role in the diet. The concept of functional food (emerged in the 80s in Japan, and later expanded in the United States and Europe), expressed implicitly that foods and food components can exert a beneficial influence on physiological functions to improve the State of health and welfare, and reducing the risk of chronic diseases such as hypertension, diabetes, obesity or cardiovascular problems (Ashwell, 2004, Menrad, 2003).

Functional foods are not separate and well defined entity. By the contrary, include numerous products of various categories food, although the more frequent of the dairy industry, confectionery, soft drinks, bakery and the market of food for babies (Kotilainen, *et al*., 2006). In this sense they are well differentiated the nutraceutical and food supplements (Menrad, 2003).

It has been proposed the following clasification for funtional foods (Spence, 2006).

• Foods fortified with extra nutrients (tagged fortified products), as fruit juices fortified with vitamin C, vitamin E, folic acid, zinc and calcium;

• Foods with new nutrient or not additional components normally found in a food in particular (tagged enriched products), as probiotics or prebiotics.

• Them food of which a component harmful has been eliminated, reduced or replaced by another with beneficial effects (products altered marked), such fibers as releasing of fat in the meat or frozen.

• Food in which components have naturally been improved (with improved commodity label), for example, eggs with increased content of omega-3 fatty acids.

In concordance with a recent report of (Leatherhead Food Reserch,) the world market of functional food increased a 26% in 2013 with regard to the value of the 2009, reaching a value of 43 thousand million dollars, and is expected to an increase similar to the 2017. Also indicates that the most demanded products are those that improve mood and provide energy (constitute 27% of the market), followed by digestive health and heart health.

The information of all the sources indicates consistently that the market of functional food is growing and that is expected that continue doing it in the future predictable. At least 168 companies are currently working in the field of functional foods in Europe. The functional foods market is growing and is expected to continue to do so in the future. With this market trend, functional foods provide high expectations to food industry companies and today, represent one of the most interesting fields of research and innovation in the food industry (Annunziata and Vecchio, 2011, Jones and Jew, 2007, Siró, *et al.*, 2008). Traditionally, the food industry has not been a sector with high research activity, but different economic and social changes described above have made that large companies should rely on research and innovation to provide solutions that adapt to the new demands of consumers.

This trend makes the production of functional ingredients, with activity demonstrated, and stabilized to permit their incorporation into a larger number of food matrices, a study area of great interest and very demanded by the food industry and in this sense is framed this thesis, oriented to the development of protection systems and

drying that they allow to obtain ingredients probiotics in stable conditions for use in the development of food.

Another rising trend, also related to the increasing of the consumer health concern, is the pursuit of natural food, free of chemical additives. At the same time and due to recent studies carried out in relation to the adverse effect of certain additives, European legislation is limiting and reducing the use of this type of additives in food.

Food additives have an important function for keep them features and the quality of them food required by them consumers and for increase your value nutritional and ensure it security and them properties organoleptic of them food from its production to its consumption.

The food additives market grew by 3% between 2004 and 2007 with a volume of 17 billion euro market. In its report, Global Industry Analysts Inc. (GIA) indicated that the additives market will reach a market of EUR 25 billion by 2015. This is due to the importance of the new processing methods and the development of a variety of new food products. The factors that will have influence on the development of the market of additives are related to health, food security and convenience foods. Therefore, natural additives may be an alternative with high market potential considering the expected growth of the sector and consumer demands and the demands of the companies' final users of additives seeking natural additives and higher nutritional value. In fact, and according to the study conducted by Frost & Sullivan in 2012, the market of antioxidants, flavorings, colorings and antimicrobial natural in the food & beverage sector reached 3.47 trillions of dollars in 2012 and is expected to reach 3.92 trillions of dollars in 2016, with an expected 3% annual growth (CAGR, 2012-2016).

As it has been mentioned above, the development of natural ingredients and/or functional foods have a great relevance for the food industry.

Probiotics and antioxidants

Developed by Pricewaterhouse Coopers report, consumers are willing to pay price premium for foods with specific health targets. And this happens even in these times difficult economically. This means that health foods are that are experiencing major growth in recent years. According to the study conducted by FEMI in 2012, in 2011, the

functional food market reached a market of 33 million euro worldwide and in Spain reached the 3,000 million euro. Also, the estimate growth market of this sector is between 8% and 14% annual for 2010 and 2020 period.

In response to statements contained in the products, the segmentation of the functional foods market is as follows:

- Fortification 9%
- Health bone 6%
- Addition of calcium 4%
- Addition of fiber 4%
- Beauty 3%
- Brain and SCN 5%
- Cholesterol reduction 6%
- Immune system 11%
- Cardiovascular health 15%
- Digestive health 38%

Considering all this, probiotics and antioxidants would be a new type of products with beneficial effect on health and with great capacity in the market and growth potential by its properties, may be fitted in more than 50% of the potential market of functional foods.

Probiotics

Probiotics are living microorganisms that administrated in adequate amounts, produce benefits to health (FAO/WHO, 2002). Probiotics for human consumption belong mostly to the genera *Lactobacillus* and *Bifidobacterium* although, not exclusively. The main species used so far are presented in Table 1.1. However, many researchers are investigating the possible use of new species, where it is established that they meet the selection criteria for a probiotic (Ramos-Clamont, *et al*., 2012). These are the following:

1. Present tolerance to acids and bile salts.
2. Be identified and classified by genotypic techniques.
3. Show antagonistic effect against pathogenic bacteria.
4. No act as opportunistic pathogens, even when the host is immunosuppressed.
5. Stimulate to the immune system enhancing the resistance against pathogenic.
6. To be able to adhere to the bowel (Ross, *et al.*, 2005).

Table 1.1. Probiotics microorganism employed in human foods (Sanders, 2008)

Genus	Specie
Lactobacillus	L.acidophilus, L.bulgaricus, L.casei, L.rhamanous GG, L.plantarum, L.johnsoni, L.lactis, L.reuteri.
Bifidobacterium	*B.adolescentis, B.bifidum,B.breve,B.infantis, B.lactis, B.longum*
Other species	*Sacharomyces boulardii, S.crevisiae, Steptococcus termophilus.*

Table 1.2. Health benefits of some commercial foods that contain probiotics.

Indication aganinst	strain	Company
Infant diarrhea	*L.rhamnosus* GG	Danimals (yoghurt)
	L.casei DN 114001	DanActive(fermented milk)
Diarrhea associated with treatment with antibiotics	*L.rhamnosus GG*	Danimals (youghurt)
	S.boulardii	Florastor (powder)
	L-casei DN 114001	Danactive(fermented milk)
Slow intestinal transit, inflammatory bowel disease	*B.animalis* DN 173 010	Activia (yoghurt)
Health maintenance	*L.reuteri* ATCC 55730	Stonyfield yoghurt
	L.casei DN 114001	Danactive (fermented milk)
	L casei shirota	Yakult
Allergy (dermatitis in children)	*L.rhamnosus GG*	Danimals (youghurt)
Lactose intolerance	*L.bulgaricus* and *S thermophilus (main strains)*	All yoghurt with live cultures
Cramps in children	*L.reuteri* ATCC 55730	Reuteri drops
Immune support	*B.lactis* HN019 (aka HOWARU^{TD} o DR10)	Milk supplements Danisco
	B. lactis Bb12	Nestlé infant formula
	L. rhamnosus GG	Danimals (youghurt).
	L.casei DN	Danactive (fermented milk)

Many international companies marketed foods with probiotics, which attributed certain beneficial effects on health; Table 1.2 summarizes some of them.

The amount of probiotics alive that we ingest to observe a positive effect on the organism, depend on the species used and the type of desired effect (Champagne, *et al.*,

2005).Generally, is considered that consuming daily 100 g of food that contains between 10^6 and 10^7 viable cfu/g, will produce a benefit effect of the health (Jayamanne and Adams, 2006, Talwalkar and Kailasapathy, 2003).

Regarding probiotics and according to the study made by FROST & SULLIVAN in relation to the probiotic market, it's a growth driven by market (Frost& Sullivan, 2013):

- The interest of the consumer by natural products
- The interest for many companies that are looking for their introduction in the sector.
- The launch of new and innovative products oriented to the prevention of problems of health related with the style of life and demographic changes of the society

According to Frost & Sullivan study, drivers of the market for probiotics between 2013 and 2019 will be those listed in Table 1.3

Table 1.3. Market drivers of probiotics in North America and Europe between 2013 and 2019.

Drivers	1-2 years	3-4 years	5-7 years
The increase of scientific studies and clinical trials to validate the benefits	M	M	H
The increase of the population´s age in North America and Europe	M	L	L
The increasing knowledge of the consumer	M	L	L

H=High, M=Medium, L=Low

However, and according to the same study, the growth of this market also has certain drawbacks, as shown in the following Table:

Table 1.4. Disadvantages for the probiotic growth market.

Disadvantages	1-2 years	3-4 years	5-7 years
High I+D costs	H	M	M
Legislative restrictions in the claim about health	M	M	M
Price	M	M	L

H=High, M=Medium, L=Low

However, despite these disadvantages, the market of the probiotics is a increasing market, with good prospects of growth as is shows in the Table 1.5.

Table 1.5. Sales, volume, and annual growth rate expected in the field of probiotics in Europe and North America between 2012 and 2019.

Sales in 2012 Million €	Sales in 2019 Million €	Annual Sales Growth 2012-2019	Volume 2012 (ton)	Volume 2019 (ton)	Annual Volume Growth 2012-2019
1294.61	2846.53	11.9%	15821.5	31312.3	10.2%

64.7% of these probiotics is used in the sector of food and dairy products and the remaining 35.3% in the development of nutritional supplements. The following table shows the volumes corresponding to the sale of probiotics in the food sector and dairy products.

Table 1.6. Sales, volume and rate of annual growth expected in the field of the probiotics applied to food and dairy products in Europe and North America between 2012 and 2019.

Sales in 2012 Million €	Sales in 2019 Million €	Annual Sales Growth 2012-2019	Volume 2012 (ton)	Volume 2019 (ton)	Annual Volume Growth 2012-2019
831.59	1826.21	11.9%	13977.6	27651.8	10.2%

Probiotics represent one of the segments of faster growth of the market being in the food sector which experience an increased consumption of them. More than 500 probiotics foods and drinks have been launched in the last ten years. The probiotic functional food market is growing, mainly considering the interest of consumers in preventative health and increase awareness of probiotics benefits on a global scale, according to a new study by Research and Markets.

Between 2009 and 2011, the volume of the probiotic functional food market grew 40%, passing from 16326.53 to 22857.14 million €. Probiotic yoghurts were the first functional dairy products on the European market, mainly from *bifidus* cultures, but as the market has developed, it has grown increasingly being more sophisticated, using different specialties of brands, cultures and mixes. These were followed by a completely new type of product - drinks with doses of active health - also with a wide range of individual and combined probiotic cultures.

The trends of the market of probiotics still remain upward. Euromonitor, predicts that worldwide sales of Probiotic supplements and foods will trigger a 50% over the next five years of 22857.14 million € in 2011 to around 34285.71 million € in 2016.

The report, "Probiotics global market categorized by product features, application and ingredients" puts emphasis on different types of probiotic products that will be aim of interest by the consumer, such as dairy products, beverages, cereals for breakfast, baked foods, probiotics and fermented meat products of dry foods, as well as the main areas of application, such as regular consumption, therapy probiotic and prevention of diseases. Our fermented product is within those groups considered as potential food target of development with interest for the consumer.

The high awareness of the benefits of probiotic yogurts and fermented milk has helped to increase the penetration of the market in Asia-Pacific and European countries. The U.S. market is also growing rapidly due to the tendency of consumers to probiotic dietary supplements and the concept of preventive health care. The Asia-Pacific area is currently the largest market for probiotics, due to the Japanese market, which introduced the concept to the world. It is expected that the innovations of those products will have an important role in the increase of the participation of these agents in the market. In addition, it is also expected that the taste and convenience are important factors to ensure market shares.

A survey made by consumerlab.com to over 10,000 users of supplements and functional foods in 2011 found that almost 28% of men and 34% of women consumed probiotics, so food developments with probiotics are widely accepted and appreciated by the consumer independently of sex.

Focusing on the Spanish market and according to data provided by Euromonitor, in Spain in 2011 the volume of Probiotic yoghurts moved 495 million €. Considering a similar distribution between liquid and spoon yogurt to the globally (55% and 45%, respectively), the liquid yoghurts have moved 271 million €.

Antioxidants

Antioxidants help organism to overcome the oxidative stress caused by free radicals. Free radicals are chemicals that contain one or more unpaired electrons, very

unstable and highly reactive, that can cause damage to other molecules by removal of electrons to achieve stability (Ali, *et al.*, 2008). Various research studies devoted to this theme suggest that free radicals cause oxidative damage mainly in lipids, proteins, carbohydrates, enzymes and nucleic acids, which can trigger some diseases (Fang, *et al.*, 2002, Prior, *et al.*, 1998). The most frequent in our organism oxidative process is which takes place on constituents, unsaturated fatty acids of cellular lipoprotein membrane; This process is also responsible for the progressive deterioration suffered by food when the rancidification of fats (Cámara, *et al*., 2011).

Antioxidants, which are found naturally in the body and in some foods, are substances that have the ability to inhibit oxidation caused by free radicals, acting at intracellular level and others in the cell membrane, always altogether to protect the different organs and systems. For this reason, there are two types of antioxidants:

- Endogenous: they are those body enzyme mechanisms (catalase, glutathione peroxidase and the Coenzyme Q). Some enzymes require metals such as copper, selenium, zinc and magnesium as cofactors in order to make the cell protection mechanism.
- Exogenous: they are introduced by diet and they should be able to neutralize the oxidative action of a free radical unstable molecule without losing its own electrochemical stability. Most important exogenous antioxidants present in foods are some vitamins (C or tocopherol), carotenoids or phenolic compounds, which prevent the oxidation of LDL cholesterol by reducing the risk of coronary alterations, as well as having anticarcinogenic effect by inhibiting the formation of carcinogenic substances (Strain and Benzie, 1999).

In the field of food preservation, the oxidation of fats is the most important food spoilage after the alterations produced by microorganisms (Calvo, 1991).

The oxidation reaction is a chain reaction, i.e., once started, continues to accelerate until the total oxidation of sensitive substances. After oxidation, smells and tastes are rancid, alters the color and texture, and it descends the nutritive value with the loss of some vitamins and polyunsaturated fatty acids. Also, the products formed in the oxidation can get to be harmful to the health.

Food industries trying to avoid the oxidation of food uses different techniques, as the packaging under vacuum or in opaque containers, but also using antioxidants. The majority of fatty products have their own natural antioxidants. Often, these are lost during processing (refining of oils, for example), loss that must be compensated. The vegetable fats are generally richer in antioxidants than the animals. Other ingredients, such as certain spices (Rosemary, for example), can also provide antioxidants to the foods processed with them.

On the other hand, the tendency to increase the unsaturated fats in the diet as a way of preventing coronary diseases makes necessary the use of antioxidants, because unsaturated fats are much more sensitive to oxidation.

Antioxidants may act through different mechanisms:

- Stopping the chain reaction of fats oxidation.
- Eliminating the oxygen trapped or dissolved in the product, or the present in the space that remains unfilled in containers, called head space.
- Eliminating traces of certain metals, such as copper or iron that facilitate the oxidation.

Those who act by the first two mechanisms are antioxidants themselves, while those who act in the third way are grouped in the legal term of "synergy of antioxidants", or more properly, chelating agents. Antioxidants slow down the reaction of oxidation, but in the process they destroy themselves. The result is that the use of antioxidants slows the oxidative alteration of food, but does not prevent it definitively. Other food additives (for example, sulphites) have some antioxidant action, in addition to the primary action which is specifically used for.

There are a number of substances with antioxidant effect which are added to foods to lengthen your life, some chemical nature as BHA or BHT and others are of natural origin such as tocopherols. There is currently a clear trend in the industry as a result of the demands of consumers worried about health and the effect of the chemical in the same additives and increasingly restrictive legislation with the use of certain additives in food, by the employment of natural alternatives for the oxidation of food control.

According to the study conducted by (Frost& Sullivan, 2012) on natural ingredients market of natural antioxidants are growing markets as shown by the data in the Table 1.7.

Table 1.7. Growth of antioxidants sales expected in the period 2012-2016.

Product	Sales of natural antioxidants in 2012 Million $	Annual Sales Growth 2012-2016	Sales of synthetic antioxidants in 2012 Million $	Total Antioxidants Sales 2012
Antioxidants	846.2	1.3%	654	1500.2

Therefore, and according to the same study quoted, the antioxidants market is a market with high appeal for its low entry barriers, markets with high growth and easy access to customers. In the following Table shows the segmentation of natural antioxidants existing in 2012 in concordance with the study from Frost & Sullivan.

Table 1.8. Segmentation of natural antioxidants in 2012.

Comercial Label	Active Ingredient	Source	Function	Application
Vitamin E	Tocopherol	Soy,palm,distilled colza oil	Nutricional and lengthening of the useful life	Foods and beverage
Rosemay extract	Carnosic acid,Rosmarinic acid	Rosemary	Lengthening of the useful life	Foods and beverage
Grape extract	Polyphenols	Grape	Functional	Foods, beverage and dietary supplements
Olive extract	Polyphenols	Olive	Lengthening of the useful life	Foods
Green tea extract	Polyphenols, EGCG	Green tea leaves	Functional	Foods, beverage and dietary supplements

However, the growth of the market of them antioxidant natural has its drivers and their restrictions as is displayed in the

Thus, the drivers that allow the growth of the market of natural antioxidants are:

- A Significant Shift from Synthetic to Natural Antioxidants Drives the Segment

This driver is part of the global “natural” Mega Trend witnessed in the food and beverage industry. Consumer preference for natural products is underlined in this driver.

- The Concept of Blending Antioxidants Reduces the Overall Cost of the Product

Blending natural antioxidants (for example, rosemary extracts with natural vitamin E) helps to reduce the total price for customers and to buffer price fluctuations.

- There is a Significant Scientific Body of Evidence for Efficacy

There is a vast consortium of research available from both academia and private organizations on the health and wellness benefits of antioxidants. Such validation has made it much easier for manufacturers to tout these extracts with their proven benefits.

- Per Capita Consumption of Antioxidants Increases

The rise in the consumption of processed foods and the development of complex food supply chains that require enhanced shelf lives have resulted in an increase in the per capita consumption of antioxidants.

Table 1.9. Natural Antioxidants Segment: Drivers and Restraints, Global, 2013-2016.

Market Drivers	**1-2 years**	**3-4 years**
A Significant Shift from Synthetic to Natural Antioxidants Drives	M	H
The Concept of Blending Antioxidants Reduces the Overall Cost of the Product	M	H
There is a Significant Scientific Body of Evidence for Efficacy	M	M
Per Capita Consumption of Antioxidants Increases	M	L
Market Restraints		
There is a lack of quality standars	M	L
Off-putting sensory and organoleptic properties hamper adoption of natural antioxidants	M	L
Severe scarcity of raw materials affects the supply-demand relstionship	M	M

H=High, M=Medium, L=Low

The main restraints to the growth of the market of natural antioxidants are:

- Severe Scarcity of Raw Materials Affects the Supply-demand Relationship

This is particularly a problem with natural vitamin E in which the scarcity of raw materials that have not been genetically modified has caused significant price increases. Until now, rosemary extracts have been harvested in the wild, leading to an unpredictable

supply. Given this challenge, companies are beginning to make concerted efforts to guarantee their supplies of raw materials.

- Off-putting Sensory and Organoleptic Properties Hamper Adoption of Natural Antioxidants.

Organoleptic properties of natural antioxidants are not completely masked in food matrices when used for shelf-life extension, which can lead to off-putting palatability issues with the finished food product. Some manufacturers are beginning to address this challenge by creating products that minimize the unwanted organoleptic properties of natural antioxidants.

- There is a Lack of Quality Standards.

Multiple purity levels, sources, product formats, and price points confuse customers and consumers when they are choosing antioxidants. However, extensive testing for quality and efficacy is expensive and time consuming, which can add to the price of natural antioxidants.

The following figure shows expected by regions, natural antioxidants, growth also boosted by its use in food supplements.

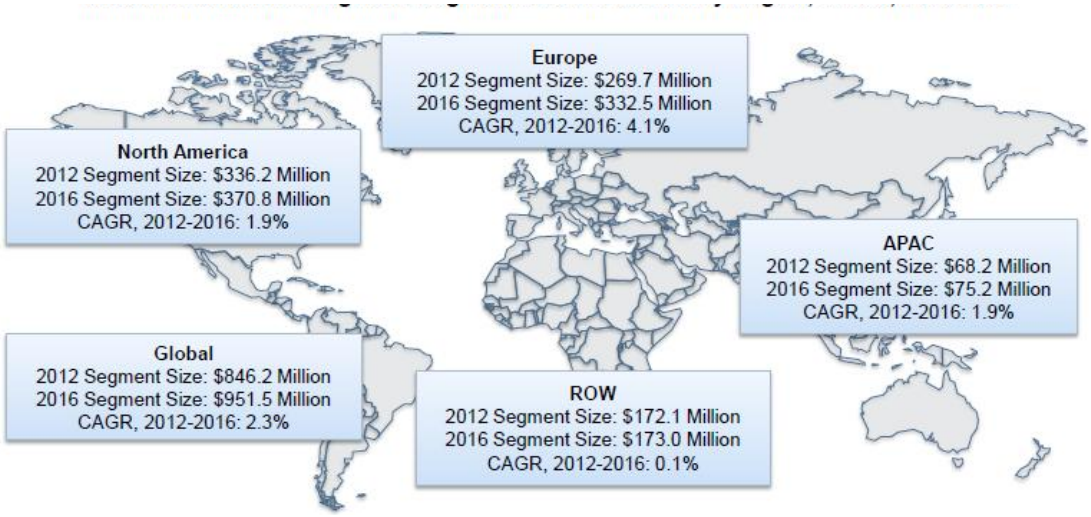

Figure 1.1. Market of the antioxidant natural by regions.

It is therefore a market with high potential that requires appropriate stabilization systems that guarantee the functionality of the ingredient throughout the preparation of the food, and at a cost acceptable to the food business.

1.2 Microencapsulation

It is a specific technology used for the manufacture of functional food that prevents the deterioration of physiologically active compounds. Microencapsulation is based on the embedding effect of a polymeric matrix, which creates a microenvironment in the capsule able to control the interactions between the internal part and the external one (Borgogna, *et al.*, 2010). Microencapsulation allows the protection of a wide range of materials of biological interest, from small molecules and protein (enzymes, hormones.) to cells of bacterial, yeast and animal origin. For this reason such versatile technology is widely studied and exploited in the high technological fields of biomedicine and biopharmaceutics, for application ranging from cell therapy to drug delivery (Smidsrød and Skjåk-Bræk, 1990). The same characteristics make microencapsulation suitable for food industry applications, in particular for the production of high value aliments and nutraceutical.

An important requirement is that the encapsulation system has to protect the bioactive component from chemical degradation, oxidation or hydrolysis to keep the bioactive component fully functional. A major obstacle in the efficacious delivery of bioactive food components is not only the hazardous events that occur during passage through the gastrointestinal tract but also the deleterious circumstances during storage in the product that serves as vehicle for the bioactive components (de Vos, *et al.*, 2010). Many food components may interfere with the bioactivity of the added bioactive food component. It is therefore mandatory that the encapsulation procedure protects the bioactive component during the whole period of processing, storage, and transport (Gibbs, *et al.*, 1999). Administration of large structures such as probiotics will require a higher efficiency of package than molecular structures such as vitamins.

Some studies have reported the success on encapsulating bioactive compounds. The most commonly applied bioactive food molecules that are already encapsulated in industrial applications are lipids, proteins, and carbohydrates. Lipids include fatty acids,

phospholipids, carotenoids, and oil-soluble vitamins (Hämäläinen, *et al.*, 2007,Mcclements, *et al.*, 2009). Bioactive proteins also might require encapsulation. Many food derived peptides act as growth factor, anti-hypertensive agent, antioxidant or immune regulatory factor (Hartmann and Meisel, 2007).

Encapsulation methods have been also widely applied to enhance viability of probiotic bacteria in commercial products. Several authors studied the probiotic strain survival under simulated gastrointestinal conditions (Mokarram, *et al.*, 2009) and similarly for liquid based products such as dairy products (Kailasapathy, 2002). In 2004, Krasaekoopt, *et al*., evaluated the influence of coating materials on some properties of alginate beads and survivability of microencapsulated probiotic bacteria. Mokarram, *et al*., (2009) studied the influence of multi stage coating on the properties of alginate beads and the survivability of microencapsulated *Lactobacillus* bacteria in the beads coated with one or two layers of alginate. In 2010, Weinbreck, *et al*., evaluated the use of microencapsulation to maintain probiotic *Lactobacillus rhamnosus* GG (LGG) viability during exposure to detrimentally high levels of water activity in order to lengthen the shelf-life of probiotic bacteria in dry products such as infant formula powder.

During recent years it has become clearer that probiotic effects are determined by the presence of specific bioactive molecules or effectors molecules in the cell envelope of probiotic bacteria (Kleerebezem and Vaughan, 2009, Van Baarlen, *et al.*, 2009). These effectors molecules are (glyco) proteins and have to be preserved in order to achieve functional effects. The survival of these effectors molecules in the product and during passage in the gastrointestinal tract is even more important than the survival of numbers of probiotics (Konstantinov, *et al.*, 2008).

1.3 Drying Technologies

Dehydration is commonly used to stabilize probiotics and bioactive compounds for storage, handling, transport and subsequent use in functional food applications. Freeze-drying is the most widespread technique for dehydration of probiotic, dairy cultures and bioactive compounds, while spray-drying has been applied to the dehydration of a limited number of probiotic cultures and bioactive compounds.

Freeze-drying has been used to manufacture probiotics and antioxidants powders for decades. Typically, cells and bioactive compounds are first frozen at 196ºC and then dried by sublimation under high vacuum (Santivarangkna, *et al.*, 2007). As the processing conditions associated with freeze-drying are milder than spray-drying, higher probiotic survival rates are typically achieved in freeze-dried powders and also high antioxidants capacity (Wang, *et al.*, 2004). It has been shown that cellular inactivation occurs mostly at the freezing step (Tsvetkov and Brankova, 1983). Indeed, To and Etzel (1997) demonstrated that 60-70% of cells that survived the freezing step can live through the dehydration step. The intracellular and extra-cellular solution concentrations will increase as temperature drops until a eutectic point is reached. There are as such two kinds of freezing methods, i.e. slow freezing and fast freezing. During slow freezing, the process of gradually dehydrating the cell as ice is slowly formed outside the cell leads to extensive cellular damage, while fast freezing can avoid solute effects and excessive cellular shrinkage (Fowler and Toner, 2005).

It has been reported that the higher the surface area of the cell, the higher the membrane damage owing to extracellular ice crystal formation during freezing (Fonseca, *et al.*, 2000). Consequently, cell size has a strong influence on survival of probiotics during freeze-drying, with small spherical cells .Removal of bound water from bacterial cells during drying leads to damage of surface proteins, cell wall and the cell membrane. Consequently, water removal during desiccation can lead to destabilization of the structural integrity of these cellular components, resulting in loss or impairment of function. It has been proposed that the lipid fraction of the cell membrane is the primary target area for damage during drying, where lipid peroxidation may occur (Linders, *et al.*, 1997). In addition, the secondary structures of RNA and DNA destabilize, resulting in reduced efficacy of DNA replication, transcription, and translation (Van de Guchte, *et al.*, 2002). Therefore, in order to achieve optimum results during the desiccation of probiotics, attention must be strongly focused on approaches to minimize damage to these cellular components.

Spray-drying commercial scale production of freeze-dried cultures is an expensive process with low yields, and as such spray drying offers an alternative inexpensive approach yielding higher production rates (Zamora, *et al.*, 2006). The spray-drying process involves the injection of the spray-drying medium at high velocity at

temperatures up to 200 C, which then blasts through a nozzle leading to formation of granules. Consequently, this process results in exposure of the drying medium to high temperatures for a short time, which can be detrimental to the integrity of live bacterial cells and affect the antioxidants capacity and polyphenols contets. During spray-drying, bacterial cells encounter heat stress, in addition to the other stresses already mentioned during freeze-drying, i.e. dehydration, oxygen exposure and osmotic stress (Teixeira, *et al.*, 1997). The effect of spray-drying on the cell membrane can lead to increased cell permeability which may result in the leakage of intracellular components from the cell into the surrounding environment (Teixeira, *et al.*, 1995). The cytoplasmic membrane is among the most susceptible sites in bacterial cells to the stresses associated with spray-drying, while the cell wall, DNA and RNA are also known to be affected, leading to loss of metabolic activity. Removal of hydrogen-bonded water from the headgroup region of phospholipid bilayers increases the headgroup packing and forces the alkyl chains together. As a result, the lipid component may undergo a transition from lamellar to gel phase, which can be seen as a dehydrated lamellar phase in which the chains are stiff and fully extended.

A number of studies have reported on the performance of a variety of probiotics during spray-drying, and in general, the survival rate of probiotic cultures depends on such factors as the particular probiotic strain used, outlet temperature, and drying medium among others. It has been shown that different bacterial species vary with respect to spray-drying tolerance, highlighting the importance of strain selection, for example *L. paracasei* NFBC 338 survived significantly better than *L. salivarius* UCC 118 at similar spray-drying conditions, which may be attributed to the greater thermal tolerance of strain *L. paracasei* NFBC 338 compared to *L. salivarius* UCC 118 (Gardiner, *et al.*, 2000). When the heat and oxygen tolerance of a number of *Bifidobacterium* species, and the relative performance of selected strains during spray-drying were compared, it was found that closely related species exhibiting superior heat and oxygen tolerance performed best, notably *Bifidobacterium animalis* subsp. *lactis* which survived spray-drying at 70% or greater in RSM (20% w/v) at an outlet temperature of 85–90ºC (Simpson, *et al.*, 2005). Outlet air temperature is a major processing parameter affecting the number of survivors during spray-drying. For example, (Kim, *et al.*, 1988) reported that numbers of *Streptococcus salivarius* subsp. *thermophilus* and *L. debrueckii* subsp. *bulgaricus* decreased with increasing outlet or

inlet air temperatures and atomizing air pressure, while similar findings were reported by Gardiner *et al*., 2000 for both *L. paracasei* NFBC 338 and *L. salivarius* UCC 118. Consequently, improved viability can be achieved by reducing the outlet temperature during spray-drying, but beyond probiotic viability, powder quality is also influenced by these parameters, with moisture content of 3.5% being preferred for shelf-stable products (Zayed and Roos, 2004).

1.4 Objetives

In this context, it has been proposed to employ microencapsulation technology as a protective barrier that combined with a novel drying technology enables the stabilization of thermosensible ingredients (probiotics and antioxidants) for the food industry. In this study, a novel technology called Near Fluidizing Microwave Drying (NFMD) was proposed as a competitive alternative method when compared with other more conventional technologies as spray drying and freeze drying. Microwave drying reduces processing times being more economical than freeze drying process. The use of microencapsulation combined with microwave drying technology in a fixed-fluidized bed having good perspectives requires an adequate control of the process. Control variables like temperature and air velocity, microwave power applied must be analyzed deeply along the different phase of drying to avoid thermal and dehydration stresses and to obtain high quality dehydrated products. Other like, processing time and energy efficiency will be considered in the different experiments carried out in order to select the most favorable operation conditions.

Consequently, the main objective of this study is to develop an elaboration process for stabilizing natural ingredients frequently used in the food industry. This elaboration process consists on the combination of microencapsulation technology and a novel microwave drying technology (NFMD). To achive this general purpose the following partial objectives have been proposed:

- Definition of the combined microencapsulation-drying elaboration process.
  - -Selection of materials and encapsulating conditions.
  - -Microwave equipment adecuation and the fluidized bed system integration.
  - -Fluidizing bed equipment design and monitoring of process variables

- Definition of a fluidizing microwave drying process of a reference encapsulating material (alginate -tylose).
  - Establishment of the microwave drying phases under near fluidizing conditions (NFMD) of encapsulating material.
  - Definition of operational strategies of NFMD on the basis of the thermal levels for air and material, along the drying phases.
  - Analysis and selection of the NFMD strategies taking into account characteristic parameters related to the thermal and dehydration stresses.

- Application of the NFMD operational strategies for reference encapsulated living cells.
  - -Firstly, employing microorganism with a wide range of survival capacity (saccharomyces cerevisiae). Preselection of NFMD strategies.
  - -Secondly, application of preselected NFMD operational conditions to probiotics bacteria such as Bifidobacterium animalis subsp. Lactis BB12®.
  - -Application of a mathematical model to be able to describe the mass and energy balances of the process for mass and heat transport parameters evaluation.Valorization of drying rates and energy consumptions.
  - -Viability valorization of the living-cells after drying.

- Comparison of the NFMD drying process respect to other conventional drying technologies (spray-drying and lyophilization).
  - -Valorization of drying cycles, thermal and dehydration stresses analysis.
  - -Analysis of the quality encapsulated dried ingredients. Viability of living-cells and antioxidant capacity.
  - -Analysis of the energy consumption and efficiency.

The results of this thesis have been structured as it follows to cover all the objectives mentioned above.

Chapter 4: Dehydration or drying of the encapsulated material containing nutritional ingredients was defined. The materials used in the microencapsulation are intended to confer protection to the ingredients, avoiding dispersion and interaction with the surrounding environment. In addition, required a proper stabilization during storage

and preparation for its addition to food processing. This requires the application of a method of drying. To reduce the problems observed in other types of drying. It is proposed in this study the development of a drying process by microwave on fluidized bed (near fluidizing microwave drying, NFMD). This chapter will explore the essential elements for the development of this innovative drying process to be applied in subsequent chapters for the preservation of specific nutritional ingredients such as probiotics and antioxidants. It begins with a definition of the materials employees for encapsulation. A definition of the operational strategies used in the application of microwave, fluidization and corresponding modeling of the process for the analysis of the operational variables effect.

Chapter 5: Once it has analyzed the fluido dynamics, kinetics, and thermal levesl in a NFMD process, the next step has been to employ this new technology of drying in microcapsules of alginate containing microorganisms (saccharomyces cerevisiae), to analyze the suitability of this technology to the subsequent viability of microorganisms. Apart from the composition, for the inclusion of living cells in the capsules, the size of these was reduced to make it more consistent with the characteristics of a food additive to assist the process of mixture with different types of food. The operational strategies were adjusted for thermal levels based on the information obtained in the previous chapter.

Chapter 6: Once the selection of the optimal operational conditions for drying NFMD with yeasts proceeded to propose new tests to the probiotic material (*Bifidobacterium animalis* subsp. *Lactis BB12*®), starting from the selected experiments and making small changes of the inlet air and the surface of the material temperatures. The next step has been to employ this novel technology of drying in alginate microcapsules containing microorganisms to analyze the suitability of this technology to the subsequent viability of microorganisms once finished the process.

Chapter 7: This chapter will take the comparison between the new NFMD process that has been described in detail in previous chapters to its application to drying of thermosensitive with other two technologies widely used such as spray drying and freeze-drying. In this chapter, you will proceed to the drying of probiotic material and a concentrate of pomegranate as common elements of reference to see the incidence of each drying technology on quality aspects, kinetic and energy consumption.

Chapter 2

FUNDAMENTALS OF ENCAPSULATION AND DRYING

2 PRINCIPLES OR THEORETICAL FUNDAMENTALS

2.1 Encapsulación technology

The protection of bioactive compounds, as vitamins, antioxidants, proteins, and lipids may be achieved using several encapsulation technologies for the production of functional foods with enhanced functionality and stability. Encapsulation technologies can be used in many applications in food industry such as controlling oxidative reaction, masking flavours, colours and odours, providing sustained and controlled release, extending shelf life, etc. In the bioactive compounds particular case, these need to be protected during the time from processing to consumption of a food product (Chávarri, *et al.*, 2012). The principal factors against them need to be protected are:

- Processing conditions (temperature, oxidation, shear, etc.)
- Desiccation (for dry food products)
- Storage conditions (packaging and environment: moisture, oxygen, temperature, etc.)
- Degradation in the gastrointestinal tract (low pH in stomach and bile salts in the small intestine).

Encapsulation technology is based on packaging of bioactive compounds in mili-, micro- or nano-scaled particles which isolate them and control their release upon applying specific conditions. The coating or shell of sealed capsules needs to be semipermeable, thin but strong to support the environmental conditions maintaining cells alive, but it can be designed to release the bioactive compounds and probiotic cells in a specific area of the human body.

Main techniques for microencapsulation

Extrusion technique

Extrusion technique is the most popular method because of its, simplicity, low cost and gentle formulation conditions that ensure high cell viability and the protection of the bioactive compunds (Krasaekoopt, *et al.*, 2003). It involves preparing a hydrocolloid solution, adding microorganisms, and extruding the cell suspension through a syringe needle. The droplets are dripped into a hardening solution (Heidebach, *et al.*, 2012). If

the droplet formation occurs in a controlled manner the technique is known as prilling. This is done by pulsation of the jet or vibration of the nozzle. The use of coaxial flow or an electrostatic field is the other common technique to form small droplets. When an electrostatic field is applied, the electrostatic forces disrupt the liquid surface at the needle tip, forming a charged stream of small droplets Figure 2.1.The method does not need organic solvents and it is easy to control the size of beads by varying the applied potential. Mass production of beads can either be achieved by multi-nozzle system or using a rotating disc Figure 2.1 Another process is the centrifugal extrusion which consists in a coextrusion process. It utilizes a nozzle with concentric orifices located on the outer circumference of a rotating cylinder. The core material is pumped through the inner orifice and a liquid shell material through the outer orifice. When the system rotates, the extruded rod breaks up into droplets that form capsules (Kailasapathy, 2002).

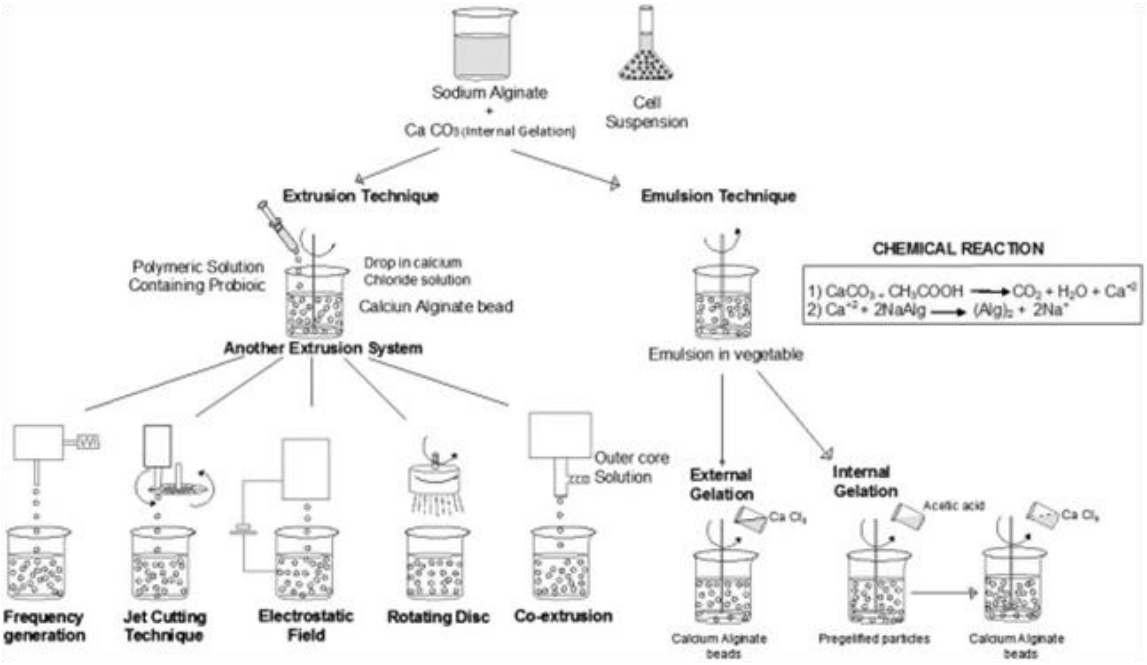

Figure 2.1. Extrusion and emulsion technologies (Martín, *et al.*, 2015).

Emulsion technique

In this technique, the discontinuous phase (cell polymer suspension) is added to a large volume of oil (continuous phase). The mixture is homogenized to form water-in-oil emulsion. Once the water-in-oil emulsion is formed, the water soluble polymer is insolubilized (cross-linked) to form the particles within the oil phase (Heidebach, *et al.*,

2012). The beads are harvested later by filtration Figure 2.1. The size of the beads is controlled by the speed of agitation, and can vary between 25 μm and 2 mm. For food applications, vegetable oils are used as the continuous phase. Some studies have used white light paraffin oil and mineral oil. Emulsifiers are also added to form a better emulsion, because the emulsifiers lower the surface tension, resulting in smaller particles (Krasaekoopt, *et al.*, 2003).

Coacervation

Microencapsulation using the coacervation technique has been attempted to encapsulate flavor oils, preservatives, enzymes as well as microbial cells (John, *et al.*, 2011, Oliveira, *et al.*, 2007a, Oliveira, *et al.*, 2007b,Park and Chang, 2000). This technique utilizes phase separation of one or more incompatible polymers from the initial coating polymer solution under specific pH, temperature or composition of the solution. The incompatible polymer(s) is added to the coating polymer solution and the dispersion is stirred. Changes in the physical parameters, as described earlier, lead to the separation of incompatible polymer and deposition of dense coacervate phase surrounding the core material resulting in formation of microspheres (Gouin, 2004, Nihant, *et al.*, 1995). If required, chemical or enzymatic cross-linking agents can be used for strengthening the microspheres. The more important processing factors to be considered for the coacervation technique are the volume of the dispersed phase, addition rate of the incompatible polymer to the coating polymer solution, stirring rate of the dispersion and core material to be encapsulated. Apart from these factors, the composition and viscosity of the coacervate and supernatant phases are known to affect the size distribution Coacervation, surface morphology and internal porosity of the final microspheres. Coacervation is a highly promising encapsulation technology in view of its good encapsulation capacity and controlled liberation of core material from the microspheres by mechanical stress, temperature and pH changes. However, higher costs and control of different critical conditions associated with composition and kinetics of reaction limit its usefulness (Freitas, *et al.*, 2005, Park and Chang, 2000). Moreover, the coacervation method may not be useful for producing microspheres that are very small (John, *et al.*, 2011).

2.2 JetCutter technology

The jet cutter technology is classified as an extrusion technique of microencapsulation. The bead production by JetCutter is achieved cutting a jet into cylindrical segments by a rotating micrometric cutting tool. The droplet generation is based on a mechanical impact of the cutting wire on the liquid jet. Some techniques as emulsion, simple dropping, electrostatic-enhanced dropping, vibration technique or rotating disc and nozzle techniques have in common that the fluids have to be low in viscosity, and not all of them may be used for large-scale applications. On the contrary, the JetCutter technique is especially capable of processing medium and highly viscous fluids up to viscosities of several thousand mPas.

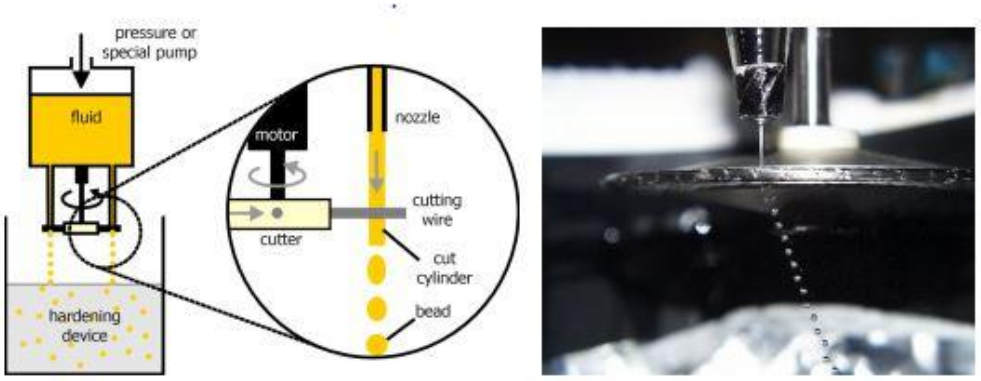

Figure 2.2. Schematic diagram of the JetCutter technology from GeniaLab.

For bead production by the JetCutter the fluid is pressed with a high velocity out of a nozzle as a solid jet. Directly underneath the nozzle the jet is cut into cylindrical segments by a rotating cutting tool made of small wires fixed in a holder Figure 2.2. Driven by the surface tension the cylindrical segments form spherical beads while falling further down, where they finally can be harvested. The size of beads can be adjusted within a range between approximately 200 μm up to several millimetres, adjusting parameters as nozzle diameter, flow rate, number of cutting wires and the rotating speed of cutting tool. Bead generation by a JetCutter device is achieved by the cutting wires, which cut the liquid jet coming out of the nozzle. But in each cut the wire produce a cutting loss. The device is designed to recover these losses, but it is important to minimize de lost volume selecting a smaller diameter of the cutting wire and angle of

inclination of the cutting tool with regard to the jet Figure 2.2. According with Pruesse and Vorlop, a suitable model of the cutting process might help to operator in the parameters selection. One of the most important parameters is the ratio of the velocities of the fluid and cutting wire, necessary to determinate the proper inclination angle (Equation 2.1), but the fluid velocity is also related with the bead size (Equation 2.2) while the diameter of the nozzle and wire determine the volume of cutting loses (Equation 2.3).

$$\alpha = \arcsin\left(\frac{u_{fluid}}{u_{wire}}\right) \tag{2.1}$$

$$D_{sph} = \sqrt[3]{3/2 \cdot D^2 \cdot \left(\frac{u_{fluid}}{n \cdot z} - d_{wire}\right)} \tag{2.2}$$

$$V_{loss} = \frac{\pi \cdot D^2}{4} \cdot d_{wire} \tag{2.3}$$

Where, α=inclination angle; u_{fluid} =velocity of the fluid; u_{wire}=velocity of the cutting wire; d_{bead} =bead diameter; D =nozzle diameter; d_{wire}=cutting wire diameter; n=number of rotations; z=number of cutting wires; V_{loss}=Volume of the overall loss.

Regarding the advantages of the JetCutter technology, besides the capacity for work with medium and highly viscous fluids, there are the narrow bead size dispersion and the wide range of possible sizes, as well as the high flow rate (approx. 0.1-5 L/h). To scale up the JetCutter technology there are two ways. First, a multi-nozzle device can be used, in which nozzles are strategically distributed in the perimeter of the cutting tool. The second way is the increase of the cutting frequency, but this approach needs also a higher velocity of the jet and a too high speed of the beads might cause problems, as coalescence or deformation in the collection bath entrance. In order to overcome this problem, the droplets can be pre-gelled prior entering the collection bath using, for example, a tunnel equipped with nozzles spraying the hardening solution or refrigerating the falling beads. The extrusion technique is the most popular microencapsulation or immobilization technique for micro-organisms and bioactive compounds that uses a gentle operation which causes no damage to the product (Krasaekoopt, et al., 2003). This technology does not involve deleterious solvents and can be done under aerobic and anaerobic conditions. The most important disadvantage of this method is that it is

difficult to use in large scale productions due to the slow formation of the microbeads (Burgain, *et al.*, 2011). Various polymers can be used to obtain capsules by this method, but the most used agents are alginate, κ-carrageenan and whey proteins (Rokka and Rantamäki, 2010).

2.3 Drying technologies

Dehydration enables to preserve food highly perishable, especially fruit and vegetables, with a content of water is typically greater than 90%. The main goal of this technology is to reduce the content moisture of foods, which decreases its activity enzyme and the ability of the microorganisms for development is about the food. The efficiency of the transport of moisture from the food is determined by the internal resistance of the tissue to the movement of the water, and a external resistance, which occurs between the solid surface and the fluid dehydrating, which in the majority of the cases it is air. The main variables that modulate the speed the movement of water in the food are the time and the temperature. As the temperature increases the Dehydration is accelerating, but those attributes qualitative initial food will change drastically the use of high dehydration temperatures damaged the appearance of the thermo sensitive products (Browning), reduces the content nutrient and induces a sweet taste as a result of the caramelization of the sugars (Zanoni, *et al.*, 1998). High levels of 5-hydroxymethylfurfural, an indicator degradation of sugars, are common in tomatoes dried at high temperatures (Muratore, *et al.*, 2008). In General, dehydration temperature decrease, it will lengthen the time of this process, but retrieved bioproduct will have better nutritional attributes, color, aroma, taste and texture (Rajkumar, *et al.*, 2007). Drying temperatures inferior to 65 ° C allow preserve the color and flavor of the tomato. At these temperatures also preserve better the compounds, such as polyphenols, flavonoids, lycopene, Ascorbic acid and β-carotene (Toor and Savage, 2006), which This fruit give a high antioxidant activity and a effect against various forms of cancer and cardiovascular diseases (Shi, *et al.*, 1999). In addition to the temperature and time of dehydrated, the increase in food contact surface with the fluid dehydrating agent also increases the speed movement of water from the food to the outside.

Solar dehydration

Dehydration by exposure to the Sun is widely practiced in the tropics and subtropics. The variant common and economic of this method consists of placing the food on the ground (conditioned or carpeted) or floor concrete, being directly exposed to the Sun. The disadvantage of this variant lies in the vulnerability of the food pollution by dust, infestation by insects and mushroom producers of aflatoxins, losses by animals and low quality of the products obtained (Bala and Mondol, 2001). The process of dehydration by direct exposure to the Sun may require 106 to 120 h (Sacilik, *et al.*, 2006). Another Variant of the drying solar is in use dehydrators solar tunnel type, where the food is protected from the environment during dehydration. The typical temperature is usually reached in these tunnels varies between 60 and 80°C, reaching in some exceptional cases up to 140°C. Typical heat flows for these dryers vary of 202.3 to 767.4 W/m^2. The dehydrated (11.5% of humidity) slices of tomato using Sun tunnels often take 82 to 96 h. The advantages of the dehydration solar lie in them low costs of operation and be eco-friendly, since generally not used power electric or derived from fossil fuels (Bala and Woods, 1994). They are designed and installed different types of solar dehydrators in different regions of the world. In general terms, the solar dehydrators can be classified into two types: dehydrators exclusively using sources of power renewable and the drying agents that include addition sources of energy not renewable already is as a source supplementary of heat or to promote the circulation of air (Bala and Janjai, 2013).

Hot air drying

The dehydrated with hot air is the method most common to dry food products, (Doymaz, 2007). In this method, the hot air removes the water on the surface of products-free State (Schiffmann, 1986). The increase in the speed of the air and the turbulence generated around the food causes a reduction of the tension in the layer of diffusion, causing an efficient dehydration (Cárcel, *et al.*, 2007). The external resistance to the movement of the water contributes significantly to the global resistance (Hawlader, *et al.*, 1991). The dehydration by this method depends on the speed used and on the air temperature (Mulet, *et al.*, 1999). Doymaz (2007) found that by increasing the air temperature from 55 to 70°C the time of dehydration decreased from 35.5 to 24 hours, respectively. The speed decreasing of the warm air (60°C) from 1.5 to 0.13 m/s increased the time of dehydration from 28 to 65 h (Tsamo, *et al.*, 2006). In general, this method of

dehydration commonly use high temperatures, which represents its main disadvantage (Sharma and Prasad, 2001), since that causes drastic changes in taste, color, content of nutrients, aromatic components, density, absorption of water and concentration of solutes (Maskan, 2001). Times and temperatures of dehydration also causes the formation of undesirable aromas and the Maillard reactions (Boudhrioua, *et al.*, 2003). The hot air flow may be upstream or in parallel. Usually the dehydration with hot air upstream, it is more efficient to that which is achieved with the air flow in parallel. (Unadi, *et al.*, 2002) showed dehydration of tomatoes (15% of humidity) was more quickly with air to upstream (5 h less) than with flow in parallel, since the transfer of heat was more efficient to the existing a contact more narrow due to the movement in opposite directions.

Osmotic dehydration

Osmotic dehydration has the advantage of maintaining organoleptic (color,) texture, flavor and aroma) and nutritional (vitamins, minerals and protective compounds) of biocompounds, which is not achieved by thermal dehydration (Jiokap Nono, *et al.*, 2001). The osmotic dehydration also allows reducing the costs production, packaging and distribution of vegetable (El-Aouar, *et al.*, 2006). Osmotic dehydration consists in place the product in contact with a solution of sugar and/or salt, to which is it called osmotic solution. During the osmotic dehydration the content of water decreases continuously in the product while the osmotic agent penetrates into it. The sugar has a lower osmotic power than other osmotic agents. Tsamo, *et al.*, (2006) compared the dehydration of slices of tomato using saturated salt solutions, sugar and salt-sugar for 20 h, finding that the product treated with salt-sugar had the lowest content of humidity, followed by those who were treated exclusively with salt and sugar, respectively. Similarly, (Askari, *et al.*, 2008)) showed that two osmotic media (40% sucrose + 5% and 40% sucrose and NaCl + 10% NaCl) presented a more dehydrating power than sucrose alone. It has been hypothesized that sucrose is a coating that reduces the exchange of materials between the product and the osmotic solution, making slower the process of dehydration (Askari, *et al.*, 2008). The reduction of water typically reached by osmotic dehydration varies from 30 to 60%. However, in some products dehydration tends to be higher (Raoult-Wack, 1994). It is important to indicate that the exchange of materials between the osmotic solution and the product cause the shrinkage and deformation of the tissue (Tsamo, *et al.*, 2006).

Microwave drying

The microwaves cause the polarization of molecules and intense mobility of their electrons, due to conversion of electromagnetic energy to kinetic energy. Because of this movement, the electrons collide each other, generating heat as a result of friction (Alibas, 2007). The application of microwave energy generate an internal warming and steam pressure within the product that gently "pumps" the humidity towards the surface, reducing the internal resistance of the food to the movement of water and causing dehydration (Turner and Jolly, 1991). The high water vapor pressure generated inside the food exposed to microwave it can induce the formation of pores in the product, which facilitates the drying process (Feng, 2002). This method of dehydration has become common, because it prevents the decrease of the quality and ensures a quickly and efficiently distribution of heat in the food (Díaz-Maroto, *et al.*, 2003). This method reduces the drying time significantly and obtains great savings of energy (Feng, 2002). The output of the microwave power plays a vital role in the dehydration of the functional foods. An increase on the power corresponds to a decrease on the drying time (Heredia, *et al.*, 2007). However, the variations of power in the high range have not a significant impact in dehydration time. (Al-Harahsheh, *et al.*, 2009) found no differences in dehydration time (20 min) (88% of humidity) of slices of tomato using microwave power on the high power range (480, 640 and 800 W). However, a decrease on the power (160 and 320 W) implied an increase from10 to 20 min in the drying time. In general, the quality of the products dried with microwave is considerably good, especially in terms of firmness and total soluble solids (Lu, *et al.*, 2011).

Lyophlization

Lyophilization or freeze drying is a process that industry employs to ensure the stability in long term and to preserve the original properties of those pharmaceutical and biological products. This process was recently applied to improve the long term stability of nanoparticles (Abdelwahed, *et al.*, 2006). The lyophilized requires the elimination of water of more than 99 % of the initially diluted solution. The total solute concentration increases rapidly and is a function only of the temperature, is therefore independent of the initial solution concentration. The water solid state during the freeze protects the elementary structure and the form of the products with a minimum volume reduction. Volatile compounds, salts and electrolytes, if they do not form a special class of

excipients, salts, acetate or baking, are eliminated easily during the stage of sublimation of the ice and therefore do not remain in the dehydrated product (Franks, 1998). (Pikal, *et al.*, 1984) mentioned that materials to be lyophilized are grouped into two classes: solids with a high content of water, as can be food products, usually placed in trays inside the lyophilizer, or solutions homogeneous as peptides or conventional drugs. States intermediate include dispersions such as liposomes or individual cells (microorganisms, yeasts). Despite the many advantages, freeze drying has always been recognized as the most expensive process for the manufacture of a dehydrated product. The freeze-drying process consists of three phases: (I) after freezing separates the water from the hydrated components of the product, by the formation of crystals of ice or eutectic mixtures. (II) Sublimation of these crystals that eliminates the product´s water working at low pressure and below the triple point temperature and providing the latent heat of sublimation. This stage takes place in the freeze dryer. (III) Evaporation or desorption of remaining water even adsorbed on the inside of the product. Once sublimated all ice, also is certain retained water in the food (bound water) this is eliminated increasing the freeze temperature keeping the vacuum which promotes the evaporation.

Spray drying

Spray drying is a method where a liquid/slurry material is sprayed in finely atomized droplets in a hot convective medium, converting the droplets into fine solid particles. The process has found many applications in food processing, particularly in the production of instant food powders (Chegini and Ghobadian, 2005, Goula and Adamopoulos, 2008). This method is commonly used to obtain powders from milk, whey, yeast, and other high-valuable products due to their good final quality (Ratti, 2013). In this drying method, a solution of soluble or suspended slurry of materials is sprayed into a drying chamber using an atomizer (e.g., a nozzle), and hot gas flows cocurrently or countercurrently with the dispersed liquid droplets, removing moisture from the particles. Dry powder particles are collected in the collection vessel. While this method has several advantages, including rapid drying, large throughput, and continuous operation, spray drying is a very expensive technique to use for low-value products, mainly because of its low energy efficiency (Jangam, 2011). Furthermore, due to the relatively high temperatures involved in spray drying processes, this drying technique may cause losses of certain quality and sensory attributes especially vitamin C, *β*-carotene, flavors, and aroma (Sagar and Suresh Kumar, 2010). Also, the oxygen present

in the large volumes of air mixed with the food droplets during spray drying can have a negative impact on heat-sensitive and oxidizable nutrients.

2.4 General rules for modeling a drying process

Two classes of processes are encountered in practice: steady state and unsteady state (batch). The difference can easily be seen in the form of general balance equation of a given entity for a specific volume of space (e.g., the dryer or a single phase contained in it):

Inputs - outputs = accumulation (2.4)

For instance, for mass flow of moisture in a solid phase, $\dot{m}$, being dried (in kg/s) this equation reads:

$$\dot{m}X_1 - \dot{m}X_2 - r_A A = m_D \frac{dX}{dt} \tag{2.5}$$

In steady -state processes, as in all continuously operated dryers, the accumulation term vanishes and the balance equation assumes the form of an algebraic equation. When the process is of batch type or when a continuous process is being started up or shut down, the accumulation term is nonzero and the balance equation becomes an ordinary differential equation respect to time.

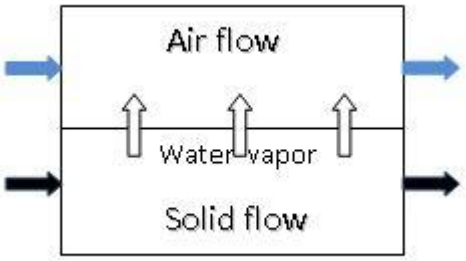

Figure 2.3. General scheme of the fluxes in a drier.

In writing Equation (2.5), we have assumed that only the input and output parameters count. Indeed, when the volume under consideration is perfectly mixed, all phases inside this volume will have the same property as that at the output. This is the principle of a lumped parameter model (LPM). If a property varies continuously along

the flow direction, the balance equation can only be written for a differential space element. Here Equation (2.6) will now read:

$$\dot{m}X - \dot{m}X + \frac{\partial X}{\partial L}dL - r_A dA = dm_D \frac{dX}{dt} \tag{2.6}$$

Or, after substituting $dA = a\,S\,dL$ and $dm = (1 - \varepsilon)\rho\,SdL$, in which S is the section of a drier of length L we obtain:

$$-\dot{m}X + \frac{\partial X}{\partial L} - r_A a\,S = (1-\varepsilon)\,\rho\,S\,\frac{dX}{dt} \tag{2.7}$$

As we can see for this case, which we call a distributed parameter model (DPM), in steady state (in the one-dimensional case) the model becomes an ordinary differential equation with respect to space coordinate, and in unsteady state it becomes a partial differential equation. This has a far-reaching influence on methods of solving the model. A corresponding equation will have to be written for another phase (gaseous), and the equations will be coupled by the drying rate expression. Before starting with constructing and solving a specific dryer model it is recommended to classify the methods, so all topic cases c an easily be identified. We will classify all topic cases when a solid is contacted with a heat carrier. Three factors will be considered:

1. Operation type; we will consider either batch or continuous process with respect to given a phase.

2. Flow geometry type; w e will consider only parallel flow, concurrent, countercurrent, and cross-flow cases.

3. Flow type; w e will consider two limiting cases, either plug flow or perfectly mixed flow.

These three assumptions for two phases present result in 16 generic cases as shown in Figure 2.4. Before constructing a model it is desirable to identify the class to which it belongs so that writing appropriate model equations is facilitated. Dryers of type 1 do not exist in industry; therefore, dryers of type 2 are usually called batch or semicontinuous dryers as is done in this text. Their principle of operation is different from any of the types shown in Figure 2.4. In the cases treated here, of microwave drying in fluidized bed

(see Chapters 3 and 4), in which air stream crosses a solid bed of particles, correspond to the case 2b or 2d.

When trying to derive a model of a dryer we first have to identify a volume of space that will represent a drier. If a dryer or a whole system is composed of many such volume s, a separate submodel will have to be built for each volume and the models connected together by streams exchanged between them. Each stream entering the volume must be identified with parameters. Basically for systems under constant pressure it is enough to describe e ach stream by the name of the component (humid gas, wet solid, condensate, etc.), its flowrate, moisture content, and temperature. All heat and other energy fluxes must also be identified. The following five parts of a deterministic model can usually be distinguished:

1. Balance equations; they represent Nature's laws of conservation and can be written in the form of Equation (2.4) (e.g, for mass and energy).

2. Constitutive equations (also called kinetic equations); they connect fluxes in the system to respective driving forces.

3. Equilibrium relationships; necessary if a phase boundary exist s somewhere in the system.

4. Property equations; some properties can be considered constant but, for example, saturated water vapor pressure is strongly dependent on temperature even in a narrow temperature range.

5. Geometric relationships—they are usually necessary to convert flowrates present in balance equations to fluxes present in constitutive equations. Basically they include flow cross-sect ion, specific area of phase contact, etc.

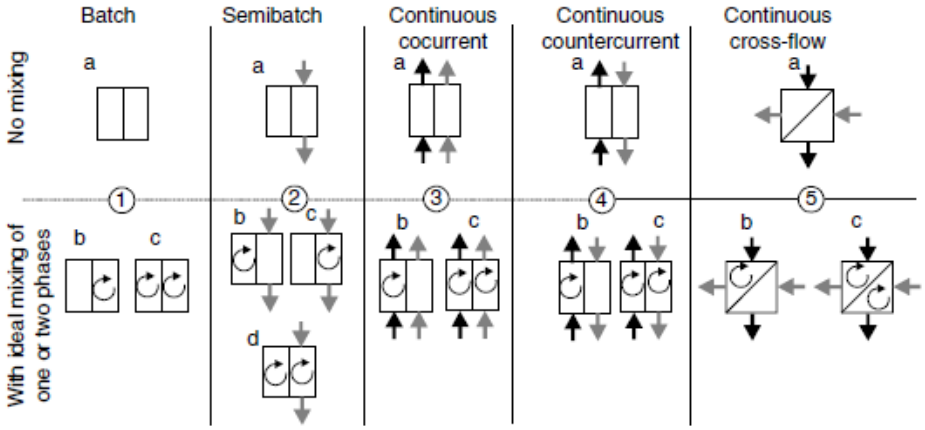

Figure 2.4. Generic types of dryers (Pakowski and Mujumdar, 2006)

Energy and balances in LPM

Input–output balance equations for a typical case of convective drying and lumped parameter model, in which we consider mean values for the properties of air and solid within the drier, assume the following form:

Mass Balances

$$\dot{m}X_1 - \dot{m}X_1 - r_A A = m_D \frac{dX}{dt} \tag{2.8}$$

$$\dot{m}_a Y_1 - \dot{m}_a Y_2 + r_A A = m_{aD} \frac{dY}{dt} \tag{2.9}$$

For solid and gas phases.

Energy Balances

$$\dot{m}Cp_1 T_1 - \dot{m}Cp_2 T_2 + \left(h\Delta T_m - r_{Am}\right)A = m_D Cp_m \frac{dT_m}{dt} \tag{2.10}$$

$$\dot{m}_a Cp_a T_{a1} - \dot{m}_a Cp_a T_2 + \left(h\Delta T_m - r_{Am} Q_{vap}\right)A = m_{aD} Cp_a \frac{dT_m}{dt} \tag{2.11}$$

For solid and gas phases.

In the above equations h is the convection heat coefficient, ΔT_m is the mean temperature increment between product and air, and r_{Am} is the mean drying rate. Accumulation in the gas phase can almost always be neglected even in a batch process as

small compared to accumulation in the solid phase. In a continuous process the accumulation in solid phase will also be neglected.

Energy and balances in DPM

In the case of distributed parameters models (DPM) properties of phases across the drier can vary for a given phase. Thus, the energy and mass balance equations read:

$$\mathrm{div}\left[\rho X u\right] - \mathrm{div}\left[D \cdot \mathrm{grad}\left(\rho X\right)\right] \pm k_G a \Delta P_w - \frac{\partial \rho X}{\partial t} = 0 \tag{2.12}$$

$$\mathrm{div}\left[\rho Cp T\, u\right] - \mathrm{div}\left[\frac{k}{\rho Cp} \cdot \mathrm{grad}\left(\rho Cp\ T\right)\right] \pm h\, a\, \Delta T \pm k_G a \Delta P_w + Q_{vap} + Q_h - \frac{\partial \rho\, CpT}{\partial t} = 0 \tag{2.13}$$

Where the terms are, respectively (from the left): in-out term, diffusion term, interfacial term, and accumulation term.

Note that density here is related to the whole volume of the phase: e.g., for solid phase composed of granular material it will be equal to $\rho\ (1\text{-}\varepsilon)$. Besides, the term Q_h represents the heat supplied by a heating device or generated by the product itself under microwave irradiation — Q_{abs}— that depends on the dielectric properties of product being dried

In some situations as we will see in the drying process detailed in chapter 4, the DPM is applied only to the solid being dried. An example is the mass and energy balance equations applied to a discrete volume of a product particle of a fluidizing bed for example under microwave irradiation. Certain terms of mass and energy balances to the solid described in Equations (2.12) and (2.13) like; in-out, diffusion, interface disappear. Thus, such equation for a general tridimensional case reduces to:

$$D\left(\frac{\partial^2 X}{\partial^2 x} + \frac{\partial^2 X}{\partial^2 y} + \frac{\partial^2 X}{\partial^2 z}\right) = \frac{\partial X}{\partial t} \tag{2.14}$$

$$k\left(\frac{\partial^2 T}{\partial^2 x} + \frac{\partial^2 T}{\partial^2 y} + \frac{\partial^2 T}{\partial^2 z}\right) + ´Q_{abs} = Cp\rho \frac{\partial T}{\partial t} \tag{2.15}$$

Equation (2.14) can be expressed also in terms of M on dry basis according to $M=X/(1-X)$. Equations (2.14) and (2.15) —this without the Q_{abs} term of microwave heating— are named Fick's law and Fourier's law, respectively, and can be solved with suitable boundary and initial conditions. Literature on solving these equations is abundant, and for diffusion a classic work is that of Crank (1975).

2.5 Lyophilization

The main principle involved in freeze drying is a phenomenon called sublimation, where water passes directly from solid state (ice) to the vapor state without passing through the liquid state. Sublimation of water can take place at pressures and temperature below triple point. The material to be dried is first frozen and then subjected under a high vacuum to heat (by conduction or radiation or by both) so that frozen liquid sublimes leaving only solid, dried components of the original liquid. The concentration gradient of water vapor between the drying front and condenser is the driving force for removal of water during lyophilization (Liberman, *et al*., 1989).

To extract water from foods, the process of lyophilization consists of:

1. Freezing the food so that the water in the food becomes ice.

2. Under a vacuum, sublimating the ice directly into water vapour.

3. Drawing off the water vapour.

4. Once the ice is sublimated, the foods are freezedried and can be removed from the machine (Neema, *et al*., 1997).

Freeze drying also known as lyophilization, is widely used for bioproducts to improve the stability and long term storage of labile compounds. Lyophilization or Freeze-drying fills an important need in food technology by allowing drying of heat-sensitive materials biologicals at low temperature under conditions that allow removal of water by sublimation, or a change of phase from solid to vapor without passing through the liquid phase (Nail, 1992). Lyophilization or freeze drying is a process in which water is removed from a product after it is frozen and placed under a vacuum, allowing the ice

to change directly from solid to vapor without passing through a liquid phase. Lyophilization is performed at temperature and pressure conditions below the triple point, to enable sublimation of ice as it can be seen in Figure 2.5. The entire process is performed at low temperature and pressure, hence is suited for drying of thermolabile compounds. Steps involved in lyophilization start from sample preparation followed by freezing, primary drying and secondary drying, to obtain the final dried product with desired moisture content. The concentration gradient of water vapor between the drying front and condenser is the driving force for removal of water during lyophilization. The vapor pressure of water increases with an increase in temperature during the primary drying. Therefore, primary drying temperature should be kept as high as possible, but below the critical process temperature, to avoid a loss of cake structure. This critical process temperature is the collapse temperature for amorphous substance, or eutectic melt for the crystalline substance. During freezing, ice crystals start separating out until the solution becomes maximally concentrated. On further cooling, phase separation of the solute and ice takes place (Adams, and Irons, 1993).

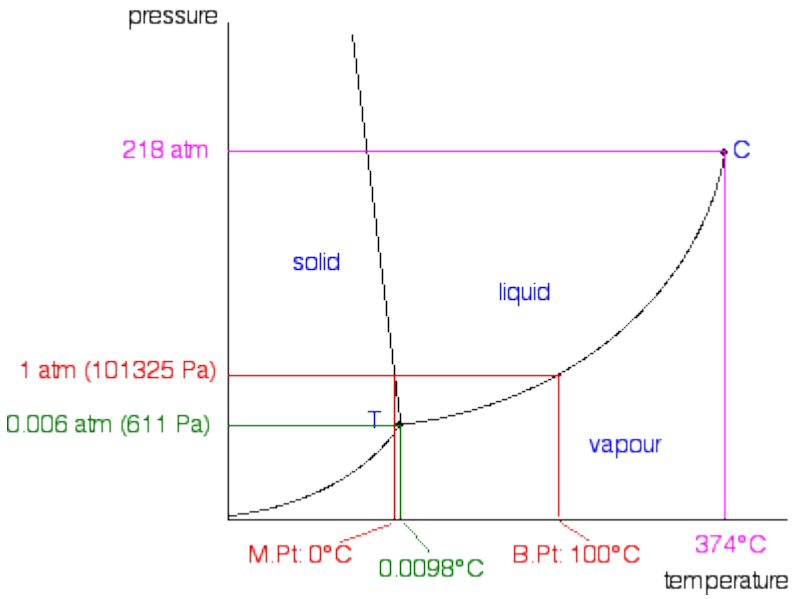

Figure 2.5. Phase diagram showing the triple point of water at 0.0098ºC, 0.006 atm.

The freeze-drying cycle

Lyophilization is the most common method for manufacturing solid products and is central to the preservation of materials which must be dried thoroughly in order to ensure stability. To meet this requirement, products' lyophilization occurs in three steps: (1)

freezing to convert most of the water into ice, (2) primary drying to sublime the ice, and (3) secondary drying to remove unfrozen water by desorption (Mackenzie, 1998). To technically realize this manufacturing process, a freeze dryer is commonly constructed with two main parts: a "drying" chamber holding temperature controlled shelves is connected by a valve to a "condenser" chamber, which contains coils capable to achieve very low temperatures between -50°C and -80°C. The freeze-drying process consists of three stages: Freezing, primary drying, secondary drying.

Freezing

Freezing is a critical step, since the microstructure established by the freezing process usually represents the microstructure of the dried product. The product must be frozen to a low enough temperature to be completely solidify. Since freeze drying is a change in state from the solid phase to the gaseous phase, material to be freeze-dried must first be adequately pre-frozen. The method of pre-freezing and the final temperature of the frozen product can affect the ability to successfully freeze dry the material (Novoa, *et al.*, 2004). Rapid cooling results in small ice crystals, useful in preserving structures to be examined microscopically, but resulting in a product that is, more difficult to freeze dry. Slower cooling results in large ice crystals and less restrictive channel in the matrix during the drying process. Products freeze in two ways, the majority of products that are subjected to freeze-drying consist primarily of water, the solvent and materials dissolved or suspended in the water, the solute. Most samples that are to be freeze dried are eutectics, which are mixtures of substances that freeze at lower temperature than the surrounding water. This is called the eutectic temperature. Eutectic point is the point where all the three phases' i.e. solid, liquid and gaseous phases coexist. It is very important in freeze-drying to pre-freeze the product to below the eutectic temperature before beginning the freeze-drying process. The second type of frozen product is a suspension that undergoes glass formation during the freezing process. Instead of forming eutectics, the entire suspension becomes increasingly viscous as the temperature is lowered. Finally the products freeze at the glass transition point forming a vitreous solid. This type of product is extremely difficult to freeze dry (Lam, *et al*., 2003).

Primary drying

After pre-freezing the product, conditions must be established in which ice can be removed from the frozen product via sublimation, resulting in a dry, structurally intact

product. This requires very carefully control of the two parameters: Temperature and pressure involved in freeze-drying system. The rate of sublimation of ice from a frozen product depends on the difference in vapor pressure of the product compared to the vapor pressure of the ice collector. Molecules migrate from the high-pressure sample to a lower pressure area. Since vapor pressure is related to temperature, it is necessary that the product temperature is warmer than the cold trap (ice collector) temperature. It is extremely important that the temperature at which a product is freeze dried is balanced between the temperatures that maintains the frozen integrity of the product and the temperature that maximizes the vapor pressure of the product.

Most products are frozen well below their eutectic or glass transition point, and the temperature is raised to just below this critical temperature and they are subjected to reduced pressure. At this point the freeze-drying process is started with the sublimation. Vacuum pump is an essential of a freeze drying system, and is used to lower the pressure of the environment around the product. The other essential is a collecting system, which is a cold trap used to collect the moisture that leaves the frozen product. The collector condenses out all condensable gases, i.e. the water molecules and the vacuum pump removes all non-condensable gases. The molecules have a natural affinity to move toward the collector because its vapor pressure is lower than that of the product. Therefore the collector temperature must be significantly lower than the product temperature.

A third component essential in freeze-drying system is energy. Energy is essential in the form of heat. Almost ten times, much energy is required to sublime a gram of water from the frozen to the gaseous state as is required to freeze a gram of water, (2700 joules per gram of ice). Heat must be applied to the product to encourage the removal of water in the form of vapor from the frozen product. The heat must be very carefully controlled, as applying more heat than the evaporative cooling in the system can warm the product above its eutectic or collapse temperature. Heat can be applied by several means one method is to apply heat directly through a thermal conductor shelf such as is used in tray drying. Another method is to use ambient heat as in manifold drying (Rendolph, *et al*., 2005).

Secondary drying

After primary freeze-drying is complete, and all ice has sublimed, bound moisture is still present in the product. The product appears dry, but the residual moisture content may be as high as 7-8% continued drying is necessary at warmer temperature to reduce the residual moisture content to optimum values. This process is called 'Isothermal Desorption' as the bound water is desorbed from the product.

Secondary drying is normally continued at a product temperature higher than ambient but compatible with the sensitivity of the product. In contrast to processing conditions for primary drying which use low shelf temperature and a moderate vacuum, desorption drying is facilitated by raising shelf temperature and reducing chamber pressure to a minimum. Care should be exercised in raising shelf temperature too highly; since, protein polymerization or biodegradation may result from using high processing temperature during secondary drying. Secondary drying is usually carried out for approximately 1/3 or 1/2 the time required for primary drying.

The general practice in freeze-drying is to increase the shelf temperature during secondary drying and to decrease chamber pressure to the lowest attainable level. The practice is based on the ice is no longer present and there is no concern about "melt track" the product can withstand higher heat input (Swarbrick, *et al*., 2004). Also, the water remaining during secondary drying is more strongly bound, thus requiring more energy for its removal. Decreasing the chamber pressure to the maximum attainable vacuum has traditionally been thought to favor desorption of water.

2.6 Spray drying

Spray drying is a unique process in which particles are formed at the same time as they are dried because of that also is considered as a microencapsulation technique (Barbosa-Cánovas and Juliano, 2005). It is very suitable for the continuous production of dry solids in powder, granulate or agglomerate form from liquid feed stocks as solutions, emulsions and pumpable suspensions. The end product of spray drying must comply with precise quality standards regarding particle size distribution, residual moisture content, bulk density, and particle shape. In the spray drying process, dry granulated powders are

produced from a slurry solution, by atomizing the wet product at high velocity and directing the spray of droplets into a flow of hot air, e.g. 150-200ºC. The atomized droplets have a very large surface area in the form of millions of micrometer-sized droplets (10-200 µm), which results in a very short drying time when exposed to hot air in a drying chamber (Morgan, *et al.*, 2006, Santivarangkna, *et al.*, 2007). Dehydrated enzymes, detergents, coffee extracts, and isolated proteins are examples of products produced by spray drying. This process is also widely used in the production of lactic acid bacteria cultures and dehydrated probiotics bacteria (Riveros, *et al.*, 2009). The concept of spray drying was first patented by Samuel Percy in 1872, and its industrial application in milk and detergent production began in the 1920s.

Every spray dryer consists of a feed pump, atomizer, air heater, air disperser, drying chamber and equipment for product discharge, transport, packaging and removing air as it can be observed in Figure 2.6. A complete air exhaust system contains fans, wet scrubbers, dampers and ducts. The atomization process is the most important part of the spray dryer. In any type of atomization, energy is needed to break up liquid bulk to create individual droplets. Depending on the type of energy used to produce the spray particles, atomizers can be classified into four main categories: centrifugal, pressure, kinetic and sonic (Barbosa-Cánovas and Juliano, 2005).

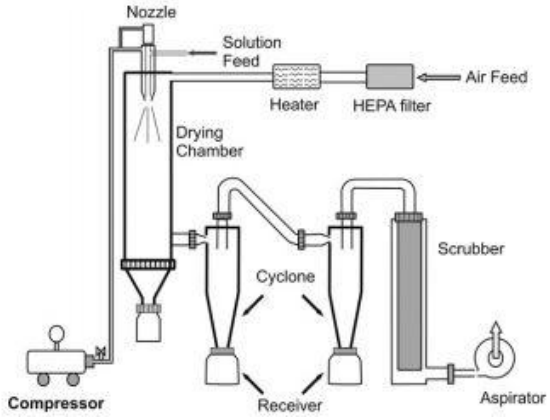

Figure 2.6. Schematic of spray dryer adopted from (Devakate, *et al.*, 2009).

Rotary atomizers or centrifugal nozzles use the energy of a high speed-rotating wheel to break up liquid bulk into droplets. They are flexible and also easy to operate and maintain. Rotary atomizers have no blockage problems and can be run for a long time

without operator interface. They operate under low feed pressure and can handle abrasive feeds. However, they cannot be used in horizontal dryers because the liquid is thrown horizontally. Rotary atomizers produce large quantities of fine particles, which can result in pollution control problems. They are also expensive compared to other types of atomizers. In pressure nozzles, the feed forced through an orifice under pressure and readily disintegrates into a spray. Pressure nozzles are small, simple to maintain, easy to replace, and low in cost. They are not applicable for viscous liquids and have clogging problems. In kinetic energy atomizers, the liquid feed and the compressed air are passed separately to the nozzle head and then the feed is broken down into small droplets. These atomizers are useful for high viscous feeds and require a smaller drying chamber. They are often used in laboratory and pilot plant spray dry applications. They are expensive to operate and require two or three times more energy than that of pressure nozzles. In sonic atomization, a sonic generator is a part of the nozzle head; when the feed passes through the head it breaks up the liquid into droplets. This device is suitable for droplets below 50 microns. The disadvantages of the sonic atomization are its capacity restrictions, low rate feeds and acoustic environmental problems (Barbosa-Cánovas and Juliano, 2005, Gohel, *et al.*, 2009).

The nature and viscosity of the feed and the desired characteristics of dried product influence the choice of atomizer configuration (Gharsallaoui, *et al.*, 2007). The atomizer must be positioned inside the drying chamber. It may be positioned at the top, side top, side base, middle and base of a spray dryer (Masters, 1985).

Spraying flow patterns

There are three types of product-air flow pattern in spray dryers: co-current, counter-current, and mixed flow. In the co-current process, the droplets and air pass through the dryer in the same direction. The droplets meet the air at the highest temperature. This causes rapid surface evaporation, while it is still wet, providing safe conditions for heat-sensitive materials. The counter-current configuration sprays the droplets in the opposite direction to the hot air flow, which exposes the dry product to high temperatures. This design can only be used for non-heat-sensitive materials and is less commonly used than the co-current configuration (Oakley, 1997). Mixed flow is a combination of co-current and counter-current flow patterns. A nozzle is positioned in the bottom of the chamber, forcing the spray to travel upward until overcome by gravity

and the downward flow of the drying medium. Mixed flow is a good method for drying relatively coarse droplets in a small chamber at small production rates because the spray has a long path through the chamber (Barbosa-Cánovas and Juliano, 2005). Typical product-air flow patterns in spray dryers are shown in Figure 2.7 (Vega-Mercado, *et al.*, 2001).

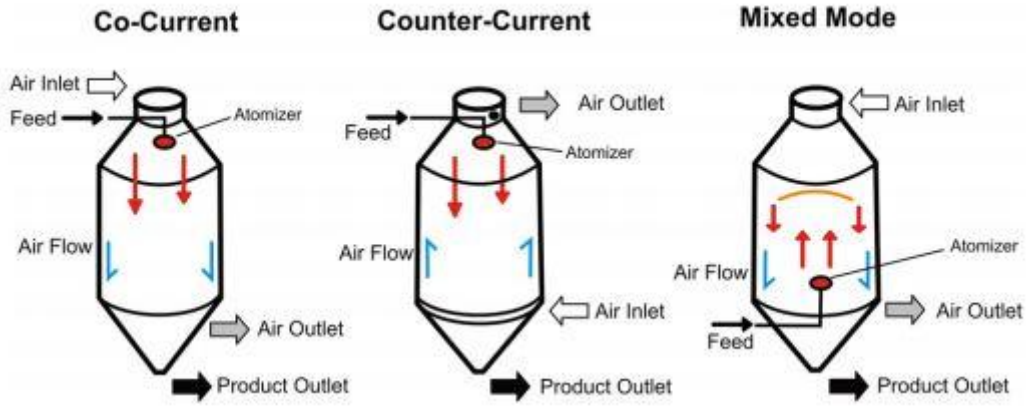

Figure 2.7. Typical air flow patterns in spray dryers adopted from (Vega-Mercado, *et al.*, 2001).

There are three types of product-air flow pattern in spray dryers: co-current, counter-current, and mixed flow. In the co-current process, the droplets and air pass through the dryer in the same direction. The droplets meet the air at the highest temperature. This causes rapid surface evaporation, while it is still wet, providing safe conditions for heat-sensitive materials. The counter-current configuration sprays the droplets in the opposite direction to the hot air flow, which exposes the dry product to high temperatures. This design can only be used for non-heat-sensitive materials and is less commonly used than the co-current configuration (Oakley, 1997). Mixed flow is a combination of co-current and counter-current flow patterns. A nozzle is positioned in the bottom of the chamber, forcing the spray to travel upward until overcome by gravity and the downward flow of the drying medium. Mixed flow is a good method for drying relatively coarse droplets in a small chamber at small production rates because the spray has a long path through the chamber (Barbosa-Cánovas and Juliano, 2005).

Two-stage spray dryer

In a two-stage spray dryer, the spray dryer is combined with a fluidized bed on the dryer outlet side. This system makes it possible to decrease the drying temperature, limiting thermal denaturation and producing powder product with very low water content

(Schuck, 2002). The investment for two-stage drying system is larger than for one stage spray drying systems, but the operating costs are lower because of energy savings. In addition, the quality of the product with a two-stage spray dryer is much better and the dried product is agglomerated, leading to good wetting dispersion properties of the final product during rehydration (Tang, *et al.*, 1999).

2.7 Microwave heating

Food preservation is the primary objective of most food-processing operations and the challenge is to ensure quality and safety of processed products. Thermal processing, which mainly includes blanching, drying, evaporation, pasteurization, and sterilization, is carried out to increase the shelf-life of foods. The thermal processing conditions normally dictate the product quality, process economics, and environmental impact in most of the food-processing operations. Conventional heating methods rely essentially on conduction or convection mechanisms. However, they suffer from drawbacks including lower energy efficiency, longer processing time, and thermal damage due to overheating, especially at the surface of materials. Some of these aspects are addressed through control and monitoring systems and intelligent design of equipment (Pereira and Vicente, 2010). With the increase in consumer demand for high-quality food products at lower prices and growing environmental concerns, efforts are being made to develop processing technologies that are energy efficient, cost effective, and environmentally friendly. Recently, electromagnetic technologies have gained increased industrial interest in food processing and have shown potential to replace, at least partially, the conventional thermal-preservation techniques. Dielectric heating, which utilizes electromagnetic radiations such as microwave (MW) and radiofrequency (RF), is gaining popularity in food processing. Amongst these two radiations, MW has shown a great potential (Chan, *et al*., 2000) to be used as an alternative to conventional heating. These novel processing technologies are regarded as volumetric forms of heating, wherein the heat is generated from inside, as compared to surface heating with conductive or convective modes of heating. The volumetric heating of materials leads to higher rates of heat and mass transfer, resulting in reduced processing times and uniform product quality.

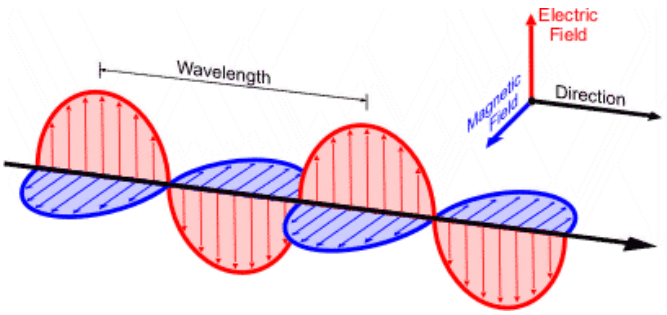

Figure 2.8. Propagation of electromagnetic wave (Jota, 2013)

Radiation may be defined as an energy streaming through space at the speed of light. Electromagnetic radiation consists of alternating electric and magnetic waves, which travel perpendicularly to one another. The electromagnetic waves can be characterized using two alternating vectors, namely, magnetic induction vector (*H*) and electric field vector (*E*) that define magnetic and electric fields, respectively. MWs are electromagnetic waves having a frequency band of 300 MHz to 300 GHz (Pereira and Vicente, 2010). These waves propagate with a time interval between peaks during oscillation, ranging from $3\ 10^{-8}$ to $3\ 10^{-11}$ s (Venkatesh and Raghavan, 2004). This range coincides with the temporal sequence of events at atomic and molecular transitions such as reactions in water, molecular dissociation and, most importantly, dielectric relaxation in water. The dielectric relaxation of water may vary from 100 MHz for bound water to 18 GHz for pure water (Miura, *et al.*, 2003) and this is the property that is studied extensively when the heating effects of MWs are investigated. The most effective conversion of MW energy into thermal energy in biological materials or in moist materials will occur in this frequency range. In the electromagnetic spectrum, MWs occupy the position between infrared and radiofrequency waves. The frequency "f" of electromagnetic wave is linked to the velocity of light "c" ($3\ 10^{8}$ m/s) and corresponding wavelength "λ" by the following equation (Knutson et al., 1987).

$$f = \frac{c}{\lambda} \tag{2.16}$$

According to the wave theory of electromagnetic radiation, waves having shorter wavelength travel with higher frequency, whereas ones with larger wavelength travel at a lower frequency. This results in propagation of all the electromagnetic waves at the same

speed, i.e. the speed of light. MW radiation is considered to be non-ionizing because they have insufficient energy (<10 eV) to ionize atoms (Piyasena, *et al.*, 2003). Since, MW is within the radar range, the frequency bands that can be used for applications other than communication are limited by Electromagnetic Compatibility (EMC) regulations. The MW frequency bands that are internationally accepted and known as Industrial and Scientific and Medical (ISM) bands used for heating are 915 MHz, 2450 MHz; 5800 MHz, and 24,125 MHz (Pereira and Vicente, 2010). While most domestic MW ovens have a frequency of 2450 MHz, many of the industrial units operate at a frequency of 915 MHz, as it has considerable advantages over 2450 MHz.

General principles of microwave heating

The heating effect of MW arises from the interaction of the electric field component of the wave with charged particles in the material. Two major effects are responsible for the development of heat in the material exposed to MW due to this interaction. If the charged particles are free to travel through the material, a current will travel in phase with the field, which is termed as ionic polarization or ionic conduction. If, on the other hand, the charged particles are bound within regions of the material, the electric field component will cause them to move until opposing forces balance the electric force. The result is a dipolar polarization in the material. The molecular movement is extremely fast due to the high frequency of the field, e.g., at MW frequency of 2450 MHz, the polarity changes 2.45 billion cycles/second. At this frequency, it creates an intense heat that can escalate as quickly as 10C per second (Lew, *et al.*, 2002). As water is a dipolar molecule and a prominent component of biological materials, its content directly influences heating. The dielectric heating leads to volumetric heating of the product. Apart from dielectric heating, there are contributions from a host of other factors influencing the heating efficiency of MW (Schiffmann, 1986) such as specific heat, thermal conductivity, and food structure Specific heat is an important property in the thermal behavior of a food subjected to MWs. Hence, produce with low specific heat such as oil may heat very rapidly, and even faster than water of the same weight. The MW-heating rates are a function of the heating system (frequency and equipment design) and the load characteristics (size, shape, dielectric properties, etc.). Any change in these parameters significantly affects the MW-heating process (Peyre, *et al.*, 1997). In solids, the molecular dipoles are no longer free to rotate as they are in liquids, but are restricted to a number of equilibrium positions, separated by potential barriers.Theoretical

treatments of this behavior have been reported to be similar to those developed for liquids.

Dielectric properties

The dielectric properties, or complex relative permittivity, are composed of dielectric constant (ε´) and dielectric loss factor (ε´´) (Mudgett, 1995).The dielectric constant reflects the ability of the material to store electric energy and the dielectric loss factor influences the conversion of electromagnetic energy into thermal energy. The dielectric properties of a material are described by the complex relative permittivity (ε^*) relative to that of free space) in the following relationship (Tang, 2005).

$$\varepsilon'' = \varepsilon' - j\varepsilon'' \tag{2.17}$$

Where $j = \sqrt{-1}$ .The ratio of the above two properties (ε0 /εv) represents another important parameter, the tangent loss angle (tan δ) which, along with thedielectric constant, determines the attenuation of MW power in foods. Mechanisms that contribute to the dielectric loss in biological materials include polar, electronic, atomic and MaxwellWagner responses of those materials in electromagnetic fields (Metaxas and Meredith, 1983). In foods, the dominant loss mechanism at MW frequencies of practical importance to industrial dielectric heating of foods are ionic conduction and dipole rotation, which are given by the following equation (Ryynänen, 1995):

$$\varepsilon'' = \varepsilon''_d + \varepsilon''_\sigma = \varepsilon_d + \frac{\sigma}{\varepsilon_0 \omega} \tag{2.18}$$

Where subscripts *d* and *σ* stand for contributions of dipole rotation and ionic conduction, respectively, *σ* (S/m) is the ionic conductivity, *ω* (rad/s) is the angular frequency, and ε_0 is the permittivity of free space or vacuum ($8.854\ 10^{-12}$ F/m).

Factors Influencing Dielectric Properties of Foods

The dielectric properties of foods are influenced by many factors such as MW frequency, material temperature, moisture content, and food compositions, in particular salt and fat contents. A few of these parameters are discussed.

Frequency Effects

The contribution of various mechanisms of the dielectric loss factor of materials as a function of frequency is shown in Figure 2.9 (Tang et al., 2002). At lower frequencies (<200 MHz) the ionic conductivity of material plays a major role, whereas both ionic conductivity and the dipole rotation of free water are important at higher MW frequencies.

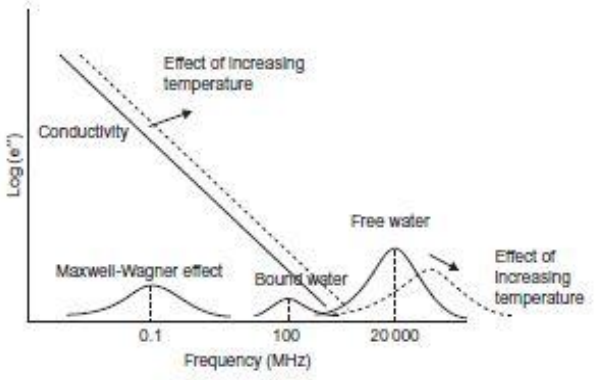

Figure 2.9. Variation of dielectric loss factor with MW frecuency (Tang et al., 2002).

The charge build-up in the interface between components in heterogenous systems is responsible for the Maxwell-Wagner polarization effect, which peaks at 0.1 MHz. For pure liquids with polar molecules, such as alcohol or water, polar dispersion dominates the frequency characteristics of dielectric properties. The polar dispersion characteristics of pure water at three different temperatures (0ºC, 25ºC, and 50ºC) are shown in Figure 2.10.

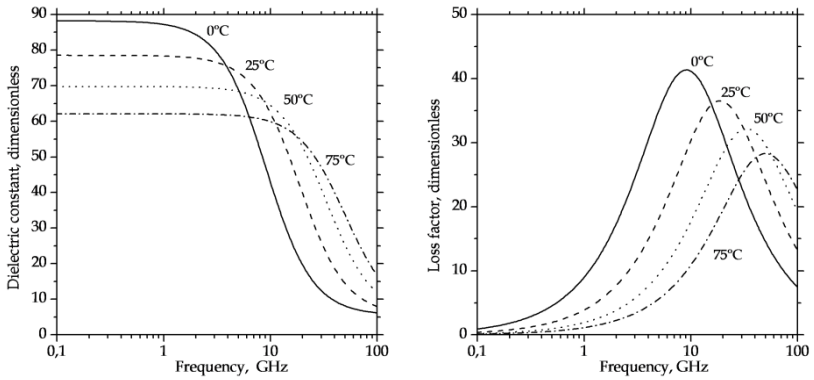

Figure 2.10. Variation of dielectric properties with frecuency at differente temperatures (Mudgett, 1985).

Dielectric constant will be relatively higher at lower frequencies (<10^3 MHz) for water having lower temperature. Aqueous solutions having charged ions behave differently from pure water with respect to dielectric characteristics, especially at low frequencies (e.g., <20,000 MHz at room temperature) and the deviation depends on the concentration of dissolved ions. The frequency and temperature dependent dielectric characteristics of pure water and aqueous solutions determine the dielectric characteristics of moist foods. For moist foods with dissolved salt, ionic conduction plays a major role in the lower end of the MW-frequency range. This was illustrated by (Guan, *et al.*, 2004) while studying the mashed potato system with different salt contents.

Temperature and Salt Effects

The effect of temperature on the dielectric properties of foods depends on many factors, including food composition, especially moisture and salt content, and MW frequency. In moist foods with lower salt content, dielectric characteristics are mainly dominated by water. The electric conductivity "σ" in ionic solutions increases with temperature because of reduced viscosity and increased mobility of the ions (Trump, 1954 and (Stogryn, 1971). The combined contribution of ionic conduction and dipole dispersion of water molecules to the dielectric characteristics of a 0.5 N sodium chloride solution as influenced by temperature is shown in Figure 2.11.

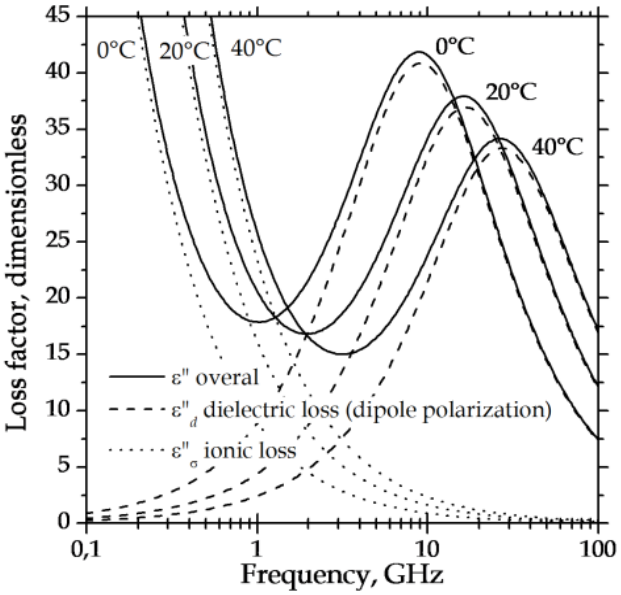

Figure 2.11. Effect of temperature on the dielectric loss factor of 0.5 N sodium chloride solution (Roebuck and Golblith, 1972)

Below a frequency band of 2000 MHz, increasing temperature raises the dielectric loss factor of the solution because of the predominant role of ionic conduction at lower frequencies. Between 2000 and 10,000 MHz, increasing temperature reduces the solution's dielectric loss factor as the peak of dielectric loss constant moves towards higher-frequency bands. This band of frequency corresponding to the transition moves to a higher-frequency range in case of solutions having increasing ionic concentrations (Tang, 2005).The temperature and frequency-dependent dielectric characteristics of water are clearly reflected in moist foods. For moist foods with salt, loss factors generally increase with increasing temperatures at lower MW frequencies, which often results in a phenomenon commonly referred to as "thermal runway" (Metaxas and Meredith, 1983). That is, a preferentially heated part of the food in an electromagnetic field accelerates its heating, often causing non-uniform heating.

Moisture Effects

Water in moist foods can be divided in to three general categories: (1) free water in intracellular spaces; (2) multilayer water with mobility between free and bound water; and (3) monolayer water tightly bound to the polar sites of solid food components. Free-water molecules in intercellular spaces have dielectric properties similar to those of liquid water, whereas bound water exhibits ice-like dielectric properties. Dielectric properties of food, in general, decrease rapidly with decreasing moisture content to a critical moisture level. Below this moisture level, e.g., about 12% for diced apples at 22ºC, the reduction in loss factor is significantly less due to the bound water. High temperature can, however, increase the mobility of bound water, reducing this critical moisture level.

Water molecules in ice are immobilized in well-defined matrices and behave similarly to bound water. Because the dielectric constant and loss factor of frozen moist foods are relatively low, their values depend, to a larger extent, on the amount of water in the unfrozen state and the ionic conductivity of the free water. All frozen foods have a very low loss factor, but after thawing the loss factor increases sharply, close to that of free water. Because of the reduced loss factor with decreasing moisture content, dehydrated foods have less ability to convert electromagnetic energy in to thermal energy. Conversely, during a MW drying process, the wet part of the product is able to

convert more MW energy into thermal energy compared to the dry part, which tends to level off the uneven moisture distribution commonly experienced in a hot air drying process where the food particle interior is wetter than the surface. This would also significantly shorten drying time (Feng, 2002).

Interactions of microwave with food components

The major food components such as water, carbohydrates, lipids, proteins and salts (minerals) interact differently with MW. Since, the primary mechanisms of MW heating is dipole rotation, water selectively absorbs the energy in intermediate and high-moisture food products (Mudgett, 1989). Low-moisture products generally heat more evenly due to their low heat capacity (Schiffmann, 1986). Alcohols and the hydroxyl groups on sugars and carbohydrates are capable of forming hydrogen bonds and undergo dipolar rotation in an electrical field. Low levels of alcohol and sugar in solution have little effect on the interaction of MW with water and dissolved ions. However, at higher concentrations (jellies and candies), sugars can alter the response of water with MW (Mudgett, 1989). Proteins have ionizable surface regions that may bind water or salts, giving rise to various effects associated with free surface charge. Lipids, other than the charged carboxyl groups of the fatty acids that are usually unavailable due to their participation in the ester linkages of triglycerides or hydrophobic in nature, interact little with MW, if water is present.

Estimation of Heat Generation

The rate of heat generation per unit volume in a food material during MW heating (Q) is characterized by the following equation (Pereira and Vincente, 2009) and is mainly attributed to dipolar rotation phenomenon:

$$Q = 2\pi f \varepsilon_0 \varepsilon'' \Delta V^2 \tag{2.19}$$

Where ΔV is the strength of the electric field, "f" is the MW frequency, ε_0 is the permittivity of free space and ε´´ is the dielectric loss factor. The heating rate due to collision of ions with the surroundings in an electric field, which is termed as ionic conduction, is expressed as below (Li and Ramaswamy, 2008).

$$\frac{P_\mu}{V_\mu} = E^2 qn\mu \tag{2.20}$$

Where E is electric field, P_μ is power, V_μ is volume of the material, q is the electric charge of the ions, μ is the level of mobility of the ions and n is the number of charges.

The Depth of Penetration of Microwaves

The penetration depth of MWs can be defined as the depth where the dissipated power is reduced to 1/e (Euler's number e ~2.718) of the power entering the surface. The penetration depth d_p in meters of MW energy in food can be estimated using dielectric properties by the following equation:

$$d_p = \frac{c}{2\pi f \sqrt{2\varepsilon' \left[\sqrt{1+(\varepsilon''/\varepsilon')^2}-1\right]}} \tag{2.21}$$

Where, c is the speed of light in free space ($3\ 10^8$ m/s).

The penetration depth of MW into a material is inversely proportional to the frequency. In addition, electromagnetic waves do not penetrate deeply into moist foods (Metaxas and Meredith, 1983), where both the dielectric constants and loss factors are high.

Dielectric properties of selected foods

The dielectric properties of a few liquid foods are presented in Table 2.1(Tang et al., 2002). The data demonstrate the effect of two MW frequencies (915 MHz and 2450 MHz) on dielectric constants and loss factors of different foods. As can be seen in Table 2.1, distilled and deionized water has a much smaller dielectric loss factor at 915 MHz than at 2450 MHz, because 2450 MHz is closer to the frequency (~16,000 MHz) corresponding to the relaxation time of water molecules at room temperature. However, with the addition of 0.5% NaCl, the ionic conduction sharply raised the dielectric loss factor of water, much more at 915 MHz than at 2450 MHz. Ice, having a very small loss factor, is almost transparent to MWs.

Table 2.1. Dielectric properties and penetration depth of a few selected foods.

Foods	Temperature (°C)	915 MHz			2450 MHz		
		ε´	ε´´	d_p(mm)	ε´	ε´´	d_p(mm)
Water Distilled/deionized	20	79.5	3.8	122.4	78.2	10.3	16.8
0.5% salt solution	23	77.2	20.8	22.2	75.8	15.6	10.9
Ice	-12	-	-	-	3.2	0.003	11615
Corn oil	25	2.6	0.18	467	2.5	0.14	220
High-protein products Yoghurt (premixed)	22	71	21	21.2	68	18	9.0
Whey protein gel	22	51	17	22.2	40	13.	9.6

Adapted from Tang et al., 2002

Oils are esters of long-chain fatty acids which have much less mobility compared to water molecules in response to oscillating electromagnetic fields. The dielectric constant and loss factor of oil are therefore very small compared to free water, as shown by the data for corn oil in Table 2.1.

2.8 Fluidization

The difficulties in prediction stem in part from the complexity and ambiguity in defining the fundamental parameters such as size, shape and density of the particles. These parameters play an important role in the calculation and prediction of dynamic behavior in fluidized beds. Most physical properties of the particles are estimated indirectly, such as estimating particle shape by the bed voidage. All factors are explicitly and implicitly significant in the estimation of the behavior of fluidization operations. Although new technology is helping us to understand and give more precise prediction in fluidization, more research is still needed. Either a gas or a liquid can fluidize a bed of particles. In this thesis, the focus is purely on gas-solid fluidization. This chapter is a short literature survey of fluidization, which will cover mainly the topics that are relevant to this work. More information about fluidization processes can be found in the references.

Fluidization basics

Fluidization is a process in which solids are caused to behave like a fluid by blowing gas or liquid upwards through the solid-filled reactor. Fluidization is widely used in commercial operations; the applications can be roughly divided into two categories, i.e.:

- Physical operations, such as transportation, heating, absorption, mixing of fine powder, etc. and
- Chemical operations, such as reactions of gases on solid catalysts and reactions of solids with gases etc.

The fluidized bed is one of the best known contacting methods used in the processing industry, for instance in oil refinery plants. Among its chief advantages are that the particles are well mixed leading to low temperature gradients, they are suitable for both small and large scale operations and they allow continuous processing. There are many well established operations that utilize this technology, including cracking and reforming of hydrocarbons, coal carbonization and gasification, ore roasting, Fisher-Tropsch synthesis, coking, aluminum production, melamine production, and coating preparations. The application of fluidization is also well recognized in nuclear engineering as a unit operation for example, in uranium extraction, nuclear fuel fabrication, reprocessing of fuel and waste disposal.

Fluidization regimes

When the solid particles are fluidized, the fluidized bed behaves differently as velocity, gas and solid properties are varied. It has become evident that there are number of regimes of fluidization, as shown in Figure 2.12. When the flow of a gas passed through a bed of particles is increased continually, a few vibrate, but still within the same height as the bed at rest. This is called a fixed bed. With increasing gas velocity, a point is reached where the drag force imparted by the upward moving gas equals the weight of the particles, and the voidage of the bed increases slightly: this is the onset of fluidization and is called minimum fluidization or homogeneous with a corresponding minimum fluidization velocity, u_{mf}. Increasing the gas flow further, the formation of fluidization bubbles sets in. At this point, a bubbling fluidized bed occurs as shown in Figure 2.12.

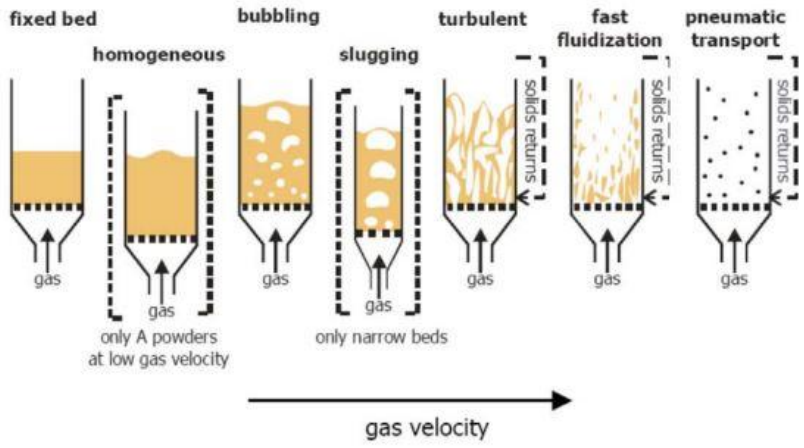

Figure 2.12. Schematic representation of fluidized beds in different regimes (based on (Kunii and Levenspiel, 1991)

As the velocity is increased further still, the bubbles in a bubbling fluidized bed will coalesce and grow as they rise. If the ratio of the height to the diameter of the bed is high enough, the size of bubbles may become almost the same as diameter of the bed. This is called slugging. If the particles are fluidized at a high enough gas flow rate, the velocity exceeds the terminal velocity of the particles. The upper surface of the bed disappears and, instead of bubbles, one observes a turbulent motion of solid clusters and voids of gas of various sizes and shapes. Beds under these conditions are called turbulent beds as shown in Figure 2.12. With further increases of gas velocity, eventually the fluidized bed becomes an entrained bed in which we have disperse, dilute or lean phase fluidized bed, which amounts to pneumatic transport of solids.

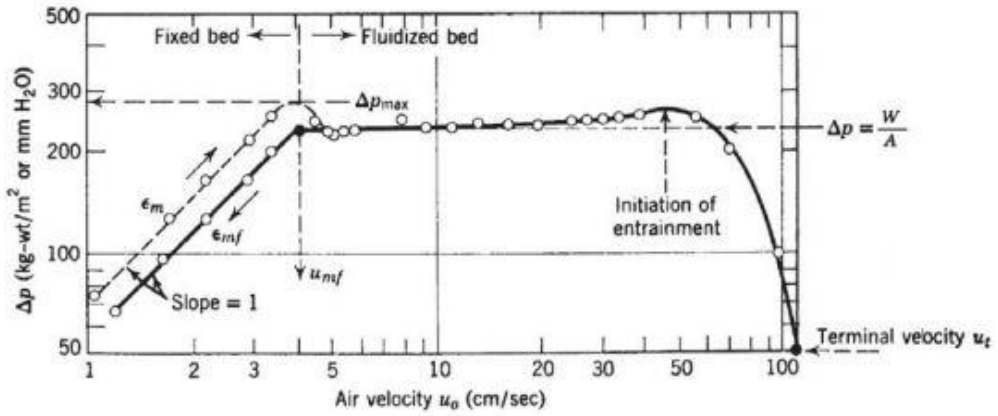

Figure 2.13. Pressure drop vs. gas velocity (Kunii and Levenspiel, 1991)

Another important issue concerning the fluidization process is pressure drop through a fixed bed. Figure 2.13 presents changes in pressure drop with changing gas velocity. At first one can observe increasing pressure drop, up to some level where it becomes constant, despite increasing gas velocity. This change in pressure drop trend can be connected with the creation of dense phase of fluidized bed and that is the moment when the fluidization occurs. The velocity at which the pressure is stabilized is called minimum fluidization velocity. Pressure drop is stable in a certain range of velocities, and then a slight increase can be observed which precede a drastic decrease in pressure drop. This is due to the entrainment of smaller particles which are suspended in the section over the dense fluidized bed. Further increase in gas velocity will cause more fractions to be carried over which leads to disappearance of dense phase and start of pneumatic transport. Although, as it will be shown later in some cases gas velocities exceeding the terminal velocity can be applied for the so called fast fluidization.

Geldart´s classic classification of powders

The behavior of solid particles in fluidized beds depends mostly on their size and density. A careful observation by Geldart (1973, 1978) is shown in Figure 2.14 in which the characteristics of the four different powder types were categorized as follows:

- Group A is designated as ‘aeratable’ particles. These materials have small mean particle size (d_p < 30 μm) and/or low particle density (<~1.4 g/cm^3). Fluid cracking catalysts typically are in this category. These solids fluidize easily, with smooth fluidization at low gas velocities without the formation of bubbles. At higher gas velocity, a point is eventually reached when bubbles start to form and the minimum bubbling velocity, u_{mb} is always greater than u_{mf}.

- Group B is called ‘sandlike’ particles and some call it bubbly particles. Most particles of this group have size 150 μm to 500 μm and density from 1.4 to 4 g/cm^3. For these particles, once the minimum fluidization velocity is exceeded, the excess gas appears in the form of bubbles. Bubbles in a bed of group B particles can grow to a large size. Typically used group B materials are glass beads (ballotini) and coarse sand.

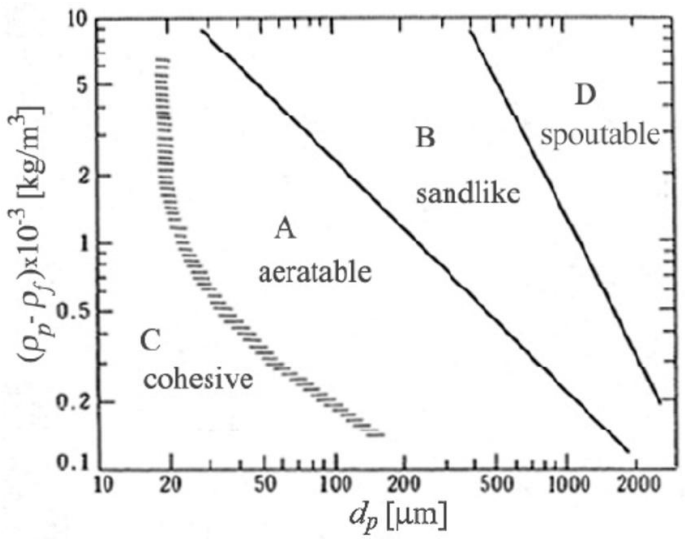

Figure 2.14. Diagram of the Geldart classification of particles. (Geldart, 1973)

- Group C materials are 'cohesive', or very fine powders. Their sizes are usually less than 30 μm, and they are extremely difficult to fluidize because interparticle forces are relatively large, compared to those resulting from the action of gas. In small diameter beds, group C particles easily give rise to channeling. Examples of group C materials are talc, flour and starch.

- Group D is called 'spoutable' and the materials are either very large or very dense. They are difficult to fluidize in deep beds. Unlike group B particles, as velocity increases, a jet can be formed in the bed and material may then be blown out with the jet in a spouting motion. If the gas distribution is uneven, spouting behavior and severe channeling can be expected. Roasting coffee beans, lead shot and some roasting metal ores are examples of group D materials.

Geldart's classification is clear and easy to use as displayed in Figure 2.14 for fluidization at ambient conditions and for u less than about $10 \cdot u_{mf}$. For any solid of a known density ρs and mean particle size d_p this graph shows the type of fluidization to be expected. It also helps predicting other properties such as bubble size, bubble velocity, the existence of slugs etc.

Minimum fluidization velocity

The superficial gas velocity, at which the bed of powder is just fluidized, is normally called the minimum fluidization velocity or designated by $u_{mf.}$ This state of incipient fluidization can be described by an equation giving the pressure drop in a gas flowing through a packed bed, such as the so-called Ergun equation:

$$\frac{\Delta P}{L} = 150\frac{(1-\varepsilon_{mf})^2}{\varepsilon_{mf}{}^3}\frac{\mu u_{mf}}{D_P{}^2} + 1.75\frac{(1-\varepsilon_{mf})}{\varepsilon_{mf}{}^3}\frac{\rho u_{mf}{}^2}{D_p} \tag{2.22}$$

In which ΔP is equal to the bed weight per unit cross-sectional area, and the particle sphericity, φ_s, is defined as the surface area of a volume equivalent sphere divided by the particle's surface area.

When applying the Ergun equation, one has to know the minimum fluidization porosity, ε_{mf}, although it is frequently an unknown. (Wen and Yu, 1966) developed an expression for the minimum fluidization velocity for a range of particle types and sizes by assuming the following approximations to hold based on experimental data:

$$\frac{1-\varepsilon_{mf}}{\phi^2\varepsilon_{mf}{}^3} \cong 11 \; and \; \frac{1}{\phi\varepsilon_{mf}{}^3} \cong 14 \tag{2.23}$$

They combined these with the Ergun equation and obtained the relation:

$$\frac{D_{sph}u_{mf}\rho_g}{\mu} = \sqrt{33.7^2 + 0.0408\frac{D_{sph}{}^3\rho_g(\rho-\rho_g)g}{\mu^2}} - 33.7 \tag{2.24}$$

Leva, (1959) obtained empirically another widely used expression:

$$u_{mf} = \frac{D_{sph}^2(\rho-\rho_{air})g}{1650\mu} \tag{2.25}$$

This equation is valid for $Re_{mf} \leq 20$ whereas for higher values of a correction factor must be applied.

2.9 Characterization parameters of drying products

Water Activity

In drying of some materials, which require careful hygienic attention, e.g., food, the availability of water for growth of microorganisms, germination of spores, and participation in several types of chemical reaction becomes an important issue. This availability, which depends on relative pressure, or water activity, a_w, is defined as the ratio of the partial pressure, P_s, of water over the wet solid system to the equilibrium vapor pressure, P_{ws}, of water at the same temperature. Thus, a_w, which is also equal to the equilibrium relative humidity of the surrounding humid air, is defined as:

$$a_w = \frac{P_{w,s}}{P_s} = \frac{RH_{eq}}{100} \tag{2.26}$$

Different shapes of the *X* versus *aw* curves are observed, depending on the type of material (e.g., high, medium or low hygroscopicity solids) and which will be discussed in the next section on sorption isotherms.

Water activity (a_w) is one of the most critical factors in determining quality and safety of the goods which are consumed every day. Water activity affects the shelf life, safety, texture, flavor, and smell of foods. It is also important to the stability of pharmaceuticals and cosmetics. While temperature, pH and several other factors can influence if and how fast organisms will grow in a product, water activity may be the most important factor in controlling spoilage. It predicts stability with respect to physical properties, rates of deteriorative reactions, and microbial growth. Foods containing proteins and carbohydrates, for example, are prone to non-enzymatic browning reactions, called Maillard reactions. The likelihood of Maillard reactions browning a product increases as the water activity increases, reaching a maximum at water activities in the range of 0.6 to 0.7 (Okos, *et al.*, 1992). In some cases, though, further increases in water activity will hinder Maillard reactions. So, for some samples, measuring and controlling water activity is a good way to control Maillard browning problems.

Table 2.2. Minimum water activity, a_w, for microbial growth and spore germination (adapted from Brockmann, 1973).

Microorganisms	Water activity
Organisms producing slime on meat	0.98
Pseudomonas, Bacillus cereus spores	0.97
B. subtilis, C. botulinum spores	0.95
C. botulinum, Salmonella	0.93
Most bacteria	0.91
Most yeast	0.88
Aspergillus niger	0.85
Most molds	0.80
Halophilic bacteria	0.75
Xerophilic fungi	0.65
Osmophilic yeast	0.62

Table 2.2 lists the measured minimum a_w values for microbial growth or spore germination. If *aw* is reduced below these values by dehydration or by adding water-binding agents like sugars, glycerol, or salt, microbial growth is inhibited. Such additives should not affect the flavor, taste, or other quality criteria, however. Since the amounts of soluble additives needed to depress a_w even by 0.1 is quite large, dehydration becomes particularly attractive for high moisture foods as a way to reduce a_w. Figure 2.15 shows schematically the water activity versus moisture content curve for and the most frequent deterioration reaction that appear at each water activity value. (Ledward, 1987) provide an extensive compilation of results on water activity and its applications shows the general nature of the deterioration reaction rates as a function of a_w for food systems. Aside from microbial damage, which typically occurs for $a_w > 0.70$, oxidation, non-enzymatic browning (Maillard reactions) and enzymatic reactions can occur even at very low aw levels during drying. Laboratory or pilot testing is essential to ascertain that no damage occurs in the selected drying process since this cannot, in general, be predicted.

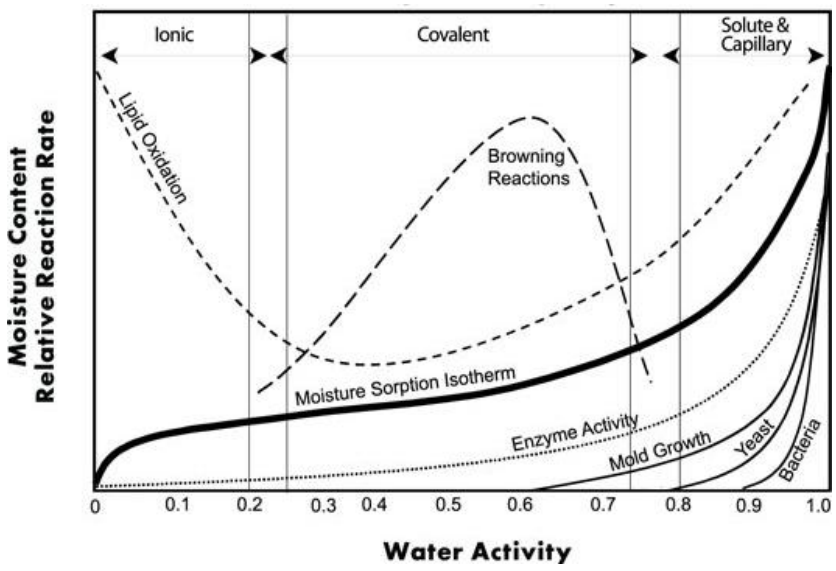

Figure 2.15. Deterioration rates as a function of water activity for food systems.

Water activity is temperature dependent. Temperature changes water activity due to changes in water binding, dissociation of water, solubility of solutes in water, or the state of the matrix. Although solubility of solutes can be a controlling factor, control is usually from the state of the matrix. Since, the state of the matrix (glassy vs. rubbery state) is dependent on temperature, one should not be surprised that temperature af-fects the water activity of the food. The effect of temperature on the water activity of a food is product specific. Some products shows an increase in water activity with increas-ing temperature, others decrease *aw* with increasing temperature, while most high mois-ture foods have negligible change with temperature. One can therefore not predict even the direction of the change of water activity with temperature, since it depends on how temperature affects the factors that control water activity in the food.

Equilibrium Moisture Content and Sorption Isotherms

The moisture content of a wet solid in equilibrium with air of given humidity and temperature is termed the equilibrium moisture content (EMC). A plot of EMC at a given temperature versus the relative humidity is termed sorption isotherm. An isotherm obtained by exposing the solid to air of increasing humidity gives the adsorption isotherm. That obtained by exposing the solid to air of decreasing humidity is known as the de-sorption isotherm. Clearly, the latter is of interest in drying as the moisture content

of the solids progressively decreases. Most drying materials display “hysteresis” in that the two isotherms are not identical.

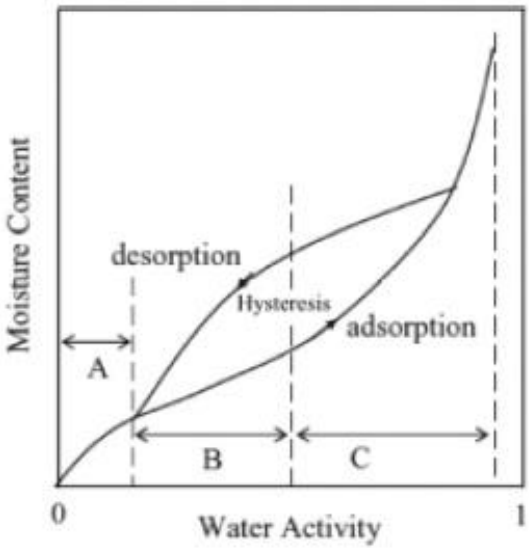

Figure 2.16. Typical sorption isotherm.(Mujumdar, 2007)

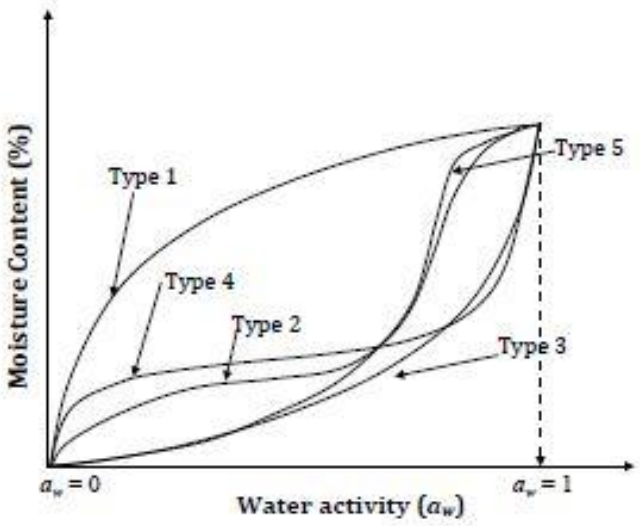

Figure 2.17. Different types of sorption isotherms (Mujumdar, 2007).

Figure 2.16 shows the general shape of the typical sorption isotherms. They are characterized by three distinct zones, A, B and C, which are indicative of different water binding mechanisms at individual sites on the solid matrix. In region A, water is tightly bound to the sites and is unavailable for reaction. In this region, there is essentially monolayer adsorption of water vapor and no distinction exists between the adsorption and

desorption isotherms. In region B, the water is more loosely bound. The vapor pressure depression below the equilibrium vapor pressure of water at the same temperature is due to its confinement in smaller capillaries. Water in region C is even more loosely held in larger capillaries. It is available for reactions and as a solvent.

Figure 2.17 shows schematically possible shapes of different sorption isotherms. Type 1 is the well known Langmuir isotherm obtained by assuming monomolecular adsorption of gas by the porous solids in a finite volume of voids. Type 2 is sigmoid isotherm generally found for soluble products. Type 3 is known as Flory-Higgins isotherm, accounts for a solvent or plasticizer such as glycerol above the glass transition temperature. The type 4 represents adsorption for swellable solids until maximum of hydration site are reached. Type 5 is the BET multilayer adsorption isotherm observed for adsorption of water on charcoal. Two isotherms commonly found in food products are types 2 and 4 (Basu, *et al.*, 2006).

The Karl Fischer method for the determination of water

The Water Determination Test (Karl Fischer Method)(Connors, 1988) is designed to determine water content in substances, utilizing the quantitative reaction of water with iodine and sulfur dioxide in the presence of a lower alcohol such as methanol and an organic base such as pyridine, as shown in the following formulae:

$$H_2O+I_2+SO_2 + 3\ C_5H_5N \rightarrow 2(C_5H_5N+H)I- + C_5H_5N\cdot SO_3$$

$$C_5H_5N\cdot SO_3 + CH_3OH \rightarrow (C5H5N+H)OSO_2\cdot OCH_3.$$

There are two determination methods different in iodine-providing principle: the volumetric titration method and the coulometric titration method. In the volumetric titration method, iodine required for reaction with water is previously dissolved in water determination TS, and water content is determined by measuring the amount of iodine consumed as a result of reaction with water in a sample. In the coulometric titration method, first, iodine is produced by electrolysis of the reagent containing iodide ion, and then, the water content in a sample is determined by measuring the quantity of electricity which is required for the electrolysis (i.e., for the production of iodine), based on the quantitative reaction of the generated iodine with water. Hereinafter in the Monographs, such a specification“not more than 4.0% (0.5 g, back titration)”indicates that when

determined by weighing about 0.5 g of the sample accurately and performing back titration, the water content is not more than 4.0% of the weight of the sample.

Method 1. Volumetric titration Apparatus Generally, the apparatus consists of an automatic burette, a back titration flask, a stirrer, and equipment for amperometric titration at constant voltage or potentiometric titration at constant current. Because water determination TS is extremely hygroscopic, the titration apparatus should be protected from atmospheric moisture. Silica gel or calcium chloride for water determination is usually used for moisture protection. Procedure As a rule, the titration of the sample with water determination TS should be performed at the same temperature as that at the standardization of the TS, while protecting from moisture. The apparatus is equipped with a variable resistor in the circuit, and the resistor is adjusted to apply a definite voltage (mV) between a pair of platinum electrodes immersed in the solution to be titrated. The change in current (μA) is measured during the dropping of water determination TS (Amperometric titration at constant voltage). As titration continues , the abrupt change in current in the circuit occurrs, but returns to the original state within several seconds. At the end of a titration, the change in current persists for a certain time (usually, longer than 30 seconds). The end point of titration is determined at this electric state. Otherwise, by adjusting the resistor, a definite current is passed between the two platinum electrodes, and the change in potential (mV) is measured during dropping water determination TS (Potentiometric titration at constant current). With the progress of titration, the value indicated by the potentiometer in the circuit decreases suddenly from a polarization state of several hundreds (mV) to the nonpolarization state, but it returns to the original state within several seconds. At the end of titration, the non-polarization state persists for a certain time (usually, longer than 30 seconds). The end point of titration is determined when this electric state attains. In the case of back titration, when the amperometric titration method is used at constant voltage, the needle of microammeter is out of scale while an excessive quantity of water determination TS remains. It returns rapidly to the original position when the titration reaches the end point. Similarly, when the potentiometric titration method at constant current is used, the needle of the millivoltmeter is at the original position while an excessive quantity of water determination TS remains. A definite voltage is applied when the titration reaches the end point. Unless otherwise specified, the titration of water with water determination TS

is performed by either of the methods below. Usually, the end point of the titration can be observed more clearly in the back titration method than in the direct titration method.

Direct titration Unless otherwise specified, proceed as directed below. Take 25ml of methanol for water determination in a dried titration flask, and titrate with water determination TS to the end point. Unless otherwise specified, weigh accurately a quantity of the sample containing 10 to 50 mg of water, transfer it quickly into the titration flask, and dissolve by stirring. Titrate the solution with water determination TS to the end point under vigorous stirring. When the sample is insoluble in the solvent, powder the sample quickly, weigh a suitable amount of the sample accurately, and transfer it quickly into the titration vessel, stir the mixture for 30 minutes while protecting it from moisture. Perform a titration under vigorous stirring. When the sample interferes with the Karl Fisher reaction, water in the sample can be removed by heating and under a stream of nitrogen gas and introduced into the titration vessel by using a water-evaporation device.

$$Water(H_2O) = \frac{Volume(mL) of\ TS\ consumed \times f\ (mg/mL)}{Weight\ of\ sample(mg)} \times 100(\%) \qquad (2.27)$$

Back titration Unless otherwise specified, proceed as directed below. Take 20ml of methanol for water determination in the dried titration vessel, and titrate with water determination TS. Weigh accurately a suitable quantity of the sample containing 10－50 mg of water, transfer the sample quickly into the titration vessel, add an excessive and definite volume of water determination TS, stir for 30 min, protecting from atmospheric moisture, and then titrate the solution with Water －Methanol Standard Solution under vigorous stirring.

$$Water(H_2O) = \frac{(V(mL) of\ TS\ con. \times f) - (V\ of\ water - Methanol\ con.(mL) \times f)}{Weight\ of\ sample(mg)} \times 100(\%) \qquad (2.28)$$

Where f = the number of mg of water (H_2O) corresponding to 1 ml of water determination TS, f' = the number of mg of water (H_2O) in 1 ml of Water－Methanol Standard Solution.

Method 2. Coulometric titration Apparatus Usually, the apparatus is comprised of an electrolytic cell for iodine production, a stirrer, a titration flask, and a potentiometric titration system at constant current. The iodine production device is composed of an anode and a cathode, separated by a diaphragm. The anode is immersed in the anolyte solution for water determination and the cathode is immersed in the catholyte solution for water determination. Both electrodes are usually made of platinum-mesh. Because water determination TS is extremely hygroscopic, the titration apparatus should be protected from atmospheric moisture. For this purpose, silica gel or calcium chloride for water determination is usually used. Procedure Take a suitable volume of an anolyte for water determination in a titration vessel, immerse in this solution a pair of platinum electrodes for potentiometric titration at constant current. Then, immerse the iodide production system filled with a catholyte for water determination in the anolyte solution. Switch on the electrolytic system and make the content of the titration vessel anhydrous. Next, take an accurately weighed amount of the sample containing 1－5 mg of water, add it quickly to the vessel, and dissolve by stirring. Perform the titration to the end point under vigorous stirring. When the sample is insoluble in the anolyte, powder it quickly, and add an accurately weighed amount of the sample to the vessel. After stirring the mixture for 5－30 minutes, while protecting from atmospheric moisture, perform the titration with vigorous stirring. Determine the quantity of electricity (C) [electric current (A) × time (s)] required for the production of iodine during the titration, and calculate the content (%) of the water in the sample by the formula below. When the sample interferes with the Karl Fisher reaction, water in the sample can be removed by heating under a stream of nitrogen gas and introduced into the titration vessel by using a water-evaporation device.

Chapter 3

MATERIALS AND METHODS

3 MATERIALS AND METHODS

In accordance with the objectives of this study, in this chapter will be revised all the elements needed to carry it out. When developing a drying process as that proposed in this study, firstly the different materials employeed in the experiments will be shown. Then, we will see all the media both relating to the drying equipment as for the experiment monitoring, as well as the technical analytical employed in the assessment of the results obtained in the different experiments. The possibility of modelling the kinetic and thermal results obtained under the consideration of the mathematical model here proposed will be also explained. For this purpose, we will see the tool FlexPDE®, employed for kinetic and thermal modelling of the different experiments. Consequently, modelling of the results enables to obtain the characteristic parameters of the system and analyze the effect of the control variables in order to obtain the most recommendable operational strategy.

3.1 Materials used for encapsulation.

Capsules should be water-insoluble to maintain their structural integrity in the food matrix and in the gastrointestinal tract. The materials are used alone or in combination to form a monolayer. In this last case, coating the microcapsule with the double membrane can avoid their exposure to oxygen during storage and can enhance the resistance of the cells to acidic conditions and higher bile salt concentrations.

Alginate

Alginate is surely the biopolymer most used and investigated for encapsulation. Alginates are natural occurring marine polysaccharides extracted from seaweed, but also they occur as capsular polysaccharides in some bacteria (Skják-Bræk, *et al.*, 1986). Being a natural polymer, alginic acids constitute a family of linear binary copolymers of 1-4 glycosidically linked α-L-guluronic acid (G) and its C-5 epimer β-D-mannuronic acid. (M). Alginates are the salts (or esters) of these polysaccharides. They are composed of several building blocks (100-3,000 units) liked together in a stiff and partly flexible chain. The relative amounts of the two uronic units and the sequential arrangements of them along the polymer chain vary widely, depending of the origin of the alginate: three

types of blocks may be found: homopolymeric M-blocks (M-M), homopolymeric G-blocks (G-G) and heteropolymeric sequentially alternating MG-blocks (M-G). This composition and block structure are strongly related to the functional properties of alginate molecules within an encapsulation matrix. Immobilisation or entrapment of probiotic bacteria in alginate it is possible due to it is a rapid, non-toxic and versatile method for cells. Dissolving alginate in water gives a viscous solution of which the viscosity will increase with the length of the macromolecule (number of monomeric units), and its solubility is also affected by the pH (at pH < 3 precipitate as alginic acid), the presence of counterions in water (alginate precipitates by crosslinking, gelling, with divalent ions such as Ca^{2+}, Ba^{2+}, Sr^{2+}…) and the sequential arrangements of the monomers (the flexibility of the alginate chains in solution increases in the order MG<MM<GG). The gelling occurs when a cation as Ca^{2+} take part in the interchain binding between G-bloks giving rise to a three-dimensional network. The advantage of alginate is that easily form gel matrices around bacterial cells, it is safe to the body, they are cheap, mild process conditions (such as temperature) are needed for their performance, can be easily prepared and properly dissolve in the intestine and release entrapped cells. However, some disadvantages are attributed to alginate beads. For example, alginate microcapsules are susceptible to the acidic environment (Chandramouli, *et al.*, 2004) which is not compatible for the resistance of the beads in the stomach conditions. Other disadvantage of alginate microparticle is that the microbeads obtained are very porous to protect the cells from its environment (Gouin, 2004). Nevertheless, the defects can be compensated by blending of alginate with other polymer compounds, coating the capsules by another compound or structural modification of the alginate by using different additives (Chávarri, *et al.*, 2010, Krasaekoopt, *et al.*, 2003).

Tylose

Condensing agent of emulsion, thickener used in food industry. Salt sodium of the polycarboximethyl ester of the cellulose, methylhydroxyethylether cellulose. It is a white powder, whose viscosity it is around 270-350 mPas (2% in H_2O at 20°C). The viscosity decreases when the temperature increases. It is soluble into cold water and insoluble in organic solvents or hot water. Its aqueous solutions have pH neutral and a density at 20°C around 1.28-1.30 g/cm³. According to their viscosity has a different numbers: MH 300 corresponding to a low viscosity, MH 1000 to a medium and MH 10000 with high viscosity. In contact with water, offers a variety of properties, which include: regular

consistency (viscosity) on vinyl and pastas, reducing spattering; It regulates water retention capacity, so it improves the process of drying and film formation; reduces sedimentation loads and pigments, avoiding the separation of phases; strengthens the adhesive strength and bonding between loads, increasing its degree of adhesion (Llave, *et al.*, 2015).

Chitosan

Chitosan is a deacetylated derivative of chitin, which is widely found in crustacean shells, fungi, insects and molluscs. This polymer is a linear polysaccharide, which can be considered as a copolymer consisting of randomly distributed β-(1,4) linked D-glucosamine and N-acetyl-D-glucosamine. The functional properties of chitosan are determined by the molecular weight, but also by the degree of acetylation (DA), which represents the proportion of N-acetyl-D-glucosamine units with respect to the total number of units (Chatelet, *et al.*, 2001). Chitosan is soluble in acidic to neutral media, but solubility and viscosity of the solution is dependent on the length of chains and the DA. As chitosan is a positively charged polymer, it forms ionic hydrogels by addition of anions such as pentasodium tripolyphosphate (TPP) and also by interaction with negatively charged polymers as alginate (Chávarri, *et al.*, 2010)or xanthan (Dumitriu and Chornet, 1998). It is possible to obtain an hydrogel by precipitation in a basic medium or by chemical crosslinking with glutaraldehyde (Jameela and Jayakrishnan, 1995). Chitosan is biodegradable and biocompatible. Nevertheless, to be used in probiotic bacteria encapsulation it is necessary to consider the antibacterial activity of this polymer. Due the possibility of a negative impact in the viability of bacteria, and due that chitosan has a very good film-forming ability, chitosan is more used as external shell in capsules made with anionic polymers as alginate. This application of chitosan can improve the survival of the probiotic bacteria during storage and also in the gastrointestinal tract (Capela, *et al.*, 2006,Zhou, *et al.*, 1998), and therefore, it is a good way of delivery of viable bacterial cells to the colon (Chávarri, *et al.*, 2010).

Saccharamyces cerevisiae

Saccharomyces cerevisiae is a yeast, a fungus unicellular, of the group of the ascomycetous. This group includes more than 60,000 species, including truffles, the morels or penicillium, the fungus which produces penicillin, but also pathogenic fungi of plants and animals, the best-known of which is Candida. In the nature is located on

substrates rich in sugars or in the exudates and SAPs sweet of some plants. The term "yeast" ("levare" within the meaning of raise or lift) refers to the visual experience of the bread dough "rising" when adding yeast to the flour. Its alternative name of "ferment" comes from the latin fervere, which means to boil and comes from the movement of the wort during the production of wine or beer. The knowledge and perception of the yeast is absolutely conditioned by its properties of fermentation of the bread, the wine or the beer (Berezc, 1999). The food interests of *Saccharomyces cerevisiae* is due to the ability of this body of fluffing the bread and on the other hand by the final product obtained by the alcoholic fermentation (beer and wine). These processes occur due to metabolizing the sugars in the dough or the wort (primarily glucose, fructose, sucrose or maltose) to generate carbon dioxide and ethyl alcohol or ethanol. The first is a gas that causes the bread dough to rise (and the Champagne bubbles), while the second is the origin of alcoholic beverages. The fermentation provides energy to it yeast regardless of the presence or not of oxygen being a reaction endogenous of oxidation-reduction (redox), during which it half of the molecule of sugar makes of donor of electrons to the other half. *Saccharomyces cerevisiae* is a body cell. More or less rounded shape, cell presents a distinct, being therefore a eukaryotic organism core (in Greek, eu - true; carion-core), as they are also the plants or animals. The yeast cells multiply quickly by budding, an asymmetric form of asexual reproduction: originates from a cell a bump that is growing and just giving rise to another cell, smaller (at the beginning) that the initial and genetically different from the original cell. In optimal conditions, this type of reproduction lasts two hours and allows the total colonization of the musts in a matter of hours or days. This is very important in wine fermentations, where there is competition from other fungi, yeasts and bacteria which can damage the wine, so it must be well controlled conditions and duration of the process to prevent the proliferation of these. The rapid growth has been a key in choosing this yeast as a tool for research and biotechnological applications (Aronsson and Rönner, 2001).

Probiotic (Bifidobacterium animalis ssp lactis BB12®)

Bifidobacterium animalis ssp lactis BB12® is a probiotic strain that has received considerable attention from the scientific community. It has tolerance to higher and lower temperatures, so as to acidic pH than other bacteria. When administered for 12 months to infants and children together with *S. thermophilus* this was associated with lower incidences of acute diarrhea (Holscher, *et al.*, 2012). Studies in different countries and

with different experimental designs confirmed these results. It was also shown that its administration did not interfere the growth or the normal weight gain of the children. *Bifidobacterium animalis ssp lactis* was associated with decreases of the fecal excretion of rotavirus during episodes of diarrhea, a fact that represents an epidemiological benefit. *Bifidobacterium animalis ssp lactis* exerts positive effects on manifestations of atopy/eczema. The statements made by some groups that infants under 4 months of age who are not breastfed should not receive probiotics have weak support if it is considered that maternal milk contains a large number and variety of strains of bacteria which may be considered as probiotics (Gibson and Roberfroid, 1995). These may not only protect from acute diarrhea but also from upper respiratory infections. Although cases of septicemia due to probiotic have been reported these represent an infinitely small proportion of the total numbers of consumers. No outbreaks have been reported that would point to invasive properties in a strain. It is not advisable to administer any living bacteria to individuals in shock or with innate or severe defects of immunity. However, carriers of HIV or patients with AIDS benefit from probiotic agents. A study carried out in Chile showed that although without evident clinical benefits *L. rhamnosus* HN001, significantly improved mucosal defense in the digestive tract (Cruchet, *et al.*, 2015).

Antioxidant (Pomanox®)

Pomegranate extract (POMANOX) was prepared according to the European Patent EP1967079 with a technology that utilizes only aqueous solutions avoiding the use of organic solvents. For manufacturing POMANOX® P30 freshly harvested pomegranate fruits growing in the Spanish Mediterranean area are used. The steps of manufacturing are an extraction of water soluble compounds including punicalagins in aqueous solution, a separation of aqueous solution from pomegranate paste, a step of adsorption chromatography, a concentration by nanofiltration and finally pomegranate aqueous extract is brought to a solid form by Spray drying. The characteristics of the pomegranate extracts (POMANOX®) were provided by Probelte Biotecnología S.L., Murcia (Spain).

Table 3.1. Specifications of POMANOX® P30

Analytical data	Specifications	Methods
Punicalagins α and β	NLT 30% (w/w as db)	Internal method (HPLC)
Loss on Drying	NMT 8 %	Thermogravimetry
Total polyphenols	NLT 50 % (w/w as gallic acid equiv.)	Spectrophotometric (Folin-Ciocalteu´s)
Microbiology		
Total plate count (cfu/g)	NMT 1000	
Yeast and Mould (cfu/g)	NMT 100	
Enterobacterium (cfu/g)	NMT 100	
Salmonella (25 g)	Absence	According European Pharmacopoeia
S. aureus (1 g)	Absence	
Escherichia coli (1 g)	Absence	

NMT: not more than, NLT: not less than.

POMANOX® has been fully characterized to all components through HPLC-TOFMS and HPLC-ITMS. POMANOX-P30® contains between 50-60 % pomegranate polyphenols, expressed as GAE (gallic acid equivalent). In addition to punicalagin-*α* and punicalagin-*ß*, other polyphenolic components that have been identified and quantified include: ellagic acid, galloylglucose, punicalin, ellagic acid glucoside, ellagic acid rhamnoside among others ellagic and gallic acid derivatives and anthocyanins such as delphinidin 3,5-diglucoside, cyanidin 3,5-diglucoside, delphinidin 3-glucoside, cyanidin 3-glucoside and pelargonidin 3-glucoside.

Table 3.2. The molecular profile of POMANOX® P30

Molecular Profile Information (per 100 g)			
	Amount	**Unit**	**Information**
Total proteins	2.2	g/100g	Distillation and acid-base titration
Total fat content	0.3	g/100g	Organic extraction
Total carbohydrates*	82.9	g/100g	Carbohydrate was calculated by difference method' (by subtracting the sum of ash, fat and protein from the dry weight of the samples
Starch	11.4	g/100g	(MET-FQ-Almidon-Al)
Glucose	1.9	g/100g	HPLC
Fructose	4.3	g/100g	HPLC
Pectin	2.2	g/100g	Expressed as monogalacturonic acid,

Table 3.2. Continuation.

Lactose	< 0.1	g/100g	HPLC
Sacarose	< 0.1	g/100g	HPLC
Maltose	< 0.1	g/100g	HPLC
Polyols	< 0.5	g/100g	HPLC
Pomegranate polyphenols	44.2	g/100g	Pomegranate polyphenols was calculated by adding the sum of punicalagins+ellagic acid+other ellagitanins+anthocyanins
Punicalagins	31.6	g/100g	HPLC
Ellagic acid	1.5	g/100g	HPLC
Other ellagitanins	11.1	g/100g (w/w as punicalagin equiv.)	HPLC
Anthocyanins	< 0.1	g/100g	Spectrophotometric
Organic acids		g/100g	
Citric acid	18.8	g/100g	HPLC-UV
Dietary fibres	≤0.05	g/100g	enzymatic degradation and gravimetric determination
Water content	4.4	g/100g	Drying at 105 °C
Ash content	10.2	g/100g	Incineration at 550 °C

*(including pomegranate polyphenols and organic acids)

3.2 Encapsulation equipment

In bead production by the JetCutter technology from geniaLab®, the fluid is pressed with a high velocity out of a nozzle as a solid jet. Directly underneath the nozzle the jet is cut into cylindrical segments by a rotating cutting tool made of small wires fixed in a holder. Driven by the surface tension, the cut cylindrical segments form spherical beads while falling further down to an area where they finally can be gathered. Bead generation with JetCutting is based on the mechanical impact of the cutting wire on the liquid jet. This impact leads to the cut together with a cutting loss, which in a first approach can be regarded as a cylindrical segment with the height of the diameter of the cutting wire. This segment is pushed out of the jet and slung aside where it can be gathered and recycled. As only a mechanical cut and the subsequent bead shaping driven by the surface tension are responsible for bead generation, the viscosity of the fluid has no direct influence on

the bead formation itself. Thus, the JetCutter technology is capable of processing fluids with viscosities up to several thousand mPa·s (Prüße, *et al.*, 2000).

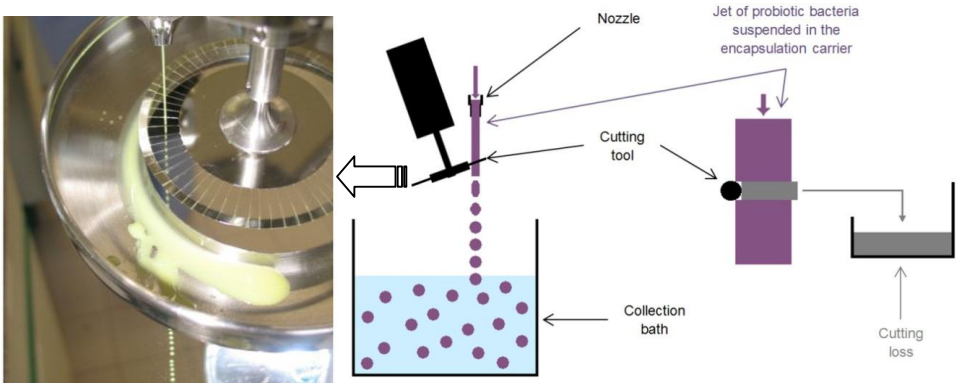

Figure 3.1. Schematic diagram of the JetCutter technology and representation of fluid losses due to the cutting wire impact (Chávarri, *et al.*, 2012).

The size of the beads can be adjusted within a range of between approx. 200 µm up to several millimeters. The main parameters are the nozzle diameter, the flow rate through the nozzle, the number of cutting wires and the rotation speed of the cutting tool. In order to get narrowly distributed beads one has to maintain a steady flow through the nozzle which may achieve with a pressure vessel or a pulsation-free pump and a uniform rotation speed of the cutting tool. The cutting tool itself also has to fulfill one major requirement. In order to produce beads of the same size, the wires have to have equal distances. This is best achieved by a circular stabilization of the wires on the outer perimeter as it is shown Figure 3.1.

This circular stabilization is essential even if the wire diameter is reduced in order to decrease the cutting losses (see also Figure 3.1). The diameter of the cutting wire may be decreased down to 30 µm. usually, stainless steel wires are used, but the application of polymer fibers is also practicable. Another requirement for the JetCutter is that a solid jet is formed. Therefore, special solid jet nozzles have to be applied. Even with these solid jet nozzles the liquid jet disintegrates after a certain length. This length depends on the viscosity and velocity of the fluid. In order to ensure a perfectly shaped jet at the point where it is cut by the wires, the cutting tool should not be too far away from the nozzle outlet, e.g. only a few millimeters.

3.3 Preparation of microcapsules

Preparation of the capsules alginate-tylose

The product used in the experiments was decided to be similar to the material that would be applied in later microencapsulation studies but without additives the material described above was used for the experiments developed along Chapter 4. The supporting material used for extrusion is sodium alginate, which is a linear heteropolysaccharide of d-mannuronic and l-guluronic acid extracted from various species of algae and a tylose suspension (1:1) of 15% (w/v) was prepared (Smidsrod, *et al*., 1972). After 24 hours period, this suspension became a jelly product that was extruded into a 5% (w/v) $CaCl_2$ solution, because divalent cations, such as Ca^{2+}, bind preferentially to the polymer of l-guluronic acid. The length of the polymer of d-mannuronic acid is, therefore, the main structural feature contributing to gel formation (Martinsen, *et al.*, 1989). One hour later, material was cut in small cylindrical pieces of 8 mm length and 5 mm diameter. This product, as fresh mass, presented before drying initial moisture of about 85% wet basis.

Preparation of yeast microcapsules

Microcapsules were prepared following a variant to that indicated in the bibliography (Chávarri, *et al.*, 2010, Krasaekoopt, *et al.*, 2003,Martín, *et al.*, 2015). In the Chapter 6 the following material was used. Dry yeast extract (*Saccharomyces cerevisiae*, ZYMAFLORE®) supplied by LAFFORT (France), containing an active cell concentration higher than 2 10^{10}/g, was used as cell culture material. A suspension of 3% alginate and 10% (w/v) of yeast extract was extruded and cut with a jet-cut device (Martín, *et al.*, 2015). Particles were dropped into a gelling solution 0.1 M $CaCl_2$, 0.2% acetic acid and 0.2% chitosan. The capsules were maintained in this solution, with stirring, during 30 minutes to obtain probiotic microcapsules with an external chitosan shell which gave them an enteric behaviour (Cook, *et al.*, 2012). Capsules were extracted from the solution by filtration and, once eliminated the superficial water, they were conveniently packaged and stored for 24 h in a freezer at 4 ºC until the start of the drying experiment. Even though diameter size for microcapsules usually is between 300 and 550 μm (Krasaekoopt *et al*., 2006), in this work, microencapsulation conditions were modified to obtain microspheres with a larger diameter to facilitate their handling during the first step of the drying process. After the gelling process, sphere microcapsules with

diameter ranged between 2000 and 2500 μm were obtained. The particles sizes and formation of microspheres were measured with a light microscope (Axioscop40, Carl Zeiss). The data analysis was performed using the software Ellix 5.0 (Microvision Instruments, France). The mean diameter of microspheres, based on 100 measurements, was 2250 μm. This value was taken as representative of the size dispersion obtained for the encapsulating conditions here used.

Preparation of probiotic BB12® microcapsules

The next step was to employ this novel technology of drying probiotic microorganisms, which is going to develop in detail in Chapter 7, to analyze the suitability of this technology to the subsequent viability of microorganisms at the end of the process. In this case a probiotic widely utilized in the dairy industry (*Bifidobacterium animalis subsp.lactis* BB12®, supplied by CHR. HANSEN (Spain) in format frozen, containing a concentration of cells active upper to 8.1 10^{10}(cfu/g). A suspension of alginate 2.5% and 83.3% of probiotic material (quantity required to obtain a concentration cell of the order of 10^9 cfu/ml, that is gripped and was cut with a jet cutter device (Chávarri, *et al.*, 2010). Microcapsules were collected in a gel-forming solution 0,1M $CaCl_2$ with 0.2% of acetic acid and 0.2% of chitosan, after adjustment of the viscosity, temperature, nozzle and cutting speed of the jet cutter to obtain the desired size of the microcapsules. After being around 30 minutes into the gelling bath the spherical microcapsules were obtained with a diameter around 2000-2500 μm. A diameter study was conducted using the optical microscope (Carl Zeiss Axioskop 40) and software Ellix 5.0 (Microvision Instruments, France). The average value of the diameter was 2250 μm as the representative size obtained at the operation parameters.

Preparation of Pomanox® microcapsules

The antioxidant material was obtained from pomegranate through the commercial company Probeltebio (Murcia, Spain) which provided the pomegranate extract commercialized as Pomanox® P30. The analysis of the drying characteristics of these microcapsules will be examinated during Chapter 8. A sodium alginate 3.1% w/w and antioxidant suspension Pomanox® P30 of 9.5% (w/w) was made. After mixing the suspension became a jelly product that was extruded and cut into a 2% (w/v) $CaCl_2$ solution, obtaining microcapsules of about 2.25 mm diameter as well as it have been

described probiotics microcapsules. The concentration of the formulation was chosen to be similar to the concentration of the extract from fresh pomegranate peel.

3.4 Microwave drying equipment.

In this work a novel process was proposed to dry particulate material and called near fluidizing microwave drying NFMD will be analyzed in detail along Chapters 4, 5 and 6. This new drying technology also will be compared with other drying technologies more extended for functional foods.

Microwave cavity and generator

The microwave drying equipment SAIREM LABOTRON 2000 used for the experiments is represented in the following Figure 3.2.

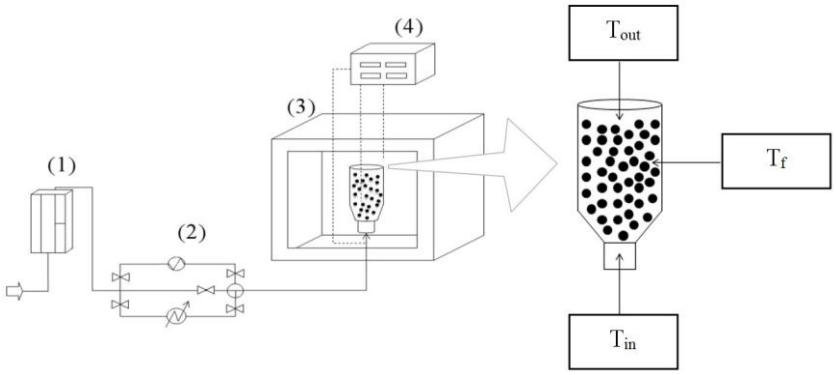

Figure 3.2. Equipment used in the experiments. (1) Dehumidifier, (2) Air cooling and heating device, (3) Microwave Chamber, (4) Temperature display. On the right side the bulk and the fibers to measure different temperatures along the drying process.

The microwave equipment was designed to hold inside a fluidizing flask containing the microcrocapsules that varied depending on the material to dry. Microwave power and air heating were changed to make possible the different variants of the NFMD process, later described in the following section. The microwave generator, which power can be adjusted up to 2000 W, works at a frequency of 2.45 GHz and the waves are driven to a multimode chamber.

Figure 3.3. Microwave chamber (3).

The main characteristics of microwave oven model SAIREM, LABOTRON 2000 are:

- Microwave power: 2 kW
- Variation of power: Continuous10-100%
- Type of applicator: multimode
- Impedance: Manual
- Maximum load weight: 4 kg

Description of the generator

- Model: MMP20T
- Frequency: 2.45 GHz
- Maximum nominal power: 2 kW
- Network consumption: 3.2 KVA

• Power supply:	400 V and 230 V single phase
• Cooling system:	Water, minimum flow rate 2 L/min.
	Temperature between 18 and 28°C, maximum dissipated in the water power: 850 W. Maximum pressure 3 bar.

Inside the chamber there is a polypropylene cylinder flask of 60 mm diameter where fluidizing microcapsules were dried as it can be showed in the Figure 4.2 on the right.

Monitoring and complementary devices

The control and monitoring of the process was followed by measuring the temperature of the microcapsules using an OPTOCON FOTEMP 4. Surface temperature of microcapsules was measured through fiber optic probes inserted in the centre of the bed.

Figure 3.4. Temperature display (4)

The air velocity was controlled and monitorized through an Airflow anemometer device, mod. PCE TA-410. The air temperature inside the cavity was also measured at the bottom and top of the bed to estimate the average temperature of surrounding air in contact with the particles.

Figure 3.5. Airflow anemometer.

The dry air flow for bed fluidization was introduced through the bottom of the bed column. A dehumidifier DONALSON ULTRAFILTER with a maximum capacity of 10 m^3/h was used to dry the air and its temperature controlled, using a heater-cooling device to regulate the air temperature before being introduced in the microwave cavity.

Figure 3.6. Dehumidifier (1).

The features of this unit are as follows:

- Flow rate maximum of air 10 m^3/h
- 7 bar operating pressure
- Drying humidity level lower to 0.5%
- 40 ℃ dew point

NFMD drying experiments planification

Microwave drying experiments under the procedure called NFMD were carried out by combining three different heat levels for inlet air temperature, (T_{in}^*) as for the surface of the product temperature (T_s^*). For the inlet air temperature the following temperatures were established: 0°C, room temperature (~ 20°C) and 40°C and the temperature of the surface of the product was set at: 5°C, 25°C and 45°C. They were designed with the two variables previously described, nine drying strategies combining the temperature of the

inlet air with two more variables such as: the surface temperature of the product and the thermal gradient between the air inlet temperature and the temperature of the product. Due to the difficulty of measuring the temperature of the interphase film in this work, is assumed a temperature on the surface of the target product, (T_s^*), assuming an adiabatic warming in which there is heat exchange with the surrounding air. This assumption was taken as a first approximation to the temperature of the surface of the material and was used to define the film temperature, (T_f^*) according to the Equation (3.1). Experimental (T_f) temperature was measured through optical fiber within the bed fibers and was controlled by adjusting the microwave power with a deviation of ±2, 5°C according to the established heat level. After which we calculated the actual temperature of the surface (T_s) achieved and calculated through the Equations (3.2) and (3.3) once known experimentally values for inlet (T_{in}) and outlet (T_{out}) air temperatures.

$$T_f^* = \frac{T_s^* + T_{in}^*}{2} \tag{3.1}$$

$$T_s = 2T_f - (T_{air}) \tag{3.2}$$

$$T_{air} = \frac{T_{in} + T_{out}}{2} \tag{3.3}$$

The applied gradient temperature was defined as the difference between the (T_s^*) and the temperature of the inlet air. This gradient can be modified by varying both, the target air temperature that must reach the product and the inlet air temperature. The experiments design can be seen in the following results chapters for each material. The thermal level designed werel obtained from combining the three heat levels for the (T_s^*) and for the (T_{in}^*) through Phases I and II, since in Phase III there is no microwave heating and inlet air temperature was the same for all experiments and used the ambient temperature , around about 20°C.

As we proceeded to finish the Phase I, Phase II proceeded in the same way unless at the start of the Phase III instead of lowering the speed of the inlet air was maintained until the end of the process so that the particles along the Phase III are in continuous fluidization. Microwave during Phase III power remained off since the microwave heating of the product with low moisture content causes a strong increase of temperature and as a result can burn the product (Pereira, *et al.*, 2007). The code used to refer each experiment refers to thermal levels: *High (*45°C), *Medium* (25°C) and *Low* (5°C). The

first letter corresponds to the target temperature of the surface of the product (T_s *) and the second refers to the temperatures of the air inlet (T_{in}*) used: 0°C, room temperature (~ 20°C) and 40°C. The letters on the left refer to temperatures that were established during phase I and the right correspond to Phase II. During the Phase III was used the room temperature for all experiments therefore not referred to within the code of the experiments.

The code used and the variables were the same in all the experiments designed for each type of microcapsules. Nevertheless, as the chapters advance experiments and thermal levels selection was done to find the more appropriate conditions for each material. For this reason, in each chapter a different fluidization velocity and thermal levels were applied because of the conditioning to the materials. The methodological characteristics of each material are described in the corresponding chapter of results.

Spray drying technology

The methodology used to dry probiotics cells of *Bifidobacterium animalis subsp. lactis* BB-12 from (CHR. Hansen BB-12). For the protection of the probiotics were used different protective materials that were added to the suspension of the probiotic to reduce thermal damage during the spray drying. The protective materials used were: maltodextrin 5% w/w, a polysaccharide that is used as a food additive, 5% inulin a prebiotic, to 5%, a natural disaccharide trehalose, lactose to 5% by weight disaccharide derived from galactose and glucose that is found in milk and 20% by weight of milk commonly used as a protective agent showing a favorable effect on the improvement of the survival of bacterial cells during the drying process.

For the experiments conducted by spray drying at laboratory scale equipment was used, the B-190 mini spray dryer Buchi, Flawil, Switzerland. Drying took place in parallel flow at a constant 100°C of the inlet air temperature and the outlet temperature was around 60-65°C.

Figure 3.7. The spray drying equipment employed.

The dissolution containing probiotic material was kept at room temperature and fed to the main chamber by a peristaltic pump with a flow of 4 mL min^{-1}, with a flow air of 37.4 m^3h^{-1}. The Resulting particulate material was collected from the base of the cyclone and was stored in sterile vials of sterile at 4°C until they were analyzed.

The spray drying experiments carried out with POMANOX®, a natural concentrate of pomegranate was used as antioxidant sample. POMANOX® is a powerful natural antioxidant with antimicrobial and antifungal properties. This concentrated natural is used to carry out different experiments for the determination of the loss of the antioxidant capacity during different drying technologies. The experiments conducted by this technology used a mini B-190 spray dryer Buchi, Flawil, Switzerland. Drying took place in parallel flow to three air inlet temperatures: 140°C, 160°C and 180°C and outlet temperature was around 90°C, 95°C and 105°C respectively. The suspension containing the antioxidant compounds was kept at room temperature and fed to the chamber by a peristaltic pump with a flow of power of 4 mL min^{-1}, with a flow of air of 37.4 $m^3 h^{-1}$.

The resulting particulate material was collected from the base of the cyclone and stored at 4°C.

Freeze drying technology

The equipment used for the freeze drying experiment was a LYOQUEST -55 from Telstar. Vacuum cavity consists of trays fitted with temperature sensors for the control of heating trays and to measure the temperature of the product.

Figure 3.8. Freeze drying equipment.

In the experiments of freeze drying microcapsules were placed in three trays evenly and were frozen under the effect of the low pressure, rapidly declining up to 600 mbar. During operation heating trays stood at 36°C while pressure decreased slightly to 200 mbar at the end of 16 hours process. This procedure was used both for the microcapsules of probiotic material such as those with antioxidants properties.

3.5 Characterization equipments

In this section a description of the equipments required for quality analysis was done to the analysis of each materials employed, both in the case of the probiotics material probiotics and in the case of the concentrated of pomegranate. The procedure of the study of the quality of each of the materials separately and the explanation of the type of analysis required in each case is described.

Mass loss analysis

Given that it is imperative to acquire a reading of the mass throughout the time of experiment has been installed a balance for this purpose. Since in the cavity cannot be used a metallic element, the balance was installed with a hook on the outside of the cavity. The hook holding the plate in which samples are placed to monitorize the mass loss of the sample. The scale used is from KERN.

Figure 3.9. Scale employed for the mass loss monitoring.

Determination of water content

A Karl-Fischer apparatus, Metrohm 860 KF, is used for the determination of water (Connors, 1988). It is based on the chemical reaction of iodine in the presence of water (Padivitage, *et al.*, 2014). This technique offers enough precision in the determination of

low water contents in dry materials, by its strong significance during storage. The analysis requires about 0.1g of sample and was repeated it in triplicate.

Figure 3.10. Equipment employed fot the water determination.

Determination of water activity

The equilibrium moisture of the samples along drying has been determined with a thermostatic chamber Novasina TH2 to follow the water activity, in this study was adopted limiting value of 0,25 assuming like in other references that microbial spoilage is avoided below it (Beuchat, 1981).

Figure 3.11. Equipment fot the water activity determination.

Analysis of Antioxidant Activity

Sample preparation

Fresh or dried pomegranate peel and microcapsules were ground in a ball mill. The ground material in amount of about 1 g were mixed with 10 mL of MeOH/water (80:20%, v/v) + 1% HCl. The mixture was sonicated at 20°C for 15 min and left for 24 h at 4°C. Then the extract was again sonicated for 15 min, and centrifuged at 15,000 g for 10 minutes.

ORAC method

The method used to evaluate the antioxidant activity of microencapsulated pomegranate extracts was Oxygen Radical Absorbance Capacity (ORAC), as described by Ou et al. (2001). Briefly, each sample was diluted with phosphate (K2HPO4 + Na2HPO4) buffer solution (75 mM, pH 7.4). Later, 0.375 ml of sample together with 2.25 mL of fluorescein (42 nM) was added in cuvettes; buffer solution was used as blank and Trolox solution (25 M trolox) as calibration solution. Fluorescence readings were taken at 5 s and then every minute thereafter. Finally, 375µL of freshly prepared AAPH reagent [2,2′- azobis(2-amidinopropane) dihydrochloride] (153 mM) was added in cuvettes every 10 s. The fluorescence spectrophotometer (Shimadzu, model RF-5301; Kyoto, Japan) was set up at an excitation wavelength of 493 nm and an emission wavelength of 515 nm and readings were recorded every 5 min for 40 min after the addition of AAPH. During the analysis all the cuvettes were incubated at 37 °C. The final ORAC values were calculated, in triplicate, using a regression equation between the

Trolox concentration and the net area under the fluorescence decay curve and final data were expressed as mmol of Trolox equivalents per 100g dry matter.

ABTS method

Additionally, the ABTS [2,2-azinobis-(3-ethylbenzothiazoline- 6-sulphonic acid)] radical cation described by Re et al. (1999). For the samples we prepared a good dilution to make the posterior analysis. Briefly, 30µL of the supernatant was mixed with 3ml of ABTS. After 6 min of reaction, the absorbance was measured at 734 nm for ABTS. The absorbance was measured in UV–Vis Uvikon XS spectrophotometer (Bio-Tek Instruments, Saint Quentin Yvelines, France). The analyses were run in three replications (n = 3) and results were expressed as mean ± standard deviation and units in mmol of Trolox equivalents per 100g dry matter.

Viability analysis of microencapsulated materials

Entrapped bacteria in uncoated alginate microspheres were released by homogenizing 0.1 g of filtered microsphere slurry in 10 mL of sodium citrate 0.1 M for 10 min and stirred. The homogenized samples were diluted to appropriate concentrations and pour plated in MRS agar. The plates were incubated for 2 days at 37 °C and the encapsulated bacteria enumerated as cfu/g ds.

3.6 Mathematical model for NFMD process.

In this study, the NFMD process will be applied to different particle geometries of encapsulated materials dried by microwave power in fluidizing conditions. In the Chapters 4, 5 and 6, the characteristically properties and the corresponding adaptations of the model according to the geometry and material properties will be described. In this Chapter the mathematical model of NFMD process is shown applied to the drying of cylindrical particles of encapsulating material whose details and results are described along Chapter 4, three main phases can be distinguished, in each of them different mechanism of mass transfer and heat transmission occur (Ingham, *et al.*, 2007). The model enables the consideration of microwave and convective heating mechanisms along the drying, although in the NFMD process microwaves are applied only during Phases I and II.

In accordance with the characteristics explained en Chapter 1, the NFMD process is a semi-batch one in which all the particles are considered perfectly mixed. Consequently, the mathematical model consists on the application of the energy and mass balance to every particle of the bed. The resolution of differential equations for mass and energy equations in the tridimensional material gives the evolution of moisture and temperature in any location

The main assumptions considered when solving the mass and energy balance expressions were:

1. The particles of material were considered to have regular cylindrical shape.
2. Heat and mass transport parameters like *D* or *h* were obtained fitting the modeled temperature and moisture profiles to the corresponding experimental data obtained in laboratory tests.
3. Volume shrinkage when assumed was considered depending on moisture content *X*.
4. Material is homogeneous in composition and properties.
5. Heat flow is considered to take place in both, axial and radial directions.
6. The evaporation process occurs completely on the external surface of the material. The largest fraction of total heat required to get the vaporization is absorbed from surrounding air, the other part from material surface.

Mass balance

Profiles of mass loss of encapsulated material in different phases of the process of drying are defined by the following equation:

$$\frac{\partial M}{\partial t} = D\left(\frac{\partial^2 M}{\partial x^2} + \frac{\partial^2 M}{\partial y^2} + \frac{\partial^2 M}{\partial z^2}\right) \tag{3.4}$$

Where, *D* refers to the effective diffusion coefficient that collects different diffusional mechanisms that act in the process. This variable is considered the same in the three spatial directions.

The Equation (3.4) corresponds to the employee balance without taking into account the contraction during the drying process. The balance used to take into consideration the contraction of particles requires the incorporation of the apparent particle density or mass of solid per volume of particle, ρ_{ap}, which includes the change in volume of the material throughout and must be included in the mass balance of particle as described in Equation (3.5).

$$\frac{\partial M\rho_{ap}}{\partial t} = D\rho_{ap}\left(\frac{\partial^2 M}{\partial x^2} + \frac{\partial^2 M}{\partial y^2} + \frac{\partial^2 M}{\partial z^2}\right) \quad (3.5)$$

Another of the equations that define the conditions of the system, below defined as boundary condition, is the moisture of the particle surface that varies along drying. Parameter. Thus, moisture $M_s(t)$ was assumed to vary between M_0 and M_e according a first order kinetic which is a characteristic coefficient β (Shivhare, *et al.*, 1994).

$$M_s = M_e + (M_0 - M_e)\exp(-\beta t) \quad (3.6)$$

According to a fitting procedure different values of the coefficient β were probed together with different diffusion coefficients D to model the experimental mass profile for a certain drying experiment,. Therefore the average value of the moisture content of the majority of the volume can be adapted to pilot the moisture content of the capsule during the time. This adaptation is possible due to the use of the FlexPDE® program. Shivhare, equation (3.5), equation relates the moisture content of the surface with the coefficient of drying of the surface. This coefficient really is the first-order kinetic constant for the variation of the humidity content at the surface, between the initial M_0 and final or equilibrium value M_e.

Initial and boundary conditions; To solve the mass balance through Equation (3.5) the following conditions were considered:

1. Initial conditions: The content of humidity of the material initial is assumes that is the same that which provide experimental data.
2. Boundary conditions: Moisture on the surface is given through the equation of Shivhare, Equation (3.5).

Calculation of the external transfer coefficient*:* Several parameters obtained in the mass and heat balance should be used for the calculation of the external transfer

coefficient. This coefficient relates the water flow, removed during drying with a gradient of pressures. The water flow or drying rate ($-dm_w/dt$) depends on the external mass transfer coefficient and the gradient of the vapor pressure vetween the surface ($P_{w,s}$) and the bed bulk ($P_{w,\infty}$).

$$\frac{dm_w}{dt}\frac{1}{V_L} = k_G a\left(P_{w,s} - P_{w,\infty}\right) \tag{3.7}$$

$$P_{w,s} = P_s a_w \tag{3.8}$$

$$P_{w,\infty} = \frac{\frac{\left(\frac{-dm_w}{dt}\right)}{PM_{H_2O}}}{\frac{Q_{air}P_{atm}}{RT_s} + \frac{\left(\frac{-dm_w}{dt}\right)}{PM_{H_2O}}} \tag{3.9}$$

During drying vapor pressure is assumed to be in equlilibrium at the surface temperature, Thus, through Equation (3.8) the vapor pressure on the surface is related to the water vapor pressure of saturation at the surface temperature T_s and the water activity. The a_w data are characteristic of each material and dependent on moisture.

Energy balance

The energy conservation for the encapsulating material in the different phases of drying process give the following set of equations (Mudgett, 1986):

Phase I/ II: During the first and second phase the power of microwave radiation is gradually modified to keep the product temperature at a constant value. In this case the energy balance of a material particle is given by Equation (3.10).

$$\rho \cdot C_p \cdot \frac{\partial T}{\partial t} = k\left(\frac{\partial^2 T}{\partial x^2} + \frac{\partial^2 T}{\partial y^2} + \frac{\partial^2 T}{\partial z^2}\right) + Q_{abs} \tag{3.10}$$

Where Q_{abs} is the heat generated and adsorbed by the material as a consequence of the microwave radiation and is described through Equation (3.11).

$$Q_{abs} = 2\pi f \varepsilon'' \varepsilon_0 \left[\left(e^{-(R-r)/d_p} + e^{-(R+r)/d_p} \right) E_{rad}^2 + \left(e^{-z/d_p} + e^{-(H-z)/d_p} \right) E_{ax}^2 \right] \quad (3.11)$$

Penetration depth (*dp*) is given through Equation (3.12)

$$d_p = \frac{c}{2\pi f \sqrt{2\varepsilon' \left[\sqrt{1 + (\varepsilon''/\varepsilon')^2} - 1 \right]}} \quad (3.12)$$

Phase III: As mentioned previously, in this Phase III the microwave source is switched off and the samples were subjected to an air flow of constant temperature, thus, heat transmission is produced by conduction from a point to another one inside of the material, and convection between the external surfaces of the material and surrounding air.

$$\rho \cdot C_p \cdot \frac{\partial T}{\partial t} = k \left(\frac{\partial^2 T}{\partial x^2} + \frac{\partial^2 T}{\partial y^2} + \frac{\partial^2 T}{\partial z^2} \right) \quad (3.13)$$

Initial and boundary conditions: to solve the energy balance through Equation (3.13) the following conditions were considered:

Initially the material is assumed to be at uniform temperature in thermal equilibrium with the environment.

$$t = 0 \quad T(x, y, z) = T_0 \quad 0 \le x \le D_c; 0 \le y \le D_c; 0 \le z \le H \quad (3.14)$$

Being, $D_c = 2R$

Boundary conditions are expressed relating the surface temperature of capsule with the external air temperature through the convective heat coefficient *h*. Due to the temperature difference between the surface of particles and the surrounding air in contact, a significant convective heat flow from outside in or viceversa arises during drying which is absorbed or emitted at the solid-gas interface. On the other hand, all of moisture vaporization takes place on the external surfaces of material. Thus, many authors agree that not all the heat required for vaporization is adsorbed on the surface of particle since an important part is absorbed directly from the microwave power that affect on the material surface. The representative term of required heat for evaporation happens, must be taken into account in the boundary conditions of the system

$$t > 0 \qquad k\left(\frac{\partial T}{\partial x}+\frac{\partial T}{\partial y}+\frac{\partial T}{\partial z}\right) = -h(T_s - T_{air}) + \frac{\partial M}{\partial t}\rho_{ap} Q_{vap}\frac{1}{S_p}w \qquad (3.15)$$

Where, $(x-2.5)^2+(y-2.5)^2 = R^2$, $0 \le z \le H$ for the lateral area of the cylinder: and for the upper bottom areas $0 \le x \le D_c, 0 \le y \le D, z = H$ ó $z = 0$

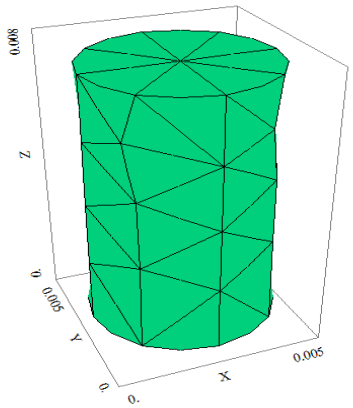

Figure 3.12. Tridimensional representation of an alginate-cellulose capsule.

In Figure 3.12, it can be observed the tridimensional representation of geometry and dimensions of a capsule, showing the dimensions of diameter D_c= 0.005 m and height H= 0.008 m material particle on the reference system used.

Physical, thermal and dielectric properties

In order to predict temperature distribution during microwave heating, it is necessary to know material properties such as bulk density, specific heat, thermal conductivity, latent heat, dielectric constant and loss factor.

Table 3.3.Physical, thermal and dielectric properties of main components of the encapsulating material described in Chapter 5. (Lide, 2005, Meda, *et al.*, 2005)

Properties	Value/Expression	Properties	Value/Expression
k_w	0.6 W/mºC	C_{paL}	4120 J/kgºC
P_w	1000 kg/m^3	ε'_{al}	6
C_{pw}	4180 J/kgºC	ε''_{al}	1.5
ε'_w	0.004T^2-0.5212T+75.241	K_{ty}	78 W/mºC
ε''_w	0.0001T^2+1.6001T+22.241	ρ_{ty}	961 kg/m^3
Q_{vap}	2257·10^3 J/kg	C_{pty}	2090 J/kgºC
k_{al}	50.22 W/m°C	ε'_{ty}	6
ρ_{aL}	1010 kg/m^3	ε''_{ty}	1.5
ρ_s (1	985.5kg/m^3	ρ_{ap} (2	148kg/m^3

(1,2 Depending on capsule composition (2 Value correspond to a capsule without shrinkage.

The properties corresponding to the whole material (ρ, C_p, k, ε) change along drying process, as they are dependent on temperature and moisture degree. Table 1 shows the thermophysical and dielectric properties of the main components of the microencapsulating material. From these, global properties of resultant material were been estimated according to Equations (3.16)-(3.19).

$$\rho = \rho_w V_W + \rho_S V_S \tag{3.16}$$

$$C_p = C_{p_w} V_W + C_{p_S} V_S \tag{3.17}$$

$$\varepsilon = \varepsilon_w V_W + \varepsilon_S V_S \tag{3.18}$$

$$k = k_w V_W + k_S V_S \tag{3.19}$$

Being V_w and V_s volumetric fraction of liquid and solid phases, respectively, calculated as:

$$V_w = \frac{\rho_s M_i}{\rho_w + \rho_s M_0} \tag{3.20}$$

$$V_s = \frac{\rho_w}{\rho_w + \rho_s M_0} \tag{3.21}$$

Se muestran también las densidades ρ_s y ρ_{ap} que corresponden respectivamente a la densidad de la partes sólida (985.5 kg/m^3, tilosa y alginato) y la densidad aparente, del sólido así constituido, referida al volumen de la cápsula

FlexPDE® software to solve the partial differential equations of the model

FlexPDE® is a powerful commercial software to obtain numerical solutions of partial differential equations in 2 or 3 dimensions. It is based on the resolution of finite element method and is capable of simulating problems both in how dynamic steady state. Among its main features can be highlighted:

- Can solve problems in 1, 2 or 3 dimensions.
- Builds the mesh, necessary to resolve the problem by using the method of finite elements, automatically.
- Refines the mesh automatically in the domain of the problem areas that required.
- Performs a dynamic control of time intervals.

- Solves nonlinear systems. In addition, you can get solutions in models formed by an unlimited number of equations also of unlimited complexity.

In this work after the material balance obtained experimentally has been used to make the energy and mass balance be able to see the interdependence of thermophysical properties with the operational variables of the process. As it can be see in the results section. The language used in the software program is described in the next table briefly and connected with the mathematical expressions defined before. In the Table 3.4 shows the FlexPDE® script corresponding to the solution of mass balance equations for the drying of encapsulating material in cylindrical geometry, included in the Annex A.

Table 3.4. FlexPDE® script to solve the mass balance equation of cylindrical capsules.

Num.	FlexPDE™ Language	Explanation
1	**TITLE** 'Mass balance for microwave dried capsules'	Title
2	**SELECT**	
3	plotintegrate	
4	**ERRLIM=0.02**	Limit error
5	**COORDINATES cartesian3**	3dimensions
	VARIABLES	
6	Hum	Total moisture content
	DEFINITIONS	
7	M=table("Esp1repexperimental esfera_M.txt")	Experimental values of moisture content dry basis
8	Zsphere = sqrt(max(0.001125^2-x^2-y^2,0))	Height of the particle
9	z1=-max(zsphere,0); z2	-
10	Humin=4.7619	Initial moisture
11	Humeq=0.0301	Equilibrium moisture
12	Beta=0.060	Shivhare coefficient
13	Hums=Humeq+((Humin-Humeq)*exp(-Beta*T)	Shivhare Equation
14	diffus1=3.2e-8	Diffusivity in Phase I
15	diffus2=4.8e-8	Diffusivity in Phase II
16	diffus3=1e-8	Diffusivity in Phase III
17	diffus= IF t<20 then diffus1 else if t >20 and then diffus2 else diffus3	Diffusivity change condition along time
18	Humav=INTEGRAL (Hum)/INTEGRAL (1)	3D Integral for the average moisture calculation
	EQUATIONS	
19	Hum: DIV (Diffus*GRAD(Hum))-dt(Hum)=0	Moisture changes with volume and time
	EXTRUSION	
20	z=z1, z2	Height
	INITIAL VALUES	
21	Hum=Humin	Initial moisture value

Table 3.4. Continuation

	BOUNDARIES	
22	surface 1	Moisture definition in each boundarie surface
23	value(Hum)=Hums	
24	surface 2	
25	value(Hum)=Hums	
	REGION 1	
26	z2=max(Zsphere,0)	
27	START(0.001125,0)	
28	value(Hum)=Hums	
29	arc(center=0,0)angle=360	
30	TIME 0 BY 5 TO 275	Time interval definition
	MONITORS	
31	for cycle=1	Grid representation
32	grid (y,z) on x=(0.000225)	
33	grid (x,y) on z=(0)	
	HISTORIES	
34	HISTORY (M, Humav,Hums) as ' name 1"#t#r#	Graphics required
35	HISTORY (Hum) at (0,0,0) as 'name 2' export format "#t#r#i"	
36	HISTORY (Hums) as 'name 3"#t#r#i"	
	END	

Detailed in Table 3.4 can be seen the main commands that are required in the FlexPDE® program.

- **TITLE:** This section is optional and is used to provide the title of the problem as showed in Table 3.4 line 1.
- **SELECT:** It serves to modify some of the criteria used by the programme in implementing resolution methods to solve the set of equations.
- **COORDINATES:** In this paragraph are defined the type of systems of coordinates to use: Cartesian of 1.2 or 3D, cylindrical, spherical. In this case Cartesian 3D.
- **VARIABLE:** This section defines the dependent variables involved in differential equations.

In the mass balance script is the moisture or Hum the variable defined in line 6. In the case of the heat balance the variable is the temperature or Temp as defined in the script that appears in the annex.

- **DEFINITIONS:** In this paragraph is defined all the constants and parameters that are needed in the differential equations, assigning them directly a value numeric or through an expression mathematical.

Here is needed to define all the data that are needed to solve the differential equations. In the script of the table 3.4 can be seen all the defined data. It can be seen how the moisture in the surface has been defined through the Shivhare´s equation in line 13 and also defined by the mathematical model in Equation (3.6). It also appeared the conditions of time for the diffusivity depending on the time interval.

- **EQUATIONS:** This section provides the needed equations to solve the problems. In this case in line 19 can be observed the mass balance equation also given in the modeled by the Equation (3.4).
- **INITIAL VALUES:** This section provides the initial conditions of the variables in the time-dependent problems. Defined in line 21 given the initial moisture content.
- **EXTRUSION:** This section only exists in 3D problems. In it is provides to the program those limits of the domain of the system in the axis Z.
- **BOUNDARIES:** The boundaries of the domain of the problem in the XY plane are provided in this section. It can e observed from line 22 to line 25 the boundaries definition through the value of Hums previously defined by Shivhare Equation in line 13.
- **MONITORS:** It is used to specify the graphics outputs that you want to observe the period during which the programme is solving the problem
- **PLOTS:** It is used to specify graphical outputs who wish to obtain the final solution of the system, or during the stage of resolution but at a given time.
- **HISTORIES:** This is optional and only valid for time-dependent problems. It specifies the variables whose evolution over time is to know and during that time interval. It also enables export to other programs in a table, the numeric value of the variable in question for different times.

The script with the heat balance is defined in the same way but it has been needed more lines in the definition section because of all the properties that must be calculated along time for each material proposed and to obtain all the properties at each instant as showed in Table 3.3 using the Equations from (3.16-3.21) of the mathematical model. Apart from that, it was also required the incorporation of the microwave heating parameters also in the definitions section defining by Equations (3.11) and (3.12).

Chapter 4

FLUIDIZED BED MICROWAVE DRYING PROCESS

4 FLUIDIZED BED MICROWAVE DRYING PROCESS

The dehydration of the encapsulated material containing nutritional ingredients was found necessary. The materials employed for the microencapsulation, have the purpose of confer a protection to the ingredients, avoiding their dispersion and interaction with the surrounding medium. In addition, it was required a correct stabilization during the storage and preparation for its addition to the food during processing. The application of a suitable drying process was required. This study proposes the development of a near fluidizing microwave drying, NFMD, to minimize the problems observed in other conventionals drying processes, as it was explained in Chapter 1.

This Chapter 4 will analyze the essential elements for the development of this innovative drying process, which will be applied in the following chapters for the preservation of specific nutritional ingredients (probiotics and antioxidants). Firstly, the definition of the materials used for the encapsulation was done according to the recommendations in this field. Then, the operational strategies employed in the microwave application, fluidization and corresponding modeling of the process were described for the analysis of the operational variables effect.

4.1 Material used for encapsulation

The material used for the experiments of the NFMD process was decided to be similar to the materials that are used for encapsulation. The encapsulation material was dried by NFMD without containing additives to stablishs the operational strategies. It was analyzed the specific effect of the dehydrated product before extend it to more complex systems. The procedure employed for the preparation of the capsules was detailed in the Chapter 3. The material used was a suspension with a ratio of 1:1 sodium alginate and tilosa 15%. This product has an initial moisture content of approximately an 85% in wet basis.

4.2 Definition of NFMD operational conditions

The drying process consists on the dehydration of particulated material in fluidized bed by microwave heating. The process requires the definition of thermal strategies through the three drying established phases under conditions of fluidization.

Microwave heating strategies

The NFMD experiments were carried out in the experimental equipment described in Chapter 3 of the methodology. The bed employed for the development of these experiments was a teflon conical container of 55 mm of diameter, in which was introduced 100 g of material to dehydrate. The drying experiments were performed combining three different thermal levels both for the inlet air temperature, (T_{in}^{*}) as for the product surface temperature (T_s^{*}). The inlet air temperature was established at 0°C, room temperature (~ 20°C) and 40°C values. The product surface temperature was set at 5°C, 25°C and 45°C. The combination of the previously described variables permit to design, nine thermal drying strategies. The surface temperature of the product and the thermal gradient stablished between the inlet air temperature and the surface temperatures were analyzed. The temperatures employed for the monitorization of the process NFMD was detailed in the Chapter 3 through the Equations (3.1-3.3).

Thermal levels designed for the experiments can be observed in the Table 4.1 obtained from the combination of three thermal levels for (T_s^{*}) and for (T_{in}^{*}) along Phases I and II, since in Phase III there is no microwave microwave heating and the inlet air temperature was maintained at the same value for all the experiments, using the room temperature (RT) (20°C-24ºC).

As we proceeded to finish the Phase I, Phase II proceeded in the same way unless at the start of the Phase III instead of lowering the speed of the inlet air was maintained until the end of the process so that the particles along the Phase III are in continuous fluidization. Microwave during Phase III power remained off since the microwave heating of the product with low moisture content causes a strong increase of temperature and as a result can burn the product (Pereira, *et al.*, 2007).

Table 4.1. Thermal levels designed for the experiments of Tylose-alginate capsules.

Exp.	Code	Phase I			Phase II			Phase III
		T_{in}^*	T_f^*	T_S^*	T_{in}^*	T_f^*	T_S^*	T_{in}^*
1	Ll/Hl	0	2.5	5	0	22.5	45	RT
2	Ml/Ml	0	12.5	25	0	12.5	25	RT
3	Hl/Ll	0	22.5	45	0	2.5	5	RT
4	Ll/Ml	0	2.5	5	0	12.5	25	RT
5	Mm/Hh	20	22.5	25	40	42.5	45	RT
6	Ml/Hm	0	12.5	25	20	32.5	45	RT
7	Hh/Hh	40	42.5	45	40	42.5	45	RT
8	Hm/Hm	20	32.5	45	20	32.5	45	RT
9	Hl/Hl	0	22.5	45	0	22.5	45	RT

The code used to refer each experiment refers to thermal levels: *High (*45°C), *Medium* (25°C) and *Low* (5°C). The first letter corresponds to the target temperature of the surface of the product (T_s^*) and the second refers to the temperatures of the air inlet (T_{in}^*) used: 0°C, room temperature (~ 20°C) and 40°C. The letters on the left refer to temperatures that were established during Phase I and the right correspond to Phase II. During the Phase III was used the room temperature for all experiments therefore not referred to within the code of the experiments.

Fluid dynamics of the drying phases

The heating strategies made for the experiments correspond to three defined phases under fluid dynamics behavior of the particles in a fixed-fluidized bed along the drying process. The flow that crosses a porous bed of particles at reduced velocity produces a head load. This is connected with the fluid velocity however; the solid particles remain innmobiles in a fixed bed.

The flow that crosses a porous bed of particles at reduced velocity produces a head loss that is related with the speed of the fluid, but the solid particles remain in fixed bed.

At a certain point, the upthrust force is equal to the weight of the particles; due to the weight loss implied in a drying process, a velocity increase is not required since the same weight decreases due to the movement and mix between them.

The fluid flow velocity in which such conditions occur is called minimum fluidization velocity and the bed of particles with mobility is named as fluidized bed. In

the Figure 4.1 can be shown a scheme of the formation of a fluidized bed starting from a fixed bed of particles. The pressure drop through the bed varies consequently until reaches the ΔP that produces fluidization (McCabe, *et al.*, 2007):

$$\Delta P = L(1-\varepsilon)(\rho - \rho_{air})g \tag{4.1}$$

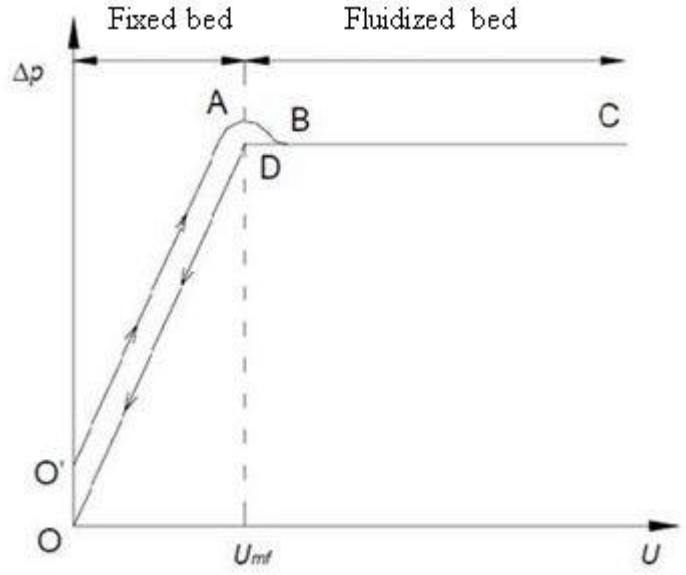

Figure 4.1. Variation of fluidized bed pressure drop with gas velocity.

Reaching the minimum of fluidization velocity, (u_{mf}), the loss of load acquires its maximum value which is maintained until the drag of the particles. Then, the head loss will decrease sharply after the drag of particles. Experimentally, a previous estimation of the minimum fluidization velocity was carried out based on density, size and other properties of the material properties. This value should be similar to the real value that is defined as:

$$\frac{1.75}{\varepsilon_{mf}^3} Re^2_{mf} + \frac{150(1-\varepsilon_{mf})}{\varepsilon_{mf}^3}\ Re_{mf} = \frac{D_{sph}^3 \rho_{air}(\rho - \rho_{air})g}{\mu^2} \tag{4.2}$$

Where,

$$Re_{mf} = \frac{D_{sph} u_{mf} \rho_g}{\mu} \tag{4.3}$$

The Equations (4.2) and (4.3) were obtained from (Levenspiel, 2014). The theoretical minimum fluidization velocity was determined for the initial two phases of

the drying process. The end of each phase was set experimentally observing the bed fluidization at the theoretical velocity.

As shown in Figure 4.2 in the initial moments there is a slight difference between the theoretical minimum fluidization velocity and the experimentally observed velocity, due to the adherents characteristics and the high moisture content of the material used. The experimental velocity requires a slight increase of the minimum fluidization velocity in the initial moments. Throughout the drying process the adherent features decrease with the loss of moisture. There is a progressive approximation from the experimental to the theoretical minimum fluidizing velocity that coincides at a value of moisture around 0.6 (g H_2O/g total). The point in which theoretical fluidization velocity and experimental converges has been employed as criterion to establish the end of the Phase I.

The end of Phase II corresponds to a strong modification in the progression of the water activity profile, as shown in Figure 4.3. After Phase II, Phase III is carried out in the absence of the microwave power to reduce the deterioration of the material and assist the homogenization of drying material; this phase is carried out in continuous fluidization. The following moisture content $X = 0.6$ and $X = 0.4$ were found as reference values for the transitions of Phase I-II and II-III in this type of material (turbulent flow, $Re_{mf} > 20$).

The fragility of the capsules as their thermosensible characteristics contribute to the use of a fixed bed in the initial phases of the process for a suitable control and monitoring of the product temperature. Alternatively, Phase III was performed in a fluidized bed due to the significant reduction of the moisture content and for the homogenization of the drying material. This procedure combined with the microwave heating that requires lower operating times, is thought that will improve the drying of the probiotic material proposed minimizing the reduction of viability.

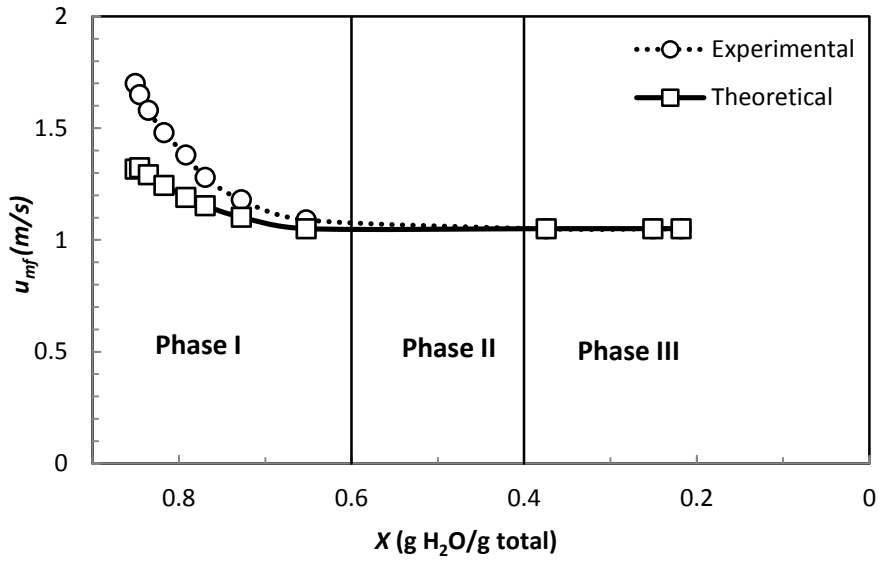

Figure 4.2. Experimental and theoretical minimum fluidization velocity.

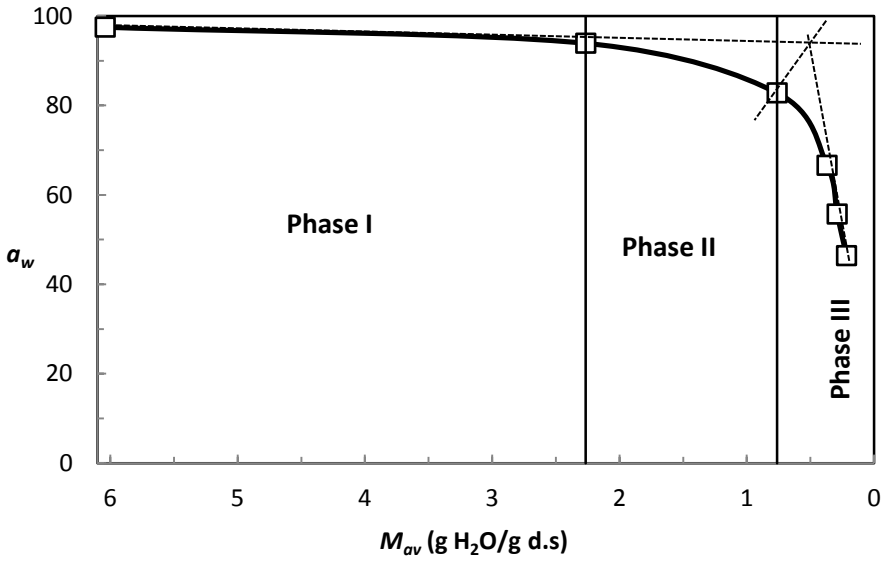

Figure 4.3. Water activity *vs.* moisture content evolution for Experiment 4 (Ll/Ml).

4.3 Analysis of drying kinetics

The evolution of the mass loss was monitored along the three phases established. At the end of each of the phase and every half an hour during phase III, the mass of the material was weighted for the kinetics monitoring of the average moisture content dry basis (M_{av}). Samples were also taken for water activity and moisture content determination at different thermal levels and processing times. The water activity profiles were analyzed as characteristics quality parameters. Figure 4.4 shows the evolution of the moisture content for Experiment 3.

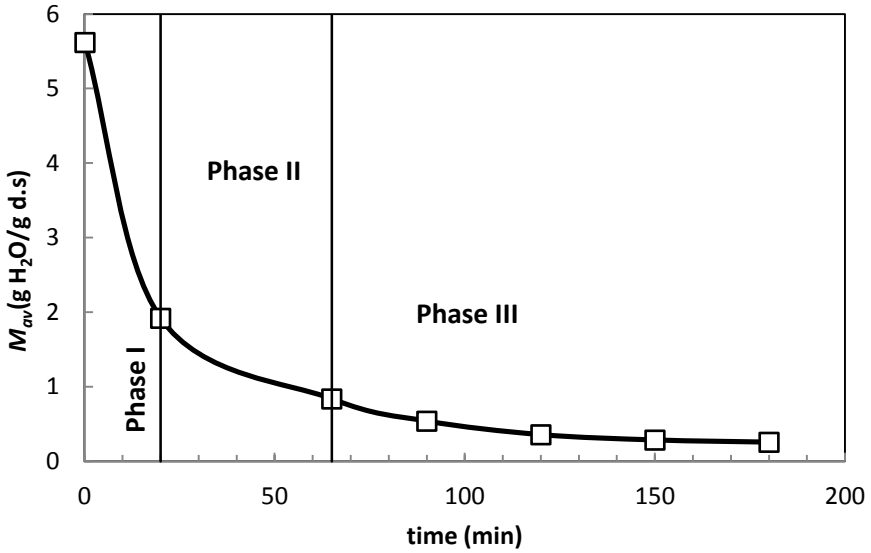

Figure 4.4. Moisture evolution dry basis along Experiment 3 (Hl/Ll).

The drying profile shown is similar to other drying processes. The drying rate increases slowly until the target temperature is achieved as shown in Figure 4.5. At this point the maximum drying rate is obtained. After the inflection point, Phase II appears with a progressive descent of the drying rate due to the diffusional resistance of the moisture content removal. Finally, the phase III is characterized by a near constant drying rate.

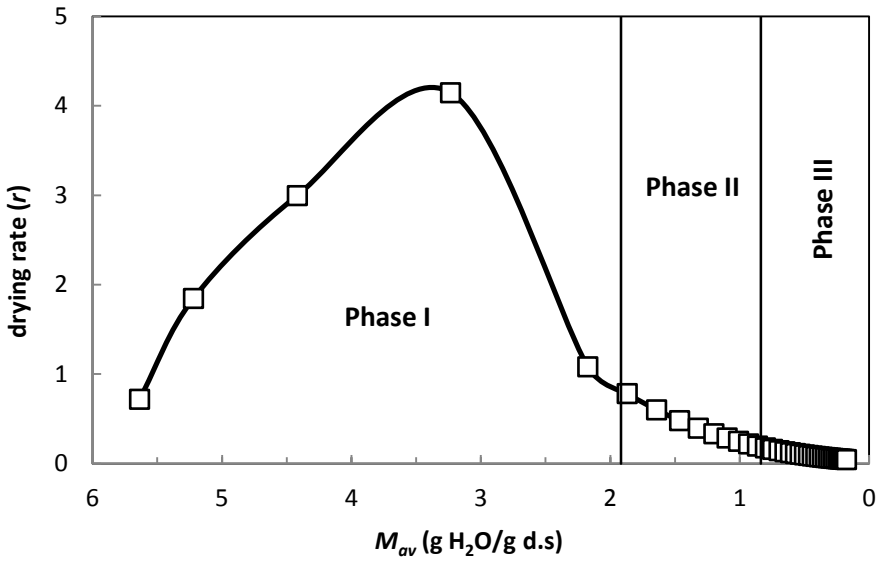

Figure 4.5. Drying rate evolution *vs*. moisture content for Experiment 3 (Hl/Ll).

Quality of the drying process

The characteristics and moisture profiles of water activity a_w along the three phases was selected as a fundamental criteria of quality, in accordance with the observations and recommendations of previous studies (Vesterlund, et al., 2012) and experience.

The moisture content was determined by the Karl-Fischer method analyzing the samples through the drying process for all the experiments. The results were obtained in wet basis, and then were transformed to dry basis once determined the dry solid. Table 4.2 shows the values of water activity and moisture for all experiments.

The dry solid content of the sample, m_{solid}, was obtained with the final dehydrated sample. Once known the water content percentage in wet basis with the Karl-Fischer titration and through the Equation (4.4) using the end mass, $m_{fin,}$ of the drying process. Therefore, average moisture content in dry basis, $M_{av,t}$, of the product for a t moment of the process is obtained using the Equation (4.5).

$$m_{solid} = m_{fin} - \left(m_{fin} KF / 100\right) \tag{4.4}$$

$$M_{av,t} = \frac{m_t - m_{solid}}{m_{solid}} \quad (4.5)$$

Table 4.2. Duration of the nine different NFMD strategies and the moisture (*M* and *X*) to achieve a_w=0.5.

Exp.	Code	t (min) a_w=0.5	*X* (g H_2O/g total)	*M* (H_2O /g d.s)
1	Ll/Hl	90	0.206	0.260
2	Ml/Ml	150	0.205	0.258
3	Hl/Ll	180	0.202	0.254
4	Ll/Ml	180	0.179	0.217
5	Mm/Hh	120	0.134	0.155
6	Ml/Hm	150	0.169	0.203
7	Hh/Hh	180	0.176	0.214
8	Hm/Hm	150	0.169	0.203
9	Hl/Hl	90	0.136	0.158

Initially, the moisture of the product is high, and drying occurs mostly at the level of the particle´s surface but, is renewed by diffused moisture from the inner layers. Consequently, the value of a_w which is a reflection of a surface moisture is keept above 0.85 during the Phases I and II. Only at the end of the Phase II a strong gradient of moisture appears. As a result, the water activity decreases as it can be observed in the Figure 4.6.

The water activity results, in contrast with the moisture average of the product M_{av}, give an idea of the moisture gradient originated inside the capsule. Therefore, the low water activity values obtained through the first drying phases can be justified as consequence of a pronounced moisture gradient. This gradient is not recommended under quality criteria of the dehydrated product.

The profile of a_w *vs. M* for the Hl/Ll strategy shown in the Figure 4.6, corresponds to a more convenient variation of the water activity with values around 0.8 at the begining of the Phase III (Vesterlund, *et al*., 2012). Thus, along the Phases I and II, a small gradient of moisture is produced at medium surface temperatures of the product. The high surface temperature of the product can be compensated as shown in the Figure 4.6, with a low inlet air temperature (T_{air} = 0°C). By the contrary, during phase III, the variation of moisture content is low but, the water activity values decrease significantly.

This suggests a significant moisture gradient that can be acceptable, only at the end of the process, but always keeping the water activity values above 0.3 (Beuchat, 1981).

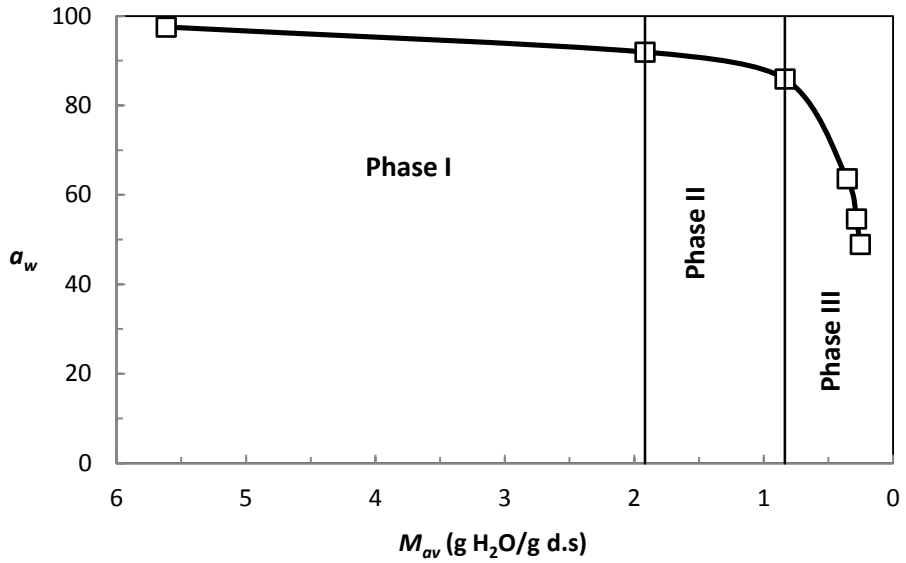

Figure 4.6. Water activity profile *vs*. moisture content for Experiment 3 (Hl/Ll).

Table 4.2 shows that experiments with high thermal levels reach earlier the desired activity. However, the moisture content is similar for all experiments or even higher. This could be explained due to the unexpected decrease of the moisture, and the very resistant layer formation that arises in the cases of high thermal levels during fundamentally the Phase II.

Analysis of phase I.

A comparison for experiments with same thermal level for the Phase II was analyzed to determine the effect of the Phase I thermal conditions. The profiles for the Experiment 2 and 7 are shown in the Figure 4.7 with a strategy (Ml) for the Phase II. Profiles present a small difference throughout Phase I, being the process faster with (Ml) than with (Ll) strategy as in Experiment 4. The different thermal history along Phase I for Experiments 2 and 4 have a strong effect in the following phases despite being carried out in the same conditions. The thermal level applied during Phase I transcends to the

Phase II so in this the kinetic behavior is different despite the use of the same drying strategy.

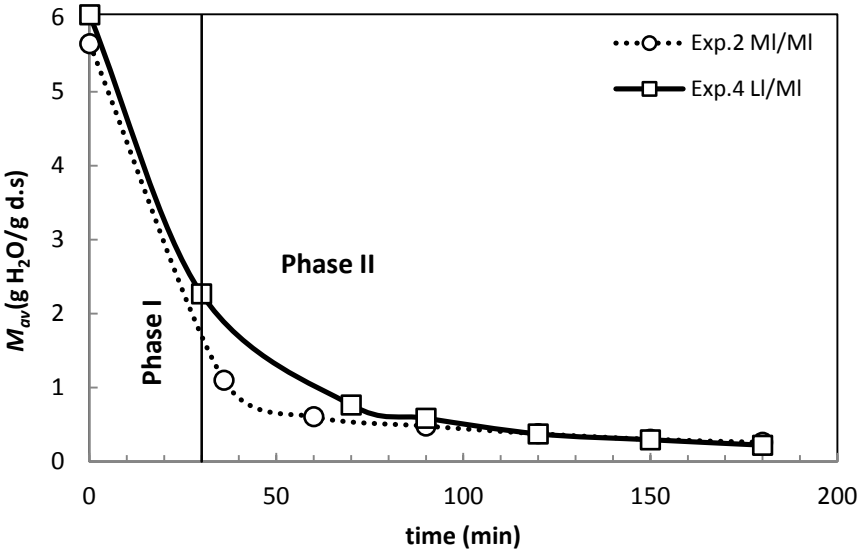

Figure 4.7. Moisture content along time for Experiments 2 and 4, with the same strategy (Ml) for the Phase II**.**

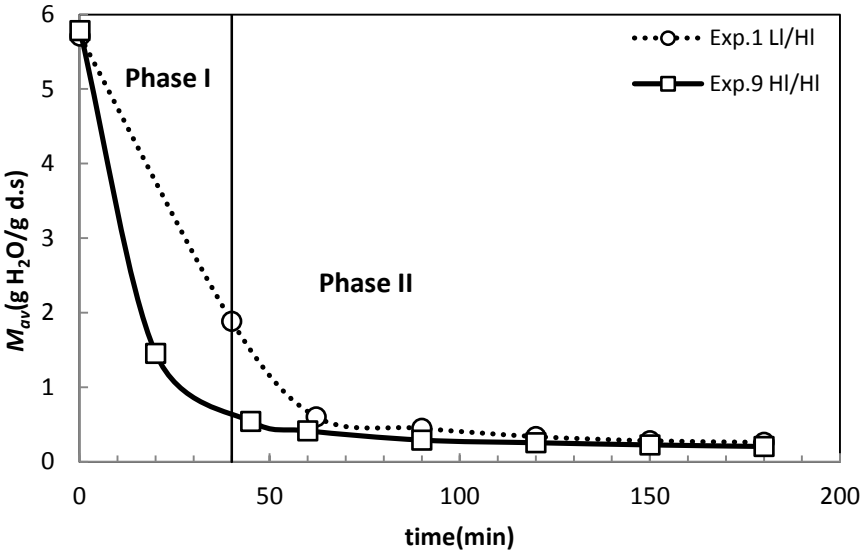

Figure 4.8. Moisture content along time for Experiments 1 and 9, with the same strategy (Hl) for the Phase II.

A similar situation to the one analyzed in the Figure 4.7 is observed comparing the Experiments 1 and 9 in the Figure 4.8 that corresponds to the effect of the Hl strategy concerning Ll strategy for the first phase. Experiment 9 presents a significant drying rate as it can be seen through the slope. By the contrary, in the Experiment 1 appears a greater diffusional resistance probably induced by the extremely low thermal level applied. Therefore, despite using the same thermal conditions (Hl) during the second phase, both moisture profiles are very different. Consequently, the thermal level employed in the Phase I has a significant effect in the diffusional resistance for the moisture removal during the Phase II.

The Experiments 5 and 7 are represented in the Figure 4.9. These experiments have a (Hh) thermal level along the Phase II. These two profiles are very similar despite the different thermal strategies in Phase I, a (Mm) and (Hh) thermal strategies for Experiment 5 and 7 respectively.

This behavior is attributed to the convective losses, higher as higher is the thermal level applied and to the kinetic process governed by external diffusional force. Therefore the thermal gradient applied has great significance in the kinetic of the product. This can be explained because of the kinetics of Experiment 5 (Mm) and the Experiment 7 (Hh) using both the same gradient temperatures corresponding to a 5°C gradient, established as the difference between the inlet air temperature (T_{in}) and the temperature of the surface (T_s) result in a same kinetic profile. The same effect occurs in Experiments 6 and 8 as shown in the Figure 4.10 corresponding to a medium gradient temperature of 25ºC.

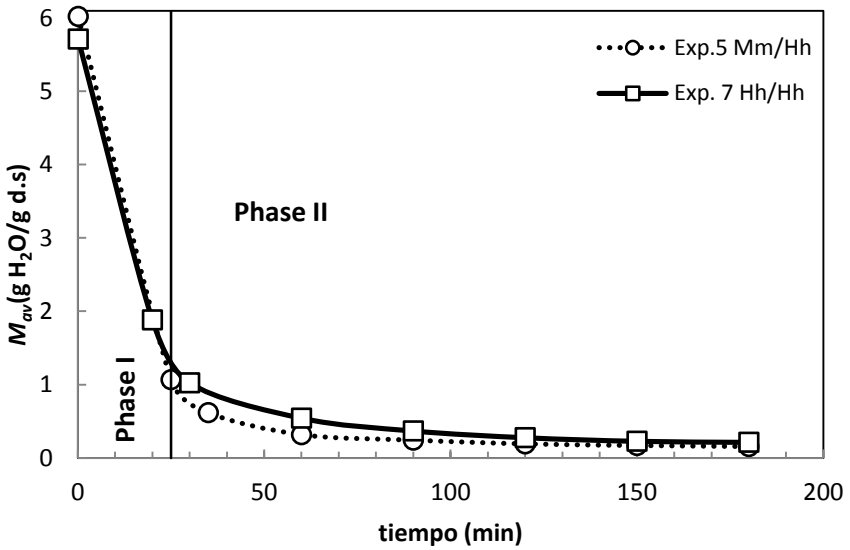

Figure 4.9. Moisture content along time for Experiments 5 and 7, with the same strategy (Hh) for the Phase II.

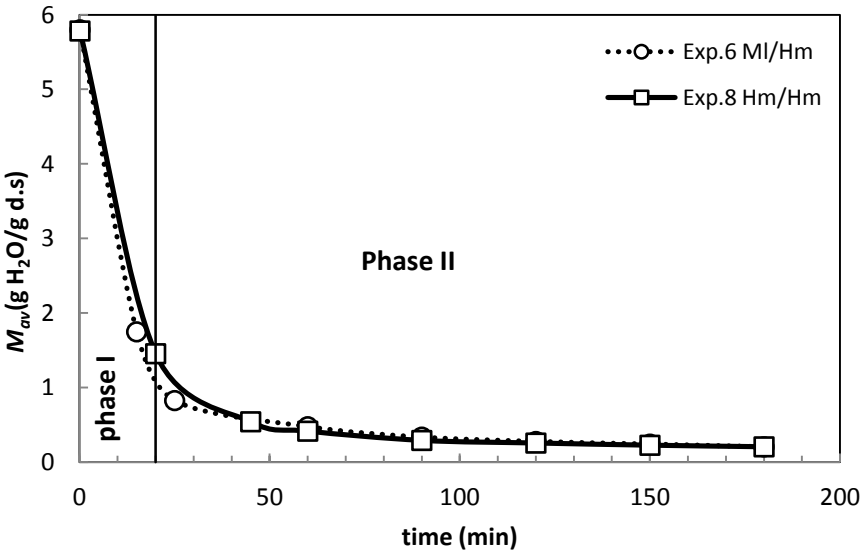

Figure 4.10. Moisture content along time for Experiments 6 and 8 with the same strategy (Hm) for the Phase II.

Analysis of phase II.

The Phase II was analyzed taking into account the experiments with the same thermal conditions along the Phase I. Experiments 1 and 4 can be seen in Figure 4.11, corresponding to a (Ll) thermal level in Phase I. As it has been mentioned previously in a similar situation, the convective losses are higher as higher is the thermal level applied 45°C (Hl) and 25°C (Ml). As a result, it can be concluded that the use of a high thermal level is not effective, since according to the observed results a similar drying kinetics are observed for both strategies (Hl and Ml) in Phase II.

On the other hand, a favorable effect can be observed if only a thermal level is increased (T_s = 45°C and 25°C for Ml and Hl) and not the gradient, around 25°C in both cases, as shown in Figure 4.12 for Experiments 2 and 6. This behavior can be justified because of the greater influence of the moisture diffusional resistance in the Phase II in which, the temperature of the surface (T_s) has a decisive influence.

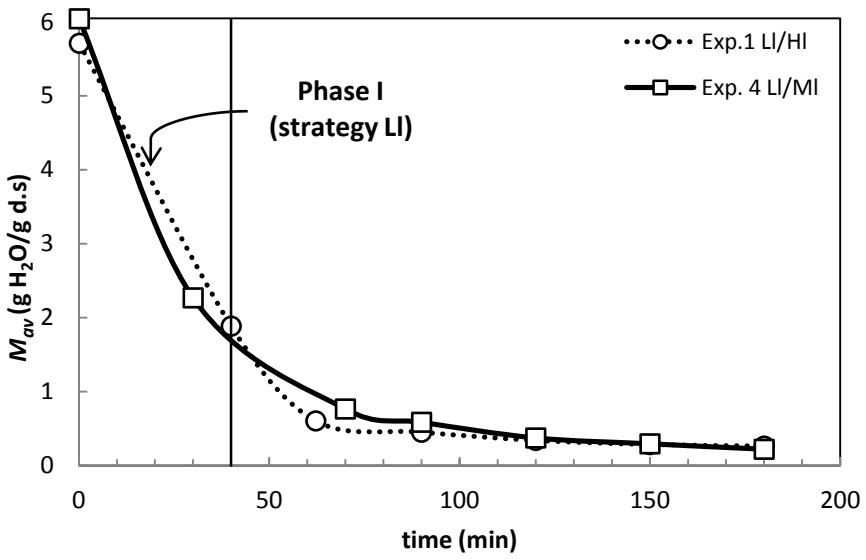

Figure 4.11. Moisture content along time for Experiments 1 and 4 with the same strategy (Ll) for the Phase I.

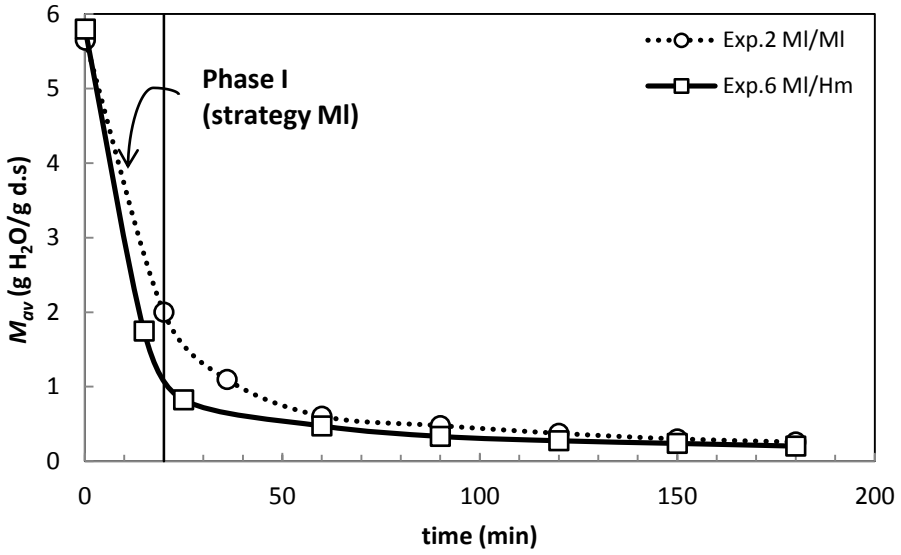

Figure 4.12. Moisture content along time for Experiments 2 and 6 with the same strategy (Ml) for the Phase I.

The gradient and the thermal level

An important conclusion that can be elucidated as a result of the experiments derives from the analysis of the thermal gradient established. This parameter has a significant effect on the drying kinetics, taking into account that the medium al low values of the established gradient prevent convective losses.

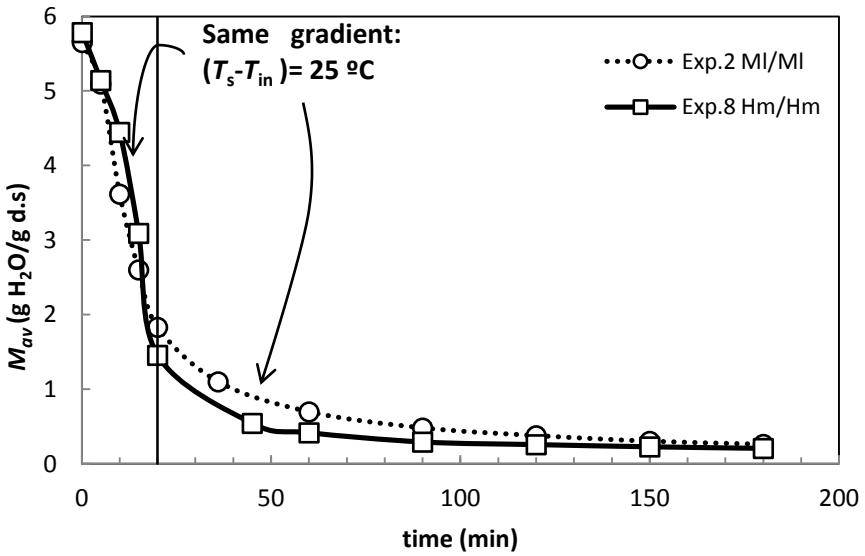

Figure 4.13. Moisture content along time for Experiments 2 and 8 with the same gradient of 25ºC for Phases I and II.

This phenomenon can be observed comparing Experiments 2 (Ml/Ml) and 8 (Hm/Hm) represented in the Figure 4.13 with the same average gradient (25°C) established during the first two phases. The evolution of the drying process is similar in both cases as it ca be seen in the Figure 4.13. The desired water activity value is reached approximately at the same processing time. Consequently, it has been observed that a medium gradient is the most suitable strategy. For the correct selection of the strategies is necessary to analyze the water activity profiles as detailed in Figure 4.14 and during rates (Figure 4.15).

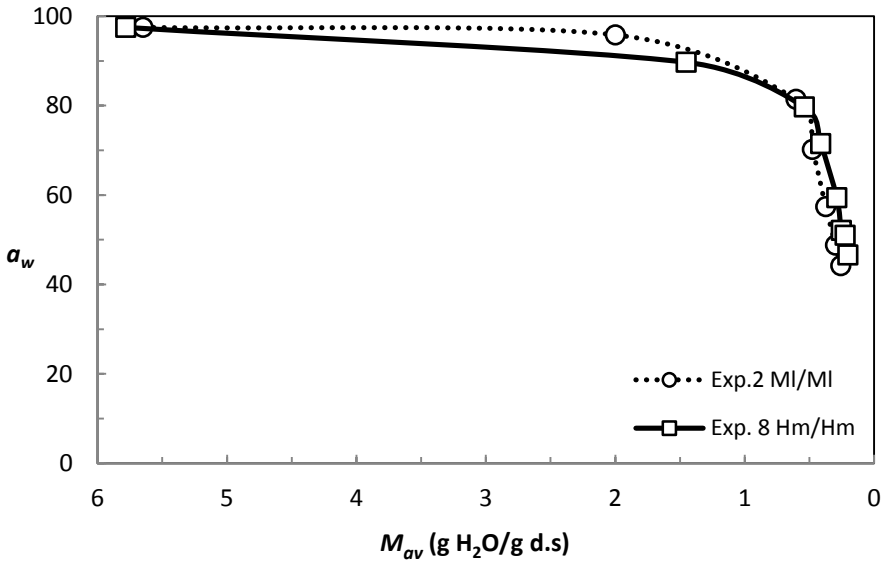

Figure 4.14. Water activity vs. moisture content for Experiments 2 and 8.

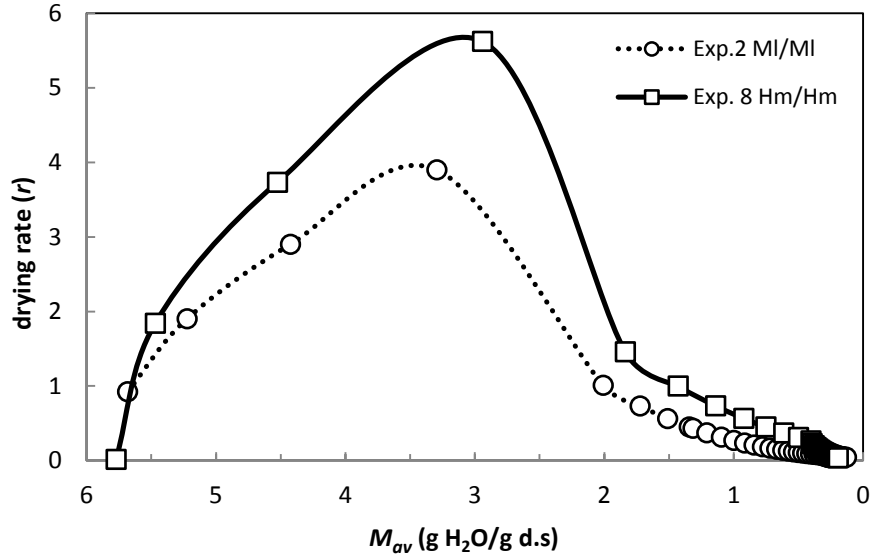

Figure 4.15. Drying rate vs moisture content for Experiments 2 and 8.

The water activity profiles present a smooth slope for the Experiment 2. This implies a homogeneous distribution of the moisture in the particle for Phases I and II, highy recommended regarding the quality of the dehydrated material better than the profile observed for Experiment 8. On the other hand, the drying rate profiles show a slight increase in the drying rate of the Experiment 8 at the begining of the drying process. Although, the total processing time required was similar. Finally, Experiment 2 was selected as the optimal strategy with a (Ml/Ml) thermal level and with a medium gradient of (25°C) established as the difference between the inlet air temperature and the surface temperature of the product. Experiment 2 was selected because of the good and acceptable results under kinetic and quality criteria. Experiment 8 with a thermal level of Hm for Phases I and II is not so favorable despite the kinetic advantages due to quality criteria because of the higher inlet air temperature applied and the abrupt change of water activity observed.

4.4 NFMD mathematical model

During the drying process proposed, was combined a microwave drying with a convective drying of the cylindrical particles. As it has been mentioned previously, can be distinguished three phases in the process. In each phase different mechanisms of mass and energy transfer take place (Ingham, *et al*., 2007).

The temperature evolution in any area inside the material is provided with differential equations, obtained from the three-dimensional material and from the energy balance of a particle in each phase.

The main assumptions for the elaboration of the mass and energy balances were:

1. The particles of material were considered to possess a regular cylindrical shape.

2. The evolution of the moisture content of the material obtained experimentally corresponds to the integrated value of the moisture gradient in the particle.

3. Material is homogeneous in composition and properties.

4. The heat flow is considered to take place in both, axial and radial directions.

5. The evaporation process occurs completely on the external surface of the material.

6. The largest fraction of the total heat required for the vaporization is absorbed from surrounding air, the other part from material surface.

Material balance

The profiles of mass loss of encapsulated material in different phases of the process of drying are defined by the Equation (3.4) that is detailed in the Chapter 3:

Where, D refers to the effective diffusion coefficient that collects different diffusional mechanisms that act in the interior of the particle and can change during the drying.

The Equation (3.4) corresponds to the employee balance without taking into account the contraction along the drying process. The balance used to take into the contraction consideration of particles requires the incorporation of the apparent density particle density, which, referred to the change in volume of the material throughout the process as described in Chapter 3 in the Equation (3.5).

Another equation that define the conditions of the system, appears defined in the Equation (3.6) and depends on the parameter β to express the surface moisture of the particle (M_s) at each the time (Shivhare, *et al*., 1994), that relates the moisture content of the surface with the drying coefficient of the surface. The coefficient β indicates the approaching velocity between the surface moisture content and the equilibrium for a set of drying conditions.

The fitting mass loss profile was obtained through different values of the drying surface coefficient, β for each experiment and with different diffusion coefficients according to the three established phases, *D*. Therefore the value of the average moisture content of the particle in its volume can be adapted to the experimental moisture content of the capsule at each time through the Equation (4.6). This adaptation is possible due to the use of the FlexPDE® program.

$$M_{av} = \frac{\int_{Vp} M \, dxdydz}{V_P} \tag{4.6}$$

Initial and boundary conditions

1 Initial conditions.The initial moisture content of the material is assumed to be the same that the experimental data provides.

2 Boundary conditions. Moisture on the surface is given through the equation of Shivhare (3.6).

Energy balance

The energy conservation for the encapsulating material in the different phases of drying process give the following set of equations (Mudgett, 1986).

Phase I/II

During the first and second phase the power of microwave radiation is gradually modified to keep the product temperatura at a constant value. In this case the energy balance of a material particle is given by the following Equations (3.10-3.12) described in Chapter 3.

Phase III

As mentioned previously, in this Phase III the microwave source is switched off and the samples were subjected to an air flow of constant temperatura, thus, heat transmission is produced by conduction from a point to another one inside of the material, and convection between the external surfaces of the material and surrounding air as has been indicated in Equation (3.13).

Initial and boundary conditions

1 Initially the material is assumed to be at uniform temperature in thermal equilibrium with the environment.

$$t = 0 \qquad T(x, y, z) = T_0 \qquad 0 \le x \le D_C; 0 \le y \le D_C; 0 \le z \le H \tag{4.7}$$

Siendo, $D_c = 2R$

2 Boundary conditions. Due to the temperatura difference between the surface of particles and the surronding air in contact, a significant convective heat flow from outside in or viceversa arises during drying which is absorbed or emitted at the solid-gas interface. On the other hand, all of moisture vaporization takes place on the external surfaces of material. Thus, many authors agree that nota ll the heat required for vaporization is adsorbed on the surface of particle since an important part, is absorbed directly from the microwave power that affect on the material surface. The representative term of required heat for evaporation happens, must be taken into account in the boundary conditions of the system.

$$t > 0 \qquad k\left(\frac{\partial T}{\partial x} + \frac{\partial T}{\partial y} + \frac{\partial T}{\partial z}\right) = -h(T_s - T_{air}) + \frac{\partial M}{\partial t}\rho_{sp} Q_{vap} \frac{1}{S_p} w \tag{4.8}$$

Where, $(x-2.5)^2 + (y-2.5)^2 = R^2$, $0 \le z \le H$ for the lateral area of the cylinder.

Ans for the upper bottom areas: $0 \le x \le D_c, 0 \le y \le D_c, z = H$ ó $z = 0$

The tridimensional representation of geometry and dimensions of a capsule can be seen in Figure 4.16, showing the dimensions of diameter of 0.005 m and a height of 0.008 m as reference.

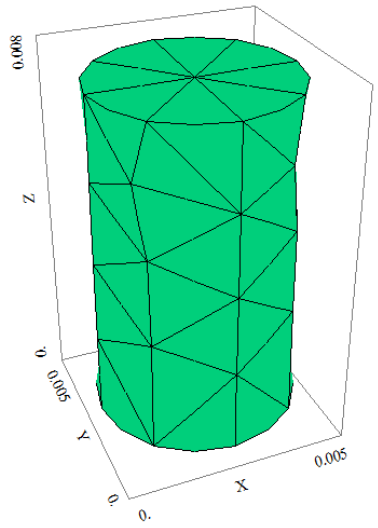

Figure 4.16. Tridimensional representation of an alginate-tylose capsule for the solution of mass and energy balances.

Physical, thermal and dielectric properties

In order to predict temperatura distribution during microwave heating, it is necessary to know material properties such as bulk density, specific heat, thermal conductivity, laten heat, dielectric constant and loss factor detailed in the following table.

Table 4.3. Physical, thermal and dielectric properties of the main encapsulated components.(Lide, 2005,Meda, *et al.*, 2005).

Properties	Value/Expression	Properties	Value/Expression
k_w	0.6 W/mºC	C_{paL}	4120 J/kgºC
P_w	1000 kg/m^3	ε'_{al}	6
C_{pw}	4180 J/kgºC	ε''_{al}	1.5
ε'_w	0.004T^2-0.5212T+75.241	K_{ty}	78 W/mC
ε''_w	0.0001T^2+1.6001T+22.241	ρ_{ty}	961 kg/m^3
Q_{vap}	2257·10^3 J/kg	C_{pty}	2090 J/kgºC
k_{al}	50.22 W/m°C	ε'_{ty}	6
ρ_{aL}	1010 kg/m^3	ε''_{ty}	1.5
ρ_s (1	985.5kg/m^3	ρ_{ap} (2	148kg/m^3

(1,2 Depending on capsule composition (2 Value corresponding to a capsule without shrinkage.

These properties are dependent on temperatura and moisture degree. Table 4.3 shows the properties of the main components of the microencapsulating material. These properties have been estimated according to Equations (3.16-3.21) seen in Chapter 3.

4.5 Mass balance

The drying kinetics has been calculated with a mathematical model. The determination of the parameters has been completed using the Equations (3.4) and (3.6). The sequence of commands (Script) is collected in the Annex A and solves the mass balance using the equations collected in the Table 4.4.

The mass loss profile was obtained after testing different values of β and (D) in accordance with a calculation strategy that compares the experimental mass loss profiles obtained with the model proposed. It was necessary to consider different values of the diffusion coefficients for each of the three drying phases for a correct fitting.

Table 4.4. Equations and fitting parameters for mass balance.

Equations	Profiles	Fitting parameters
$\frac{\partial M}{\partial t} = D\nabla^2 M$	*M vs t*	β,*D*
$M_s = M_e + (M_0 - M_e)\exp(-\beta t)$	M_s *vs t*	

The experiments carried out with the cylinders of alginate-tilosa were adjusted with different values of the parameter β, defined through the Equation of Shivhare (3.6), and *D* for each experiment. The model runed on the Flexpde® program was employed for the adjustment of the model to the experimental moisture profiles.

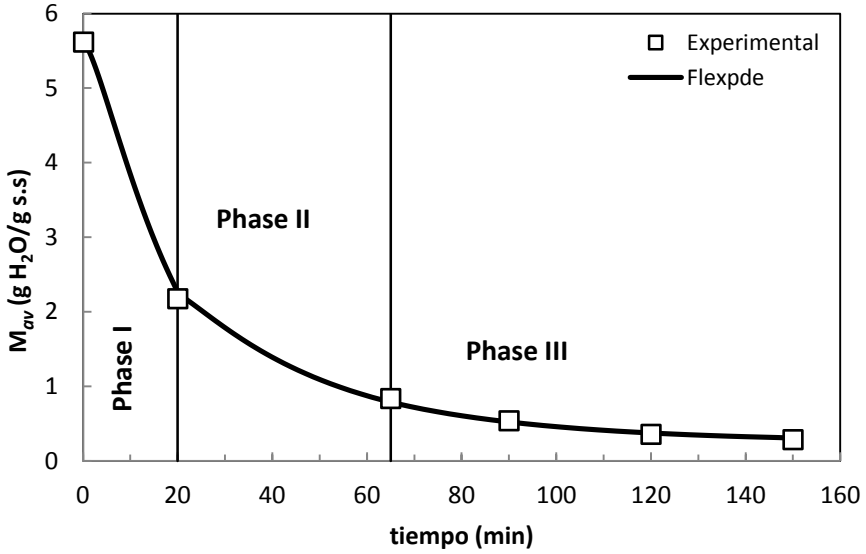

Figure 4.17. Experimental and modeled profile for Experiment 3 (Hl/Ll).

Figure 4.17 shows, the good fitting obtained with the program applying the previously model described and comparing it with the experimental data. The β parameter was decisive through the regulation of the surface moisture (M_s) which must be below the average moisture values. The adjustment of the experimental data requires a suitable β value for each experiment and appropriate diffusion coefficients for each established phase in the drying process. The average moisture value of the capsule given by the model fits with the moisture of the capsule obtained experimentally.

The drying process along the Phases I and II implies the elimination of the greater amount of water, due to the elimination of the free water towards outside the particle. In the initial phase, moisture profiles are affected by boundary conditions through the parameter β. This affects to the surface moisture content of the material depending on drying conditions. The β values vary from 0.04 to 0.20 min^{-1} as collected in Table 4.5, depending on the thermal conditions for each proposed experiment.

The described adjustment has been made for the fitting of the different operational variations applied, obtaining for each condition the values of the diffusion coefficients seen in Table 4.5.

Table 4.5. Diffusion coefficients D_1, D_2, D_3, and coefficient β values for the experiments.

Exp.	Código	β(min^{-1})	D_1(m^2/min)	D_2(m^2/min)	D_3(m^2/min)
1	Ll/Hl	0.040	5.8E-8	9.8E-8	7.1E-8
2	Ml/Ml	0.110	36E-8	77E-8	6.1E-8
3	Hl/Ll	0.170	9.5E-8	2.5E-8	2.3E-8
4	Ll/Ml	0.146	6.4E-8	2.1E-8	2.5E-8
5	Mm/Hh	0.080	16E-8	36E-8	4.1E-8
6	Ml/Hm	0.127	34E-8	71E-8	4.2E-8
7	Hh/Hh	0.060	9.3E-8	18E-8	1.3E-8
8	Hm/Hm	0.120	9.1E-8	20E-8	3.2E-8
9	Hl/Hl	0.164	45E-8	7E-8	3E-8

The diffusivity is an effective parameter that describes the water diffusion in liquid and gas phase and also incorporates the structural changes due to the contraction of the particle. Table 4.5 shows that the diffusivity through Phases I and II is slightly higher, since diffusion occurs in liquid phase, along Phase III the diffusional mechanism is in gas phase. The highest diffusivity values are obtained in Experiments 2, 6 and 9 in which the established gradient between the inlet air temperature and the temperature of the surface is the highest. In general, the value of the diffusion coefficient in Phase II is the highest, although there are some exceptions due to the combination of the diffusivity in gas and liquid phase. As the drying process advances the diffusional mechanism in liquid phase is gradually less important. By the contrary, in the Experiments 1 and 2 the previous drying condition, with a low inlet air temperature, imply a more open structure with a higher diffusivity value along the third phase.

Volume shrinkage consideration

In the previous mathematical model the volume of the particle has been considered constant so that the effective diffusivity incorporates the phenomenon of contraction. The volume decrease affects the corresponding *D* coefficients values of each phase.

In this case, the parameter β does not vary since the drying kinetics for each experiment is the same. The mathematical model previously described has been replicated in the same way, but in this case the density of the particle has been incorporated to introduce the volume changes as described in Equation (3.5). The contraction rate is a new parameter which is defined for each phase and obtained by the Equation (4.9) for the radial contraction and for the axial contraction considering the reduction of the height. This parameter depends on the relationship between the radio (*r*) and (*h*) with the times of phase changes. According to the three drying phases, three different values were established v_{r1}, v_{r2}, v_{r3}, v_{h1}, v_{h2} v_{h3}.

$$v_r = \frac{\Delta r}{\Delta t} \tag{4.9}$$

$$v_h = \frac{\Delta h}{\Delta t} \tag{4.10}$$

El cálculo del valor de *r* se calcula mediante la siguiente expresión:

$$\frac{X - X_e}{X_0 - X_e} = \frac{r - r_e}{R - r_e} \tag{4.11}$$

A good linear correlation between *X* and *r*, was found where, r_e is the radio value of the final equilibrium conditions (Ochoa, *et al*., 2002). These equations permit to calculate the value of the radio for each phase. Due to the geometry of the material there is also a reduction of cylinders height calculated with a modification of the Equation (4.11) which implies the substitution of *r* and r_e by *H* and h_e for the initial and the final heignt in the equilibrium respectively. The different experiments rates are collected in Table 4.6. The maximum contraction values are reached in the first phase due to the drying kinetic. On the other hand, the value obtained for Experiment 5 is slightly superior to that obtained in

the first phase due to the thermal level (Hh) employed in the second phase that has contributed to the contraction of the material respect to the first phase in which medium temperatures are used for the product and the inlet air.

Table 4.6. Axial and radial shrinkage rates for all experiments.

Exp.	Code	v_{r1}(m/s)	v_{r2}(m/s)	v_{r3}(m/s)	v_{h1}(m/s)	v_{h2}(m/s)	v_{h3}(m/s)
1	Ll/Hl	4.59E-7	3.08E-7	9.49E-10	2.51E-7	9.38E-7	2.09E-8
2	Ml/Ml	6.33E-5	1.44E-5	1.75E-7	4.52-5	5.00E-5	1.32E-6
3	Hl/Ll	1.17E-6	3.89E-8	9.80E-10	9.21E-7	1.85E-7	1.96E-8
4	Ll/Ml	5.02E-7	1.25E-7	2.08E-8	3.90E-7	4.58E-7	2.08E-8
5	Mm/Hh	4.67E-7	8.33E-7	1.48E-8	6.33E-7	1.92E-6	1.48E-8
6	Ml/Hm	1.45E-6	3.00E-7	4.00E-9	8.95E-7	1.17E-6	2.00E-8
7	Hh/Hh	1.09E-6	3.67E-7	1.39E-9	1.26E-6	1.00E-6	1.39E-8
8	Hm/Hm	8.58E-7	2.00E-7	1.59E-9	1.42E-6	5.33E-7	1.59E-8
9	Hl/Hl	2.44E-6	1.22E-7	6.67E-10	1.60E-6	1.72E-6	1.33E-8

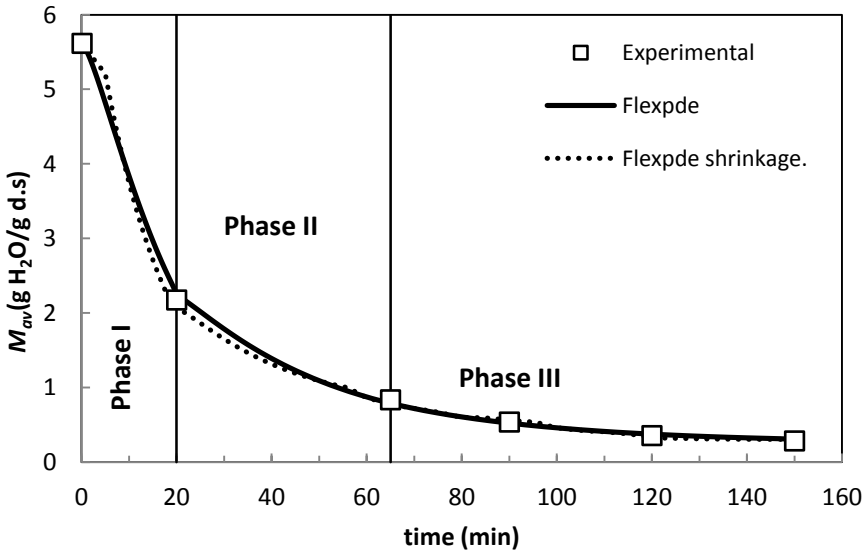

Figure 4.18. Experimental and modeled profile for Experiment 3 with and without shrinkage consideration (Hl/Ll).

The consideration of the density together with the axial and radial contraction affects to the diffusivity values, decreasing the values obtained without shrinkage consideration. The diffusivity values obtained for the model without contaction (shaded rows) and with contraction consideration are collected in Table 4.7. As shown in the table the diffusivity values during the second phase are higher with a few exceptions such as the observed in Experiment 3, in which the thermal conditions of the first phase are

(Hl) with respect to the second phase with a thermal level of (Ll) that lowers the diffusion ability. The values of thermal diffusivity in which has taken into account the contraction of the material involves a reduction of diffusivity due to the difficulty to diffuse if the structure of the material is reduced over time, making more complicated the water removal. As shown in Figure 4.18, can be observed the best fitting of the model with the contraction consideration to the experimental data.

Table 4.7. Values of diffusion coefficients with and without shrinkage consideration.

Exp.	Código	D_1(m^2/min)	D_2(m^2/min)	D_3(m^2/min)
1	Ll/Hl	5.8E-8	9.8E-8	7.1E-8
1	Ll/Hl	2.5E-8	2.5E-8	7.9E-8
2	Ml/Ml	36E-8	77E-8	6.1E-8
2	Ml/Ml	4.6E-8	5.7E-8	8.1E-8
3	Hl/Ll	9.5E-8	2.5E-8	2.3E-8
3	Hl/Ll	2.0E-8	1.0E-8	3.3E-8
4	Ll/Ml	6.4E-8	2.1E-8	2.5E-8
4	Ll/Ml	4.4E-8	1.5E-8	3.0E-8
5	Mm/Hh	16E-8	36E-8	4.1E-8
5	Mm/Hh	5.6E-8	9.2E-8	3.1E-8
6	Ml/Hm	34E-8	71E-8	4.2E-8
6	Ml/Hm	1.4E-8	7.1E-8	1.2E-8
7	Hh/Hh	9.3E-8	18E-8	1.3E-8
7	Hh/Hh	4.3E-8	6.0E-8	4.0E-8
8	Hm/Hm	9.1E-8	20E-8	3.2E-8
8	Hm/Hm	8.3E-8	7.0E-8	9.8E-8
9	Hl/Hl	45E-8	7E-8	3E-8
9	Hl/Hl	65E-8	5.0E-8	3.0E-8

External transfer coefficient calculation

Several parameters obtained in the mass and heat balance are used for the calculation of the external transfer coefficient. This coefficient relates the water flow removed with the vapor pressure gradient in the surface of the particle. The water flow ($-dm_w/dt$) is also known as the drying rate, the surface vapor pressure ($P_{w,s}$) and vapour pressure gradient at the end ($P_{w,\infty}$), which are related through the Equations (3.7-3.9) described in the methodology chapter.

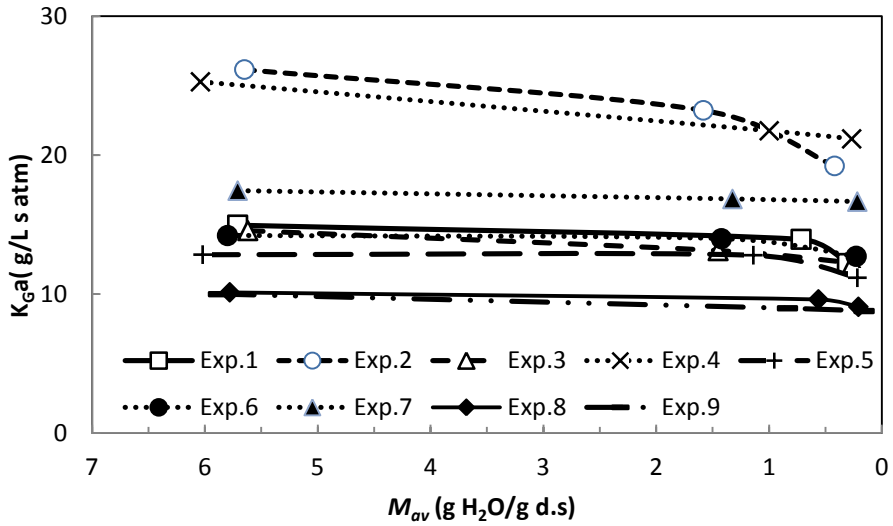

Figure 4.19. Representation of external transfer coefficient for all the experiments.

According to Equation (3.8) the surface vapour pressure of the material depends on the temperature through the pressure saturation of water and the water activity.

Once the mass and energy balances have been adjusted. The transfer coefficient has been calculated $k_G\,a$ as shown in Equation (3.7). The parameters obtained in mass and energy balances are used for the calculation of this coefficient. The coefficient values are represented with the average values of mass loss as shown in Figure 4.19 to permit the comparison. Generally, in the figure can be noticed that the initially value of the coefficient is more or less constant with a slight descent for low moisture content values. There are differences between the values obtained for each experiment. The Experiments 2 and 4 have the highest values compared with the other experiments. These cases correspond to intermediate thermal gradients (T_s-T_{in}) ≈ 25°C. The convective heat flow to the outside of the particle connects with the mass transport mechanisms favouring the elimination of vapor generated at the surface of the particle.

The results shown in Figure 4.19 indicate that the fall of fluid temperature of in the surroundings of the material is a decisive parameter of the $K_G\,a$, increasing the vapor flows, obtaining lower $K_G\,a$ values. Convective heat and mass flows connection generally favors the elimination of vapor if these correspond to moderate thermal gradients of ≈ 25°C. Thus, Experiments 8 and 9 with high thermal gradients or high temperatures on the surface, the convective heat flow can be high, compromising negatively to the

vaporization of the surface moisture. The rest of the cases correspond to high product temperatures with low thermal and medium gradients of 5ºC to 25°C, respectively. All of them correspond to transfer coefficient values between 12 and 17 (g/ L s atm).

4.6 Energy balance

The model has been used to calculate the energy balance through Equations (3.10-3.13) described in Chapter 3. The script is collected in the Annex A. The surface temperature profiles of the material is needed to determine the value of the convection coefficient that was h = 150 W/m^2 °C for all experiments and for each proposed phases. This value is within the range (100-400W/m^{2}K) employed by other authors (Abbasi Souraki and Mowla, 2008). The microwave power was set around 220W for these experiments. Figure 4.20 shows the fitting of the experimental data with the the proposed energy model. In the Figure 4.21 can be observed the fraction of microwave on time taking as nominal power 220W.

Table 4.8. Microwave time on and energy consumption.

Exp.	1	2	3	4	5	6	7	8	9
time (min)	12	20	34	29	17	18	16	25	27
G_{mw}**(kJ/cm^3)**	158.4	264	448.8	382.8	224.4	237.6	211.2	330	356.4

At the beginning of the experiments, the microwave energy was used to reach the surface target temperature of the material. Once this temperature was reached and exceeded, the temperatue was regulated with the microwave power applied. Because of this, the fraction of the microwave on power varies due to the control of the temperature via the microwave power. Microwave power was used in the first and second phase but in the third phase was switched off. The microwave on fraction was defined by the parameter b employed in the program. Applied microwave power is regulated through this parameter. It can take values of zero and one. The value of b = 1 is taken to indicate that microwaves are active and b = 0 when are turned off. If the experimental surface temperature is greater than the target temperature, this parameter will take the value of 0.

On the contrary, if the experimental temperature is lower than the target temperature will take the value of 1.

The *b* parameter, prior calculation of the accumulated value (b_{ac}), obtained by integration of the value of *b* in a finite time, allows to obtain the consumption G_{mw} of the microwave power generator through the Equation (4.13). The value of b_{ac} is between 0 and 1 that represents the fraction of microwave throughout the processing time. Figure 4.21 represents for Experiment 8 the change of b_{ac} which is introduced for a time on determination t_{on} at specific time *t* in the Equation (4.12).

$$t_{on} = \int_0^t b_{ac}(t)dt \tag{4.12}$$

$$G_{mw} = W_{nom}\int_0^t b_{ac}(t)dt \tag{4.13}$$

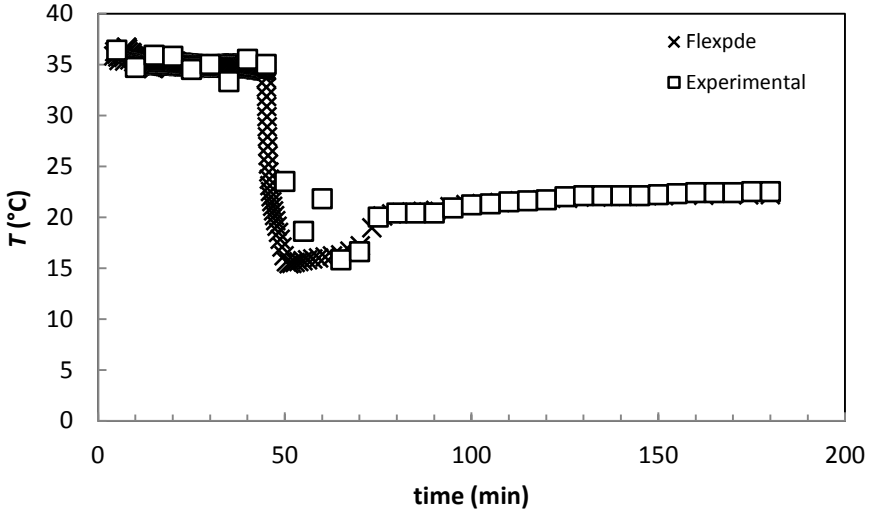

Figure 4.20. Experimental surface temperature and modeled profile for Experiment 8 (Hm/Hm).

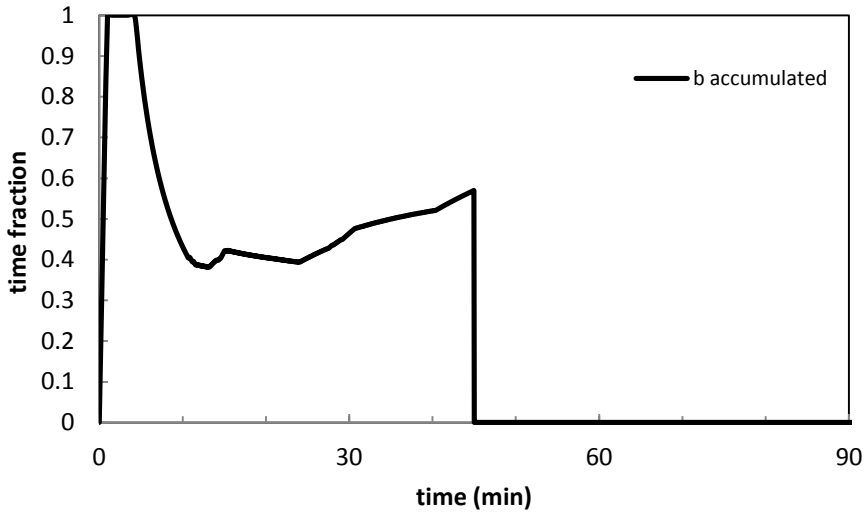

Figure 4.21. Representation of b_{ac} for Experiment 8 (Hm/Hm).

As all experiments have the same nominal potential of 220W, it will be compared the microwave activated time, shown in Table 4.8. The greater is the time of activated microwave power the greater is its consumption. Experiment 1 has the lowest consumption with thermal conditions of Ll/Hl. On the other hand, in Experiment 3, as requires longer period of activated microwaves with thermal conditions of Hl/Ll.

.

Capítulo 5

SECADO DE MICROORGANISMOS ENCAPSULADOS

5 SECADO DE MICROORGANISMOS ENCAPSULADOS

Una vez que se ha analizado la fluidodinámica, la cinética y el nivel térmico en un proceso de secado NFMD, el siguiente paso ha sido emplear esta nueva tecnología de secado en microcápsulas de alginato con un contenido de microorganismos (*saccharomyces cerevisiae*), para poder analizar la adecuación de esta tecnología a la posterior viabilidad de los microorganismos una vez finalizado el proceso.

Aparte de la composición, derivada de la inclusión de células vivas en las cápsulas, se disminuyó el tamaño de éstas para hacerlo más acorde a las características de un aditivo alimentario para favorecer el proceso de mezcla con los distintos tipos de alimentos.

Las estrategias operacionales, aunque dentro de un mismo planteamiento general, se ajustó en el valor de los niveles térmicos e intervalo de condiciones en base a la información obtenida en el capítulo anterior.

5.1 Descripción del material empleado

En este caso se partió de extracto de levadura (*saccharomyces cerevisiae*, ZYMAFLORE® F15), suministrado por LAFFORT (Francia), conteniendo una concentración de células activas superior a $2\ 10^{10}$ cfu/g de extracto seco de levadura. Se utilizó una suspensión al 3% de alginato y al 10% (g/L) de extracto de levadura que se extruyó y se cortó con un equipo *jet cutter* (Chávarri, *et a*l., 2012). Las microcápsulas se recogieron en una disolución al 2% de $CaCl_2$, previo ajuste de la viscosidad, temperatura, boquilla y velocidad de corte del *jet cutter* para la obtención del tamaño de las microcápsulas. Comúnmente el diámetro de las partículas conocidas como microcápsulas suele oscilar entre 400 y 800µm (Burgain, *et al.*, 2011). En este trabajo para favorecer la manipulación del material sobre todo en los primeros momentos del secado, se modificaron las condiciones de formación de las microcápsulas para obtener tamaños superiores. Después del proceso de gelificación llevado a cabo en el baño de cloruro de calcio, se obtuvieron microcápsulas esféricas con un diámetro en torno a 2000-2500 µm. Se realizó un estudio granulométrico empleando el microscopio óptico (Axioskop 40, Carl Zeiss) y el software Ellix 5.0 (Microvision Instruments, Francia). En consecuencia

el valor medio del diámetro obtenido fue de 2250 µm como representativo del tamaño que se obtiene a la temperatura y parámetros de operación empleados. Las microcápsulas una vez extraídas del baño de cloruro de calcio, fueron cubiertas y almacenadas no por más de 24 horas en un refrigerador a 4ºC hasta su empleo en el experimento de secado correspondiente.

5.2 Equipo experimental de secado NFMD

El equipo empleado para realizar los experimentos de secado se muestra en el Capítulo 3. Se utilizó un microondas SAIREM LABOTRON 2000 para realizar los experimentos.

El equipo de microondas lleva en su interior un lecho fluidizado conteniendo las microcápsulas para hacer posible las diferentes variantes del proceso aquí denominado NFMD y que se describen en el Capítulo 3 de metodología. En el interior de la cámara se encuentra un lecho cilíndrico de propileno de 60 mm de diámetro en el cuál se secaron las microcápsulas. El seguimiento de la pérdida de masa se realizó con una balanza en la que a diferentes tiempos del proceso de secado se colgó el lecho para proceder a la medición de la masa. El control y monitorización del proceso se siguió a través de las temperaturas de las microcápsulas empleando el OPTOCON FOTOTEMP 4. La temperatura de la superficie de las microcápsulas se midió a través de unas sondas de fibra óptica insertadas en el interior del lecho. La temperatura del aire también se controló tanto a la entrada como a la salida del lecho, para estimar la temperatura media del aire circundante en contacto con las microcápsulas. El caudal de aire seco se introdujo por la parte inferior del lecho. Se utilizó un deshumidificador de aire DONALSON ULTRAFILTER con una capacidad máxima de $10 m^3/h$ para secar el aire y su temperatura se controló empleando un dispositivo de calentamiento y enfriamiento del aire para regular la temperatura de entrada del aire antes de ser introducido en la cavidad de microondas.

Un equipo de liofilización LYOQUEST-55 de la casa Telstar se usó para realizar los experimentos de comparación respecto al NFMD. La cavidad de vacío viene provista de bandejas calefactables con sondas para el control del las temperaturas. En los experimentos de liofilización las microcápsulas se colocaron en las bandejas y se

congelaron bajo el efecto de disminución de presión, alcanzando rápidamente valores por debajo de los 600 mbar. A lo largo del proceso las bandejas calefactables se mantuvieron a 31.6 ºC mientras la presión desciende a 200 mbar hacia el final del proceso.

El contenido de humedad del producto previo al proceso de secado NFMD se determinó en un horno BINDER, modelo ED53 a 60ºC hasta alcanzar una pesada constante. En las últimas fases del secado el contenido de humedad se llevó a cabo a través del método de Karl-Fischer con un valorador modelo Methrom 860KF, acoplado a un horno modelo 702 SM. La actividad de agua (a_w) fue también medida en una cámara termostática modelo Novasina TH2 que da la presión de vapor ($P_{w,s}$) a 24ºC para obtener así:

$$a_w = \frac{P_{w,s}}{P_s} \tag{5.1}$$

Siendo P_s la presión de vapor de saturación a 24ºC.

Unas 10 microcápsulas a diferentes tiempos se tomaron como muestras para poder medir la a_w, empleada como parámetro indicador del final del proceso el cuál se estableció en valores entre 0.2 y 0.3.

5.3 Experimentos NFMD para secado de microcápsulas de levadura

Los experimentos fueron llevados a cabo según el procedimiento NFMD, consistente en secar material particulado en condiciones de fluidización o próximas a la fluidización, mediante el suministro de calor por microondas. La potencia de microondas se reguló en el transcurso del proceso de secado a fin de conseguir determinados valores de temperatura en las microcápsulas y en la temperatura del aire que se introduce en el lecho de partículas. En este estudio se analizaron nueve estrategias térmicas, combinando tres niveles para la temperatura de entrada del aire (T_{in}^*) con los tres niveles establecidos para la temperatura de la superficie del producto (T_s^*). La temperatura de entrada del aire en este caso tomó los siguientes valores: 5ºC, RT (room temperatura, 20 - 24ºC) y 40ºC. Los diferentes experimentos diseñados se basaron en la combinación de estas tres temperaturas del aire con las diferentes temperaturas de superficie objetivo de las microcápsulas. Debido a la dificultad de medir directamente la temperatura de las

microcápsulas, la temperatura de la superficie se estimó midiendo la temperatura de la película de aire en contacto con la sonda de fibra óptica introducida dentro del lecho de partículas. Los experimentos se definieron a través de temperaturas objetivo: (T_s^*), para la superficie y (T_{in}^*), para la temperatura de entrada del aire. A lo largo del proceso de secado, la potencia de microondas fue regulada para alcanzar la temperatura objetivo (T_f^*) tal y como se observa en la Ecuación (3.1). Los valores experimentales de la temperatura en el interior del lecho, (T_f) asumido como la media aritmética de la temperatura del aire, (T_{air}) y la temperatura de la superficie (T_s) tal y como se observa en la Ecuación (3.2). Mientras que (T_{in}), a la entrada del aire, se mantuvo en valores muy cercanos al valor objetivo establecido (T_{in}^*) mediante el correspondiente enfriamiento ó calentamiento del aire, la (T_{air}) puede variar significativamente dependiendo de la fase de secado. El aire a su paso por el lecho puede llegar a experimentar un incremento de hasta 20ºC, en los primeros momentos del secado y cuando, además, la diferencia entre la temperatura del aire a la entrada y del producto es más elevada. A pesar de que se midieron las temperaturas experimentales: (T_{out}, T_{in} y T_s), tal y como se indica en la Figura (5.3). Las temperaturas (T_{in} y T_s) no coinciden con las temperaturas objetivo (T_s^* y T_{in}^*) y muestran cierta variabilidad debido al control manual de la potencia. Empleando las temperaturas medidas experimentalmente (T_f), y (T_{air}) se estima la temperatura de la superficie experimental del material (T_s), obtenida a través de las Ecuaciones (3.2) y (3.3) (Bergman, *et al*., 2011).

La temperatura de entrada del aire (T_{in}^*) y el correspondiente gradiente térmico establecido desde el interior hacia la superficie del material ($T_s^* - T_{in}^*$) fueron utilizados para definir los experimentos de NFMD junto con la T_s^*.

A la hora de diseñar las distintas estrategias de calentamiento se realizó un planteamiento semejante al expuesto en el Capítulo 4 sólo que, en base a los resultados obtenidos, se acorto el intervalo de (T_{in}^*) (ahora de 5 a 40ºC) evitando temperatura de 0ºC por problemas operacionales de congelación en el inicio del proceso. Así mismo, se acortó la variación de (T_s^*), ahora de 15 a 45ºC y se evitan los niveles térmicos altos en la primera fase que ocasionan elevadas pérdidas energéticas por convección sin claro beneficio en la calidad. El diseño de experimentos puede verse en la Tabla 5.1. A lo largo de cada uno de los experimentos, los equipos de control tanto de la potencia de microondas como de la temperatura de entrada del aire se regularon para el ajuste de los

valores de (T_f) y (T_{in}) a las temperaturas objetivos previamente fijadas (T_f^*) y (T_{in}^*). Como la (T_s) se estima a través de la Ecuación (3.2) empleando la (T_{air}) en lugar de la (T_{in}), se observa cierta diferencia respecto de la temperatura objetivo (T_s^*).

Table 5.1 Definition of the thermal levels applied in the drying experiments.

Exp.	Code	Phase I			Phase II			Phase III
		T_{in}^*	T_f^*	T_S^*	T_{in}^*	T_f^*	T_S^*	
1	Ll/Ml	5	10	15	5	17.5	30	
2	Ml/Mm	5	17.5	30	20	25	30	
3	Ll/Lh	5	10	15	40	27.5	15	
4	Mm/Ml	20	25	30	5	17.5	30	40-20˚C
5	Lm/Mm	20	17.5	15	20	25	30	
6	Lm/Hh	20	17.5	15	40	42.5	45	
7	Lm/Hm	20	17.5	15	20	32.5	45	
8	Lh/Hh	40	27.5	15	40	42.5	45	
9	Mh/Hm	40	35.5	30	20	32.5	45	

El código empleado en la Tabla 5.1 hace referencia a las condiciones térmicas empleadas en las Fases I y II. Las primeras dos letras se corresponden a las condiciones empleadas en la Fase I y las siguientes dos letras separadas por una barra hacen referencia a las Fase II. En cada fase la primera letra en mayúscula se refiere a la temperatura de la superficie (T_s^*) que puede adoptar los siguientes valores y el correspondiente código: L=15° C (*Low*), M = 30 ° C (*Medium*) y H = 45 ° C (*High*). La segunda letra hace referencia a la temperatura objetivo de entrada del aire (T_{in}^*) empleando la misma terminología pero con la letra en minúsculas: *l* = 5 °C, *m* = 20 ºC and *h* = 40 °C. Por ejemplo, en el Experimento 3 (Ll/Lh), se empleó tanto en la Fase I como en la Fase II un nivel térmico bajo para la temperatura de la superficie, exceptuando en la Fase II que se utilizó una temperatura de 40ºC para la entrada del aire.

5.4 Descripción de las fases de secado en el proceso NFMD

La diferenciación de las fases se hizo de acuerdo a cierto procedimiento experimental. A continuación, se procede a la descripción de uno de los experimentos llevado a cabo en el equipo experimental. Inicialmente, se introducen unos 200 g de material en el lecho. Después, el recipiente se suspendió en el interior de la cámara. A continuación se colocaron apropiadamente las fibras ópticas para medir la temperatura de entrada del aire, (T_{in}), la temperatura de salida (T_{out}) y la temperatura en el interior del

lecho (T_f). Durante el proceso NFMD se consideraron tres fases en las que además de cambiar las temperaturas objetivo (T_{in}^*) y (T_f^*) correspondientes a cada fase, debe disminuirse continuamente la velocidad del aire a medida que las partículas se hacen cada vez más pequeñas y ligeras cuando el lecho fluidiza. La velocidad del aire es una variable fundamental para el establecimiento de las fases del proceso NFMD. Debido a la adherencia que presentan las microcápsulas en las etapas iniciales del secado, la velocidad mínima de fluidización experimental o real no coincide con la obtenida teóricamente en función de las propiedades de la partícula (Pata, *et al.*, 1988). De trabajos anteriores se estimó experimentalmente que la velocidad de mínima de fluidización inicial es 1.39 m/s en el espacio libre de la columna de fluidización y que es aproximadamente tres veces superior a la calculada teóricamente a partir de las propiedades físicas de las microcápsulas tal y como se verá en detalle en la sección siguiente. A medida que avanza el secado se observa una progresiva aproximación de la velocidad experimental a la teórica de mínima fluidización. Ambas velocidades experimental y teórica coinciden (≈ 0.30 m/s) cuando las partículas pierden cualquier tipo de adherencia, lo que corresponde a un contenido acuoso entorno a 0.50 g/g producto en base húmeda tal y como se observa en la Figura 5.1 y se emplea en este trabajo para marcar el comienzo de la última Fase III. En el periodo de secado anterior al momento de igualación de las velocidades de mínima fluidización experimental y teórica, se produce la eliminación de más del 80 % de la humedad de la partícula por lo que se consideraron a su vez dos fases para un mejor control. Para el establecimiento de la transición de la Fase I a la II, se tomó el valor medio entre la velocidad inicial 1.39 m/s y la de comienzo de la Fase II (0.32 m/s). En consecuencia las tres fases del proceso NFMD quedan definidas de la siguiente forma:

Fase I: En esta fase la velocidad de entrada del aire se estableció en 1.39 m/s (velocidad mínima observada experimentalmente) en el espacio libre de la columna de fluidización. Durante esta fase la temperatura de entrada del aire se controló próxima a la temperatura objetivo (T_{in}^*) y la potencia de microondas se reguló para que la temperatura experimental del interior del lecho (T_f) se aproximará a los valores establecidos de temperatura del film objetivo (T_f^*).

Fase II: Esta fase comienza cuando la velocidad de mínima fluidización desciende al valor medio entre el valor inicial y el de igualación (0.32 m/s). La potencia de

microondas se reguló para obtener las temperaturas prefijadas de la temperatura del lecho (T_f^*) y la temperatura de entrada del aire (T_{in}^*) para esta fase.

Fase III: De manera similar, esta fase comienza cuando la velocidad del aire desciende a 0.32 m/s. En esta fase las microondas permanecieron apagadas y el lecho se mantuvo fluidizando hasta el final del proceso definido como el momento en el que se alcanza un valor de actividad del agua entre 0.2-0.3 (Iaconelli, *et al.*, 2015). En todos los experimentos, al comienzo de esta fase, la temperatura de entrada del aire se elevó a 40ºC como una manera de acelerar el proceso de la dificultosa eliminación de la humedad adsorbida. La temperatura de entrada del aire se reduce del valor inicial de 40 °C empleando una rampa de temperatura descendente de 5°C por hora.

Al final de cada una de las fases y cada media hora en la Fase III se realizaron tomas de muestra para la determinación y análisis de los parámetros de la cinética de secado, actividad de agua y contenido en humedad de las diferentes muestras a los diferentes niveles térmicos establecidos.

Tal como se ha comentado anteriormente, se empleó la velocidad del aire como variable indicadora para la definición de las tres fases del secado, en lugar de la humedad del producto mucho menos accesible a la hora de su determinación. Dado que el proceso NFMD se lleva a cabo en condiciones de mínima fluidización, la velocidad del aire debe ser disminuida cuando el lecho entra en fluidización a medida que las partículas se hacen más ligeras por efecto del secado. Por tanto, existe una relación estrecha entre el contenido acuoso de las microcápsulas y la velocidad del aire empleada a lo largo del proceso. Las microcápsulas obtenidas según se indica en secciones anteriores presentan un contenido de humedad en torno al 85 % en base húmeda al inicio del secado. En esas condiciones las microcápsulas presentan una elevada adherencia de manera que la velocidad de mínima fluidización del lecho inicialmente es considerablemente superior a la obtenida teóricamente a través de las Ecuaciones (4.2) y (4.3) del capítulo anterior (Levenspiel, 2014).

Se llevó a cabo un estudio de fluidización durante el proceso NFMD con temperaturas objetivo medias para la (T_s^*) y la (T_{in}^*). Inicialmente, la velocidad de mínima fluidización experimental, u_{mf}^*, fue de 1.39 m/s, unas tres veces superior a la velocidad mínima de fluidización teórica, u_{mf}, obtenida de acuerdo a las ecuaciones

anteriores. La u_{mf}^{*} decrece rápidamente a medida que avanza el secado, mientras que en la u_{mf} el descenso es menor sólo afectado por el descenso de la densidad y del d_p de la partícula medido a lo largo del secado. Cuando la humedad de las partículas desciende en torno a X=0.5(g H_2O/g totales) tal y como se puede observar en la Figura 5.1, las microcápsulas pierden la adherencia mostrada al inicio del proceso de manera que la velocidad de mínima fluidización experimental llega a igualarse a la teórica. En esa situación: $u_{mf}^{*} = u_{mf} = 0.32$ m/s y se fijó en este estudio como referencia para la definición del comienzo de la Fase III en la que la humedad residual de las partículas se elimina exclusivamente por calentamiento convectivo, sin aplicación de microondas. A la hora de llevar a cabo los diferentes experimentos NFMD, es preciso tener en cuenta que el proceso de descenso de la velocidad se efectúa en intervalos de tiempo de 2 ó 3 minutos siempre y cuando el lecho de microcápsulas fluidiza. Por tanto, los valores de la velocidad mínima de fluidización asociados a los cambios de fase indicados anteriormente son una referencia difícil de reproducir con precisión, observándose variaciones por las condiciones propias de cada experimento y seguimiento del proceso.

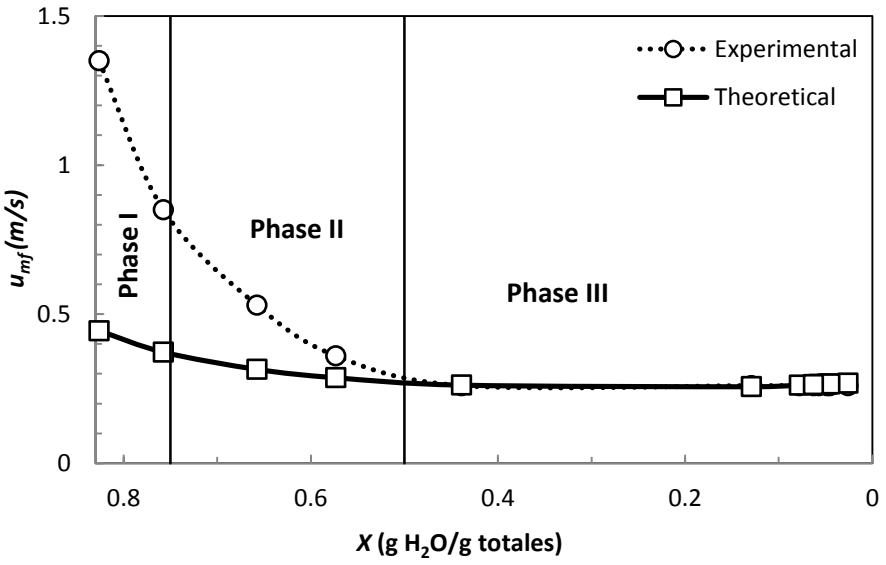

Figure 5.1. Theoretical and experimental minimum fluidization velocity for yeast experiments.

En la Tabla 5.2, para los todos los experimentos de NFMD realizados, puede verse el valor del tamaño de las microcápsulas, la velocidad de mínima fluidización experimental y el contenido acuoso de la partícula, en el inicio del proceso y al final de cada fase junto con el tiempo de proceso.

Table 5.2. Data of X, u_{mf}, d_p and time at the end of each phase for the different NFMD strategies

Code	X_{in}[1]	u_{mf}^*/u_{mf}[2]	Phase I				Phase II				Phase III		
			t(min)	X[1]	d_P (m)	u_{mf}^*/u_{mf}[2]	t(min)	X[1]	d_P (m)	u_{mf}^*/u_{mf}[2]	t(min)	X[1]	d_P (m)
Ll/Ml	0.83	1.35/0.45	20	0.66	2.00E-03	0.72/0.32	35	0.44	1.69E-03	0.30/0.32	275	0.05	1.13E-03
Ml/Mm	0.83	1.35/0.45	10	0.77	2.18E-03	0.94/0.39	30	0.49	1.76E-03	0.30/0.30	195	0.07	1.16E-03
Ll/Lh	0.84	1.37/0.46	8	0.78	2.18E-03	1.02/0.40	18	0.55	1.86E-03	0.38/0.28	240	0.07	1.16E-03
Mm/Ml	0.85	1.38/0.46	10	0.77	2.18E-03	0.94/0.39	25	0.49	1.76E-03	0.30/0.30	240	0.07	1.16E-03
Lm/Mm	0.84	1.37/0.46	10	0.78	2.18E-03	0.95/0.40	25	0.57	1.88E-03	0.40/0.30	235	0.07	1.16E-03
Lm/Hh	0.82	1.34/0.45	10	0.70	2.08E-03	0.76/0.35	20	0.39	1.63E-03	0.30/0.30	210	0.07	1.16E-03
Lm/Hm	0.82	1.34/0.45	10	0.74	2.12E-03	0.78/0.36	23	0.48	1.75E-03	0.28/0.32	240	0.08	1.17E-03
Lh/Hh	0.86	1.39/0.47	5	0.79	2.20E-03	1.04/0.40	15	0.54	1.84E-03	0.28/0.36	240	0.08	1.18E-03
Mh/Hm	0.86	1.39/0.47	10	0.75	2.14E-03	0.85/0.37	20	0.5	1.78E-03	0.32/0.30	240	0.07	1.16E-03

[1]Units of X_{in} and X: gH_2O/g w.b. [2]Units of u_{mf}^*/u_{mf}: m/s

Es preciso tener en cuenta que la velocidad de mínima fluidización obtenida al final de la Fase II se mantiene hasta el final del secado por lo que la Fase III se desarrolló en continua fluidización. Puede observarse, de los datos de contenido de humedad expresados en la Tabla 5.2, una aceptable correspondencia de X con los valores de velocidad mínima de fluidización empleados en cada fase. Así los valores medios de X correspondientes al final de la Fase I y II fueron 0.75 y 0.49 con una desviación típica de de ± 0.04 y ± 0.05 respectivamente que puede considerarse aceptable dadas las distintas condiciones de operación en los experimentos.

5.5 Análisis de las fases de secado

La evolución del contenido de humedad en base seca y los perfiles de velocidad se muestran en la Figura 5.2 para los Experimentos 1 y 9 como representativos de dos estrategias térmicas extremas. Las curvas modeladas se obtuvieron tras la aplicación del modelo matemático que se detallará en secciones posteriores. Las curvas se corresponden a una suave curva de forma sinusoidal, característica de este tipo de procesos de secado con el punto de inflexión correspondiente a la mayor velocidad de secado.

La velocidad de secado normalmente comienza a incrementarse suavemente hasta que se alcanza la temperatura de control deseada. En este momento, aparece el máximo de la velocidad de secado que coincide con la Fase I, según el criterio seguido para el establecimiento de las diferentes fases del secado en función de velocidad mínima de fluidización. Después del punto de inflexión da comienzo la Fase II donde se observa un fuerte descenso de la velocidad de secado, originado por la resistencia difusional a la eliminación de la humedad. El descenso de la velocidad de secado es tanto más acusado cuantos mayores son las temperaturas de proceso. En la Figura 5.2, se pueden observar como en el Experimento 9 (Mh/Hm), en el que las temperatura de proceso son más elevadas que en el Experimento 1 (Ll/Ml). En consecuencia, se produce en el Experimento 9 un cambio mucho más acusado en la velocidad de secado que parece afectar negativamente a la duración del ciclo de secado, como se desprende al analizar los tiempos de secado de ambos experimentos. Finalmente, la Fase III se caracteriza por una casi constante velocidad de secado y cuyo valor se encuentra claramente por debajo de 0.1 g/g min.

El secado por microondas presenta un efecto favorable a la cinética de secado debido al gradiente de humedad originado desde el interior hacia el exterior muy diferente del que se produce en otras tecnologías de secado.

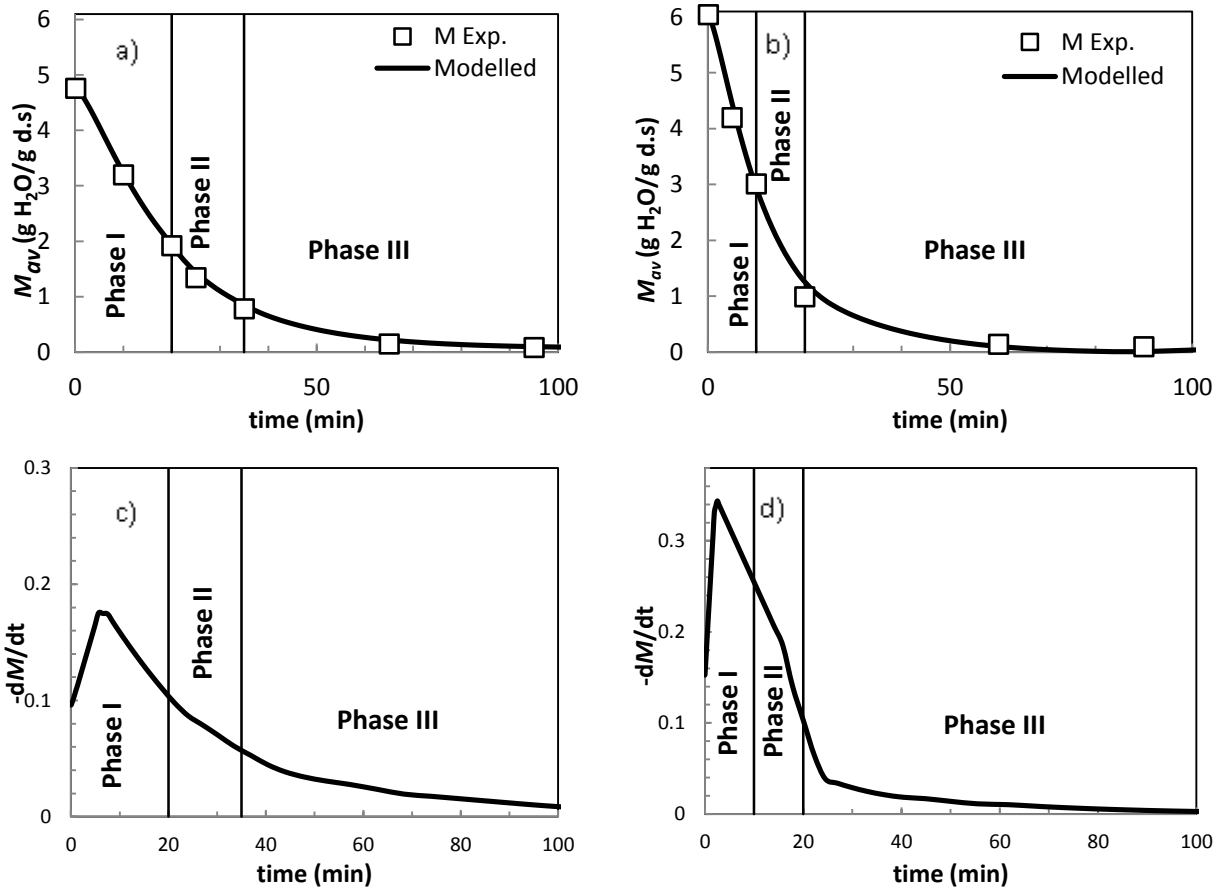

Figure 5.2. Moisture content, M_{av}, and drying rate profiles: (a) and (c) for Experiment 1(Ll/Ml). (b) and (d) for Experiment 9 (Mh/Hm).

Las estrategias de secado en NFMD se analizaron en base a los niveles térmicos establecidos con las temperaturas objetivo (T_f^*) y (T_{in}^*) definidas para las Fases I y II. La potencia de microondas y la temperatura de entrada del aire deben de estar convenientemente reguladas para conseguir las temperaturas objetivos deseados para cada una de las fases. La Fase I se caracteriza por un pequeño incremento de la velocidad de secado en el que la temperatura del producto alcanza un equilibrio dinámico de acuerdo a las condiciones del aire circundante y de la potencia de microondas suministrada. La temperatura de la superficie del producto se estabiliza rápidamente por lo que el calentamiento convectivo y por microondas (negativo a bajas T_{air}) iguala la energía necesaria para la vaporización de la humedad. Durante la Fase II, la velocidad de secado decrece continuamente tanto en cuanto las microcápsulas se van secando. La

temperatura del producto es relativamente estable a lo largo de este periodo, desde que el calor absorbido de microondas decrece en consonancia con el contenido de agua, el cuál va disminuyendo. En este trabajo la transición de la Fase II a la III tiene lugar en el momento en el que el lecho comienza a fluidizar y se apagan las microondas, ya que el contenido de humedad es bajo y el calentamiento por microondas podría afectar negativamente a la calidad del material encapsulado.

En la Figura 5.3, se representa el contenido en humedad M_{av} (en base seca) de las microcápsulas a lo largo de cada fase, en el que se observa una pendiente acusada durante las Fases I y II, aunque en la Fase II la velocidad de secado comienza a descender intensamente. Es por ello que al comienzo de la Fase III, una vez que ya se ha eliminado más del 80% del contenido de humedad inicial la pendiente del perfil de humedad es considerablemente bajo. A continuación, se desconectan las microondas y se observa una ligera pendiente descendiente en el contenido de humedad hasta el final del proceso cuando el material alcanza el valor de actividad de agua necesario según los requerimientos de calidad. Todas las cinéticas aparecen recogidas en el Anexo B

Durante los experimentos se han monitorizado tanto la masa como la temperatura. La pérdida de masa se tomó a diferentes tiempos y siempre al final de cada fase. La diferencia entre la temperatura de entrada, la de salida y la de la superficie del producto se observa en la Figura 5.3 correspondiente al Experimento 1 (Ll/Ml)**.** Todas las cinéticas y las diferentes temperaturasaparecen recogidas en el Anexo B para cada uno de los experiemntos.

Durante el primer periodo la temperatura de entrada del aire se controló a 5ºC, y la temperatura de la superficie fue entorno a 15ºC, mientras en la segunda fase, la temperatura de la superficie se incrementó hasta los 30ºC. Tal y como se ha mencionado en el apartado experimental la (T_s) se controla indirectamente a través de la temperatura en el interior del lecho, (T_f) y estimada con la temperatura media del aire (T_{air}). Como la (T_{out}) puede presentar un incremento significativo respecto a la (T_{in}) la estimación de los valores experimentales de (T_s) pueden tener diferencias respecto a los valores (T_s^*).

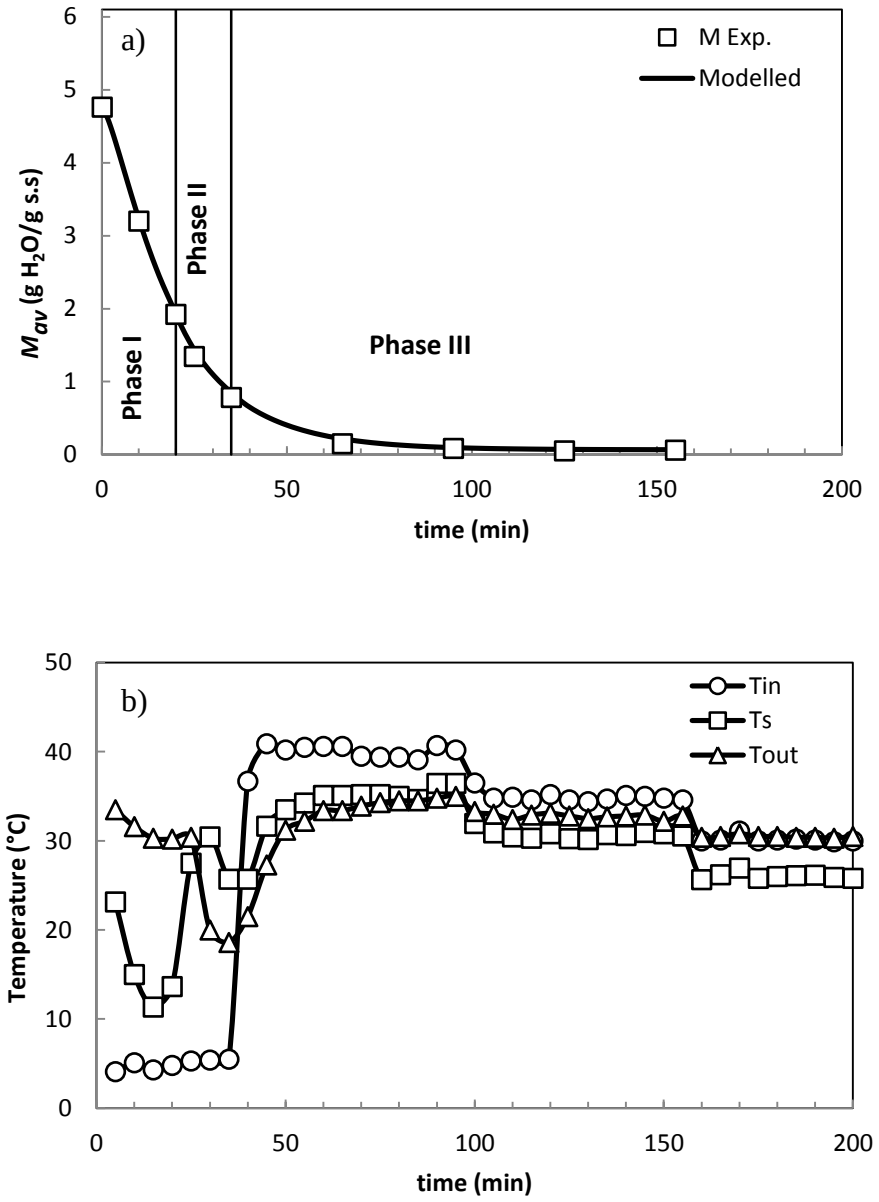

Figure 5.3. Moisture content and temperature profiles during Experiment 1 (Ll/Ml). (a) *M vs* time. (b) T_{in}, T_s, T_{out} *vs* time

Al final del proceso de secado en la Fase III se puede observar una pequeña diferencia entre las temperaturas de entrada, salida y de la superficie del material como se muestra en la FiguraFigure 5.3b. Se cree que la vaporización en la interfase requiere del calor obtenido ya sea de la superficie de la partícula o del aire circundante, en una cantidad variable para cada uno, durante el proceso. No obstante, en ocasiones, como en el experimento referido en la Figura 5.3, la pérdida de calor debido a la convección por la baja temperatura de entrada puede ser 2 ó 3 veces superior a la de vaporización. Esta conclusión se obtuvo de los estudios de modelización realizados gracias al programa

FlexPDE® y que se expondrán en las secciones posteriores. La Figura 5.3 corresponde al Experimento 1 (Ll/Ml) en el que se empleó una temperatura del aire a la entrada de 5 ºC, manteniendo un elevado nivel térmico en el producto. En consecuencia, puede verse como la temperatura del aire a la salida experimenta una fuerte elevación por el flujo de calor convectivo, sobre todo en la Fase I, para descender posteriormente como consecuencia del menor espesor del lecho.

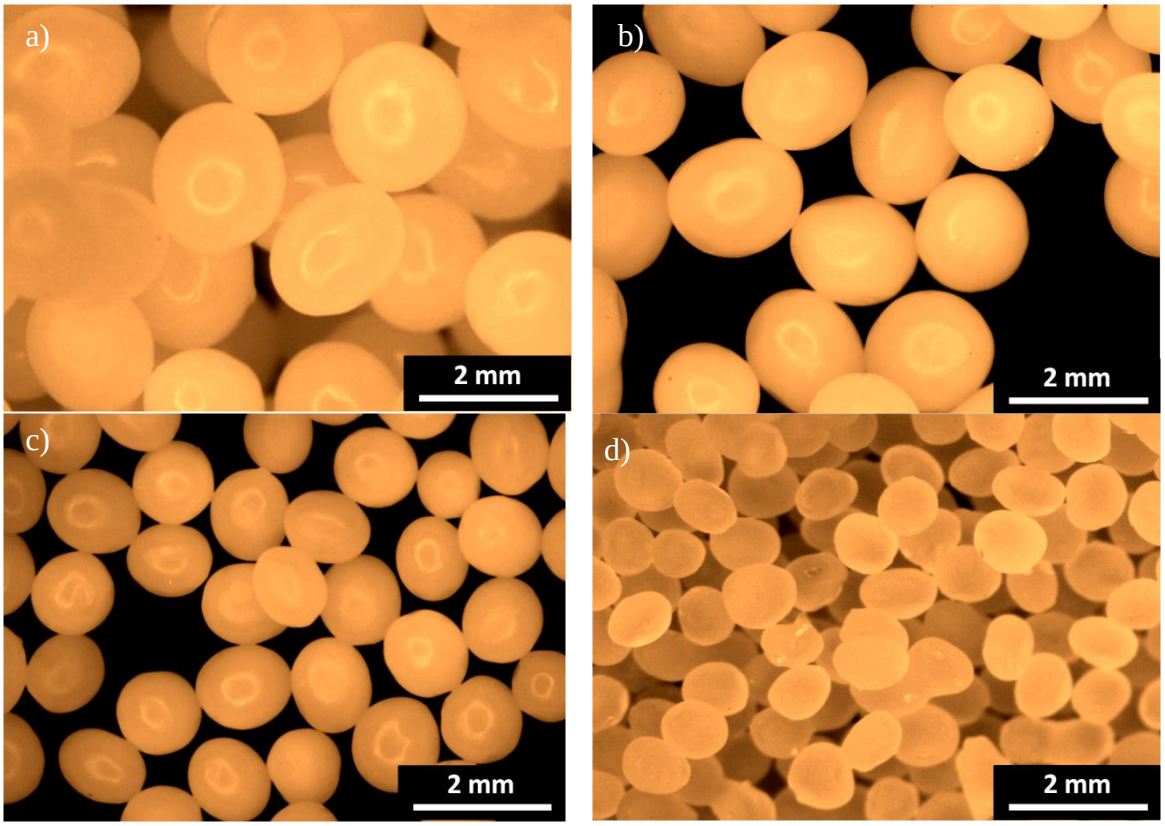

Figure 5.4. Micrograph of the microcapsules at different drying times for Experiment 7(Lm/Hm). a) X_{in}=0.80, d_p=2.12mm; b) X_{in}=0.51, d_p=1.8mm; c) X_{in}=0.24, d_p=1.4mm; d) X_{in}=0.05, d_p=1.1mm

A la hora de analizar los perfiles térmicos, es preciso tener en cuenta la fuerte reducción de masa durante las Fases I y II que afecta directamente al espesor del lecho de partículas a través de una reducción de su tamaño, como se ha podido comprobar en la Tabla 5.2 anterior. Una idea de la reducción del tamaño asociado a la perdida de humedad puede observarse en la Figura 5.4 para el Experimento 7 (Lm/Hm).

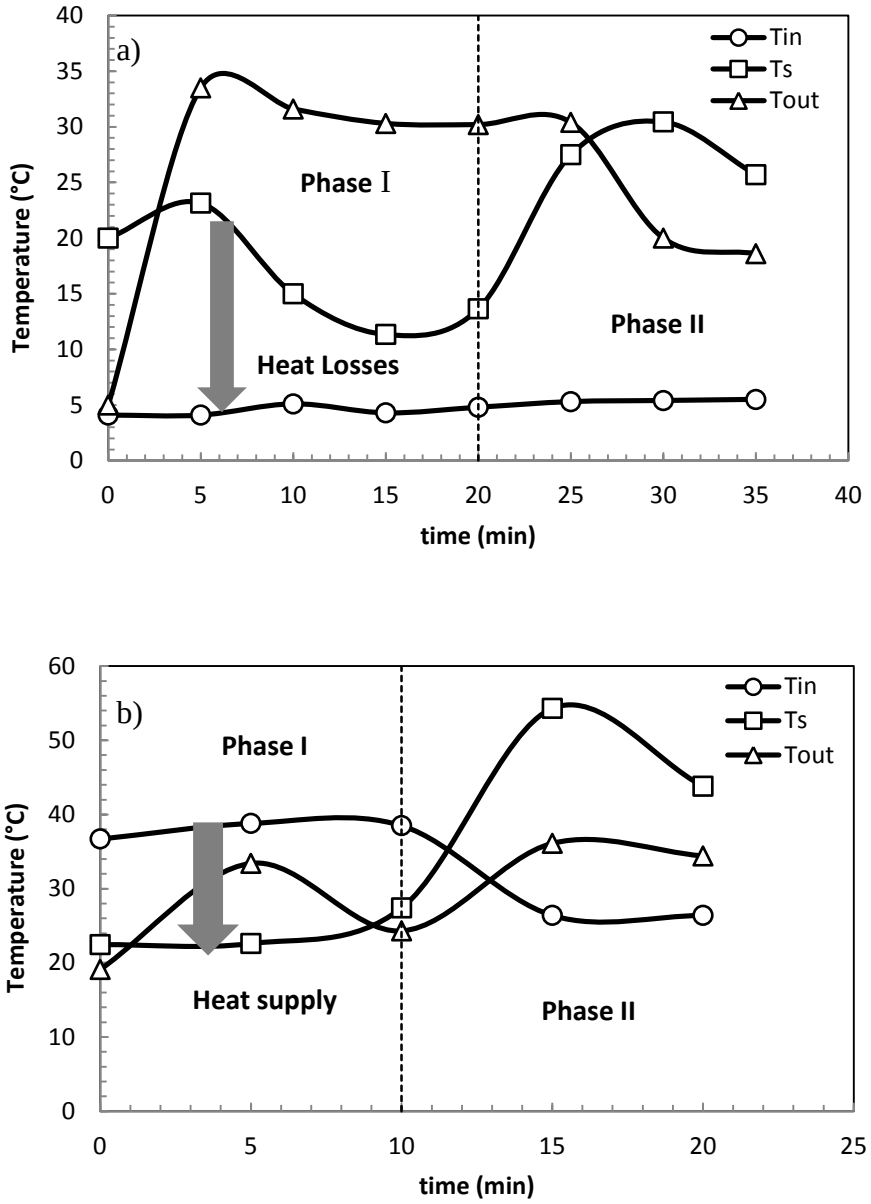

Figure 5.5. Inlet, outlet and surface experimental temperatures *vs* time on the phases I and II (microwaves on). (a) for Experiment 1 (Ll/Ml) (b) for Experiment 9 (Mh/Hm).

Así en la Figura 5.4 a y b corresponden al inicio y final de la Fase I, observándose la importante variación con respecto al resto del secado, Figura 5.4 c y d. Como consecuencia se ha observado una reducción en el espesor del lecho de partículas estimado en torno a un 25 % del valor inicial al final de la Fase II. De esta manera, el tiempo de contacto del aire con el sólido durante la Fase II desciende sensiblemente debido a la reducción del espesor del lecho que explicaría el comportamiento de la temperatura, T_{out} respecto de la T_{in} en los Experimentos 1 y 9 que se recogen en la Figura 5.5, donde puede observarse los efecto de flujos convectivo contrarios. En el

Experimento 9 (Mh/Hm) se produce preferentemente un flujo de calor convectivo que supone un calentamiento extra, aparte de las microondas, que ocasiona un descenso de la temperatura T_{out} respecto de la T_{in} en la Fase I (Figura 5.5 b). Una situación contraria se da en el Experimento 1 (Ll/Ml) causando una elevación de la T_{out} (Figura 5.5 a). En la Fase II, el intercambio calorífico entre el producto y el aire es mucho menos acusado por la reducción importante de la altura del lecho y la temperatura T_{out} se aproxima a T_{in}. El resto de experimentos con las temperaturas experimentales obtenidas se muestran en el Anexo B.

El comportamiento extremo de los Experimentos 1 y 9, como se ha podido observar, da lugar a un efecto contrario en el consumo de energía por microondas. No obstante, a pesar de que éste es mayor para el Experimento 1, hay un gradiente del interior hacia el exterior que favorece los mecanismos de eliminación de humedad y parece ser un factor importante en la calidad final del producto observada como se verá en el apartado siguiente.

5.6 Calidad del producto deshidratado

A la hora de determinar la calidad final del producto deshidratado se tuvieron en cuenta dos parámetros: la actividad del agua, y la viabilidad del producto antes y después del proceso de secado. En relación con la viabilidad de los probióticos, así como la contaminación microbiana en los alimentos, el término de la actividad del agua es más importante que el contenido de humedad. La actividad de agua (a_w) define el agua libre (moléculas de agua no ligadas a moléculas del alimento) en el producto, el cual está disponible para reacciones metabólicas de los microorganismos. Cuanto menor sea la actividad del agua, mejor será la estabilidad del probiótico en el producto deshidratado, pero a valores muy bajos de la actividad del agua, incluso la oxidación de las membranas lipídicas puede reducir la viabilidad (Viernstein, *et al*., 2005).

Los probióticos son microorganismos, que deben de ser viables cuando se suministran con el fin de ejercer sus efectos beneficiosos para la salud. Por otra parte, en productos en los que se anuncia un beneficio para la salud, la dosis necesaria para un efecto positivo en la salud debe ser etiquetado en el producto, que debe incluir también el

número de microorganismos viables que se encuentran al final de la vida útil del producto, en lugar de sólo mostrar los presentes inicialmente (FAO / OMS, 2002).

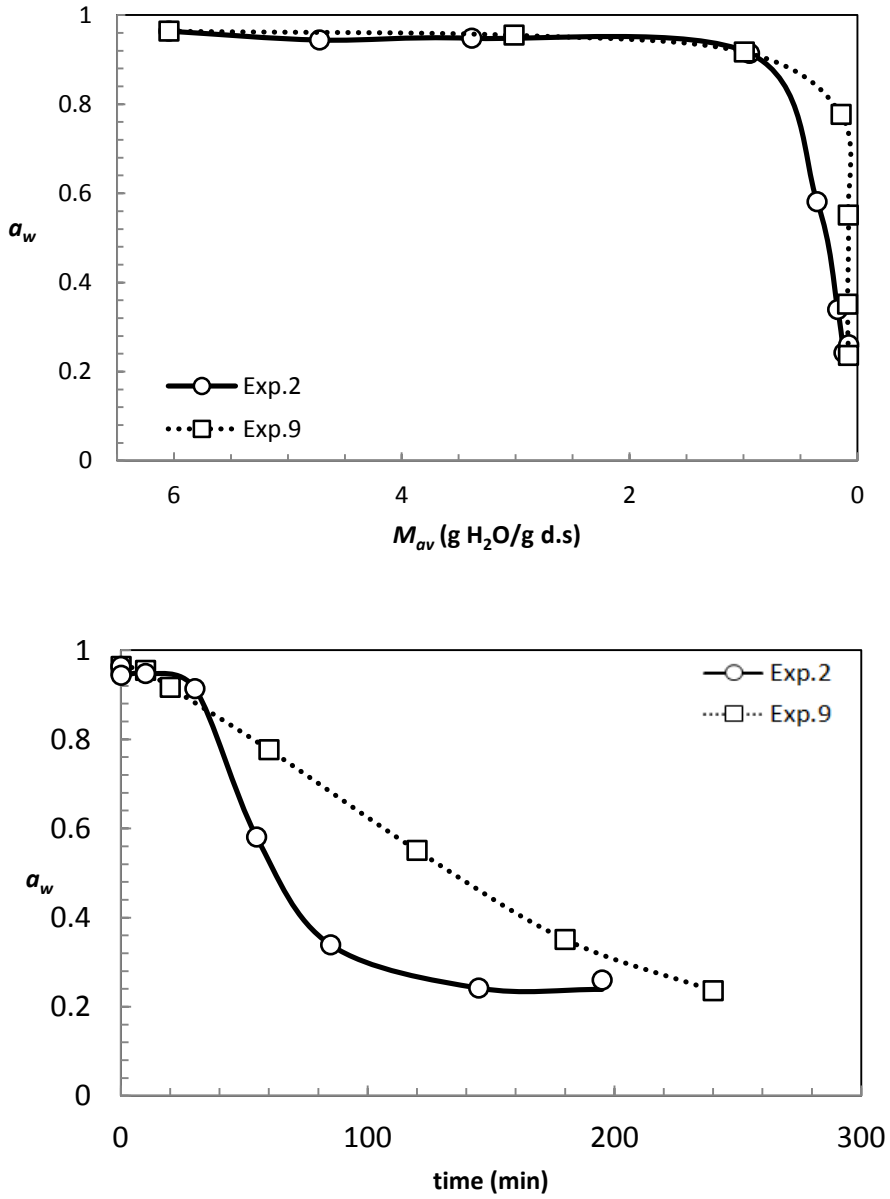

Figure 5.6. Water activity *vs* moisture profiles for Experiments 2 and 9. (a) a_w *vs* M_{av} (b) a_w *vs* time.

La actividad del agua final deseada se estableció alrededor de 0.25 a fin de asegurar la estabilidad del material deshidratado (Chávez yLedeboer, 2007, Manojlovic, *et al.*, 2010, Viernstein, *et al.*, 2005). Este valor de actividad de agua se consiguió teniendo en cuenta los estudios previos para averiguar el tiempo de procesamiento necesario para cada gradiente térmico para alcanzar el valor de actividad de agua deseado. El contenido de humedad se determinó por el método de Karl-Fischer. Los resultados correspondientes

expresados de forma porcentual (KF) expresan el contenido de agua de la muestra en base húmeda. El KF final se utilizó para la determinación de la masa de sólido seco contenida en la muestra, para cada experiemnto de secado realizado. A partir de ese valor se puede establecer el valor de $M_{av,t}$ en base seca para cada momento a través de las Ecuaciones (4.4) y (4.5) descritas anteriormente.

Los resultados de actividad del agua se analizaron para determinar la homogeneidad de la distribución del contenido de agua a lo largo del proceso de secado, como se muestra en la Figura 5.6. Durante la Fase I y II, los valores más altos de la velocidad de secado se da lugar alrededor de la transición de la Fase I a la II y los perfiles de humedad *M vs* tiempo muestran una pendiente casi constante y la velocidad de secado disminuye progresivamente hasta conseguir de un 80 a un 90% del contenido de agua inicial contenido. Durante la Fase III, el contenido total de humedad no sufre un cambio apreciable, pero la actividad del agua disminuye significativamente a lo largo del tiempo como se puede ver en la Figura 5.6 b. El suave descenso de la actividad del agua a lo largo del Experimento 9 no fue favorable según los resultados de viabilidad. Por el contrario, en el Experimento 2 según los datos de viabilidad obtenidos se observó un comportamiento no tan perjudicial debido a la transición rápida por los valores de actividad del agua críticos (Aronsson y Rönner, 2001).

$$Survival(\%) = \frac{Log\ cfu_{fin}/g}{Log\ cfu_0/g}100 \qquad (5.9)$$

Los análisis de la viabilidad de los probióticos (dado como porcentaje de supervivencia) se obtuvieron tras realizar un recuento de las unidades formadoras de colonias (cfu) de las muestras iniciales para compararlas con las muestras finales obtenidas tras el proceso de secado obteniendo el resultado como se puede ver en la Ecuación (5.9) (Chávarri, *et al.*, 2010b). En la Tabla 5.3, se muestran, el valor promedio de la velocidad de secado para cada experimento, el tiempo de procesamiento, la actividad de agua, el *KF* (%), y el de supervivencia (%) del proceso en general al final de cada una de las fases de secado establecidas.

La liofilización se tomó como referencia para la selección de las condiciones óptimas para los probióticos. Teniendo en cuenta que los datos de la actividad del agua y el contenido de humedad (*KF*) no difieren significativamente, unos experimentos de

otros. La reducción del tiempo en este nuevo proceso de secado es significativamente positiva a través del secado por microondas respecto de la liofilización. Teniendo en cuenta la cinética y los criterios de calidad se observó que los Experimentos 2, 3 y 5 mostraron los valores de viabilidad más altos que los obtenidos en la liofilización.

Table 5.3. Quality parameters obtained for all experiments

Exp.	r_{I-II}	$M_{fin\ II}$	r_{global}	time (min)	*KF*(%)	Survival (%)	Code
1	0.114	0.783	0.017	275	6.726	74.4	Ll/Ml
2	0.126	0.946	0.024	195	7.522	96.3	Ml/Mm
3	0.219	1.245	0.021	240	7.706	94.1	Ll/Lh
4	0.184	0.945	0.023	240	7.577	88.9	Mm/Ml
5	0.163	1.309	0.023	235	7.458	92.2	Lm/Mm
6	0.198	0.646	0.022	210	7.599	87.7	Lm/Hh
7	0.159	0.907	0.019	240	8.414	77.7	Lm/Hm
8	0.349	1.184	0.026	240	8.830	74.2	Lh/Hh
9	0.254	0.992	0.025	240	7.726	55.0	Mh/Hm
Lyo.			0.007	720	8.855	91.1	-

*Units: $r_{I,\ II}$ and r_{global}: g H_2O/g d.s. min, $M_{end\ phase\ II}$: g H_2O/g d.s.

A nivel global, los mejores resultados se muestran en el Experimento 2. A pesar de que la velocidad de secado a lo largo de las Fases I y II (r_{I-II}: 0.126 g H_2O/g d.s. min) fue la más baja. La velocidad de secado global fue muy similar y bastante superior a la de los Experimentos 3 y 5.

5.7 Modelo matemático del proceso NFMD para microcápsulas esféricas.

Durante el proceso de secado estudiado, se combina un secado por microondas con un secado convectivo de las partículas cilíndricas de material. Como se ha mencionado anteriormente, se pueden distinguir tres fases en el proceso, en cada una de las cuales tienen lugar diferentes mecanismos de transferencia de materia y de energía (Ingham, *et al.*, 2007).

La evolución de la temperatura en cualquier zona del interior del material se proporciona a partir de ecuaciones diferenciales, obtenida a partir del material tridimensional y del balance de energía para una partícula en cada fase.

Las principales suposiciones para la elaboración de las expresiones de los balances de materia y de energía son:

1. Las partículas del material se considerada que poseen una forma esférica regular.
2. El contenido de humedad del material experimental observado corresponde al valor medio de todas y cada una las cápsulas (mezcla completa).
3. El material es homogéneo en su composición y propiedades físicas, térmicas y dieléctricas (isotropía).
4. El flujo de calor se transfiere en dirección radial.
5. El proceso de evaporación ocurre completamente en la superficie externa del material.
6. Una fracción del total del calor requerido para la vaporización es absorbido por el aire que rodea al material y la otra parte por la propia superficie del material.

Balance de materia

Para la obtención de la pérdida de masa del material encapsulado y a fin de ajustar al perfil de masa obtenido experimentalmente se procedió de forma semejante a lo expuesto en el Capítulo 3, resolviendo las Ecuaciones (3.4-3.6), según si se considera o no la contracción y la humedad superficial de la partícula. La resolución se hizo de la misma forma con ayuda de programa FlexPDE®, con la única diferencia que en este caso, para las microcápsulas de levadura, se aplicó a la geometría esférica en lugar de cilíndrica. Esta diferencia se recoge en el programa de resolución correspondiente al (*script*) del Anexo B, en el apartado REGION, donde se define la geometría del producto.

Balance de energía

También en este caso se procedió de manera semejante a lo realizado en el Capítulo 4 con la resolución de las Ecuaciones (3.10-3.13). Las diferencias corresponden a la geometría esférica a la que se aplica en este caso que se reflejan a la hora de definir la ecuación para el calor absorbido y las condiciones de contorno.

Así, el Q_{abs} es el calor generado por la fuente de microondas y directamente absorbido por el producto, para geometría esférica, se expresa en la siguiente ecuación:

$$Q_{abs} = 2\pi f \varepsilon'' \varepsilon_0 \left(e^{-(R-r)/d_p} + e^{-(R+r)/d_p} \right) E^2 \quad (5.10)$$

Condiciones iniciales y de contorno

Se plantean de forma semejante a lo expuesto en el Capítulo 4 introduciendo las adaptaciones para su aplicación a geometría esférica.

1. Condiciones iniciales. En primer lugar se asume que el material se encuentra a una temperatura uniforme y en equilibrio térmico con el ambiente.

$$t = 0 \qquad T(x,y,z) = T_0 \quad -D_{sph} \le x \le D_{sph}; -D_{sph} \le y \le D_{sph}; -D_{sph} \le z \le D_{sph} \quad (5.11)$$

Siendo, $D_{sph} = 2R$

2. Condiciones de contorno. Debido a la diferencia de temperatura entre la superficie de las partículas y el aire circulante en contacto, se presenta un flujo de calor por convección significativo durante el proceso de secado que se absorbe desde el exterior en la interfase solido-gas. Por otra parte, la vaporización de toda la humedad del material tiene lugar en la superficie externa. Además, muchos autores coinciden en que el calor necesario para la vaporización no se obtiene a partir del material, sino que también se absorbe de la potencia de microondas que actúa directamente sobre la superficie del material (Abbasi Souraki y Mowla, 2008). El término representativo del calor requerido para la evaporación, debe tener en cuenta las condiciones de contorno del sistema.

$$t > 0 \qquad k\left(\frac{\partial T}{\partial x} + \frac{\partial T}{\partial y} + \frac{\partial T}{\partial z} \right) = -h(T_s - T_{air}) + \frac{\partial M}{\partial t} \rho_s Q_{vap} \frac{1}{S_p} w \quad (5.12)$$

Donde,

$$x^2 + y^2 + z^2 = R^2$$

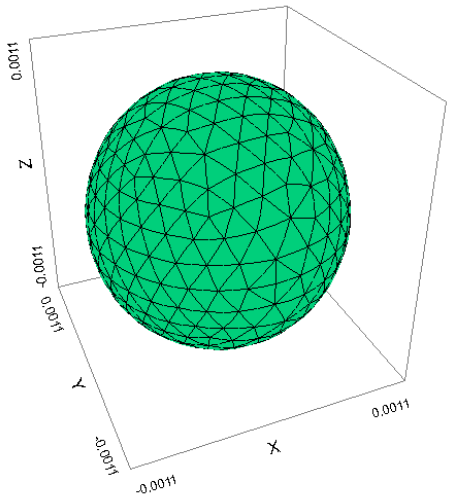

Figure 5.7. Tridimensional representation of a yeast microcapsule showing nodes according to the FlexPDE® solving process.

En la Figura 5.7, se puede observar la representación tridimensional de las dimensiones de la partícula de 0.001125 m de radio de referencia del sistema usado con la distribución de nodos empleada en la resolución de la ecuaciones de los balances de materia y energía.

Propiedades físicas, térmicas y dieléctricas.

Para predecir la distribución de la temperatura durante el calentamiento por microondas es necesario conocer algunas propiedades del material como la densidad, el calor especifico, la conductividad térmica, el calor latente, la constante dieléctrica y el factor de pérdidas que aparecen detalladas en la siguiente Tabla.

Table 5.4. Physical, thermal and dielectric properties of main components of the encapsulating material. (Lide, 2005,Meda, *et al.*, 2005).

Properties	Value/Equation	Properties	Value/Equation
K_w	0.6 W/m°C	C_{paL}	4120 J/kg˚C
P_w	1000 kg/m^3	ε'_{al}	6
C_{pw}	4180 J/kg˚C	ε''_{al}	1.5
ε'_w	0.004T^2-0.5212T+75.241	K_{lev}	0.157 W/m°C
ε''_w	0.0001T^2+1.6001T+22.241	ρ_{lev}	1479 kg/m^3
Q_{vap}	2257·10^3 J/kg	C_{plev}	1720 J/kg˚C
k_{al}	50.22 W/m°C	ε'_{lev}	6
ρ_{aL}	1010 kg/m^3	ε''_{lev}	1.5
ρ_s (1	1368 kg/m^3	ρ_{ap} (2	178kg/m^3

(1,2 Depending on capsule composition (2 Value corresponding to a capsule without shrinkage.

Estas propiedades experimentan cambios durante el experimento de secado debido a la dependencia con la temperatura y el grado de humedad. Para calcular las propiedades del material contendiendo el extracto de levaduras se tiene en cuenta la composición de las microcápsulas según las Ecuaciones (3.16-3.21) del Capítulo 3.

5.8 Balance de materia. Análisis de la cinética de secado.

Se ha empleado un modelo matemático para el cálculo de la cinética del proceso de secado. La determinación de estos parámetros se ha completado usando las Ecuaciones del Capítulo 3 (3.4-3.6). La secuencia de comandos (Script) se recoge en el Anexo B y resuelve el balance de materia empleando las ecuaciones recogidas en la Tabla 5.5.

Table 5.5. Equations and fitting parameters for mass balance.

Equations	Profiles	Fitting parameters
$\frac{\partial M}{\partial t} = D\nabla^2 M$	*M vs t*	β, *D*
$M_s = M_e + (M_0 - M_e)\exp(-\beta t)$	M_s *vs t*	

Para lograr el perfil de pérdida de masa, se analizaron los diferentes valores de β y *D.* Los valores de los coeficientes de difusión fueron diferentes para cada una de las fases de secado establecidas. Para la verificación de los valores empleados se compararon los perfiles obtenidos con el modelo, con los datos experimentales.

Los experimentos realizados con las microcápsulas de levaduras se ajustaron con diferentes valores del parámetro β, definido a través de la Ecuación de Shivhare (3.6) recogida en la Tabla 5.5, y de *D* para cada uno de los experimentos. El modelo se ejecuta en el programa FlexPDE®. De acuerdo con el procedimiento de cálculo el programa simula la cinética de secado para determinados valores de *D* y β a fin de los valores que proporcionen la evolución simulada del contenido de humedad del producto que mejor se ajuste al perfil de humedad obtenido experimentalmente. Como el programa de cálculo proporciona la distribución de la humedad en la partícula *M* (*x*,*y*,*z*) a cada tiempo, al igual que se hizo también en el Capítulo 4, deben reprocesarse los datos para proporcionar el

valor promedio $M_{av}(t)$, según la Ecuación (4.6). Debe ajustarse al valor experimental de la partícula o microcapsula.

En la Figura 5.8 se puede observar, el buen ajuste obtenido de los datos obtenidos con el programa aplicando el modelo previamente descrito con los datos experimentales. El parámetro β debe ajustarse previamente los datos a través de la humedad de la superficie (M_s) cuyo valor no puede exceder el valor medio de humedad de las partículas. El aumento del valor de β, hace que el perfil de humedad descienda de manera notable, especialmente a lo largo de la Fase I, tal y como se observa en la Figura 5.8.

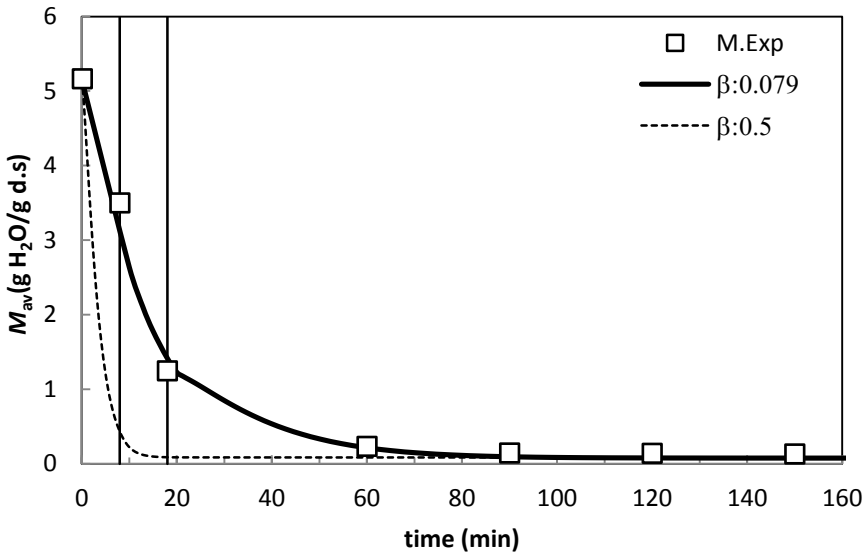

Figure 5.8. Different drying profiles depending on β for Experiment 3(Ll/Lh).

El secado al final de la Fase II implica ya la eliminación de más del 80% del contenido inicial de agua en la partícula. En la fase inicial, los perfiles de humedad se ven afectados por las condiciones de contorno a través del parámetro β. Esto afecta al contenido de humedad en la superficie del material dependiendo de las condiciones de secado. Los valores de β oscilan entre 0.057 y 0.150 min^{-1} dependiendo de las condiciones establecidas para cada uno de los experimentos propuestos.

El proceso de ajuste descrito se ha realizado para el ajuste de los diferentes niveles térmicos aplicados obteniendo para cada uno de ellos los valores de los coeficientes de difusión y β recogidos en la Tabla 5.6.

Table 5.6. Diffusion coefficients: D_1, D_2, D_3 and coefficient β values for the experiments.

Exp.	Code	β(min^{-1})	D_1(m^2/min)	D_2(m^2/min)	D_3(m^2/min)
1	Ll/Ml	0.060	3.20E-08	4.80E-08	0.70E-08
2	Ml/Mm	0.057	4.20E-08	4.50E-08	3.20E-08
3	Ll/Lh	0.079	6.00E-08	8.00E-08	0.99E-08
4	Mm/Ml	0.077	2.20E-08	6.00E-08	1.20E-08
5	Lm/Mm	0.055/0.06	5.00E-08	5.00E-08	0.97E-08
6	Lm/Hh	0.098	6.10E-08	8.00E-08	1.00E-08
7	Lm/Hm	0.075	3.40E-08	5.60E-08	1.00E-08
8	Lh/Hh	0.120	10.00E-08	10.00E-08	1.08E-08
9	Mh/Hm	0.150	1.30E-08	1.30E-08	0.95E-08

La difusividad es un parámetro efectivo que describe la difusión del agua en fase líquida e incorpora el fenómeno de contracción del volumen del material, cuando no es contemplado en el modelo matemático. La Tabla 5.6 muestra que la difusividad a lo largo de las Fases I y II son más altos debido a que la difusión se da en fase líquida y la humedad del producto es claramente superior a la unidad. Los mayores valores de las difusividades se consiguen en el Experimento 8, en el que el gradiente establecido entre la temperatura de la superficie del aire y el de la superficie fue el más alto, seguido de los Experimentos 5 y 6. En general, el valor de del coeficiente de difusión en la Fase II es el más alto, aunque hay algunas excepciones debido a la combinación de la difusividad en fase gas y líquida y a la estructura más contraída que se da en la Fase III. Así en el Experimento 2 el elevado valor de D_3 parece deberse a las condiciones de secado de las Fases I y II. Una temperatura de entrada del aire baja, implica que se obtenga una estructura más abierta con una mayor difusividad a lo largo de la tercera fase.

Consideración de la contracción

Los cálculos anteriores de D se obtuvieron sin considerar que el volumen inicial sufrió cambios importantes durante el proceso, debido a la reducción del contenido en humedad del interior de la microcápsula. También este caso, de la microcápsulas esféricas con levaduras, se procedió a realizar el estudio del efecto de la contracción sobre la difusividad.

Table 5.7. Rates of the different thermal experiments.

Exp.	Code	v_{r1}(m/s)	v_{r2}(m/s)	v_{r3}(m/s)
1	Ll/Ml	1.71E-05	9.10E-06	3.56E-07
2	Ml/Mm	1.64E-05	1.48E-05	6.36E-07
3	Ll/Lh	2.33E-05	2.49E-05	5.80E-07
4	Mm/Ml	2.20E-05	1.70E-05	4.15E-07
5	Lm/Mm	1.73E-05	2.78E-06	1.92E-07
6	Lm/Hh	2.28E-05	1.71E-05	8.74E-07
7	Lm/Hm	2.25E-05	1.82E-05	4.74E-07
8	Lh/Hh	2.39E-05	1.53E-06	1.48E-07
9	Mh/Hm	2.40E-05	2.00E-06	3.13E-08

Table 5.8. Values for yeasts experiment with and without shrinkage consideration.

Exp.*	Code	β (min^{-1})	D_1(m^2/min)	D_2(m^2/min)	D_3(m^2/min)
1	Ll/Ml	0.060	2.00E-08	3.00E-08	5.00E-09
1	Ll/Ml	0.060	3.20E-08	4.80E-08	0.70E-08
2	Ml/Mm	0.057	1.00E-08	1.50E-08	8.00E-09
2	Ml/Mm	0.057	4.20E-08	4.50E-08	3.20E-08
3	Ll/Lh	0.079	4.00E-08	6.00E-08	2.00E-09
3	Ll/Lh	0.079	6.00E-08	8.00E-08	0.99E-08
4	Mm/Ml	0.077	1.00E-08	4.00E-08	2.00E-09
4	Mm/Ml	0.077	2.20E-08	6.00E-08	1.20E-08
5	Lm/Mm	0.055/0.06	5.00E-08	5.00E-08	6.33E-09
5	Lm/Mm	0.055/0.06	5.00E-08	5.00E-08	0.97E-08
6	Lm/Hh	0.098	4.00E-08	6.00E-08	8.00E-09
6	Lm/Hh	0.098	6.10E-08	8.00E-08	1.00E-08
7	Lm/Hm	0.075	1.00E-08	3.50E-08	5.00E-09
7	Lm/Hm	0.075	3.40E-08	5.60E-08	1.00E-08
8	Lh/Hh	0.120	5.00E-08	5.00E-08	4.83E-09
8	Lh/Hh	0.120	10.00E-08	10.00E-08	1.08E-08
9	Mh/Hm	0.150	0.80E-08	0.80E-08	1.32E-09
9	Mh/Hm	0.150	1.30E-08	1.30E-08	0.95E-08

*Shaded rows: Shrinkage consideration, White rows: Not shrinkage consideration

Las velocidades de los diferentes experimentos se recogen en la Tabla 5.7. Los valores máximos de contracción se alcanzan en la primera fase al producirse la mayor pérdida de humedad. En el Experimento 3, en cambio, es ligeramente superior v_{r2} a v_{r1}, debido al bajo nivel térmico empleado en la primera fase. La consideración de la de contracción afecta a los valores de difusividad, haciendo que disminuyan respecto a los valores sin contracción y posibilita un mejor ajuste a los datos experimentales de pérdida de masa. Los valores de las difusividades con (filas sombreadas) y sin contracción como para el que no lo contempla aparecen recogidos en la Tabla 5.8.

Cálculo del coeficiente de transferencia externa

Para el cálculo del coeficiente de transferencia de materia $k_G\,a$ se emplearon las Ecuaciones de (3.7-3.9) en base a los datos de pérdida de masa y gradiente de presión de vapor en el exterior de la partícula. Para la estimación de la presión de vapor sobre superficie de las partículas se midió la actividad de agua de las muestras extraídas a lo largo del proceso NFMD. De esta manera fue posible obtener la correspondencia de la a_w frente al contenido acuoso del producto (Figura 5.9).

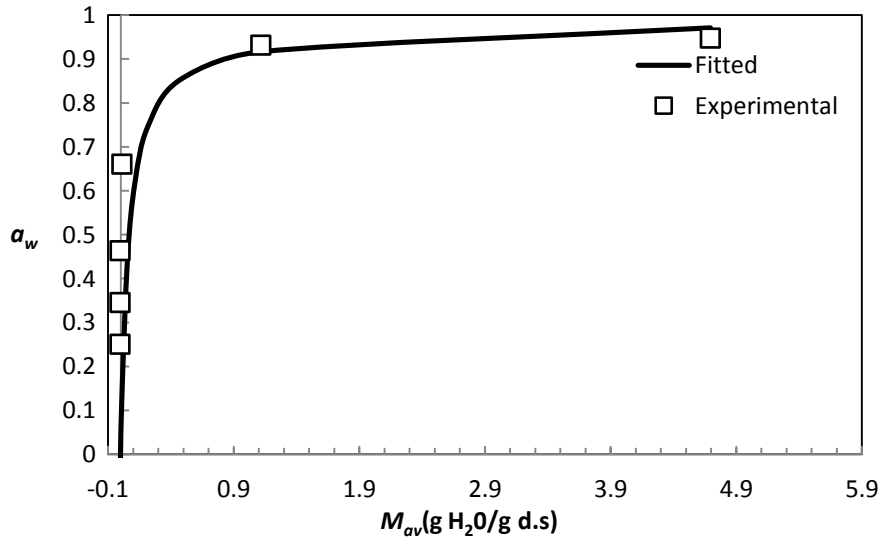

Figure 5.9 Profile for the determination of the moisture content that corresponds to each water activity value.

Una vez que se han realizado y ajustado los balances tanto de materia como de energía, se ha calculado el coeficiente de transferencia $k_G\,a$ según las Ecuaciones (3.7-3.9) y el procedimiento explicado anteriormente. Se puede observar que para el cáculo de este coeficiente se emplean parámetros obtenidos en los balances de materia y energía. Para poder comparar el valor del coefciente de transferencia obtenido para cada uno de los experimentos, se representan los valores del coeficiente con los valores medios de perdida de masa tal y como se muestra en la Figura (5.9). Se observa para la mayoría de casos que inicialmente el valor del coeficiente desciende levemente y al llegar a valores bajos del contenido en humedad cae de forma más pronunciada. Existen diferencias entre los valores obtenidos para cada uno de los experimentos. Los Experimentos 8 y 6 tienen los valores más altos comparandolos con los demás experimentos. Parece ser que que los

valores bajos de la temperatura de la superficie del material en la primera fase y el gradiente térmico aplicado tiene un efecto favorable sobre el parametro $k_G\ a$ y se corresponden con los casos que preentan mayor difusividad y cineticas de secado más rápidas (Tabla 5.3 y 5.8).

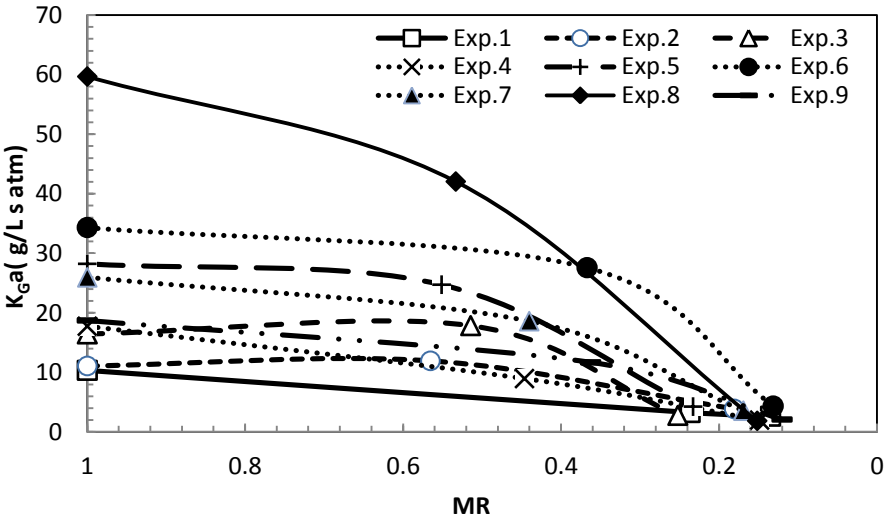

Figure 5.10. External coefficient for the NFMD experiments analyzed.

El comportamiento de $k_G\ a$ en el secado de microcapsulas esféricas contrasta con el comportamiento obsevado con partículas mayores que se explica en el Capítulo 4. En cualquiera de los dos casos, el gradiente en la película de fluido en contacto con la partícula parece esencial. No obstante, mientras que en las particulas grandes de alginato-tilosa los gradientes intermedios (T_s-$T_{in}\approx$ 20 ºC) son los mas recomendables, en el caso de las microcápsulas esféricas lo son, los gradientes termicos altos (T_s-$T_{in}\approx$ 40 ºC) sobretodo asociados a bajas temperaturas en el producto. Como se expuso en el Capitulo 4, el movimiento convectivo en la película de fluido circundante favorece en general el coeficiente externo de eliminación del vapor pero sin llegar a comprometer el aporte calorífico en la superficie de las partículas. Dada la configuracion de experimentos en el caso de la microcápsulas de levadura los gradientes térmicos elevados al contrario de los experimentos del Capitulo 4, suponen un aporte calorífico extra en lugar de pérdida convectiva sin tener efectos para la vaporización de la humedad. Salvo el Experimento 8 donde se da esta característica especial, los valores son muy semejanetes a los obtenidos para las cápsulas cilíndricas de tamaño mas grande.

5.9 Balance de energía. Análisis del consumo energético.

En el modelo que se ha utilizado para realizar el balance de energía se han empleado las Ecuaciones (3.10-3.13) con las modificaciones introducidas de Q_{abs} y condiciones de contorno expuestas en el modelo matemático. El programa se recoge en el Anexo.B. Para lograr el ajuste de los perfiles de temperatura de la superficie experimental del material con el modelo propuesto se probaron diferentes valores del campo eléctrico como único parámetro de ajuste. El resto de valores necesarios se tomaron como constantes. Los coeficientes de convección dependen básicamente de la velocidad de fluidización tendiendo a disminuir a lo largo del secado obteniendo los valores de: 166.7 W / m^{2o}C y 116.7 W / m^{2o}C para las Fases I y II - III, respectivamente a los caudales definidos. Estos valores están dentro del rango (100-400W/m^2K) que otros autores emplean, en secados de características similares al aquí descrito (Abbasi Souraki y Mowla, 2008).

El tiempo de encendido de las microondas se define a través del parámetro β en el programa ya empleado y definido en el Capítulo 4 a través de la Ecuación (4.12). La potencia de microondas aplicada se reguló a través de este parámetro tal como se expuso en dicho Capítulo. La integración de b_{ac} en tiempo finito permite obtener la fracción de tiempo encendido a lo largo del proceso (b_{ac}) que sirve para estimar el tiempo real en el que las microondas están encendidas.

El b_{ac} a cada tiempo se representa en la Figura 5.11 para el Experimento 1. El área bajo la curva del perfil del b_{ac} permite estimar el tiempo real de encendido de las microondas en el proceso. El correcto ajuste obtenido para el Experimento 8 de levaduras se muestra en la Figura 5.12. Las fluctuaciones que se observan en la figura están relacionadas con el empleo del parámetro *b*. Estas oscilaciones son frecuentes en modelos de simulación de calentamiento por microondas (Gulati, *et al.*, 2015) por la alternancia de los periodos de conexión y desconexión para ajustarse a la temperatura experimenal T_s al aplicar un determinado campo eléctrico *E* en las Fases I y II. Éste fue seleccionado en cada experimento para evitar fuertes oscilaciones superiores a ±5ºC en el ajuste. Los resultados del campo eléctrico se recogen la Tabla 5.9. El campo eléctrico se definió como un valor único para todas las fases; sin embargo, en los Experimentos 4 y 5 fue necesario el empleo de dos campos eléctricos. El alto contenido de humedad durante la primera fase facilita alcanzar la temperatura de la superficie objetivo con un menor

campo eléctrico. En cambio, por el bajo contenido de humedad en la segunda fase se necesitó un mayor campo eléctrico para el ajuste.

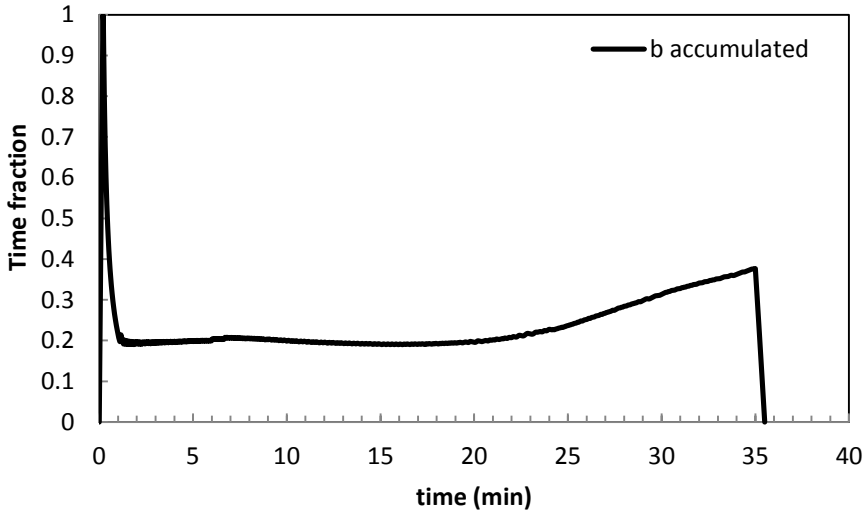

Figure 5.11. Representation of b accumulated value for Experiment 1 (Lm/Ml) of yeasts.

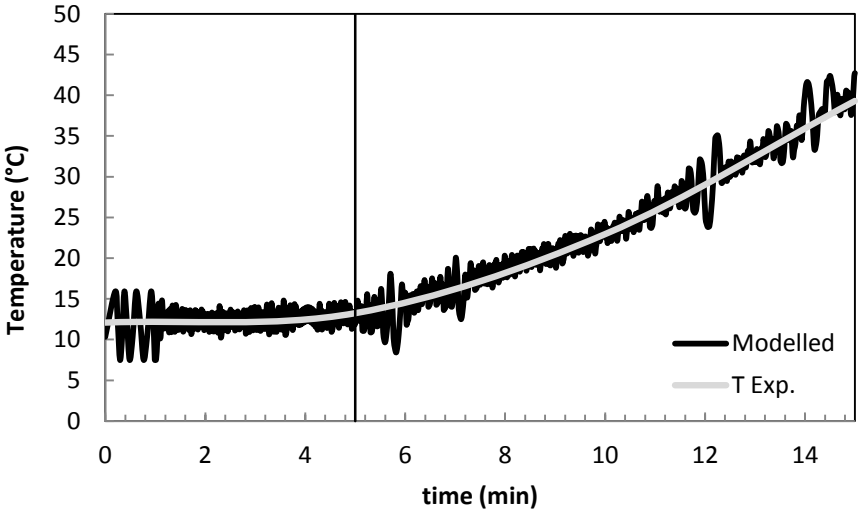

Figure 5.12.Temperature modelled and experimental in Experiment 8 (Lh/Hh) for yeasts.

Table 5.9. Electric field (*E*) for different experiments.

Exp.	Code	*E*(V/m)
1	Ll/Ml	1800
2	Ml/Mm	1750
3	Ll/Lh	1600
4	Mm/Ml	600/1800
5	Lm/Mm	1000/2500
6	Lm/Hh	1720
7	Lm/Hm	1820
8	Lh/Hh	2000
9	Mh/Hm	1900

Existe un compromiso entre la primera y segunda fase ya que un campo eléctrico bajo hace que no se alcancen las temperaturas objetivo y un campo eléctrico alto en cambio provoca el sobrecalentamiento del material durante la primera fase. En general, el campo eléctrico es muy similar en todos los experimentos de secado. El valor más alto se obtuvo para el Experimento 8, debido a la alta temperatura de la superficie a alcanzar (45°C).

La modelización del proceso NFMD permite estimar la cantidad de energía de microondas requerida según las condiciones operacionales aplicadas. Con el fin de evaluar la energía consumida por los diferentes experimentos de levaduras, se define *G* mediante la siguiente ecuación:

$$G = \int_0^t Q_{abs}(t)dt \tag{5.13}$$

Donde Q_{abs} es el calor específico absorbido (J/m^{3}min).

La Figura muestra el calor absorbido (Q_{abs}) del Experimento 1 y *G* se obtuvo tras el cálculo del área bajo la curva.

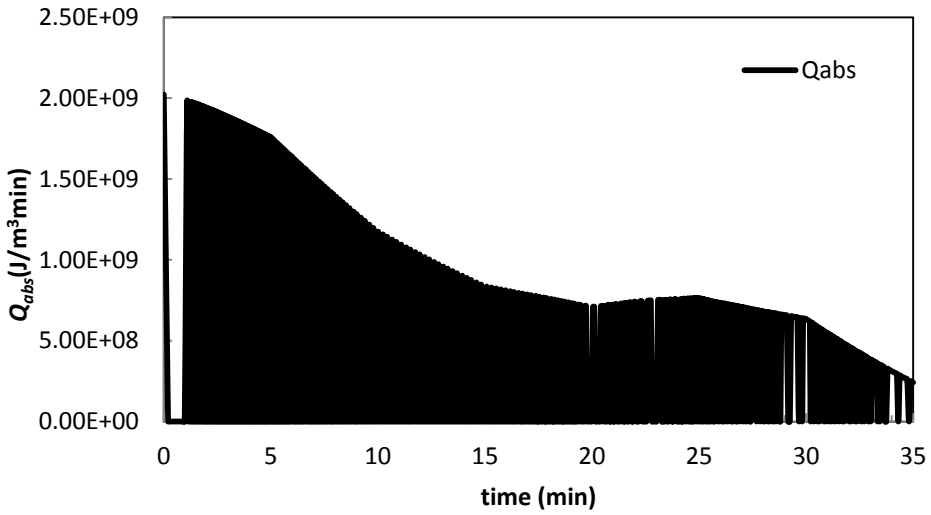

Figure 5.13. The diagram of $Q_{absorbed}$ for the Experiment 1 (Ll/Ml).

$$G_{\max} = \frac{G}{t_{on}} \cdot t_{total} \tag{5.14}$$

El valor de Q_{abs} disminuye con la reducción del contenido de humedad. Además, el consumo máximo, se puede calcular utilizando la Ecuación (5.14) que sería como si la energía de microondas hubiese estado activa durante todo el proceso.

El uso de G_{max} durante el proceso experimental no vale la pena porque produce daños en el producto final. Este valor se ha calculado para la estimación del consumo máximo. Toda esta información se recoge en la Tabla 5.10.

En general, el consumo de energía se puede dividir en tres partes: la pérdida por convección, el calentamiento del material y la vaporización. La energía de vaporización empleada en el proceso de secado es de aproximadamente 2.02 kJ /cm^3 relacionado con el calor latente de vaporización (Lide, 2005). El resto de la energía se emplea en la pérdida convectiva y el calentamiento del material termo-sensible.

Table 5.10. Microwave energy consumption for drying of yeast microcapsules

EXP.	CODE	t_{on} (min)	G(kJ/cm^3)	G_{max}(kJ/cm^3)
1	Ll/Ml	8.46	10.66	44.09
2	Ml/Mm	8.52	10.99	38.68
3	Ll/Lh	5.41	5.20	17.33
4	Mm/Ml	12.36	11.41	23.07
5	Lm/Mm	13.25	8.99	16.96
6	Lm/Hh	6.33	6.20	19.61
7	Lm/Hm	7.47	11.45	35.27
8	Lh/Hh	8.19	10.58	19.37
9	Mh/Hm	7.33	13.70	37.37

El Experimento 3 de levaduras tiene las pérdidas más bajas debido a que durante la primera fase se aplica un gradiente térmico bajo usando 15°C para la temperatura de la superficie y 5ºC para la temperatura de entrada del aire. En la segunda fase, la temperatura de entrada del aire es alta (40°C) lo que favorece un aporte convectivo extra al producto a 15°C, reduciendo así el tiempo de encendido de la energía de microondas. Por el contrario, el Experimento 9 tiene las mayores pérdidas convectivas debido al alto gradiente térmico, principalmente durante la segunda fase con una temperatura de entrada del aire de ~20°C y una temperatura de la superficie objetivo de 45°C. Se puede concluir que las pérdidas se incrementan con la diferencia entre la temperatura de entrada y la

superficie. Siendo energéticamente favorable cuando la temperatura del aire de entrada es mayor que la temperatura de la superficie.

Todos estos valores tienen un valor magnificado debido a la evolución térmica del producto. El calor absorbido se calcula considerando que durante el proceso no se realizan paradas (extracción de muestras para seguimiento de masa y a_w) con lo que ese valor lleva asociada este error más elevado en los experimentos en los que operó a temperaturas del producto altas o bajas (H o L). Sin embargo, este hecho no puede ser evitable ya que las muestras deben ser tomadas para recopilar información acerca de la masa y algunos otros parámetros como la actividad de agua (a_w).

Teniendo en cuenta aspectos cinéticos, las condiciones más favorables, requieren un alto consumo de energético. Por lo tanto, debe buscarse un compromiso entre la cinética de secado y y el consumo energético a la hora de seleccionas la estrategia más favorable.

Capítulo 6

APLICACIÓN DEL PROCESO NFMD AL SECADO DE MATERIAL PROBIÓTICO

6 APLICACIÓN DEL PROCESO NFMD AL SECADO DE MATERIAL PROBIÓTICO

Una vez realizada la selección de las condiciones operacionales óptimas para el secado en NFMD con levaduras se procedió a proponer nuevos ensayos para el material probiótico, partiendo de los experimentos seleccionados y realizando pequeñas modificaciones en la temperatura de entrada del aire y de la superficie del material. El siguiente paso ha sido emplear esta novedosa tecnología de secado en microcápsulas de alginato con un contenido de microorganismos para poder analizar la adecuación de esta tecnología a la posterior viabilidad de los microorganismos una vez finalizado el proceso.

6.1 Obtención de material probiótico microencapsulado

En este caso se partió de material probiótico ampliamente empleado en la industria láctea BB12® (*Bifidobacterium animalis subsp. lactis* suministrado por CHR HANSEN, España) en formato congelado, conteniendo una concentración de células activas superior a 8,1 10^{10} cfu/g. Se utilizó una suspensión al 2.5% de alginato y el 83.3% de probiótico (cantidad requerida para obtener una concentración celular del orden de 10^9 cfu/ml, que se extruyó y se cortó con un equipo de *jet cutter* (Chávarri, *et al.*, 2010a).

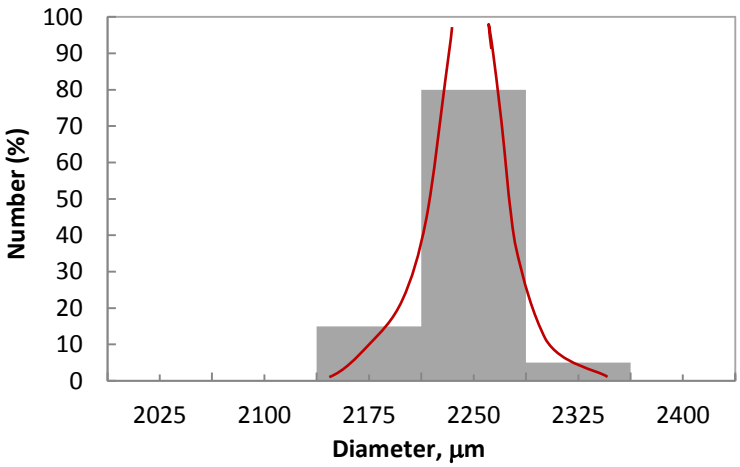

Figure 6.1.The results of grainsize analysis

Se controló la temperatura (12-13ºC) y viscosidad 4660 cP) de la mezcla, diámetro de la boquilla y velocidad de corte del *jet cutter* antes de proceder a la formación de las microcápsulas que se se recogen en una disolución gelificante 0.1M de $CaCl_2$ con un 0.2% de acético y un 0.2% de quitosano, para la obtención del tamaño de las

microcápsulas deseadas. Después del proceso de gelificación llevado a cabo en el baño de cloruro de calcio, se obtuvieron las microcápsulas esféricas con un diámetro en torno a 2100-2400 µm.

Figure 6.2. Micrograph of the microcapsules before the drying process

Para estimar la desviación del tamaño de las microcápsulas se realizó un estudio granulométrico empleando el microscopio óptico (Axioskop 40, Carl Zeiss) y el software Ellix 5.0 (Microvision Instruments, Francia). El valor medio del diámetro obtenido fue de 2250 µm como representativo del tamaño que se obtiene a la temperatura y parámetros de operación empleados tal y como se puede observar en la Figura 6.1. Las microcápsulas una vez extraídas del baño, fueron cubiertas y almacenadas durante un tiempo no superior a 24 horas en un refrigerador a 4ºC hasta su empleo en el experimento de secado correspondiente. En la Figura 6.2, se aprecia el aspecto de las cápsulas antes del proceso de secado Para poder determinar la eficiencia de la encapsulación para el material probiótico empleado se realizó el cálculo con la siguiente ecuación, obteniéndose un resultado del 71.1%, valor muy razonable teniendo en cuenta la infinidad de variables que afectan a la viabilidad de los microorganismos.

$$EY = \left(\frac{N}{N_0} \right) X\ 100 \qquad (6.1)$$

Donde, N es el número de células encapsuladas viables y N_0 es el número de de células libres que se encuentran en la suspensión biopolimérica previa a la encapsulación.

6.2 Equipo experimental de secado NFMD

El equipo empleado para realizar los experimentos de secado se muestra en el Capítulo 3 en la Figura 3.2. Se utilizó un microondas SAIREM LABOTRON 2000 para realizar los experimentos. Otros elementos necesarios para el seguimiento del secado como: sensores de temperatura de fibra óptica, deshumidificador de aire a la entrada, pirómetro óptico, medidor de caudal de aire se encuetran detallados en el Apartado 3.4. En el interior de la cámara se encuentra un lecho cilíndrico de vidrio de 24.4 mm de diámetro y 320 mm de altura, en el cuál se secaron las microcápsulas. El seguimiento de la pérdida de masa se realizó con una balanza en la que a diferentes tiempos del proceso de secado se colgó el lecho para proceder a la medición de la masa.

6.3 Planificación de experimentos NFMD para secado de probióticos

En base a los resultados obtenidos en el capítulo precedente se observó en muchos casos la no conveniencia de emplear niveles térmicos elevados al tomar en consideración aspectos energéticos y de calidad. Así, en este estudio se analizaron seis estrategias térmicas, previa selección de las condiciones y niveles térmicos que resultaron más favorables para el secado de las levaduras, combinando dos niveles para la temperatura de entrada del aire (T_{in}^{*}) con los dos niveles establecidos para la temperatura de la superficie del producto (T_s^{*}). La temperatura de entrada del aire en este caso tomó los siguientes valores: 5ºC y temperatura ambiente (RT, 20 a 24ºC).

Los diferentes experimentos diseñados se basaron en la combinación de estas dos temperaturas del aire con las diferentes temperaturas de superficie objetivo de las microcápsulas. Al igual que se explicó en el Apartado 3.4. Los experimentos se definieron a través de temperaturas objetivo: (T_s^{*}) para la superficie y (T_{in})* (para la temperatura de entrada del aire. A lo largo del proceso de secado, la potencia de microondas fue regulada para alcanzar la temperatura objetivo (T_f^{*}) tal y como se observa en la Ecuación (3.1).

Los valores experimentales de la temperatura en el interior del lecho, (T_{out}), (T_{in}) que junto a (T_f) considerado como la media de la película de aire que rodea las partículas (Figura 3.2) se estiman la temperatura de la superficie T_s según las Ecuaciones (3.2-3.3).

Al igual que en el Capítulo 3 la temperatura de entrada del aire (T_{in}^*) y el correspondiente gradiente térmico establecido desde el interior hacia la superficie del material (T_s^*-T_{in}^*) fueron utilizados para definir los experimentos de NFMD junto con la T_s^*. Los elementos de control del proceso fueron también en este caso la T_{in} y la potencia de microondas que incide más directamente sobre el valor de T_f.

Table 6.1 Definition of the thermal levels applied in the NFMD experiments of microencapsulated probiotics.

Exp.	Code	Phase I			Phase II			Phase III
		T_{in}^*	T_f^*	T_S^*	T_{in}^*	T_f^*	T_S^*	
1	Mm/Mm	20	25	30	20	25	30	RT
2	Ml/Mh	5	17.5	30	40	35	30	RT
3	Ml/Mm	5	17.5	30	20	25	30	RT
4	Ml/Ll	5	17.5	30	5	10	15	RT
5	Hm/Hm	20	32.5	45	20	32.5	45	RT
6	Hm/Ml	20	32.5	45	5	17.5	30	RT

El código empleado en la Tabla 6.1 hace referencia a las condiciones térmicas empleadas en las Fases I y II. Las primeras dos letras se corresponden a las condiciones empleadas en la Fase I y las siguientes dos letras separadas por una barra hacen referencia a la Fase II. En cada fase la primera letra en mayúscula se refiere a la temperatura de la superficie (T_S^*) que puede adoptar los siguientes valores y el correspondiente código: L=15° C (*Low*), M = 30 ° C (*Medium*) y H = 45 ° C (*High*). La segunda letra hace referencia a la temperatura objetivo de entrada del aire T_{in}^* empleando la misma terminología pero empleando la letra en minúsculas: l = 5 °C y m = 20 ºC. Por ejemplo, en el Experimento 1 (Mm/Mm), se empleó tanto en la Fase I como en la Fase II un nivel térmico medio para la temperatura de la superficie del material.

6.4 Fases del proceso NFMD para el secado de probióticos microencapsulados

A continuación, se procede a la descripción de uno de los experimentos NFMD llevado a cabo en el equipo experimental detallado en la Figura 3.2. Inicialmente, se introducen unos 70-75 g de material en el lecho. Después, el recipiente se suspendió en el interior de la cámara. A continuación se colocaron apropiadamente las fibras ópticas para medir la temperatura de entrada del aire, (T_{in}), la temperatura de salida (T_{out}) y la temperatura en el interior del lecho (T_f). Durante el proceso NFMD se consideraron tres fases en las que además de cambiar las temperaturas objetivo T_{in}^* y T_f^* correspondientes a cada fase, debe disminuirse continuamente la velocidad del aire a medida que las

partículas se hacen cada vez más pequeñas y ligeras cuando el lecho fluidiza. Al igual que en el capitulo anterior aplicado a microcápsulas con levadura, en este caso también se consideraron tres fases que se diferenciaron a través del valor de la velocidad de mínima fluidización. A pesar de ser de un tamaño muy similar al del Capítulo 5, la variación en la composición dio lugar a pequeñas variaciones en valores de velocidad mínima de fluidización encontrados.

Se realizó un estudio de fluidización con temperaturas objetivo medias para la (T_s^*) 30 ºC y la T_{in}^*(22-24 ºC) para la determinación de la evolución de las velocidades experimentales u_{mf}. Dado que el proceso NFMD se lleva a cabo en condiciones de mínima fluidización, la velocidad del aire debe ser disminuida cuando el lecho entra en fluidización a medida que las partículas se hacen más ligeras por efecto del secado. Por tanto, existe una relación estrecha entre el contenido acuoso de las microcápsulas y la velocidad del aire empleada a lo largo del proceso.

Las microcápsulas obtenidas según se indica en secciones anteriores presentan un contenido de humedad en torno al 85 % en base húmeda al inicio del secado. En esas condiciones las microcápsulas presentan una elevada adherencia de manera que la velocidad de mínima fluidización del lecho inicialmente es considerablemente superior a la obtenida teóricamente a través de las Ecuaciones (4.2) y (4.3) (Levenspiel, 2014) que aparecen en el Capítulo 4.

Como resultado del estudio de fluidización se obtuvo que inicialmente la velocidad de mínima fluidización experimental, u_{mf}^*, fue de 1.35 m/s, unas tres veces superior a la velocidad mínima de fluidización teórica, u_{mf}, obtenida de acuerdo a las ecuaciones indicadas anteriormente. La u_{mf}^* decrece rápidamente a medida que avanza el secado, mientras que en la u_{mf} el descenso es menor sólo afectado por el descenso de la densidad y del d_p de la partícula medido a lo largo del secado.

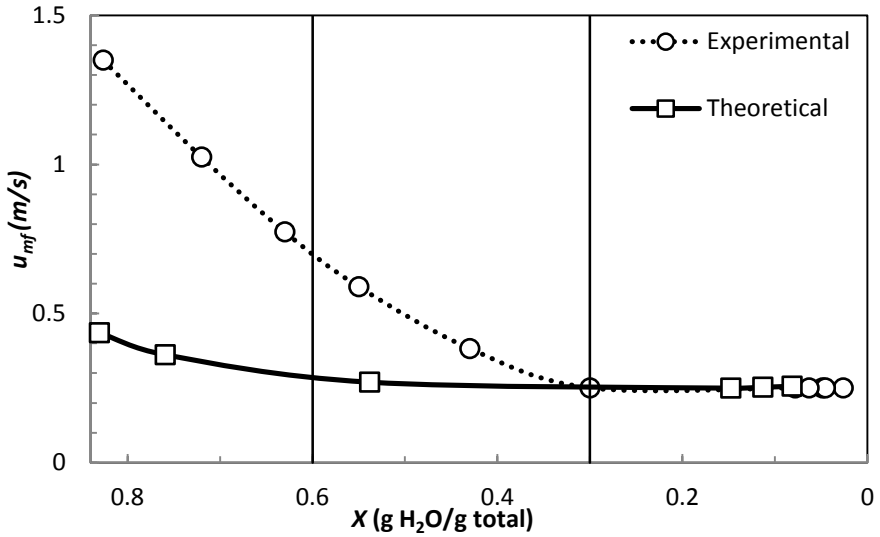

Figure 6.3. Theoretical and experimental minimum fluidization velocity for probiotics.

Cuando la humedad de las partículas desciende en torno a X=0.3 (g H_2O/g totales) tal y como se puede observar en la Figura 6.3, las microcápsulas pierden la adherencia mostrada al inicio del proceso de manera que la velocidad de mínima fluidización experimental llega a igualarse a la teórica. En esa situación: $u_{\mathrm{mf}}^{*} = u_{\mathrm{mf}} = 0.25\,\mathrm{m/s}$ y se fijó en este estudio como referencia para la definición del comienzo de la Fase III en la que la humedad residual de las partículas se elimina exclusivamente por calentamiento convectivo, sin aplicación de microondas. A la hora de llevar a cabo los diferentes experimentos NFMD, es preciso tener en cuenta que el proceso de descenso de la velocidad se efectúa en intervalos de tiempo de 2 ó 3 minutos siempre y cuando el lecho de microcápsulas fluidiza. Por tanto, los valores de la velocidad mínima de fluidización asociados a los cambios de fase indicados anteriormente son una referencia difícil de reproducir con precisión, observándose variaciones por las condiciones propias de cada experimento y seguimiento del proceso. Como consecuencia del estudio del comportamiento de la u_{mf}, las tres fases del proceso NFMD quedan definidas de la siguiente forma:

Fase I: En esta fase la velocidad de entrada del aire se estableció en 1.35 m/s (velocidad mínima observada experimentalmente) en el espacio libre de la columna de fluidización. Durante esta fase la temperatura de entrada del aire se controló próxima a la temperatura objetivo (T_{in}^{*}) y la potencia de microondas se reguló para que la temperatura

experimental del interior del lecho (T_f) se aproximará a los valores establecidos de temperatura del film objetivo (T_f^*).

Fase II: Esta fase comienza cuando la velocidad de mínima fluidización desciende al valor medio entre el valor inicial y el de igualación (0.25 m/s), que corresponde a un contendio acuoso $X \approx 0.6$. La potencia de microondas se reguló para obtener las temperaturas prefijadas, según el experimento, de la temperatura del lecho (T_f^*) y la temperatura de entrada del aire (T_{in}^*) para esta fase.

Fase III: De manera similar, esta fase comienza cuando la velocidad del aire desciende a 0.25 m/s, que corresponde a un $X=0.3$. En esta fase las microondas permanecieron apagadas y el lecho se mantuvo fluidizado hasta el final del proceso definido como el momento en el que se alcanza un valor de actividad del agua entre 0.2-0.3 (Iaconelli, *et al.*, 2015). En todos los experimentos, al comienzo de esta fase, la temperatura de entrada del aire se mantuvo a temperatura ambiente (20 a 24ºC).

Al final de cada una de las fases y cada media hora en la Fase III se realizaron tomas de muestra para la determinación y análisis de los parámetros de la cinética de secado, actividad de agua y contenido en humedad de las diferentes muestras a los diferentes niveles térmicos establecidos.

La Tabla 6.2 muestra para los todos los experimentos de NFMD realizados, el valor del tamaño de las microcápsulas, la velocidad de mínima fluidización experimental y el contenido acuoso de la partícula, en el inicio del proceso y al final de cada fase junto con el tiempo de proceso.

Es preciso tener en cuenta que la velocidad de mínima fluidización obtenida al final de la Fase II se mantiene hasta el final del secado por lo que la Fase III se desarrolló en continua fluidización. Puede observarse, de los datos de contenido de humedad expresados en la Tabla 6.2 a una aceptable correspondencia de X con los valores de velocidad mínima de fluidización empleados en cada fase. Así los valores medios de X correspondientes al final de la Fase I y II fueron 0.60 y 0.30 con una desviación típica de de ± 0.07 y ± 0.05 respectivamente que puede considerarse aceptable dadas las distintas condiciones de operación en los experimentos.

Table 6.2. Data of X, u_{mf}, d_p and time at the end of each phase for the different NFMD strategies.

Code	X_{in}[1]	u_{mf}^*/u_{mf}[2]	Phase I				Phase II				Phase III		
			t (min)	X[1]	d_P (m)	u_{mf}^*/u_{mf}[2]	t (min)	X[1]	d_P (m)	u_{mf}^*/u_{mf}[2]	t (min)	X[1]	d_P (m)
Mm/Mm	0.83	1.36/0.43	27	0.54	1.81E-03	0.50/0.27	39	0.15	1.22E-03	0.25/0.25	165	0.08	1.13E-0.3
Ml/Mh	0.79	1.22/0.39	80	0.52	1.78E-03	0.46/0.26	97	0.14	1.21E-03	0.25/0.25	247	0.09	1.14E-03
Ml/Mm	0.81	1.29/0.41	55	0.52	1.78E-03	0.46/0.26	70	0.32	1.48E-03	0.25/0.25	195	0.09	1.14E-03
Ml/Ll	0.82	1.32/0.42	25	0.68	2.02E-03	0.86/0.32	40	0.44	1.67E-03	0.33/0.25	130	0.09	1.13E-03
Hm/Hm	0.79	1.22/0.39	15	0.69	2.03E-03	0.90/0.32	28	0.34	1.52E-03	0.25/0.25	175	0.08	1.12E-03
Hm/Ml*	0.90	1.58/0.51	60	0.64	1.97E-03	0.75/0.30	70	0.40	1.61E-03	0.33/0.25	150	0.08	1.12E-03

[1]Units of X_{in} and X: gH_2O/g w.b. [2]Units of u_{mf}^*/u_{mf}: m/s

*Sample prepared with suspension of 3.3% alginate and 30% of probiotic.

Estudio calorimétrico de las fases del secado

El momento en el que la velocidad de mínima fluidización observada coincide con la obtenida experimentalmente parece corresponder a un determinado contenido de humedad que resulta característico de cada material. Una vez eliminada una determinada cantidad de humedad las partículas pierden su adherencia, situación que ha sido elegida a la hora de definir el comienzo de la Fase III. El contenido de humedad correspondiente a la presencia mayoritaria de un determinado tipo de agua caracterizado por una mayor interacción con el material sólido de la microcápsula.

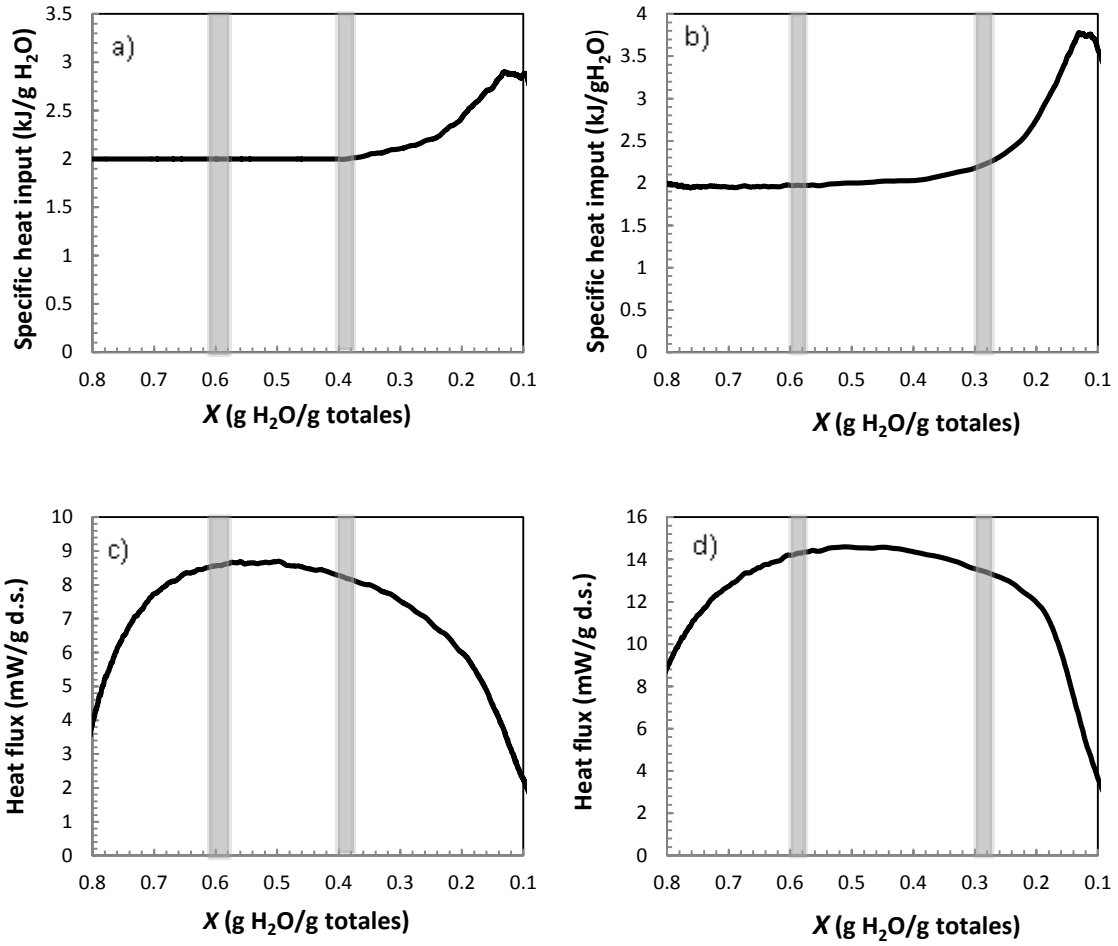

Figure 6.4. Specific heat input and heat flux related to de water content wet basis for alginate-tyose capsules (a) and (c). Probiotic microcapsules (b) and (d).

Se realizó un estudio calorimétrico de la energía necesaria para la eliminación de la humedad durante el proceso de secado. El estudio se realizó en un calorímetro Setaram TG-DSC 111 (que permite la medida simultánea de las variaciones de masa y entalpía),

acoplado en línea a un espectrómetro de masas Thermostar de Balzers Instruments, mediante una línea calorífuga (que evita la condensación de los productos). Este equipo dispone de un conmutador de gas para la introducción programada de gas activo o inerte a la cámara. El procedimiento experimental consiste en un rampa de temperatura de 20 a 85 ºC a una velocidad de 2 ºC/min, simultáneamente se siguen las señales de agua (m/z=18) y CO_2 (m/z=44), a fin de poder identificar las distintas fases de secado de la muestra así como su descomposición térmica si la hubiera.

En la Figura 6.4 se puede observar el calor requerido para la evaporación del agua de los diferentes materiales a la derecha y los cambios de fase de cada uno de los materiales empleados. El fin de Fase I viene definido por el máximo valor de calor suministrado necesario en ambos casos se ha realizado el ensayo con las microcápsulas esféricas con contenido probiótico y en las figuras de la izquierda en cambio se trata del material empleado en el Capítulo 4, es decir, los cilindros de alginato y tilosa que no contienen microorganismos en su interior. En cambio el cambio de Fase II tiene lugar cuando es necesario un aporte de calor más intenso y se observa un cambio de pendiente creciente. Se puede observar que el agua se encuentra más retenida a lo largo de la Fase III en el caso del material de alginato y tilosa. A pesar, de que las fases que hemos considerado no tienen exactamente el mismo comportamiento al mostrado en los resultados de la calorimetría. Se ha empleado el criterio de mínima fluidización para la definición de las fases. De todos modos, el momento del cambio de fase que se establece a través de la velocidad mínima de fluidización parece estar ligado al contenido de humedad en base humeda, a pesar de que los datos de la calorimetría solo proporcionen información sobre la retención del agua en la matriz sólida de cada producto para los casos estudiados.

6.5 Análisis de las fases de secado

La evolución del contenido de humedad en base seca y los perfiles de velocidad se muestran en la Figura 6.5 para los Experimentos 1 y 4 como representativos de dos estrategias térmicas diferentes. Pueden verse los datos experimentales junto con la curva ajustada por aplicación del modelo matemático que se detallará en los siguientes

apartados. Las curvas de forma sinusoidal, características de este tipo de procesos de secado presentan un punto de inflexión correspondiente a la mayor velocidad de secado.

La velocidad de secado normalmente comienza a incrementarse suavemente hasta que se alcanza la temperatura de control deseada. En este momento, aparece el máximo de la velocidad de secado que coincide con la Fase I, según el criterio seguido para el establecimiento de las diferentes fases del secado en función de la velocidad mínima de fluidización. Después del punto de inflexión da comienzo la Fase II donde se observa un fuerte descenso de la velocidad de secado, originado por la resistencia difusional a la eliminación de la humedad. El descenso de la velocidad de secado es tanto más acusado cuantos mayores son las temperaturas de proceso. En la Figura 6.5, se pueden observar como en el Experimento 1 (Mm/Mm), en el que las temperatura de proceso son más elevadas que en el Experimento 4 (Ml/Ll). En consecuencia, se produce en el Experimento 1 un cambio mucho más acusado en la velocidad de secado que parece afectar negativamente a la duración del ciclo de secado, como se desprende al analizar los tiempos de secado de ambos experimentos. Finalmente, la Fase III se caracteriza por una casi constante velocidad de secado y cuyo valor se encuentra claramente por debajo de 0.01 g/(g s.s. min).

El secado por microondas presenta un efecto favorable a la cinética de secado debido al gradiente de humedad originado desde el interior hacia el exterior muy diferente del que se produce en otras tecnologías de secado. Las estrategias de secado en NFMD se analizaron en base a los niveles térmicos establecidos con las temperaturas objetivo (T_f^*) y (T_{in}^*) definidas para las Fases I y II. La potencia de microondas y la temperatura de entrada del aire deben estar convenientemente reguladas para conseguir las temperaturas objetivo deseadas para cada una de las fases. La Fase I se caracteriza por un pequeño incremento de la velocidad de secado en el que la temperatura del producto alcanza un equilibrio dinámico de acuerdo a las condiciones del aire circundante y de la potencia de microondas suministrada. La temperatura de la superficie del producto se estabiliza rápidamente por lo que el calentamiento convectivo y por microondas (negativo a bajas T_{air}) iguala la energía necesaria para la vaporización de la humedad. Durante la Fase II, la velocidad de secado decrece continuamente por el progresivo aumento de la resistencia difusional al establecerse un gradiente de humedad en el interior de la partícula.

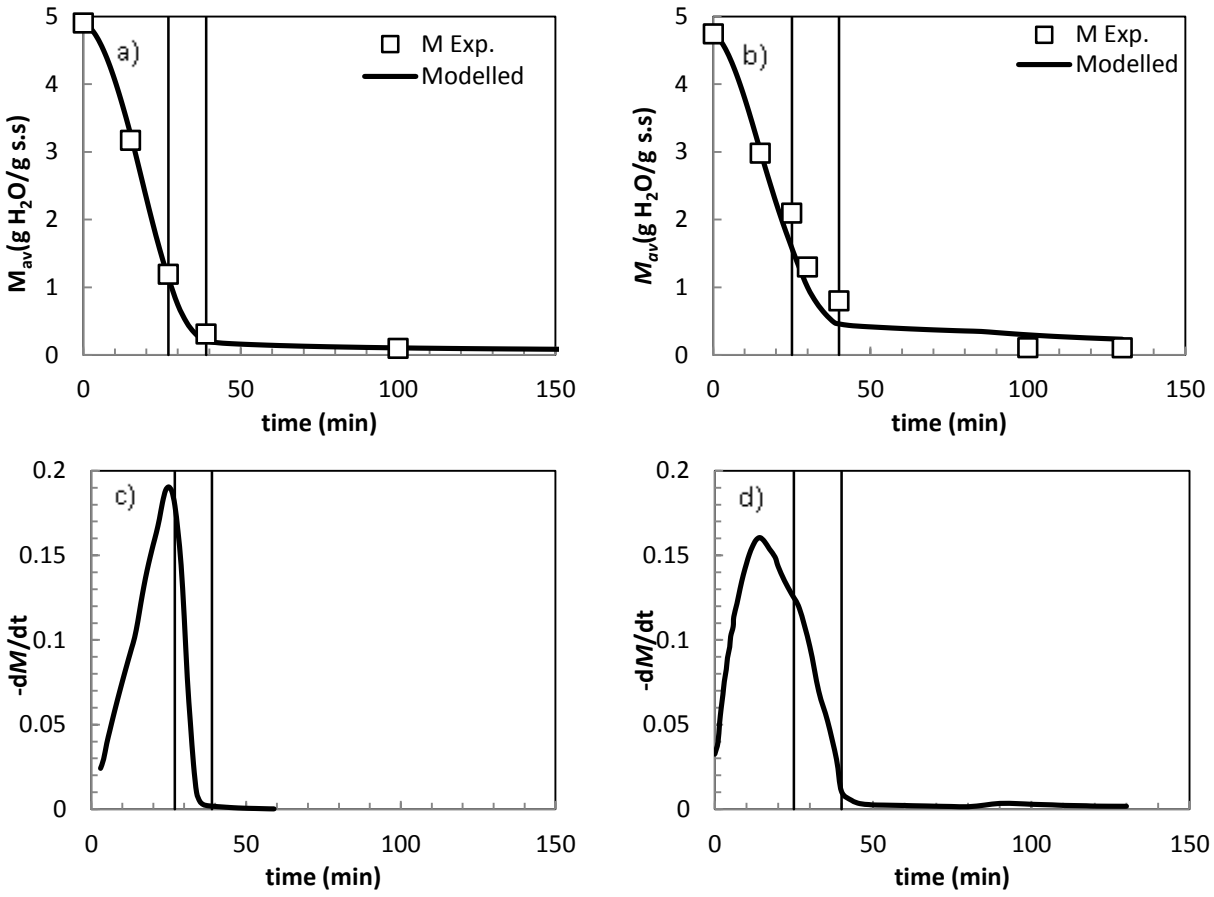

Figura 6.5. Moisture content, M_{av}, and drying rate profiles: (a) and (c) for Experiment 1(Mm/Mm). (b) and (d) for Experiment 4 (Ml/Ll).

La temperatura del producto puede ser difícil mantenerla constante a lo largo de la Fase II, desde que el calor absorbido de microondas decrece en consonancia con el contenido de agua, el cuál disminuye fuertemente. La transición de la Fase II a la III tiene lugar en el momento en el que el lecho comienza a fluidizar y se apagan las microondas, ya que el contenido de humedad es bajo y el calentamiento por microondas podría afectar negativamente a la calidad del material probiótico. En otros casos, la Fase II se puede llegar a extender a menores niveles de humedad, con lo que se reduce también el tiempo del proceso (Scaman, *et al.*, 2014).

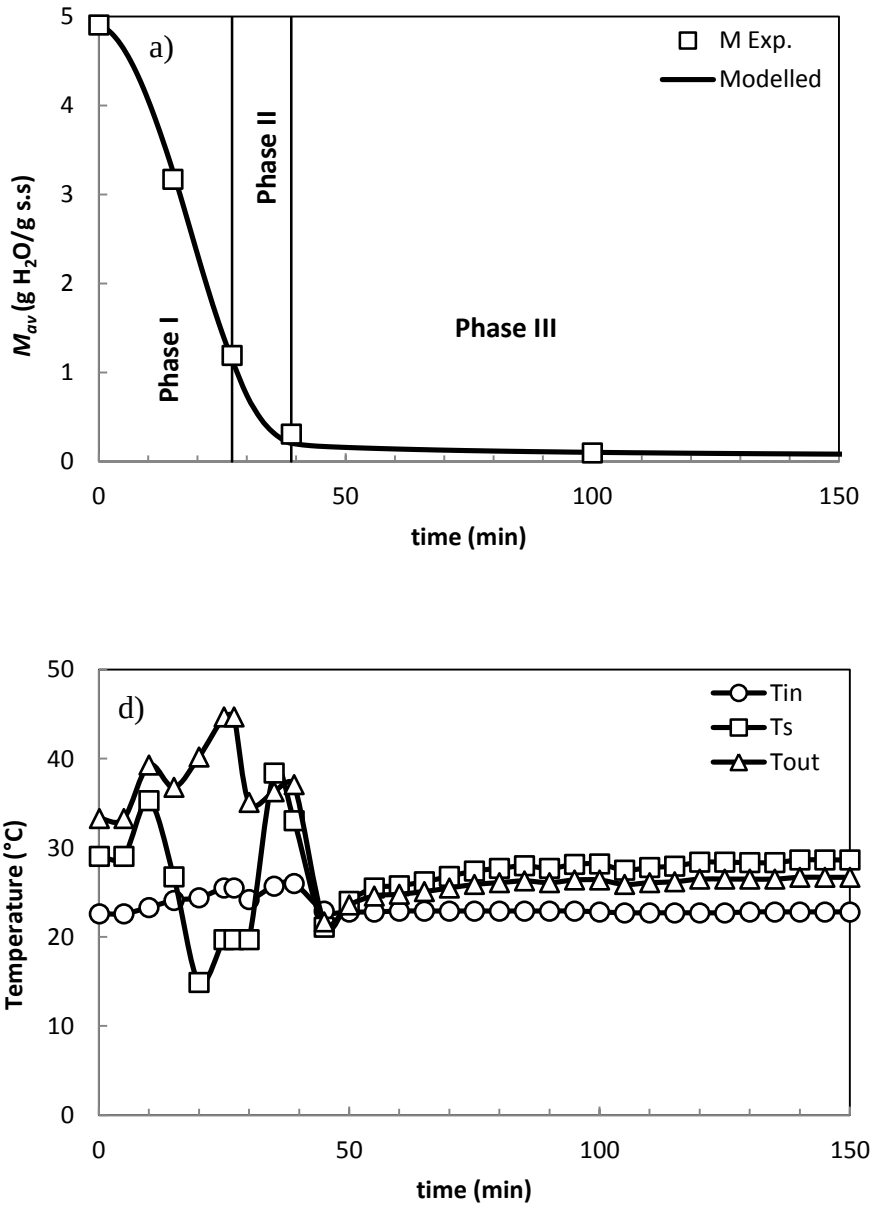

Figure 6.6. Moisture content and temperature profiles during Experiment 1 (Mm/Mm). (a) M_{av} *vs* time. (b) T_{in}, T_s, T_{out} *vs* time

En la Figura 6.6a, se representa el contenido de humedad M_{av} (en base seca) de las microcápsulas a lo largo de cada fase para el Experimento 1. Se observa una pendiente acusada durante las Fases I y II, aunque en la Fase II la velocidad de secado comienza a descender intensamente. Es por ello que al comienzo de la Fase III, una vez que ya se ha eliminado más del 80% del contenido de humedad inicial la pendiente del perfil de humedad es considerablemente bajo. A continuación, se desconectan las microondas y se observa una ligera pendiente descendiente en el contenido de humedad hasta el final del

proceso cuando el material alcanza el valor de actividad de agua necesario según los requerimientos de calidad.

Durante los experimentos se han monitorizado tanto la masa como la temperatura. La pérdida de masa se tomó a diferentes tiempos y siempre al final de cada fase. La diferencia entre la temperatura de entrada, la de salida y la de la superficie del producto se observa en la Figura 6.6b correspondiente al Experimento 1 (Mm/Mm)**.** Durante el primer periodo la temperatura de entrada del aire se mantuvo entre 20 y 24ºC, y la temperatura de la superficie fue entorno a 30ºC, y durante la segunda fase se mantuvieron las mismas condiciones. Tal y como se ha mencionado en el apartado experimental, la T_s se controla indirectamente a través de la temperatura en el interior del lecho (T_f) y estimada con la temperatura media del aire (T_{air}). Como la (T_{out}) puede presentar un incremento significativo respecto a la (T_{in}) la estimación de los valores experimentales de (T_s) pueden tener diferencias respecto a los valores (T_s^*).

Al final del proceso de secado en la Fase III la diferencia entre las temperaturas de entrada, salida y de la superficie del material es pequeña como se muestra en la FiguraFigure 5.3b.La vaporización en la interfase requiere del calor obtenido ya sea de la superficie de la partícula o del aire circundante, en una cantidad variable que depende de la velocidad del aire y gradiente de temperatura y signo en cada momento. La pérdida de calor debido a la convección por la baja temperatura de entrada puede ser 2 ó 3 veces superior a la de vaporización para gradientes exteriores a la partícula extremos. La valoración de estos detalles energéticos se dedujeron tras la modelización de las temperaturas observadas durante el secado que, como las mostradas en la Figura 6.6b. La modelización del comportamiento térmico se realizó mediante el programa FlexPDE® como se verá en el apartado siguiente.

A la hora de analizar los perfiles térmicos, es preciso tener en cuenta la fuerte reducción de masa durante las Fases I y II que afecta directamente al espesor del lecho de las partículas a través de una reducción de su tamaño, como se ha podido comprobar en la Tabla 6.2 anterior. Como consecuencia, se ha observado una reducción en el espesor del lecho de partículas estimado en torno a un 25 % del valor inicial al final de la Fase II de forma similar a lo observado para las microcápsulas de levaduras. De esta manera, el tiempo de contacto del aire con el sólido durante la Fase II desciende sensiblemente debido a la reducción del espesor del lecho que explicaría la tendencia a disminuir de la

temperatura T_{out}, al final de la Fase II, en los Experimentos 1y 3 que se recogen en la Figura 6.7. Por otro lado, en el Experimento 1 (Mm/Mm) se produce también un flujo de calor convectivo que supone un calentamiento extra, aparte de las microondas durante la Fase II (Figura 6.7b).

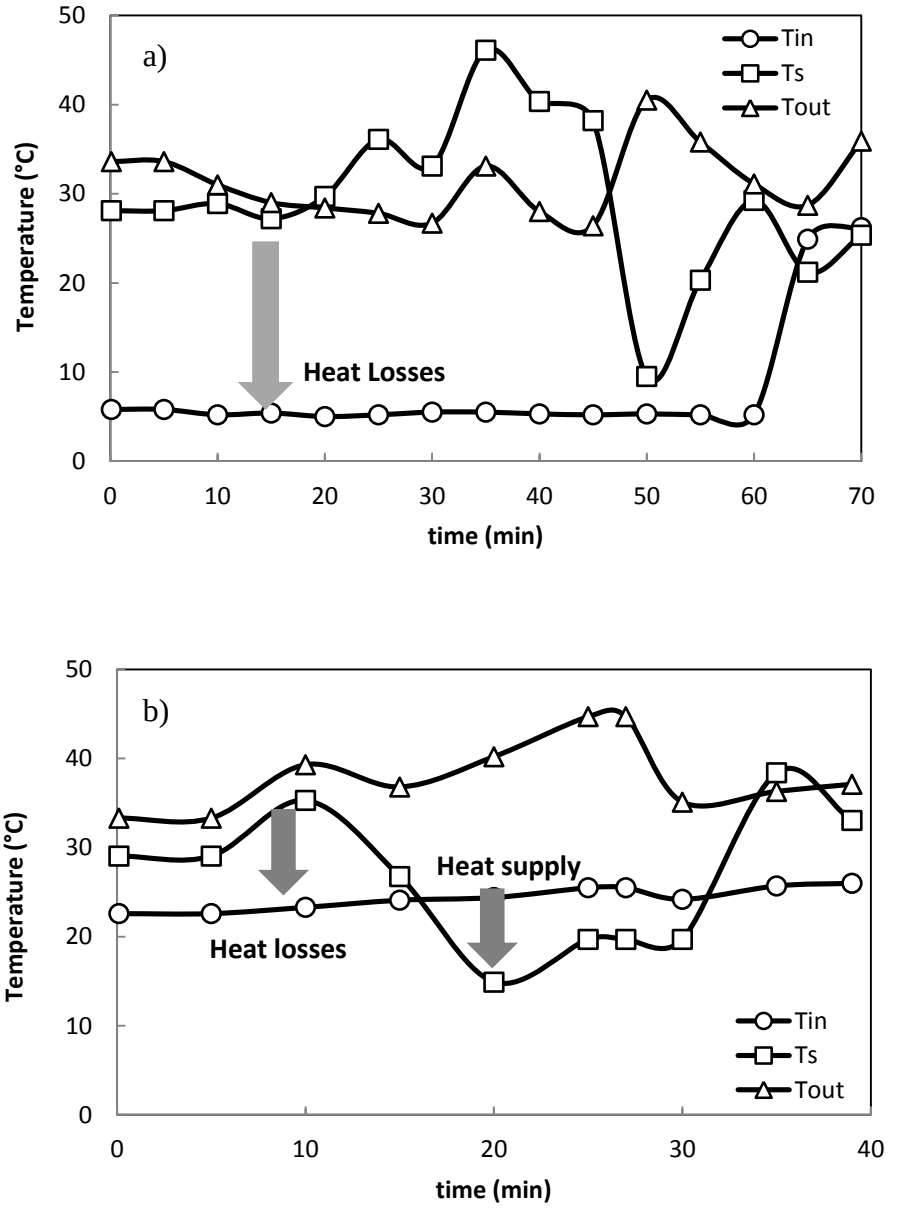

Figure 6.7. Inlet, outlet and surface experimental temperatures *vs* time on the phases I and II (microwaves on). (a) for Experiment 3 (Ml/Mm) (b) for experiment 1(Mm/Mm).

Una situación diferente se da en el Experimento 3 (Ml/Mm) donde se produce en todo momento perdidas convectivas. En la Fase II, el intercambio calorífico entre el producto y el aire es mucho menos acusado por la reducción importante de la altura del lecho y la temperatura (T_{out}) se aproxima a (T_{in}). También puede deducirse, sobre todo

del Experimento 1, la diferencia de temperatura en el lecho por la diferencia entre de (T_{in}) y (T_{out}), de forma un valor medio deducido a partir de la temperatura experimental (T_f.) Los Experimentos 1 y 3, como se ha podido observar, dan lugar a un efecto contrario en el consumo de energía por microondas. Éste es mayor para el Experimento 3, no obstante el gradiente térmico hacia el exterior que favorece los mecanismos de eliminación de humedad y parece ser un factor importante en la calidad final del producto observada como se verá en el apartado siguiente.

6.6 Calidad del material probiótico deshidratado por NFMD

De la misma forma que en el Capítulo 5 para el caso de las levaduras se tuvieron en cuenta los criterios de calidad de los alimentos deshidratados en relación con el contenido acuoso y actividad del agua. Siguiendo el protocolo experimental indicado en el Apartado 5.6 En cada experimento usando el método de Karl- Fischer se determinó la cantidad de sólido seco y el valor promedio de la humedad en base seca según las Ecuaciones (5.7) y (5.8). La actividad del agua se analizó en relación con el contenido de humedad. Valores de la a_w elevados indican un bajo gradiente de humedad en la partícula. En la Figura 6.8 se representan los perfiles de a_w de los Experimentos 5 y 6 que corresponden a los experimentos que han conseguido los mejores resultados de viabilidad y se compara su perfil con el Experimento 2 que obtuvo datos más desfavorables de la viabilidad. Durante la Fase I y II, los valores más altos de la velocidad de secado se da lugar alrededor de la transición de la Fase I a la II y los perfiles de humedad M_{av} *vs* tiempo muestran una pendiente casi constante y la velocidad de secado disminuye progresivamente hasta conseguir entre un 80 a un 90% de eliminación del contenido de agua inicial. Durante la Fase III, el contenido total de humedad no sufre un cambio apreciable, pero la actividad del agua disminuye significativamente a lo largo del tiempo como se puede ver en la Figura 6.8b. El suave descenso de la actividad del agua a lo largo del Experimento 2 no fue favorable según los resultados de viabilidad con una velocidad de descenso de la actividad de agua de 0.004 min^{-1}. Por el contrario, en los Experimentos 5 y 6 según los datos de viabilidad obtenidos se observó un comportamiento no tan perjudicial debido a la transición más rápida por los valores de actividad del agua críticos con una velocidad en torno a 0.008 (Aronsson y Rönner, 2001, Foerst y Kulozik, 2012).

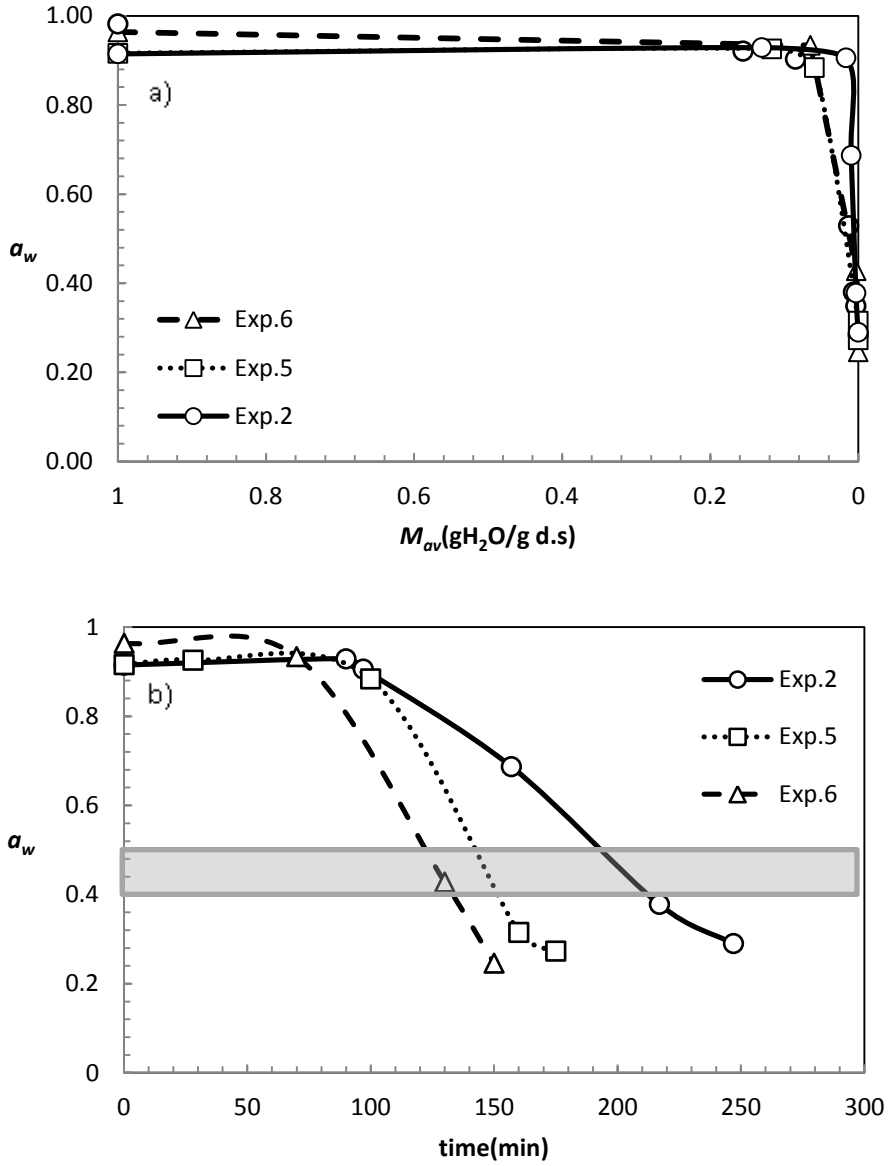

Figure 6.8. Water activity *vs* moisture profiles for Experiments 2,5 and 6. (a) a_w *vs* M_{av} (b) a_w *vs* time.

Table 6.3. Quality parameters obtained for all experiments.

Exp.	$r_{I\text{-}II}$	$M_{fin\ II}$	r_{global}	time (min)	KF(%)	Survival (%)	Code
1	0,122	0.173	0.029	165	8.87	48.71	**Mm/Mm**
2	0.038	0.163	0.015	247	10.08	53.14	**Ml/Mh**
3	0.056	0.466	0.022	195	10.52	89.77	**Ml/Mm**
4	0.099	0.799	0.036	130	9.54	46.22	**Ml/Ll**
5	0.117	0.521	0.021	175	8.76	85.92	**Hm/Hm**
6	0.124	0.672	0.062	150	8.81	90.39	**Hm/Ml**
Lyo.	-	-	0.008	585	9.15	90.45	-

*Units: $r_{I,\ II}$ and r_{global}: g H_2O/g d.s. min, $M_{end\ phase\ II}$: g H_2O/g d.s.

Los análisis de la viabilidad de los probióticos (dado como porcentaje de supervivencia) se obtuvieron tras realizar un recuento de las unidades formadoras de colonias (cfu) de las muestras iniciales para compararlas con las muestras finales obtenidas tras el proceso de secado obteniendo el resultado como se puede ver en la Ecuación (5.9) (Chávarri, *et al.*, 2010b). En la Tabla 6.3, se muestra: el valor promedio de la velocidad de secado para cada experimento, el tiempo de procesamiento, la actividad de agua, el KF o contenido de agua porcentual final, el porcentaje de supervivencia de la viabilidad de las células BB12® y las velocidades de secado del proceso en general y la media durante las Fases I y II.

La liofilización se tomó como referencia para la selección de las condiciones óptimas para los probióticos. Teniendo en cuenta que los datos de la actividad del agua y el contenido de humedad (KF) no difieren significativamente, unos experimentos de otros. La reducción del tiempo en este nuevo proceso de secado es significativamente positiva a través del de secado por microondas respecto de la liofilización. Teniendo en cuenta la cinética y los criterios de calidad se observó que los Experimentos 3, 5 y 6 mostraron los valores de viabilidad más altos que los obtenidos en la liofilización. A nivel global, los mejores resultados de viabilidad se dieron en el Experimento 6 que presenta además la velocidad de secado más elevada en las Fases I y II ($r_{I\text{-}II}$: 0.124 g H_2O/g d.s. min).

6.7 Modelización del proceso NFMD para el secado de microcápsulas de probiótico.

Se llevó a cabo la modelización de secado de microcápsulas de probiótico BB12® siguiendo el modelo matemático descrito en el Apartado 5.7 del Capítulo 5, dadas las semejanza geométrica y de tamaño. Por consiguiente, el planteamiento del los balances de materia y energía, así como las condiciones iniciales y de contorno fueron exactamente las mismas.

Propiedades físicas, térmicas y dieléctricas.

Para predecir la distribución de la temperatura durante el calentamiento por microondas es necesario conocer algunas propiedades del material como la densidad, el

calor especifico, la conductividad térmica, el calor latente, la constante dieléctrica y el factor de pérdidas que aparecen detalladas en la siguiente tabla.

Table 6.4. Physical, thermal and dielectric properties of main components of the encapsulating material. (Lide, 2005,Meda, *et al.*, 2005).

Properties	Value/Equation	Properties	Value/Equation
k_w	0.6 W/mºC	C_{paL}	4120 J/kgºC
ρ_w	1000 kg/m^3	ε'_{al}	6
C_{pw}	4180 J/kgºC	ε''_{al}	1.5
ε'_w	$0.004T^2$-0.5212T+75.241	K_{prob}	0.54 W/mºC
ε''_w	$0.0001T^2$+1.6001T+22.241	P_{prob}	1043 kg/m^3
Q_{vap}	$2257 \cdot 10^3$ J/kg	C_{prob}	3980 J/kgºC
k_{al}	50.22 W/mºC	ε'_{prob}	67.5
ρ_{aL}	1010 kg/m^3	ε''_{prob}	13.2
ρ_s (1	1042 kg/m^3	ρ_{ap} (2	166 kg/m^3

(1,2 Depending on capsule composition (2 Value corresponding to a capsule without shrinkage.

Estas propiedades experimentan cambios durante el experimento de secado debido a la dependencia con la temperatura y el grado de humedad. La Tabla 6.4 muestra las propiedades térmicas y dieléctricas de los principales componentes del material encapsulado. A partir de las propiedades se obtiene de la mezcla empleada para la obtención de la microcápsulas de BB12®, que al igual que en el Capítulo 5 se obtuvieron previa estimación de la fracción volumétrica correspondiente al contenido acuoso y del sólido seco empleando las Ecuaciones (3.16-3.21).

6.8 Valoración de la cinética del proceso NFMD.

Se ha empleado un modelo matemático para la valoración de la cinética del proceso NFMD aplicado a microcápsulas de probiótico BB12®. La determinación de estos parámetros se ha completado usando las Ecuaciones (3.4-3.6). La secuencia de comandos (Script) se recoge en el Anexo C y resuelve el balance de materia empleando las ecuaciones recogidas en la Tabla 6.5.

Tabla 6.5. Equations and fitting parameters for the mass balance of the product.

Equations	Profiles	Fitting parameters
$\frac{\partial M}{\partial t} = D\nabla^2 M$	*M vs t*	β, *D*
$M_s = M_e + (M_0 - M_e)\exp(-\beta t)$	M_s *vs t*	

Los experimentos realizados con las microcápsulas de levaduras se ajustaron con diferentes valores de los parámetros β, definida a través de la Ecuación de Shivhare (3.6), y *D* para cada uno de los experimentos. El modelo se ejecuta en el programa FlexPDE® que se emplea para realizar el ajuste del modelo con los perfiles de humedad experimentales.

El programa de cálculo proporciona la distribución de la humedad en la partícula $M(x,y,z)$ a cada tiempo, al igual que se hizo también en el Capítulo 4, deben reprocesarse los datos para proporcionar el valor promedio $M_{av}(t)$, según la Ecuación (4.6) del capítulo anterior:

El valor de $M_{av}(t)$ obtenido con el modelo matemático propuesto tras resolver la integral de la Ecuación (4.6), en la que V_p es el volumen de la partícula o microcápsula, debe ajustarse al correspondiente valor experimental, a través de las Ecuaciones (4.4) y (4.5) con el conocimiento de la humedad final del secado KF_{fin}.

En la Figura 6.9 se puede observar, el buen ajuste obtenido de los datos obtenidos con el programa aplicando el modelo previamente descrito con los datos experimentales. El secado a lo largo de la Fase II implica la eliminación de la mayor cantidad de agua de todo el proceso debido a la eliminación del agua libre hacia el exterior de la partícula. En la fase inicial, los perfiles de humedad se ven afectados por las condiciones de contorno a través del parámetro β. Esto afecta al contenido de humedad en la superficie del material dependiendo de las condiciones de secado.

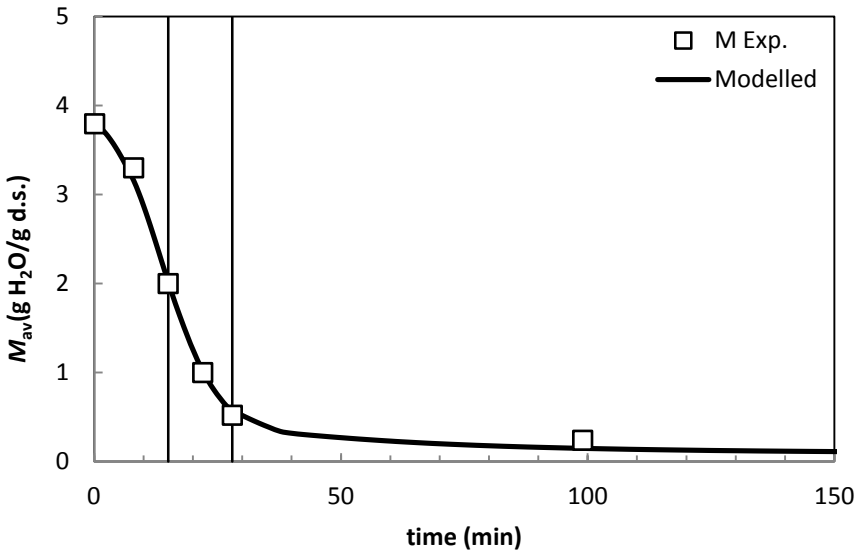

Figure 6.9. The simulation result in Experiment 5 (Hm/Hm).

El proceso de ajuste descrito se ha realizado para el ajuste de los diferentes niveles térmicos aplicados obteniendo para cada uno de ellos los valores de los coeficientes de difusión y β recogidos en la Tabla 6.6. Para el correcto ajuste de la cinética con el modelo matemático propuesto se requirió el empleo de dos valores de β tal y como aparece definida en la Ecuación (6.2) para proceder al ajuste a través de una cinética de primer orden que nos permite ajustar el valor según avanza el proceso de secado.

$$\beta = \beta_{\min} + \frac{\beta_{\max} - \beta_{\min}}{M_0 - M_e}(M_0 - M_{av}) \qquad (6.2)$$

Table 6.6. Diffusion coefficients: D_1, D_2, D_3 and coefficient β values for the experiments.

EXP.	CODE	β(min^{-1})	D_1(m^2/min)	D_2(m^2/min)	D_3(m^2/min)
1	Mm/Mm	0.022/0.11	2.00E-08	2.30E-08	2.00E-09
2	Ml/Mh	0.01/0.05	0.40E-08	3.49E-08	8.00E-09
3	Ml/Mm	0.012/0.043	1.00E-08	4.23E-08	3.10E-09
4	Ml/Ll	0.023/0.08	2.00E-08	2.00E-08	0.36E-09
5	Hm/Hm	0.025/0.085	3.50E-08	1.00E-08	1.50E-09

Por su carácter efectivo, la difusividad D mide la capacidad de difusión del agua en la estructura de la mezcla de alginato y probiótico, incorporando el fenómeno de la

contracción del volumen del material. La Tabla 6.6 muestra que la difusividad a lo largo de la Fase II es generalmente más alta debido a que la difusión se da en fase líquida y coincide con las velocidades de secado más elevadas con el gradiente de humedad en el interior de la partícula muy pequeño. En las Fase I las difusividades son en general algo más bajas dado que incorporan un espacio temporal transitorio hasta alcanzar la temperatura de control, salvo los Experimentos 4 y 5 en los que se emplean niveles térmicos iguales o superiores a los de la Fase II. Los mayores valores de las difusividades se consiguen en el Experimento 5, donde se deduce un claro efecto de la temperatura del producto sobre la difusividad. A esta conclusión podemos llegar también al observar las difusividades de microcápsulas de probiótico son claramente inferiores, por los mayores niveles térmicos empleados en las estrategias analizadas a las de levadura obtenidas en el Capitulo 5 (Tabla 5.6) Según avanza el proceso, el mecanismo difusional en la fase líquida se hace gradualmente más difícil hasta llegar a valores cercanos a cero a lo largo de la Fase III. Excepcionalmente en el Experimento 2, por las condiciones de secado previas a una temperatura de entrada del aire baja, implica que se obtenga una estructura más abierta con una mayor difusividad a lo largo de la Fase III.

Consideración de la contracción

Se llevó a cabo para el secado de microcápsulas de probiótico un estudio paralelo a los realizados en los Capítulos 4 y 5, a fin de analizar el alcance de la contracción. Este estudio requiere el cálculo de las velocidades de contracción radial en cada una de las tres fases establecidas: v_{r1},v_{r2} y v_{r3}, en base a los datos de contracción realizados que se pueden observar por los datos de contracción recogidos en la Tabla 6.6 anterior. Las velocidades de contracción de los diferentes experimentos se estimaron de la misma forma que en el Capitulo 5 empleando las Ecuaciones (4.8) y (4.10) y se recogen en la Tabla 6.7. Los valores máximos de contracción se alcanzan en la Fase II en consonancia con la mayor pérdida de agua, salvo para el Experimento 3 por el bajo nivel térmico empleado en la Fase I.

Table 6.7. Rates of the different thermal experiments.

EXP.	CODE	v_{r1}(m/s)	v_{r2}(m/s)	v_{r3}(m/s)
1	Mm/Mm	1.61E-05	8.61E-06	1.97E-07
2	Ml/Mh	5.16E-06	7.18E-06	5.53E-08
3	Ml/Mm	2.85E-06	1.98E-06	1.33E-07
4	Ml/Ll	1.20E-05	1.43E-06	3.19E-07
5	Hm/Hm	1.78E-05	2.63E-06	2.80E-07

Los valores de las difusividades obtenidos tanto con contracción como sin considerar contracción aparecen recogidos en la Tabla 6.8. Tal y como se observa los valores de difusividad a lo largo de la segunda fase son mayores salvo algunas excepciones como las observadas en el Experimento 5 en el cual las condiciones térmicas de la primera fase son (Hm) son los más elevados e iguales a la segunda que hace que aumente la capacidad de difusión en ella.

Table 6.8. Values for probiotics experiments with and without volume shrinkage consideration.

EXP. *	CODE	β (min^{-1})	D_1(m^2/min)	D_2(m^2/min)	D_3(m^2/min)
1	Mm/Mm	0.022/0.11	1.00E-08	1.38E-08	0.50E-09
1	Mm/Mm	0.022/0.11	2.00E-08	2.30E-08	2.00E-09
2	Ml/Mh	0.01/0.05	0.40E-08	2.33E-08	8.00E-09
2	Ml/Mh	0.01/0.05	0.40E-08	3.49E-08	8.00E-09
3	Ml/Mm	0.012/0.043	1.00E-08	3.25E-08	3.00E-09
3	Ml/Mm	0.012/0.043	1.00E-08	4.23E-08	3.10E-09
4	Ml/Ll	0.023/0.08	2.00E-08	2.00E-08	0.30E-09
4	Ml/Ll	0.023/0.08	2.00E-08	2.00E-08	0.36E-09
5	Hm/Hm	0.025/0.085	3.50E-08	1.00E-08	0.80E-09
5	Hm/Hm	0.025/0.085	3.50E-08	1.00E-08	1.50E-09

*Shaded rows: Shrinkage consideration. White rows: No shrinkage consideration

Al analizar los valores de difusividad en los que se tuvo en cuenta la contracción del material se observó un descenso poco significativo y tanto menor cuanto menor el valor de la difusividad. En consecuencia, el fenómeno de contracción presenta poca significación en las propiedades difusionales durante el secado de las microcápsulas de probiótico por los menores noveles térmicos empleados en este caso en comparación con el secado de microcápsulas de levaduras del Capítulo 5.

Cálculo del coeficiente de transferencia externa

Para realizar el cálculo del coeficiente de transferencia externa se emplearon los datos de pérdida de agua ($-dm_w/dt$) de la totalidad del producto sometido al proceso de secado, una vez ajustados los datos de pérdida de masa al modelo matemático propuesto. El valor de $k_G\,a$ se obtuvo con las Ecuaciones (3.7-3.9), empleadas en los Capítulos 4 y 5, previa determinación del gradiente de presiones exterior a las partículas. Para la determinación del coeficiente de transferencia $k_G\,a$ según las ecuaciones y procedimiento explicado anteriormente. Para poder comparar el valor del coeficiente de transferencia obtenido para cada uno de los experimentos, se representan los valores del coeficiente con los valores medios de perdida de masa tal y como se muestra en la Figura 6.10. De manera general en la figura se observa que inicialmente el valor del coeficiente se mantiene mas o menos constante con un leve descenso al llegar a valores bajos del contenido en humedad. Existen diferencias entre los valores obtenidos para cada uno de los experimentos. Los Experimentos 1 y 4 tienen los valores más altos comparandolos con los demás experimentos. Este comportaiento podría explicarse por los gradiente de temperatura intermedios y bajos (T_s-T_{in} entre 25 ºC y 10 ºC). Gradientes de temperatura inferiores como el Experimento 1 (Mm/Mm) que presentan coeficientes de transporte inferiores. Gradientes más elevados o mantenidos durante las Fases I y II como en el Experimento 5 (Hm/Hm) provocan un flujo de calor convectivo más elevado que compromete el neceasrio aporte calorífico para la vaporización.

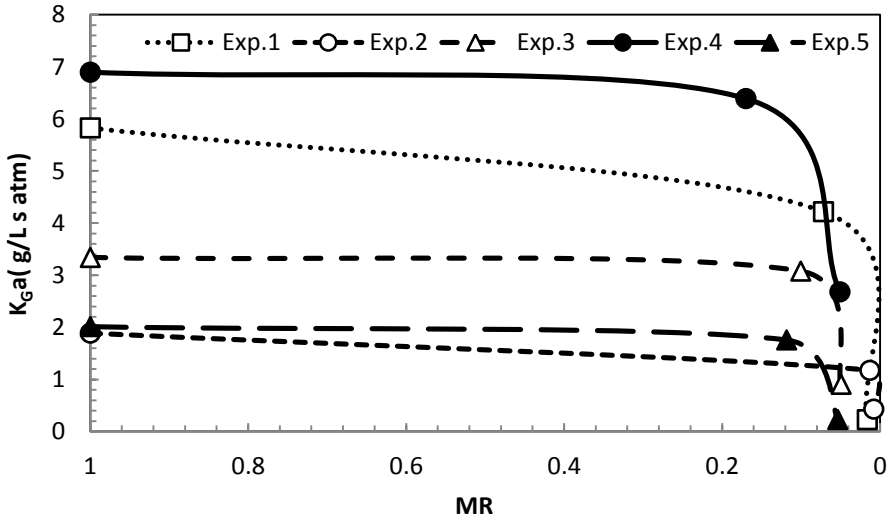

Figure 6.10. External coeffcient for the NFMD experiments analyzed.

Dadas las condiciones operacionales de las microcápsulas de probiótico por su tamaño y fluidodinámica, la caída de la temperatura de la capa de fluido en torno a la partículas es el parámetro determinante de la $k_G\,a$. Como se recoge en la Figura 6.10, los valoeres de $k_G a$ obtenidos se encuentran entre 2 y 7 (g/L s atm), proporcionado los mejores resultados cuando el gradiente térmico exterior en la película de aire se mantiene en niveles bajos o intermedios.

6.9 Estimación de consumo de energía por microondas en el proceso NFMD

Para la estimación del consumo energético se procedió al cálculo de Q_{abs} que se obtiene según la Ecuación 5.10 para una geometría esférica. En el modelo que se ha utilizado para realizar el balance de energía se han empleado las Ecuaciones (3.10-3.13) y también empleadas para la microcápsulas con levadura. El programa de cálculo (*script)* correspondiente se recoge en el Anexo C con el que para para lograr el ajuste de los perfiles de temperatura de la superficie experimental del material con el modelo propuesto se probaron diferentes valores del campo eléctrico como único parámetro de ajuste. El resto de valores necesarios se tomaron como constantes de la Tabla 6.4. Por la similitud tamaño y condiciones fluidodinámicas del lecho en los casos de microcápsulas de levaduras y probiótico, los coeficientes de convección *h*, para cada una de las tres fases, fueron los mismos. Estos valores fueron de 166.7 W / m^{2o}C tanto para el periodo de accionamiento microondas (Fases I y II) como para la Fase III. El efecto de la disminución de tamaño parece equilibrar el derivado de la disminución continua de la velocidad del aire lo largo del proceso haciendo que el valor de *h* se mantenga constante. El ajuste de los datos de temperatura se realizó en las dos fases en las que se aplican la energía de microondas (Fase I y Fase II).

Al igual que en el Apartado 5.9, se calculó para los secados de material probiótico el tiempo de accionamiento de las microondas (t_{on}) según Ecuación4.11 previo cálculo del parámetro b_{ac} que expresa la fracción de tiempo de encendido a lo largo del tiempo de proceso que se explica en detalle en el mismo Apartado 5.9. El b_{ac} a cada tiempo se representa en la Figura 6.11 para el Experimento 3. El área bajo la curva del perfil del *b* acumulado permite estimar el tiempo real de encendido de las microondas en el proceso. La obtención de b_{ac} se consigue tras contabilizar los tiempos de accionamiento de las

microondas a fin de ajustar la T_s modelada al valor medio experimentalmente a través de T_f. Un ejemplo del ajuste obtenido con el modelo puede verse para el Experimento 5 de microcápsulas de levaduras que se muestra en la Figura 6.12. Estos ajustes se repitieron para cada uno de los experimentos propuestos, en los que se obtuvo el campo eléctrico *E* para evitar oscilaciones de temperatura no superiores a ±5 ºC; los resultados se recogen en la Tabla 6.9.

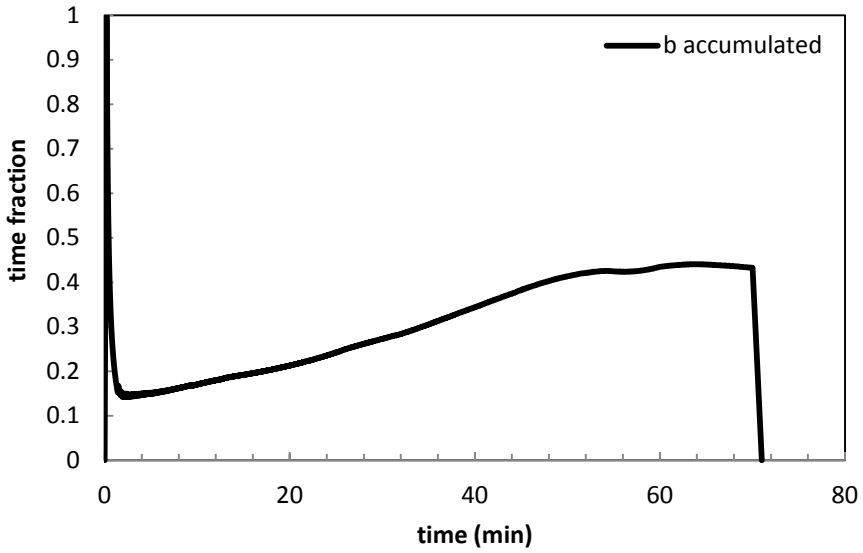

Figure 6.11. Representation of b accumulated value for Experiment 3 (Ml/Mm) of BB12®.

El campo eléctrico se definió como un valor único para todas las fases. Existe un compromiso entre la primera y la segunda fase ya que un campo eléctrico bajo hace que no se alcancen las temperaturas objetivo y un campo eléctrico alto, en cambio, provoca el sobrecalentamiento del material durante la primera fase. En general, el campo eléctrico es muy similar en todos los experimentos de secado. El valor más alto se obtuvo para el Experimento 5, debido a la alta temperatura de la superficie a alcanzar (45°C) en ambas fases del proceso de secado. Para el resto de los experimentos al estar en niveles térmicos más próximos debido a la selección realizada con los resultados obtenidos para los experimentos llevados a cabo con las levaduras, se puede observar que el campo eléctrico no varía mucho de unos ensayos a otros.

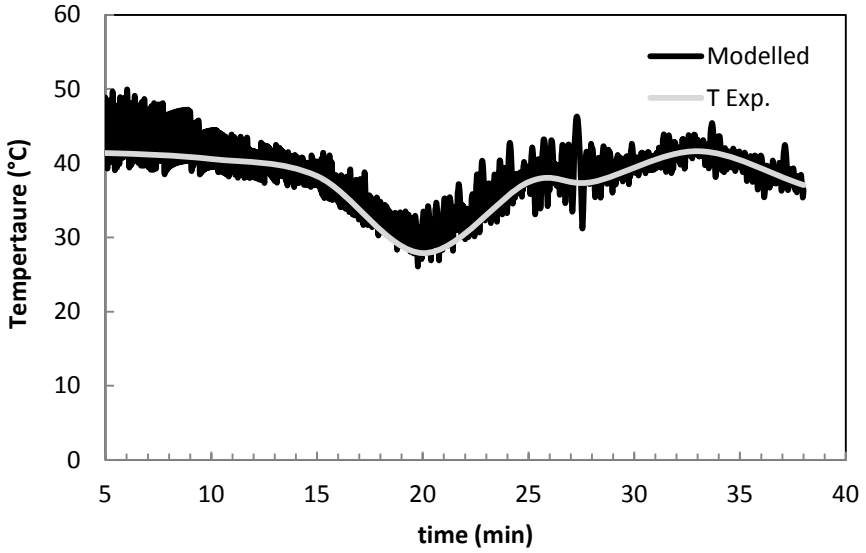

Figure 6.12.Temperature modelled and experimental in Experiment 5 (Hm/HM)) for BB12®.

Table 6.9. Electric field (*E*) for different experiments.

Exp.	Code	*E*(V/m)
1	Mm/Mm	1750
2	Ml/Mh	1700
3	Ml/Mm	1700
4	Ml/Ll	1600
5	Hm/Hm	1900

La consecución de una tecnología de secado eficiente pasa por reducir al mínimo la cantidad de energía requerida. Con el fin de evaluar la energía consumida por microondas para los diferentes experimentos de levaduras, se define *G* mediante la Ecuación (5.14).

La Figura muestra el calor absorbido (Q_{abs}) del Experimento 5 y *G* se obtuvo tras el cálculo del área bajo la curva. El valor de Q_{abs} disminuye con la reducción del contenido de humedad. Además, el consumo máximo, se puede calcular utilizando la Ecuación (5.14) que sería la energía de microondas si hubiese estado activa durante todo el proceso. Los resultados de consumo *G* para todos los experimentos se recogen en la Tabla 6.10.

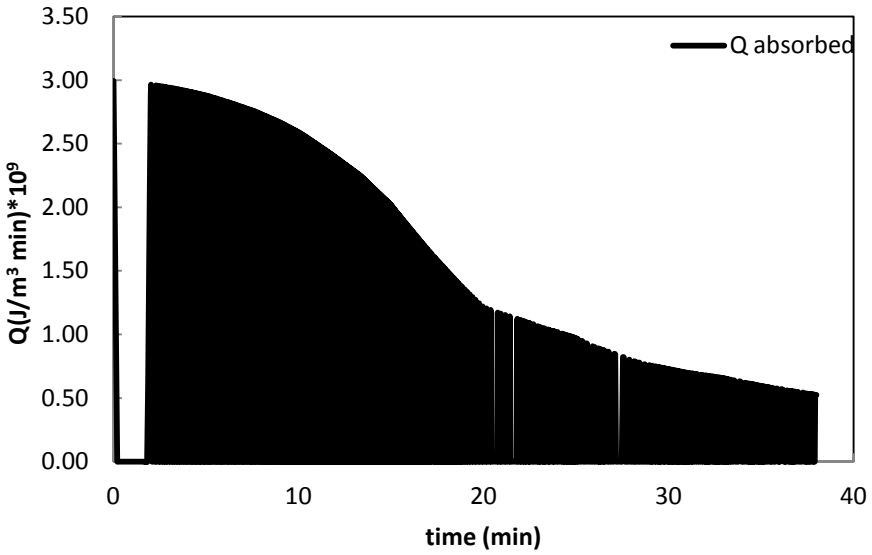

Figure 6.13. The diagram of Q_{abs} for the Experiment 5 (Hm/Hm).

El consumo de energía o cantidad de energía calorífica de origen microondas que recibe el producto tiene 3 diferentes destinos: pérdidas por convección, el calentamiento del material y la vaporización. La energía de vaporización empleada en el proceso de secado es de aproximadamente 2,02 kJ /cm^3 relacionado con calor latente de vaporización (Lide, 2005). El resto de la energía se emplea en la pérdida convectiva y el calentamiento del material termo-sensible.

Table 6.10. Information about Energy consumption for probiotics.

EXP.	CODE	t_{ON}(min)	G(kJ/cm^3)	G_{max}(kJ/cm^3)
1	Mm/Mm	7.52	10.01	51.95
2	Ml/Mh	21.14	28.66	131.49
3	Ml/Mm	21.68	35.36	114.18
4	Ml/Ll	16.61	19.71	47.47
5	Hm/Hm	6.62	12.65	72.59

Es preciso tener en cuenta que a la hora de hacer una valoración energética del proceso debe calcularse la energía eléctrica según se indica en el Capítulo 4 (Apartado 4.6) y expresada como G_{mw} y calculada a través de potencia nominal W_{nom} teniendo en cuenta el tiempo de microondas activo. El valor de G_{mw} o consumo eléctrico del dispositivo generado de microondas es superior a G y la relación entre los corresponde al rendimiento de conversión

en calor de la energía microondas que se verá en el Capítulo 7 a la hora de comparar diferentes tecnologías de secado. El Experimento 1 tiene las pérdidas más bajas debido a que durante la primera fase se aplica un gradiente térmico medio usando 30°C para la temperatura de la superficie y la temperatura ambiente para la temperatura de entrada del aire. En la segunda fase, las condiciones térmicas son iguales lo que favorece a lograr la temperatura de la superficie objetivo del producto y a evitar los periodos de adecuación térmica a las condiciones de la segunda fase, reduciendo así el tiempo de encendido de la energía de microondas. Por el contrario, el Experimento 3 tiene las mayores pérdidas debido al gradiente térmico, principalmente durante la primera fase con una temperatura de entrada del aire de 5°C y una temperatura de la superficie objetivo de 30°C. Se puede concluir que las pérdidas se incrementan con la diferencia entre la temperatura de entrada y la superficie. Siendo energéticamente favorable cuando la temperatura del aire de entrada es mayor que la temperatura de la superficie.

El calor absorbido se calcula considerando que durante el proceso no se realizan paradas con lo que ese valor lleva asociada este error. Sin embargo, este hecho no puede ser evitable ya que las muestras deben ser tomadas para recopilar información acerca de la masa y algunos otros parámetros como la actividad de agua (a_w).Teniendo el tiempo de operación, es mejor lograr un alto valor de β, que corresponde también a los casos de mayor difusividad, con el fin de maximizar la velocidad de secado y reducir así los costes asociados al tiempo de proceso. Sin embargo, si se tienen en cuenta las pérdidas convectivas, las condiciones cinéticas más favorables, requieren un alto consumo de energético. Por lo tanto, existe un compromiso entre conseguir la cinética de secado más rápida y el consumo energético más bajo no siempre coincidentes.

Como criterio final de selección es preciso tener en cuenta la calidad del producto final cuyos resultados se expusieron en el Apartado 6.6 anterior. Al incluir este criterio resulta como más favorable el Experimento 5 (Hm/Hm). En cambio, el Experimento 3 (Ml/Mm), aunque sería también recomendable desde el punto de vista de la calidad del producto deshidratada al mostrar buena viabilidad de las células después del proceso NFMD (Tabla 6.3), resulta poco recomendable desde el punto de vista energético debido esencialmente al empleo de baja temperatura del aire en la Fase I que derivan en pérdidas caloríficas convectivas y elevado consumo energético.

..

Capítulo 7

COMPARATIVA DEL PROCESO NFMD CON OTRAS TECNOLOGÍAS DE SECADO

7 COMPARATIVA DEL PROCESO NFMD CON OTRAS TECNOLOGÍAS DE SECADO

En este capítulo se va a realizar la comparativa entre el nuevo proceso NFMD que se ha descrito con detalle en los capítulos anteriores para su aplicación al secado de materiales termosensibles con otras dos tecnologías ampliamente empleadas como son el secado por aspersión o *spray drying* y la liofilización. En este capítulo se va a proceder al secado de material probiótico y de un concentrado de granada como elementos comunes de referencia para ver la incidencia de cada una de las tecnologías de secado en aspectos de calidad, cinéticos y de consumo energético.

7.1 Introducción

Los procesos de secado implican la eliminación de gran cantidad de agua, que en el caso de los probióticos afecta a la estructura celular lo que puede llegar a inducir la muerte celular. La presencia de una determinada cantidad de microorganismos vivos o activos en las formulaciones probióticas se considera un criterio esencial para ser beneficioso para la salud (Cruchet, *et al*., 2015). Para prolongar la estabilidad durante largos periodos de almacenamiento, es importante preservarlos de forma deshidratada reduciendo el contenido de humedad. Para el secado de probióticos se pueden emplear diversas tecnologías que pueden afectar a la viabilidad de los microorganismos. El diseño de unas estrategias óptimas para la protección de probióticos durante este tipo de procesos es crucial. De este modo se mantiene la viabilidad y el éxito en la aplicación de cada tecnología de secado. El secado también se plantea en frutas y vegetales frescos por ser productos altamente perecederos (debido a su alto contenido de humedad alrededor del 80%) que se deterioran en un período corto de tiempo si se manejan incorrectamente. Con el secado se evita el crecimiento de microorganismos de descomposición, así como las reacciones enzimáticas en la matriz del material conservando así la estructura, características sensoriales y valor nutricional del material de partida (Vega-Mercado, *et al*., 2001).

De entre las distintas tecnologías de secado que se emplean más comúnmente para la deshidratación de este tipo de materiales destacaremos aquí: El secado por aspersión o

spray drying muy orientada hacia la obtención del material deshidratado en partículas y la liofilización que se aplica comúnmente a materiales sólidos. Las características de estas tecnologías de secado se van a analizar a continuación.

Secado por aspersión ó atomización (Spray drying)

El secado por aspersión o atomización es un método de secado rápido y económico (Peighambardoust, *et al*., 2011) sobre disoluciones con capacidad para producir partículas esféricas con propiedades tales como: un específico contenido de humedad residual, un aspecto y distribución de tamaños uniforme. En una primera parte del proceso, el líquido de alimentación se atomiza en forma de aerosol de pequeñas gotas que entran en contacto con el gas a alta temperatura en la cámara de secado. Se pueden aplicar tres tipos diferentes de modelos de intercambio de calor dependiendo de la dirección de entrada del líquido y del aire en la cámara de secado, flujo en paralelo, a contracorriente o flujo mezclado. Como los probióticos y los compuestos antioxidantes son organismos termosensibles, es importante aplicar el intercambio en paralelo. En este modelo, las gotas con mayor contenido en humedad entran en contacto con la temperatura más alta y las partículas más secas con las temperaturas más bajas, lo que minimiza el riesgo de sufrir daños por las altas temperaturas. Finalmente esta tecnología conlleva el secado de las partículas en lecho fluidizado.

Durante el proceso *spray.drying* las partículas más grandes y pesadas se separan por la parte baja de la cámara de secado por gravedad. Las partículas más pequeñas y finas se recogen en ciclones o filtros de mangas. Las partículas que se recogen en el colector son materiales que se puede comercializar y usar. Las partículas secas se forman en diferentes fases. En la primera, se alcanza el estado de equilibrio entre las gotas y el aire caliente suministrado. Tras el contacto con el aire caliente, el agua comienza a evaporarse inmediatamente. Como se puede mantener la saturación de la superficie de las gotas, esta evaporación se caracteriza inicialmente por un periodo de secado a velocidad constante, donde la temperatura de las partículas se define por la temperatura de bulbo húmedo. Una vez que las condiciones de saturación de la superficie de las partículas húmedas no se pueden mantener, comienza la segunda fase del secado con un descenso de la velocidad de secado. Como las partículas húmedas se contraen, se forma una capa debido a la cristalización de los materiales disueltos o suspendidos en la alimentación. La velocidad de evaporación después de la formación de la corteza depende de la difusión de

la humedad a través de la capa seca. Con el incremento de la evaporización, la capa irá haciéndose más gruesa y la velocidad de evaporación disminuirá. La temperatura del producto se incrementa hasta llegar a aproximarse a la temperatura del aire caliente que se introduce que en muchos casos se sitúa en torno a 100 ºC o superior (Ananta, et al., 2005). En esta última fase, las células probióticas tienden a la inactivación térmica y los compuestos antioxidantes son susceptibles de degradarse debido a las reacciónes de Maillard (Summa, *et al*., 2008).

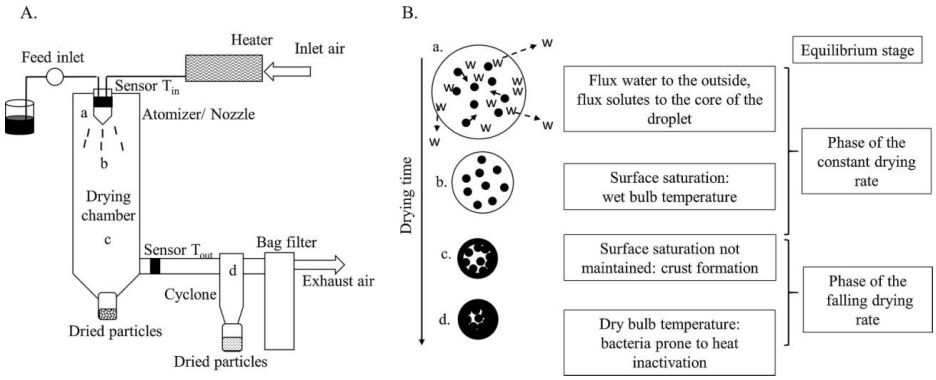

Figure 7.1. The spray drying process. (A) A schematic overview of a spray dryer. (B) A schematic overview of the different stages during the drying process with indication of the important heat and dehydration stresses. Black dots: bacterial cells, w: water molecules. (Broeckx, *et al.*, 2016)

Esta tecnología de secado parece ofrecer grandes ventajas si se compara con otras tecnologías de secado convencionales. Este proceso es rápido, continuo y económico en el que se pueden obtener grandes cantidades de productos deshidratados.

Durante el secado por aspersión, los probióticos y los compuestos antioxidantes experimentan diversas tensiones que incluyen el estrés térmico, la deshidratación, y el estrés oxidativo. Se cree que el estrés ocasionado por el calor y la deshidratación son los dos principales mecanismos que conducen a la inactivación y la pérdida de viabilidad de los probióticos y al deterioro de las propiedades antioxidantes de los compuestos. Sin embargo, los mecanismos de inactivación de las bacterias probióticas durante el secado por aspersión no se entienden todavía completamente. Las conclusiones generales de los diferentes estudios publicados en torno a esta área resaltan la dificultad debido a los diferentes resultados obtenidos para diferentes géneros y especies de bacterias, pero también específicos de cada cepa.

Estrategias de protección

Mientras que diversos factores de estrés pueden afectar la capacidad de supervivencia de los probióticos y la capacidad antioxidante de los compuestos durante y después del secado por aspersión, la mayoría de estos factores, al menos en parte, se pueden minimizar realizando una selección óptima de estrategias de protección adecuadas. En general, se pueden distinguir tres estrategias principales de protección: la adición de agentes protectores, y la adaptación de los parámetros del proceso. Estas estrategias no sólo afectan a la viabilidad del probiótico y a la capacidad antioxidante de los compuestos inmediatamente después del proceso de secado sino que también durante el almacenamiento.

Agentes protectores

La adición de sacáridos ó hidratos de carbono, principalmente disacáridos, es una de las estrategias más comúnmente aplicadas para proteger productos termosensibles como los probióticos y los compuestos antioxidantes. Para comprender el efecto protector de los azúcares sobre las membranas bacterianas y las proteínas, se pueden encontrar varias hipótesis en la bibliografía (Garvey, *et al*., 2013), incluyendo la teoría de la vitrificación, la hipótesis de recambio de agua y la hipótesis de las fuerzas de hidratación. En primer lugar, es importante considerar una membrana bajo circunstancias fisiológicas normales. En la forma hidratada, la bicapa se encuentra en fase laminar del fluido. Las colas de ácido graso se sitúan en la región hidrofóbica de la bicapa, mientras que los grupos de cabeza polares están orientados hacia las moléculas de agua. Durante la deshidratación esta bicapa puede sufrir una transición a fase gel. En esta fase, las colas lipídicas se presionan en el plano de la membrana y los grupos de cabeza polares se acercan, lo que puede causar defectos que pueden afectar a la reversibilidad de la rehidratación, que conduce a la posible salida de componentes intracelulares y la muerte celular. Los sacáridos pueden prevenir las consecuencias perjudiciales de la pérdida de integridad de la membrana por vitrificación. Como se extrae el agua de la suspensión bacteriana se concentrarán los agentes protectores en esta suspensión, favoreciendo el estado vítreo sobre el gomoso de las células. Las células probióticas están embebidas en una matriz vidriosa con mayor estabilidad química y física. La transición desde el estado vidrioso al estado gomoso se produce a la temperatura de transición vítrea, que es característico de cada sacárido.

Parámetros de proceso

Durante el secado por aspersión, la pérdida de viabilidad se produce debido a las altas temperaturas utilizadas en el proceso. Se ha hecho una amplia investigación sobre la influencia de la temperatura de salida (Corcoran, *et al*., 2004). Como se explica anteriormente, se trata de la temperatura que alcanzan las células probióticas al acercarse al final del proceso de secado. Esta temperatura no puede controlarse individualmente puesto que es dependiente de la temperatura de entrada y de la velocidad de alimentación. A mayores velocidades de alimentación, se introduce más líquido en la cámara lo que aumentará la humedad del gas circundante. Esto da como resultado una temperatura más baja a la salida, obteniendo así probióticos con mayor viabilidad. Sin embargo, cuanto mayor sea el contenido de humedad de los alrededores del gas, mayor será la posibilidad de terminar con un producto incompletamente seco, que puede ser perjudicial para un almacenamiento a largo plazo (Santivarangkna, *et al*., 2007)

La liofilización

Desde hace décadas, la liofilización, es el método más conveniente y ampliamente utilizado para la extracción de agua para mejorar la estabilidad de almacenamiento de los probióticos. La liofilización se puede dividir en 3 etapas: congelación, secado primario y secado secundario (Ratti, 2013). Durante la congelación, se forman cristales que pueden dañar los probióticos. El crecimiento de los cristales de hielo depende de la velocidad de congelación y la temperatura. Se prefiere emplear una velocidad alta de congelación en lugar de una velocidad de congelación lenta, ya que así se previene la formación de pequeños cristales de hielo evitando así daños celulares (Abadias, *et al*., 2001). Además, durante la congelación se concentran los solutos en la fracción restante, que conduce al daño químico y osmótico. En el secado primario el agua congelada se elimina por sublimación a vacío, mientras que en el secado secundario, se elimina el agua sin congelar por desorción. Como el agua desempeña un papel importante en la integridad celular y estabilidad, su eliminación de las células probióticas puede dañar a las proteínas de la superficie, la pared celular y la membrana de la célula, disminuyendo su viabilidad después del proceso de secado (Golovina, *et al*., 2009). La liofilización es un proceso costoso que requiere de elevados tiempos de procesado, que se traduce en la producción de una torta seca. Un paso de procesamiento adicional es necesario para obtener las partículas individuales del polvo (Sosnik y Seremeta, 2005). Sería recomendable prestar

atención extra cuando se trabaja con diferentes especies bacterianas en una cámara de liofilización, para garantizar el uso adecuado del equipo y evitar contaminaciones. Sin embargo, la liofilización es una técnica valiosa, que es ampliamente utilizada con diversas estrategias para la mejora de la tasa de supervivencia de los probióticos incorporados.

Estrategias de protección

Incluyen muchas de las estrategias de protección que se han desarrollado anteriormente para mejorar la viabilidad bacteriana durante la liofilización, agregar excipientes al medio de secado, control de los parámetros de proceso, cambio de las condiciones de fermentación de los probióticos. Sin embargo, la eficacia de estas estrategias depende de la tolerancia intrínseca al proceso de secado ya que ésta varía también según la cepa utilizada. Por ejemplo, se evaluó el efecto de la adición de excipientes y la viabilidad de diferentes cepas como la *Lactobacillus gasseri* CRL 1412 y *L. gasseri* CRL 1421 (Otero*, et al.,* 2007). Esta última demostró ser más resistente a la congelación producida durante el proceso de secado. Esta dependencia de la cepa dificulta establecer directrices y conclusiones generales.

Agentes protectores

La adición de crioprotectores a la suspensión bacteriana es una de las estrategias más ampliamente empleadas para su protección y actúan rebajando su punto de fusión. La adición de crioprotectores amplía la fracción sin congelar, dando más espacio a los probióticos, que conduce a un menor daño celular por estrés mecánico o estrés osmótico. Por el contrario, los lioprotectores protegen las células probióticas durante el secado cuando el agua se retira. Los mecanismos subyacentes de protección son similares a los mencionados durante el proceso de secado por aspersión. Algunos azúcares pueden actuar tanto como crioprotectores como lioprotectores, por ejemplo la adición de sacarosa y trehalosa presentan efectos positivos sobre la viabilidad de los probióticos después de la liofilización (Abadias, *et al*., 2001)). Por ejemplo, las bacterias *Lactobacillus helveticus*, originadas del kéfir, mostraron una viabilidad inferior del 10% cuando se liofilizaron sin protector. La adición de un 10% (p/v) de sacarosa o trehalosa había incrementado la viabilidad en un 50% y en un 20%, respectivamente. De todas maneras una vez más el efecto de la adición de un excipiente es específica de cada cepa y que el efecto de la adición de agentes protectores puede tener diferentes efectos sobre el

proceso de secado y posterior almacenamiento. Esto hace difícil por lo tanto predecir el resultado final. Sin embargo, en general, la utilización de trehalosa o sacarosa, solos o en combinaciones con otros productos, mejoran la viabilidad (Castro, *et al*., 1997).

Parámetros de proceso

Los parámetros de proceso, también en gran medida pueden afectar a la viabilidad de los probióticos durante la liofilización, siendo un parámetro clave la temperatura a la cual se congelan los probióticos. Diversos estudios han demostrado que cuanto menor sea esta temperatura, mejores son los resultados de viabilidad (Abadias, et al., 2001, Broeckx, *et al*., 2016, Perdana, *et al*., 2013). Las bajas temperaturas de congelación darán lugar a cristales de hielo más pequeños, limitando así el daño celular, como se mencionó anteriormente. Sin embargo, se debe concluir que una mayor velocidad de congelación no siempre corresponde con los mejores resultados de viabilidad. Al evaluar las velocidades de congelación, puede notarse una clara diferencia en la viabilidad. En primer lugar, una velocidad más rápida de descenso da mejores resultados de supervivencia de los probióticos congelados, hasta llegar a la óptima velocidad de congelación. Un aumento posterior de la velocidad vuelve a ser más perjudicial para los probióticos conservados. Sin embargo, la tasa óptima de congelación depende del lioprotector utilizado.

7.2 Ensayos de referencia con otras metodologías de secado.

Secado por aspersión (Spray drying) de los probióticos.

Se utilizaron células probióticas de *Bifidobacterium animalis subsp lactis* BB-12 (BB-12, Chr. Hansen) descritas en el Capítulo 3 de metodología. Para la protección de los probióticos se emplearon diferentes materiales protectores que fueron agregados a la suspensión del probiótico para reducir el daño térmico durante los experimentos de secado por aspersión. Los materiales protectores se agregaron a la disolución de probiótico en la siguiente proporción: maltodextrina 5% w/w, un polisacárido que se usa como un aditivo alimenticio, inulina al 5% un prebiótico, trehalosa al 5%, un disacárido natural, la lactosa al 5% en peso disacárido derivado de la galactosa y la glucosa que se encuentra en la leche y 20% en peso de leche descremada comúnmente utilizado como agente protector, mostrando un efecto favorable sobre la mejoría de la supervivencia de las células bacterianas durante el proceso de secado por aspersión.

Para los experimentos llevados a cabo mediante el secado por aspersión se empléo un equipo a escala de laboratorio, el B-190 mini spray dryer, Buchi, Flawil, Suiza. Se realizó el secado en flujo paralelo a una temperatura de entrada del aire constante de 100 ºC y la temperatura de salida que estuvo en torno a 60-65 ºC. La disolución de alimentación que contiene las *Bifidobacterium* BB-12® se conservó a temperatura ambiente y se alimentó a la cámara principal a través de una bomba peristáltica, con un flujo de alimentación de 4 mL min^{-1} y con un caudal de aire de 37.4 m^3h^{-1}. El material particulado resultante se recolectó de la base del ciclón y fueron almacenados en viales estériles sellados a 4 ºC. En los casos que se utilizaron protectores

Spray drying sobre material antioxidante.

Como muestra antioxidante se emplea POMANOX® suministrado por Probelte Biotecnología S.L., Murcia (Spain), un concentrado natural de granada obtenido mediante una tecnología propia patentada, utilizando procedimientos físicos de purificación, libre de disolventes, con un alto grado de pureza y estandarizado a su contenido de punicalaginas ver las Tablas 3.1 y 3.2 del Capítulo 3. POMANOX® es un potente antioxidante natural con propiedades antimicrobianas y antifúngicas. Se empleó este concentrado natural con una concentración del 9.5 % en peso ver apartado correspondiente en el Capítuo de metodología, para realizar los diferentes experimentos para la determinación de la pérdida de la capacidad antioxidante durante cada uno de los procesos de secado analizados.

Para los experimentos llevados a cabo mediante el secado por aspersión se empleó un equipo a escala de laboratorio, el B-190 mini spray dryer, Buchi, Flawil, Suiza. Se realizó el secado en flujo paralelo a tres temperaturas de entrada del aire: 140ºC, 160ºC y 180ºC y la temperatura de salida estuvo en torno a 90ºC, 95ºC y 105ºC respectivamente. La suspensión que contiene los compuestos antioxidantes se conservó a temperatura ambiente y se alimentó a la cámara principal a través de una bomba peristáltica, con un flujo de alimentación de 4 mL min^{-1}, con un caudal de aire de 37,4 m^3h^{-1}. El material particulado resultante se recolectó de la base del ciclón y fueron almacenados en viales estériles sellados a 4 ºC.

Liofilización de los Antioxidantes y de los probióticos.

Se utilizó un equipo LYOQUEST -55 de Telstar para los experimentos de liofilización. La cavidad de vacío consta de bandejas provistas de sondas de temperatura para el control de la calefacción de las bandejas y para poder medir la temperatura del producto. En los experimentos de liofilización se emplearon las microcápsulas conteniendo probióticos o antioxidantes. La composicón de probióticos y los antioxidantes se detalla en el Apartado 3.3. Tanto con la microcápsulas de conteniendo probiótico, como con antioxidante, se procedió colocando el material en las tres bandejas uniformemente y fueron congeladas bajo el efecto de la presión baja, disminuyendo rápidamente hasta 600 μbar. Durante la operación la calefacción de las bandejas se mantuvo a 36ºC mientras que la presión disminuyó ligeramente a 200 μbar al final del ciclo de 16 horas. Este procedimiento se empleó tanto para las microcápsulas de material probiótico como aquellas de material antioxidante.

7.3 Análisis comparativo de las cinéticas de secado

En este apartado se procedió a realizar la comparativa de las cinéticas del proceso de secado NFMD propuesto con dos de las tecnologías más ampliamente empleadas y mencionadas anteriormente que son la liofilización y el secado por aspersión o spray drying. Uno de los grandes inconvenientes de los procesos de secado son los tiempos de procesado, en el caso de la liofilización los tiempos de proceso son muy elevados en el caso de los materiales empleados en torno a 13 horas, y en cambio el proceso de spray drying en cuanto a tiempos de procesado es muy rápido. En la Figura 7.2 se puede observar las cinéticas de los diferentes procesos de secado que se van a analizar y comparar. Dentro del proceso NFMD se muestra el más lento (Experimento 2 con probiótco) y más rápido (Experimento 9, con levaduras); experimentos referidos en el Apartado 6.5 y Apartado 5.5, respectivamente.

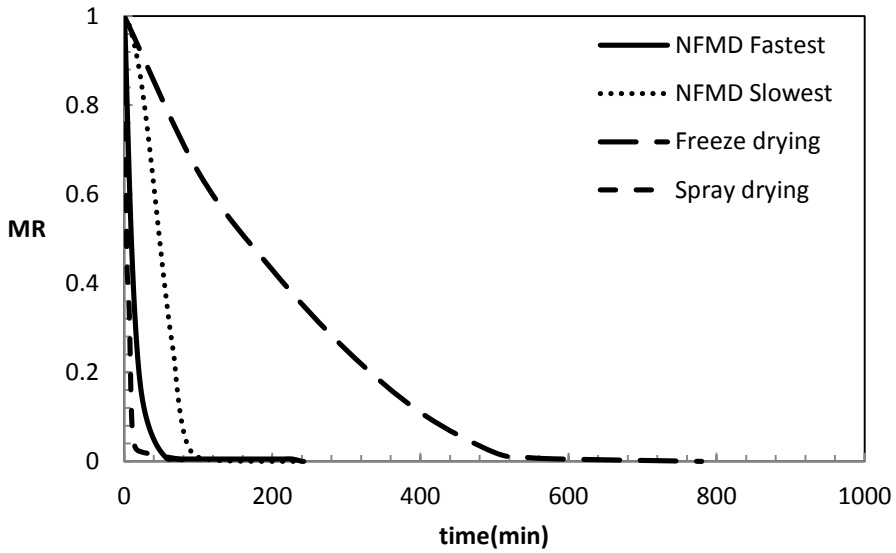

Figure 7.2. Drying kinetics of the NFMD compared with freeze-drying and spray-drying.

El calentamiento por microondas presenta un efecto favorable sobre la cinética debido al gradiente inverso que se origina respecto a otras tecnologías de secado. En la Figura 7.2, se comparan los perfiles de la pérdida de masa de los experimentos NFMD en términos de MR (moisture ratio). Se compara la tecnología se secado propuesta con el secado por aspersión y la liofilización. El tiempo de secado en el proceso NFMD es claramente más bajo que el requerido para la liofilización pero algo mayor que el tiempo observado en el proceso de *spray drying*. Los niveles térmicos aplicados en el proceso NFMD son considerablemente más bajos que los aplicados en el proceso de secado por aspersión como se verá en la sección siguiente. En consecuencia, el NFMD presenta características muy favorables para el secado de materiales termosensibles con eficacias similares a las obtenidas por *spray-drying*, teniendo en cuenta la duración de los ciclos de secado y el consumo energético

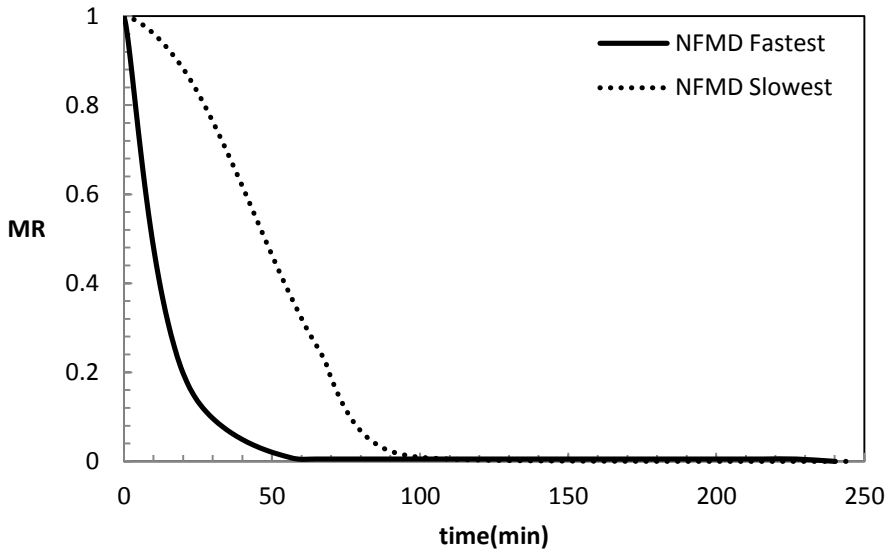

Figure 7.3. Drying kinetics of the fastest NFMD experiment (Exp. 9 yeast Mh/Hm) and the slowest (Exp.2 BB12® Ml/Mh).

Table 7.1. Kinetics drying rates for the selected NFMD experimentes.

Exp.	Code	r_{I-II}	$M_{fin\ II}$	r_{global}	time (min)
2	Ml/Mh	0.038	0.163	0.015	247
9	Mh/Hm	0,254	0,992	0,025	240

*Units: $r_{I,\ II}$ and r_{global}: g H_2O/g d.s. min, $M_{end\ phase\ II}$: g H_2O/g d.s.

En la Figura 7.3 se pueden observar en detalle los dos de los experimentos NFMD llevados a cabo con el proceso de secado. El experimento 9 llevado a cabo con las levaduras es el que cinéticamente es más favorable respecto a los demás experimentos desarrollados a lo largo del trabajo. El experimento 2 llevado a cabo con el material probiótico y con unas condiciones operacionales de niveles térmicos medios para la superficie del producto y una temperatura de entrada del aire de 5ºC en la primera fase ha dado lugar a la cinética más lenta del proceso. En cambio en el experimento 9 se ha empleado una temperatura alta para la entrada del aire en la Fase I y se ha utilizado una temperatura media en la segunda fase pero con una temperatura alta a su vez para la temperatura de la superficie del producto, lo que ha favorecido a la cinética global del proceso tal y como se puede observar también en la Tabla 7.1. De todas maneras en las próximas secciones se va a proceder a realizar un análisis tanto de la calidad como de los factores térmicos y de consumo energético que se ven implicados en este tipo de procesos ya que es necesario realizar una selección conjunta de las condiciones más

favorables cinéticamente, térmicamente y de calidad junto con los aspectos del consumo energético requerido.

7.4 Análisis de los perfiles de temperatura

A la hora de realizar el análisis térmico del proceso de secado llevado a cabo con la tecnología NFMD, se procedió a realizar el análisis de las condiciones que implicaban un aporte de calor y de aquellas condiciones en las que se contemplaban pérdidas convectivas. En la Figura 7.4 se observa como el Experimento 9 de levaduras que en el apartado cinético se ha visto como el más rápido, se puede observar como térmicamente también cuenta con condiciones favorables debido al calor que aporta la temperatura de entrada del aire superior a la temperatura de la superficie del material. Esta circunstancia es favorecedora no sólo de la cinética de secado si no también como a la hora de realizar la valoración energética del proceso.

En contraposición, en la Figura 7.5 se observa el efecto contrario térmicamente, en donde una baja temperatura de entrada del aire dificulta y promueve la pérdida de calor por convección.

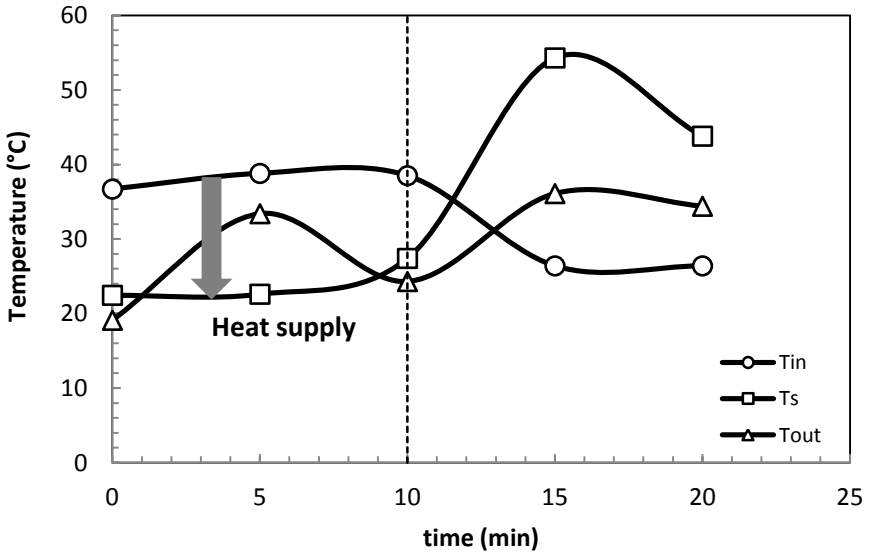

Figure 7.4. Thermal profile of Experiment 9 of yeast (Mh/Hm).

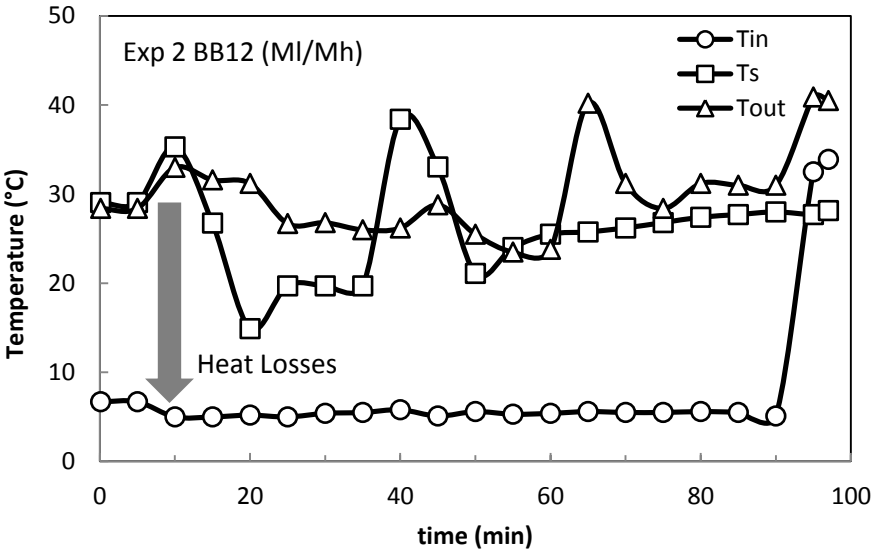

Figure 7.5. Thermal profile of Experiment 2 of BB12® (Ml//Mh).

El aporte calorífico o las pérdidas convectivas observados en ese aportado tendrán su influencia en el apartado siguiente en el que se realizará una valoración del consumo energético requerido para cada uno de los experimentos llevado a cabo con la tecnología NFMD. De todas maneras el análisis del proceso de secado NFMD requiere de una visión global y generalizada de los resultados obtenidos, tanto cinéticamente como energéticamente al que hay que añadir una valoración de la calidad a través de la viabilidad de los probióticos y de la capacidad antioxidante del concentrado de granada empleado en los productos sometidos a secado

7.5 Calidad del producto deshidratado

En este apartado se va a proceder a describir las características de calidad que hemos analizado para cada uno de los materiales empleados, tanto en el caso del material probiótico como en el caso del concentrado de granada. Por ello se va a proceder al estudio de la calidad de cada uno de los materiales por separado y explicando el tipo de análisis realizado en cada caso para su determinación.

Análisis de la capacidad antioxidante de las muestras

Para la preparación del extracto se tomaron entre 0.7-1.1g de muestra y se mezclaron con 10 mL de MeOH/agua (80:20% v/v) + 1% HCl, dispersada con

ultrasonidos a 20 °C durante 15 min y almacenada durante 24 h a 4°C. A continuación, el extracto fue de nuevo introducido en el baño de ultrasonidos durante 15 min y se centrifugó a 15.000 Gs durante 10 minutos. A continuación se analizó la capacidad antioxidante tanto por el método Orac como poel ABTS, decritos en el Capítulo 3 de metodología.

Los resultados que se muestran en la Tabla 7.2 corresponden al secado por *spray drying* del Pomanox®(concentrado de granada comercial), se puede observar como los valores de actividad de agua y de contenido de humedad obtenidos entran dentro de los parámetros de calidad para un almacenamiento prolongado de las muestras (Beuchat, 1981).

Table 7.2. Water activity, moisture content and antioxidant activity results analyzed by Orac and ABTS method for the spray-drying experiments.

Exp.	Protectant	T_{in}	Orac (mmolTE/100g ds)	ABTS (mmol TE/100g ds)	a_w	KF
Pomanox®	-	-	125.64 ± 5.60	371.11 ± 0.52	0.24	6.62
1	-	140	163.50 ± 9.33	482.95 ± 0.89	0.25	6.61
2	-	160	146.76 ± 4.88	433.48 ± 0.35	0.16	5.11
3	-	180	186.20 ± 7.08	549.98 ± 0.59	0.21	5.83
4	maltodextrin	140	175.93 ± 4.83	519.64 ± 0.23	0.14	4.36
5	maltodextrin	160	165.50 ± 3.50	488.86 ± 0.60	0.15	4.91
6	maltodextrin	180	172.83 ± 1.17	510.50 ± 0.78	0.14	4.56
7	Arabic gum	140	165.76 ± 0.69	489.62 ± 1.18	0.16	5.34
8	Arabic gum	160	137.52 ± 3.21	406.20 ± 2.35	0.17	5.54
9	Arabic gum	180	140.88 ± 4.00	416.13 ± 3.89	0.15	4.77
10	Inulin	140	169.85 ± 2.05	501.69 ± 0.98	0.16	5.40
11	Inulin	160	168.87 ± 5.08	498.80 ± 0.73	0.17	5.16
12	Inulin	180	164.97 ± 3.00	487.28 ± 0.48	0.18	5.15

La capacidad antioxidante del concentrado de granada sin ningún tipo de agente protector en todos los casos es inferior a la capacidad antioxidante observada en el resto de los experimentos llevados a cabo con protectores y a temperaturas superiores a 120ºC. El aumento producido en la capacidad antioxidante puede deberse a que a elevadas temperaturas se favorece la aparición de los productos de la reacción de Maillard provocando así un aumento de la capacidad antioxidante del producto. Según estudios realizados en torno a este fenómeno concluyen que los procesos de calentamiento como los que se dan en un proceso de secado por aspersión o *spray drying*, a pesar de que

originan una pérdida parcial de compuestos naturales con actividad antioxidante, las propiedades antioxidantes podrían mantenerse e incluso mejorarse gracias a la formación de nuevos compuestos originados por las reacciones de Maillard. Estos compuestos se forman durante el tratamiento térmico utilizado en la fabricación de alimentos como el chocolate y son capaces de neutralizar la actividad de radicales libres como el ABTS, en función del grado de tostado (Summa, *et al.*, 2008).

Normalmente, la temperatura de entrada utilizada para la técnica de *spray drying* es en torno a 150-220ºC. El contenido de humedad disminuyó con el aumento de la temperatura de secado, debido a la rápida transferencia de calor entre el producto y el aire de secado tal y como se puede observar en la Tabla 7.2. A temperaturas más altas del aire de entrada, hay un mayor gradiente de temperatura entre el alimento pulverizado y el secado de aire y se produce una mayor fuerza impulsora para la evaporación del agua. A pesar de que en este caso sólo se ha tenido en cuenta el análisis de la capacidad antioxidante de las muestras y éste se ha visto favorecido con el incremento de la temperatura de entrada del aire se conoce por otras investigaciones que la temperatura del aire de entrada influyó considerablemente en los pigmentos de zumos de fruta deshidratada. (Quek, *et al.*, 2007) estudió el efecto de la temperatura de entrada (145-175ºC) sobre la estabilidad del licopeno y del β-caroteno en el deshidratado de zumo de sandía. El resultado mostró que, el contenido de licopeno disminuyó al aumentar la temperatura de entrada. Algo similar observaron en el secado de pulpa de tomate (Goula and Adamopoulos, 2005). La reducción del contenido de licopeno fue probablemente debida a la degradación térmica y a la oxidación. La deshidratación con aire expone a los carotenoides al oxígeno, que puede causar una gran degradación de carotenoides. Los productos deshidratados que tienen una gran proporción de superficie respecto a su masa son especialmente susceptibles a la descomposición oxidativa durante el secado y almacenamiento. Los carotenoides se oxidan fácilmente debido al gran número de dobles enlaces conjugados que poseen. Este tipo de reacciones causa la pérdida de color de los carotenoides en los alimentos y es de los mecanismos de degradación más importantes y que más preocupan en este tipo de secado. Debido a la estructura altamente conjugada, no saturada de los carotenoides, los productos de su degradación son muy complejos. Durante la oxidación, se forman inicialmente epóxidos y compuestos carbonilicos. La extensa oxidación dará lugar a la decoloración de los pigmentos carotenoides y a la pérdida de color (Phisut, 2012). La temperatura de entrada también afectó la estabilidad

de las antocianinas en el deshidratado de zumo de acai (Tonon, *et al.*, 2008). El aumento de la temperatura del aire de entrada disminuyó las antocianinas, debido a la alta sensibilidad de estos pigmentos a las altas temperaturas.

Por todo lo expuesto anteriormente, se cree necesario en el caso de los antioxidantes realizar unos análisis complementarios para poder analizar la pérdida de nutrientes asociada a las condiciones de procesado de cada tecnología de secado.

En cuanto al agente protector empleado según los resultados obtenidos la maltodextrina parece mostrar los mejores resultados tal y como se ve reflejado en la Tabla 7.2. Según las investigaciones realizadas la baja concentración del agente puede originar partículas muy adherentes. Queck, *et al*., 2007 investigaron el efecto de la concentración de maltodextrina a diferentes concentraciones (0, 3 y 5%) sobre las propiedades de las partículas de zumo de sandía deshidratadas. La adición de maltodextrina al 5% a la alimentación dió mejores resultados que la adición de maltodextrina al 3%. Estos resultados mostraron que la maltodextrina es útil para el secado del zumo de sandía y como resultado mejoró el rendimiento del producto. Así mismo la adición de maltodextrina podría aumentar el contenido total de sólidos en la alimentación y por lo tanto, reducir el contenido de humedad del producto.

A continuación se va a proceder a realizar el análisis del concentrado de granada previamente encapsulado y secado mediante la tecnología NFMD y la liofilización tal y como se observa en la Tabla 7.3. Si se comparan estos resultados con los obtenidos por el secado por aspersión se puede observar el descenso de la capacidad antioxidante del material. Tal y como se ha mencionado anteriormente se cree que gran parte de la capacidad antioxidante mostrada en el caso anterior es debida a las altas temperaturas y a las reacciones de Maillard. Por ello se cree necesario realizar análisis adicionales a los realizados para ver la incidencia de cada uno de los procesos de secado en otros compuestos importantes a nivel nutricional como pueden ser las antocianinas, los flavonoides, etc.

Table 7.3. Water activity, moisture content and antioxidant activity results analyzed by Orac and ABTS method for NFMD and Lyofilization.

Exp.	Orac (mmolTE/100g ds)	ABTS (mmol TE/100g ds)	a_w	KF
Fresh	119.89 ± 0.25	389.02 ± 0.47	0.99	-
NFMD(Mm/Mm)	31.56 ± 0.38	110.48 ± 0.35	0.28	8.75
NFMD(Hl/Hl)	81.15 ± 0.52	284.04 ± 0.11	0.27	9.38
Lyofilization	58.38 ± 0.82	205.88 ± 1.84	0.20	9.21

Según los resultados mostrados en la Tabla 7.3 los mejores resultados se obtienen para el experimento llevado a cabo a baja temperatura de entrada del aire (5ºC) y a una alta temperatura del material en torno a (40ºC) parece según los datos obtenidos también para la liofilización que el empleo de una baja temperatura en los procesos de deshidratación de materiales con alta capacidad antioxidante es muy favorable y permite la mejor conservación de sus características nutricionales iniciales. Según varios autores la pérdida de compuestos bioactivos, tales como los flavonoides totales, flavonas, catequinas, así como resinas fenólicas resultó ser poco significativa en productos liofilizados (Asami, *et al.*, 2003, Zainol, *et al.*, 2009). Algunos autores incluso han observado un incremento en las concentraciones de fenólicos y antocianinas totales entre un 17-52% y un 7-26% respectivamente, el nivel de incremento depende del tipo de material (arándanos, frambuesas, *Alpinia Zerumbet* (jengibre) ó hojas Elatior), y del sistema de producción (Chan, *et al.*, 2009, Lin, *et al.*, 1998, Sablani, 2006). Según (Abonyi, *et al.*, 2002) observaron una casi completa retención del caroteno durante el proceso de liofilización del 96% de las zanahorias, carambolas, papayas, melón y fresas (Regier, *et al.*, 2005, Shofian, *et al.*, 2011). Además, muchos autores han obtenido un máximo (hasta un 94% en algunos casos y en todos los demás casos superiores al 60%) de retención de ácido ascórbico (Santos y Silva, 2008) como se observa en la guayaba liofilizada (Nogueira, *et al.*, 1978), tomates (Chang, *et al.*, 2006), pimientos (Martínez, *et al.*, 2005), fresas (Abonyi, *et al.*, 2002), zanahorias (Lin, *et al.*, 1998).

Así que tras el análisis realizado en varios compuestos con alto contenido antioxidante con compuestos de gran valor nutricional cabe señalar que el empleo de bajas temperaturas es favorable para la conservación de la mayoría de compuestos con alto contenido nutricional como los carotenoides y las antocianinas que tal y como se ha comentado disminuían significativamente en el proceso de secado por aspersión. Parece

que la tecnología de secado NFMD requiere de análisis complementarios para su verificación pero tras, el análisis bibliográfico realizado de las tecnologías de secado más convencionales. Todo parece indicar que este proceso puede llegar a obtener resultados similares o mejores a los obtenidos en la liofilización con la consiguiente reducción de costes y de tiempo tal y como se verá con detalle a lo largo de este capítulo.

Análisis comparativo de la viabilidad de las muestras probióticas deshidratadas

En este caso se partió de material probiótico ampliamente empleado en la industria láctea (*Bifidobacterium animalis subsp. Lactis* BB12®, suministrado por Chr HANSEN (España) en formato congelado, conteniendo una concentración de células activas superior a 8,1 10^{10} ufc/g. Se utilizó una suspensión al 2,5% de alginato y el 83,3% de probiótico (cantidad requerida para obtener una concentración celular del orden de 10^9 ufc/ml, que se extruyó y se cortó con un equipo de *jet cutter* para la obtencion microcápsulas de entre 2000-2500 µm de diámetro, según se indica en Apartados 3.2 y 3.3. La viabilidad de las muestras probióticas se analizó a través de la metodología descrita en el Capítulo 3 Apartado 3.4.

Las muestras deshidratadas por aspersión están expuestas a altas temperaturas en la cámara de secado. A pesar de que las temperaturas de secado pueden ser tan altas como 200°C, las células probióticas no están constantemente sujetas a temperaturas tan altas. Como se mencionó anteriormente, durante la fase de secado constante, la temperatura de los probióticos está limitada a la temperatura de bulbo húmedo. Por lo tanto, la inactivación térmica es más probable que ocurra durante la fase de velocidad de secado descendente. En esta etapa, las células probióticas pueden llegar a la temperatura del aire de secado circundante. Las partículas secas a menudo permanecen en la máquina hasta el final del ciclo de secado, pudiendo llegar a calentarse hasta alcanzar la temperatura de salida, lo que lo convierte en un parámetro crítico que influye en la viabilidad. Las altas temperaturas pueden provocar la desnaturalización de las proteínas y desestabilizar las membranas, posiblemente conduciendo a la muerte celular. Sin embargo, es importante tener en cuenta que el contenido de humedad y la actividad de agua (a_w) del material deshidratado obtenido están relacionados con la temperatura de salida. La a_w tiene un papel importante durante el almacenamiento de los probióticos. Las temperaturas más altas reducen el valor de a_w y generalmente conlleva a una mayor estabilidad durante el almacenamiento. Así que, es importante encontrar una temperatura

de salida óptima, lo suficientemente alta como para obtener valores de a_w y asegurar la estabilidad, pero evitando el letal daño celular.

La inactivación causada por la deshidratación a menudo ocurre simultáneamente con el estrés térmico. Durante la deshidratación, las moléculas de agua se extraen de las células y su entorno, lo que limita las reacciones químicas y las actividades metabólicas. Como las moléculas de agua desempeñan un papel importante en la estabilización de varios componentes de la célula, su eliminación tendrá implicaciones fisiológicas en la integridad de la célula y en su estructura. La bicapa lipídica de la membrana celular es estabilizada por un equilibrio entre repulsión de hidratación y fuerzas de atracción de van der Waals. Esta estabilidad se debilita por la deshidratación, provocando la fuga de compuestos intracelulares, posiblemente provocando la muerte celular. Perdana, *et al*., (2013) realizó experimentos de secado en solo una gota con *Lactobacillus plantarum WCFS1* y evaluó el efecto de la temperatura y la deshidratación en la inactivación de los probióticos (Perdana, *et al.*, 2013). Sus resultados mostraron que con el uso de temperaturas inferiores a 45°C, la inactivación por deshidratación era predominante. En contraposición con los resultados obtenidos a temperaturas superiores a 45°C, donde la inactivación por estrés térmico y la deshidratación estaban presentes. Propusieron también que cuanto mayor es el tiempo de secado, las células probióticas son más propensas al estrés por deshidratación. Al extrapolar sus resultados a un equipo a escala de laboratorio, los investigadores sugirieron que el factor de estrés importante que afecta la viabilidad durante el secado por aspersión es la inactivación térmica ya que el tiempo de secado requiere de tiempos cortos (Broeckx, *et al.*, 2016). Para poder evitar el daño térmico y el debido a la deshidratación de las muestras probióticas se emplean diferentes agentes protectores para reducir en lo posible los efectos del proceso de secado.

Table 7.4. Water activity, moisture content and Survival results for Spray drying.

Exp.	Protectant	a_w	KF	Survival (%)
1	No protectant	0.613	8.955	75.81 ± 3.08
2	Skim milk	0.538	8.656	69.49 ± 3.80
3	Inulin	0.552	8.502	84.60 ± 2.42
4	Lactose	0.545	7.940	68.96 ± 2.20
5	Maltodextrin	0.571	6.921	90.08 ± 1.04
6	Trehalose	0.457	8.516	94.09 ± 3.21

Los resultados obtenidos en la Tabla 7.4 muestran los datos obtenidos de viabilidad con diferentes agentes protectores, la actividad de agua de las muestras y el contenido de humedad de las mismas. Algunos azúcares como la trehalosa y la sacarosa pueden también actuar como protectores compatibles. Como el tiempo de procesado durante el secado por aspersión es corto los solutos compatibles deben ser incorporados a la suspensión probiótica antes del proceso de secado. Además, la incorporación de estos compuestos a los medios de crecimiento permite a los probióticos ocupar el soluto deseado durante su crecimiento. Diferentes comportamientos de la viabilidad de bacterias lácticas se observan cuando se emplean diferentes solutos compatibles. La trehalosa, conocido como un soluto compatible, ejerce efectos positivos sobre diferentes cepas de *L. plantarum* según los resultados obtenidos y mostrados en la Tabla 7.4 se puede observar como el secado por aspersión llevado a cabo con trehalosa como agente protector ha mostrado los mejores resultados en cuanto a viabilidad . También los prebióticos como la inulina y fructo-oligosacáridos pueden influir positivamente a la viabilidad después del secado por aspersión y durante el almacenamiento de varias cepas de *lactobacillus*, entre los que destacan: *L. rhamnosus* B442, *Lactobacillus kefir* CIDCA 8321 y L. kéfir *CIDCA* 8348.

Table 7.5. Water activity, moisture content and Survival results for Spray drying.

Exp.	Protectant	a_w	KF	Survival (%)
1	Trehalose 2%	0.111	5.83	92.15 ± 3.05
2	Maltodextrin 2,5% + Trehalose 2,5%	0.106	6.40	84.68 ± 3.20
3	Maltodextrin 2%	0.088	7.09	94.92 ± 2.50
4	Maltodextrin 4%+ trehalose 1%	0.109	6.15	90.08 ± 3.52

En otros experimentos, se han empleado, maltodextrinas o leche descremada reconstituida como protector a la solución de alimentación, según los resultados obtenidos parecen tener un efecto positivo sobre la viabilidad bacteriana después del secado en los resultados que se muestran en la Tabla 7.4 se puede observar el buen resultado de viabilidad obtenido en las muestras probióticas empleadas. Los altos valores obtenidos en los resultados de la actividad del agua se deben a la gran higroscopicidad de las muestras y al no correcto de las muestras hasta su análisis en esta tanda de experimentos. Tras analizar los resultados de la Tabla 7.5 se procedió a combinar varios

de los protectores utilizados anteriormente para poder observar si se puede conseguir una mejoría en los resultados de la viabilidad de los microorganismos.

A tenor de los resultados que se muestran en la Tabla 7.5 se puede observar como la combinación de los agentes protectores en el caso de las muestras probióticas empleadas no ha repercutido en un aumento de la viabilidad de las muestras, es más los resultados más favorables se han obtenido para las muestras en las que tan solo se ha empleado un agente protector como la trehalosa al 2% con un resultado del 92.15% de células viables y el mejor resultado se observó para la maltodextrina al 2% con un resultado superior al 94%. Tanto los resultados de actividad de agua como los del contenido de humedad están dentro de los valores requerido para un almacenamiento prolongado (Aronsson y Rönner, 2001).

Table 7.6. Water activity, moisture content and Survival results for NFMD and Lyofilization.

Exp.	Code	a_w	KF	Survival (%)
1	Mm/Mm	0.26	8.87	48.71± 2.03
2	Ml/Mh	0.29	10.08	53.14 ± 1.88
3	Ml/Mm	0.28	10.52	89.77 ± 3.15
4	Ml/Ll	0.28	9.54	46.22 ± 5.30
5	Hm/Hm	0.27	8.76	85.92 ± 2.50
6	Hm/Ml*	0.24	8.81	90.39 ± 3.05
Lyo.	-	0.21	9.15	90.45 ± 3.25

*Sample prepared with suspension of 3.3% alginate and 30% of probiotic.

En la Tabla 7.6 se muestran los resultados obtenidos en el proceso de secado NFMD para las muestras probióticas. Tal y como se puede observar en la Tabla, los resultados obtenidos tanto para los Experimento 3,5 y 6 son superiores en cuanto a la viabilidad al 85% siendo incluso entorno al 90% para el Experimento 6, valor muy cercano al obtenido en el experimento de la liofilización. Estos resultados óptimos se pueden deber al efecto protector de los cationes de Ca^{2+} que contiene el alginato de calcio que forma la cápsula protectora. En un estudio reciente, el efecto protector de la leche descremada se atribuyó a la presencia de Ca^{2+} y proteínas en lugar de la presencia de lactosa. De hecho, también demostraron que Ca^{2+} juega un papel en la mejora de la resistencia térmica de las bacterias lácticas. Se puede concluir que los resultados obtenidos por las diferentes tecnologías de secado son similares en todos los casos si se tiene en cuenta la desviación asociada a cada una de las muestras analizadas.

7.6 Valoración energética

En este apartado se va a estimar el coste energético de cada una de las tecnologías que se han analizado en este capítulo para poder hacer una valoración global del proceso de secado NFMD propuesto frente a otras tecnologías más convencionales y establecidas en la industria alimentaria.

Proceso de secado NFMD

El proceso de secado descrito en este trabajo y el análisis energético del mismo se ha ido realizando a lo largo de cada uno de los capítulos. El consumo energético debido al uso de la energía de microondas se ha determinado con el análisis de la Q_{abs}.

$$G = \int_0^t Q_{abs}(t)dt \tag{7.1}$$

Donde Q_{abs} es el calor específico absorbido (J/m^{3}min).

Uno de los aspectos que hasta este momento no se ha tenido en cuenta, es la energía requerida para el calentamiento del aire de entrada al lecho de partículas, es decir la energía requerida para el calentamiento del aire que ha sido calculada a través de la ecuación siguiente:

$$G_{cal,1} = \frac{Q_{air}\, c_{p,air}\, \rho_{air}(T_{in} - T_{room})}{m_o} t \tag{7.2}$$

Otro aspecto que se ha tenido que tener en consideración en el proceso de secado NFMD es la energía empleada por el deshumidificador del aire tal, que conlleva a su vez una descompresión del aire y se ha calculado tal y como se muestra a continuación.

$$G_{pump} = \frac{Q_{air}\, \Delta P}{m_o} t \tag{7.3}$$

Una vez que se han definido todos los consumos implicados en el proceso de secado NFMD, se puede estimar el consumo eléctrico del proceso.

Consumo eléctrico:

$$GE_{mw} = G_{mw} / \eta_{mw} + G_{cal,1} / \eta_{cal,1} + G_{pump} / \eta_{pump} \quad (7.4)$$

Donde η es el rendimiento de cada uno de los requerimientos energéticos necesarios para poder llevar a cabo el proceso de secado por microondas denominado NFMD.

Table 7.7. Parameters needed for the heating and mechanical energy calculations for NFMD.

Heating Energy		**Mechanical Energy**	
Q_{air}/m_o	1.18(L/min g)	Q_{air}/m_o	1.18(L/min g)
$c_{p,air}$	1.012(J/g K)	ΔP	7.5bar
ρ_{air}(20ºC)	1.2 (g/L)	$t_{cal,1}$	15
(T_{in}-T_{room})	(40-20)(ºC)	t	240 (min)

Table 7.8. Energy consumption for yeasts and probiotics BB12® in NFMD.

Exp.Yeast	**CODE**	t_{on}**(min)**	G**(kJ/cm^3)**	G**(kJ/g)**
1	Ll/Ml	8.46	10.66	9.93
2	Ml/Mm	8.52	10.99	10.23
3	Ll/Lh	5.41	5.20	4.84
4	Mm/Ml	12.36	11.41	10.62
5	Lm/Mm	13.25	8.99	8.37
6	Lm/Hh	6.33	6.20	5.77
7	Lm/Hm	7.47	11.45	10.66
8	Lh/Hh	8.19	10.58	9.85
9	Mh/Hm	7.33	13.70	12.76
Exp.BB12®	**CODE**	t_{on}**(min)**	G**(kJ/cm^3)**	G**(kJ/g)**
1	Mm/Mm	7.52	10.01	9.60
2	Ml/Mh	21.14	28.66	27.48
3	Ml/Mm	21.68	35.36	33.90
4	Ml/Ll	16.61	19.71	18.90
5	Hm/Hm	6.62	12.65	12.13

En la Tabla 7.7 se muestran todos los parámetros necesarios para estimar el consumo calorífico del aire y el consumo del deshumidificador. En la Tabla 7.8 se muestran los consumos de cada uno de los experimentos debido al calor suministrado por la energía de microondas tal y como se ha ido desarrollando a lo largo de cada uno de los capítulos para cada uno de los materiales empleados. El consumo producido por el calentamiento del aire y del deshumidificador se ha estimado de igual manera para todos

los experimentos NFMD realizados. En cambio, en el caso del calor de microondas absorbido, *G*, el cálculo se ha realizado de manera más rigurosa mediante aplicación del modelo matemático, como se ha visto en capítulos precedentes.

Proceso de secado por aspersión o spray drying

En el secado por aspersión se dan solo dos fenómenos de requerimiento energético que son el necesario para calentar el aire, y el de la bomba necesaria para alimentar la cámara. Las ecuaciones necesarias para su determinación se han descrito previamente siendo las Ecuaciones (7.2) y (7.3).

Consumo eléctrico:

$$GE_{sd} = G_{cal,1}\eta_{cal,1} + G_{pump}\eta_{pump} \tag{7.5}$$

Table 7.9. Parameters needed for the heating and mechanical energy determinations for spray drying technology.

Heating Energy		**Mechanical Energy**	
Q_{air}/m_o	6.23(L/min g)	Q_{air}/m_o	4.00E-05(L/min g)
$c_{p,air}$	1.012(J/g K)	ΔP	2bar
ρ_{air}(20ºC)	1.2(g/L)		
(T_{in}-T_{room})	(140-20)(ºC)	t	10 (min)

Proceso de secado por liofilización

El secado por liofilización que se ha empleado en nuestros ensayos consta de una placa calefactora además del sistema de refrigeración y de la bomba de vació habituales en este tipo de procesos de secado.

Consumo generado por el calentamiento con la placa calefactora:

$$G_{cal,2} = \frac{\frac{k}{e_l}(T_{f,2} - T_{cal})}{\frac{m_o}{A_{cal}}} t \tag{7.6}$$

Donde m_o se define por la siguiente ecuación teniendo en cuenta el espesor (e_l), la porosidad (ε), densidad (ρ) y el área calefactora de la placa (A_{cal}).

$$m_o = e_l A_{cal}(1-\varepsilon)\rho \tag{7.7}$$

El consumo producido por el sistema de refrigeración implica la eliminación del calor generado por la placa calefactora, teniendo en cuenta la eficiencia (*E*) del sistema de refrigeración.

$$G_{sr} = \frac{G_{cal,2}}{E} \tag{7.8}$$

El consumo requerido para el cambio de fase está implícito en el sistema de calefacción.

$$G_{phc} = (1-W_{ds})\lambda_{sub} \tag{7.9}$$

$$k_l = k_{air}V_{air} + k_w V_W + k_s V_s \tag{7.10}$$

La ecuación necesaria para la energía de la bomba es la misma que la mencionada anteriormente en la Ecuación (7.3) pero el caudal corresponde al aire extraido para mantener el vacío.

Table 7.10. Parameters needed for the heating and mechanical energy determinations for lyophilization.

Heating Energy		**Mechanical Energy**	
κ_l	1.75 (W/mºC)	Q_{air}/m_o	5.85E-04(L/min g)
$(T_{f,2}-T_{cal})$	$(T_{f,2}$-31.6)(ºC)	ΔP	1 bar
ρ	1074.10(kg/m^3)	W_{ds}	0.15
ε	0.32	λ_{sub}	2591(kJ/kg)
e_l	0.02(m)	E	1.5
		t	720 (min)

El consumo eléctrico generado por el equipo de liofilización se define como:

$$GE_{Lyo} = G_{sr}/\eta_{sr} + G_{cal,2}/\eta_{cal,2} + G_{pump}/\eta_{pump} \tag{7.11}$$

Comparativa del Consumo de las tres tecnología de secado

Una vez que se han definido cada una de las ecuaciones y los parámetros empleados para realizar la valoración energética de cada una de las tecnologías de secada que se han desarrollado a lo largo del capítulo. En la Tabla 7.11 se recogen los datos del consumo producido por cada uno de los sistemas tanto mecánicos como caloríficos

requeridos por cada una de las tecnologías de secado, así como el consumo eléctrico de cada una de ellas.

Table 7.11. Energy requirements and consumption for each drying technology.

Technology	**Heating Energy**			**Mechanical Energy**		**GE**
	G_{mw}(kJ/g)	$G_{cal,1}$(kJ/g)	$G_{cal,2}$(kJ/g)	G_{pump}(kJ/g)	G_{sr}(kJ/g)	
NFMD	4.84	0.43	-	2.12E-3	-	6.91
Spray Drying	-	9.08	-	1.25E-4	-	9.56
Lyophilization	-	-	16.35	8.42E-7	10.90	44.47

Según los datos que se muestran en la Tabla 7.11 el consumo energético del proceso de secado NFMD es muy competitivo frente a la liofilización que es la que mayor coste lleva asociado. Cabe destacar que la liofilización, es un método de conservación muy largo y costoso debido a las bajas velocidades de secado generadas por el sistema de refrigeración y el sistema de la bomba que aumenta los costes energéticos (Liapis, *et al.*, 1996, Ratti, 2001). Ratti (2001) ha cuantificado los costes de la liofilización de entre 4 a 8 veces superior al secado por aire caliente. En el caso del consumo producido por la tecnología NFMD se ha tomado el menor consumo energético debido a las microondas. Pero aún así, se observa que los consumos pueden incluso en el caso de consumos más elevados estar en torno a los valores que se han obtenido para la tecnología de secado por aspersión o *spray drying*.

El secado con microondas es una alternativa de secado que ha ido ganando popularidad en los últimos años para una gran variedad de productos industriales (Krokida, *et al.*, 2000). Puede considerarse como un proceso de deshidratación rápido que reduce el tiempo de secado, hasta el 89% del tiempo según algunos autores (Maskan, 2001, Therdthai y Zhou, 2009). Un proceso de secado por microondas consiste en tres períodos de secado: el primero consiste en un período de calentamiento en el cual la energía de microondas se convierte en energía térmica dentro del material húmedo y la temperatura del producto aumenta con el tiempo, el segundo es el periodo de secado rápido durante el cual se utiliza la energía térmica para la vaporización de la humedad y el tercero se corresponde con el periodo de menor velocidad de secado durante el cual la humedad local se reduce a un punto que la energía necesaria para la vaporización de la humedad es menor que la energía térmica inducida por las microondas (Maskan, 2001, Zhang, *et al.*, 2006). El secado por microondas puede considerarse un proceso de calentamiento volumétrico ya que la energía electromagnética es absorbida directamente

por el agua de los materiales energía que se convierte en calor por la agitación molecular (Khraisheh, *et al.*, 1997,Piyasena, *et al.*, 2003). Cabe destacar, que el secado por microondas ha demostrado tener entre bajos y moderados consumos energéticos (Tulasidas, *et al.*, 1997, Sagar y Suresh Kumar, 2010, Motevali, *et al.*, 2011). La energía de microondas (generalmente a frecuencias de 2450 y 915 MHz) se ha utilizado en el secado de hierbas (Özbek y Dadali, 2007), patatas (Bouraoui, *et al.*, 1994), manzanas y setas (Feng y Tang, 1998), zanahorias (Jia, *et al.*, 2003), kiwis (Maskan, 2000). En general, la aplicación de microondas se ha extendido para mejorar la calidad general del producto con gran aroma, color y retención de nutrientes, las velocidades relativamente rápidas de rehidratación, así como el considerable ahorro energético (Maskan, 2000, Torringa, *et al.*, 2001, Orsat, *et al.*, 2007, Ghanem, *et al.*, 2012). La combinación del secado de microondas con la protección de los materiales debida a la tecnología de la encapsulación junto con la combinación durante el proceso del secado en lecho fijo-fluidizado hacen de la tecnología propuesta NFMD una tecnología particularmente conveniente para el secado de materiales sensibles al calor y ofrece la oportunidad de reducir los tiempos de procesado y mejorar la calidad del producto en comparación con otras tecnologías de secado en el que se emplea únicamente la tecnología de microondas.

Chapter 8

CONCLUSIONS

8 CONCLUSIONS

In recent decades, there has been a change in the trends of food in developed countries, and the concept of a balanced diet has come to mean maintaining a proper diet based on foods that promote health and well-being. In this sense, a growing number of consumers are aware that foods are not only necessary for nutrition and sustenance, but also play an important role in improving the quality of life and the prevention of chronic diseases in today's society. On the other hand, the level of health is directly associated with the health expenditure for and the frequent incidence of these diseases, the increase in life expectancy and the aging of the population have had great impact on the increase in the cost of health care, promoting public policies to improve practices and dietary habits of the population.

In this context of health and wellness, functional foods play a key role in the diet. The concept of functional food (emerged in the 80s, in Japan), implicitly express that food and components food can exercise a beneficial influence on physiological functions to improve the state of health and welfare and reduce the risk of chronic diseases as the hypertension, diabetes, obesity or cardiovascular problems.

The information consistently indicates that functional foods market is growing and is expected to continue to do so in the foreseeable future. At least 168 companies are working in the field of functional foods in Europe. This trend makes that the production of functional ingredients, with demonstrated activity and stabilized for its incorporation to a greater number of food matrices, is an area of study of great interest and very demanded by the food industry .In this sense this thesis has been framed, oriented to the development of protection and drying systems that allow to obtain probiotic ingredients and antioxidant in stable conditions for the use in the special food elaboration.

The dehydration is used to stabilize probiotics and bioactive compounds for its storage, handling, transport and later use in applications in functional food. The freeze-drying is frequently applied technology for the dehydration of probiotics and bioactive compounds, while spray.drying has been applied to the dehydration of a limited number of probiotics and bioactive compounds. The inactivation of the probiotic cells occurs mostly during the freezing stage during freeze drying. The elimination of the water

content causes the damage of membrane proteins causing the loss of the function of the cells. Spray drying, on the other hand, is a significantly shorter process but leads cells to a high thermal stress due to the high temperatures required during the process (100-200°C). The effect of spray drying can lead to increase permeability of the cell which can cause the exit of intracellular cell components to the environment. The cytoplasmic membrane is a very susceptible part in bacterial cells to tensions associated with the spray drying, leading to the cell activity loss.

These two technologies have been taken as reference for the analysis of the proposed process, called Near Fluidizing Microwave Drying (NFMD), to become an alternative drying technology for the previously mentioned, decreasing the thermal stress of the samples because of the temperatures used during this process (5-45 °C) and its corresponding monitoring. The proposed technology combines the technology of microencapsulation for the protection of the natural ingredients with the drying process by applying microwave on a fixed-fluidized bed of particulated material. For the study of the NFMD process has been needed a systematic experimental work of the proposed method to select the processing conditions.

After the analysis of the results obtained and exposed throughout this thesis, as general conclusion can be considered that the operational parameters of the combined process of microencapsulation with the NFMD have been established. Thus, the problems originated in other reference drying technologies have been minimized. A mathematical model has been applied, describing satisfactorily the process. This enables to analyze the interrelation of the operational variables and its effect, allowing to design the most favorable drying process under quality and energy efficiency criteria.

Then, the most relevant conclusions drawn from each experimental chapter will be extracted.

Combination of encapsulation and drying process

It has been selected, after a literature review, the use of alginate as a suitable encapsulating material for the use in the extrusion technique. The definition of the required composition of alginate was obtained (2-3.5% w/w), according to encapsulated

ingredients (probiotics or antioxidant) for a 2.5 mm particle size. The encapsulated probiotic material´s concentration was adjusted to contain a number of viable cells around 8.0 10^{10} cfu/g mix. A viscosity value around 4500 cP was found as the most appropriate for the extrusion.

The definition of the NFMD process was established through the control variables: inlet temperature, bed temperature and the air velocity. Defined the process, the microwave power of the equipment was varied (150-350 W), depending on the material employed and on the size of the bed (70-200 g).

The adequacy of the bulk size of fluidizing bed was determined for the correct monitoring of the temperature of the product, due to the strong reduction (more than 75 %) of the particle bed thickness estimated along the three phases.

Air velocity has played a key role in the definition of the three drying phases together with the microwave power applied for the control of the temperature of capsule surface and that of the inlet air as control elements for the determination of thermal levels. An essential aspect in the estimation of the phase transitions was the convergence between the experimental and theoretical minimum fluidization velocities. This convergence was found characteristic of the Phase II-III transition and corresponds to certain moisture content with slight oscillations depending on the capsule composition.

The results obtained have served to establish the bases for the application of the NFMD technology to obtain dehydrated encapsulated probiotic material. About 90% of the initial water content was eliminated in Phases I and II where the heating is applied by microwave. In Phase I, near 50% of the humidity is eliminated reaching the maximum of the drying rate, while in Phase II appears the diffusional control, decreasing the drying rate. Moreover, the Phase III, of little importance regarding the water removal, is employed to reach the value of water activity required under quality criteria.

For the selection of the different strategies, monitoring the water activity and its decreasing rate through the critical interval (0.6 – 0.4) was found transcendental for the final quality of the dehydrated product. Thus, the highest thermal levels applied initially can develop in the capsule a high resistance to the moisture diffusion during Phases II and III. A slow decreasing rate of the water activity has proved to cause undesirable effects on the quality of the dried material.

Application of the NFMD process to reference encapsulated microorganism

For a better control of the process, were considered three phases after a review of the correspondence between theoretical minimum and experimental fluidization velocity. The results show characteristic values of the particles moisture (wet basis) around 0.75 and 0.49 for the end of the Phase I and II, respectively, for the yeast (*saccharomyces cerevisiae*).

The average value of the drying rate in the experiments on yeast microcapsules was found around 0.02 g H_2O/g d.s with no significant variations, spite of the sensible differences on the drying time observed in Phases I and II. The large duration of the Phase III absorbs the variations of the previous phases.

The operation conditions employed and the thermal gradient (from the product to the air or *viceversa*) generate a convective flow that supposed: a calorific contribution or losses. Nevertheless, low or medium air temperatures seem to be a favorable effect for the quality of the dehydrated product, despite the negative effect on the energy consumption. .

The NFMD process has resulted to be a good technology for the dehydration of the microencapsulated probiotics. In spite of the greater thermal-sensitivity of the species BB12® (*Bifidobacterium animalis subsp. lactis*), the results reveal that the NFMD process can be applied satisfactorily with temperatures in the product up to 45 °C and temperatures of ≈25 °C in the surrounding air. In these conditions, the best kinetic and quality results of the dried material were achieved with survival results around 90% of initial living-cells. For the correct application of the NFMD process, the definition of the three phases after the corresponding fluid-dynamic study show characteristic mean values of the moisture (wet basis) around 0.60 and 0.30 for the end of Phases I and II, respectively, in the case of probiotics. Such values seem to be related to changes in the necessary heat applied for the vaporization of the moisture retained in the solid matrix. These changes were obtained through calorimetric studies (DSC) to estimate the heat power input associated to the vaporization of the microcapsules moisture.

The mathematical model applied in this work, describes adequately the kinetics and thermal profiles of the NFMD process, either in the microwaves-on phases (Phase I and II) or in the microwave-off phase (Phase III). A good fitting of the model to the

experimental kinetics values requires also modeling the moisture change at the particle surface along drying. The change rate of moisture boundary value at the particle surface is described through the first order kinetic constant β. Thus, coefficient β must be considered together with the effective diffusivity *D* for the simulation of drying.

D values change according to the stages as a result of the temperature of the product (Phases I and II) and the structure of the solid matrix (Phase III). The diffusivity during the Phase II presents the highest value coinciding with the maximum drying rate as higher is the temperature of the product.

The NFMD process was evaluated with and without consideration of the shrinkage effect. The diffusivity values become lower when the shrinkage effect is introduced in the model. However, the lowering effect on *D* was not significant for microcapsules of BB12®, if compared with yeast microcapsules, in which the diffusivity values found were comparatively higher. Consequently, shrinkage of microcapsules does not significantly alter the diffusional mechanisms for diffusivity values around 2 E8 m^2/min or lower.

The resolution of the energy balance was applied in the drying of probiotics (BB12®) microcapsules. This has allowed to estimate the electric field *E* in a range between 1600 and 1900 V/m, in order to achieve an adequate thermal control of the process depending on the pre-defined operational strategy. This *E* range is very similar to the observed in the case of yeasts microcapsules.

Other analyzed parameter involved in the energy balance, apart from the electric field *E*, was the convection coefficient *h*. Consequently, the absorbed heat by the product and microwave energy consumption could be calculated. The low thermal level (15ºC) and medium air temperature (20ºC) imply a reduction of the energy consumption, which corresponds to the most efficient strategies associated to the kinetics.

Comparison of the NFMD process with other reference drying technologies

A sensible difference was found regarding drying kinetics. The NFMD process gives intermediate drying rates around 0.03 g/min while the technology of spray drying is the fastest with a drying rate of 0.06 g/min. On the other hand, freeze-drying was found to be slowest process with a drying rate around 0.005 g/min.

Spray drying requires higher process temperatures in some cases higher than 150 °C. On the other hand, the freeze-drying could be a more favorable process if used on small loads but this requires a greater heating surface and size of the freeze-drying equipment.

The viability after drying (survival) of highly thermosensible probiotics was analyzed showing that both processes: freeze-drying and spray drying were affected by the heat stress due to the freezing and to the high temperatures respectively. Instead, the cell survival results of the proposed NFMD process were higher than 90%, only affected by the dehydration stress appearing in the three analyzed technologies. The heat stress in NFMD process was reduced due to the heat control and the employed temperatures (15-45°C). Concretely, it was observed that the cases with water activity profiles showing a fast transition through critical water activity interval (0.4-0.6) gave the most satisfactory results of cell viability in the dehydrated product.

The NFMD process applied to antioxidant compounds showed a small drop of the antioxidant capacity which is justified due to the oxidative deterioration due to the increasing of the product specific surface. In the case of spray drying was observed an increase in the antioxidant capacity even more than the initial values, which according to references is due to the apparition of Maillard reaction compounds. This increase of the antioxidant capacity has been highly questioned in the literature since it can be a consequence of the thermal degradation of the material.

Energy consumption was analyzed in comparison with reference drying technologies. The NFMD process energy consumption was around 4.84 kJ/g being very competitive respect to the spray drying value of 6.91 kJ/g. The consumption of the proposed NFMD process, giving also good cell viability results, was found 30% lower than the value obtained in the process of spray drying and a sixth of the consumption required by freeze-drying.

Capítulo 9

NOMENCLATURA

9 NOMENCLATURA

A	Área de interfase aire-sólido en secado de sólidos, m^2.
a	Superficie específica del lecho de partículas , m^2/m^3.
A_{cal}	Área calefactora de la placa, m^2.
a_w	Actividad del agua, adimensional.
b	Indicador de encendido (1)/ apagado(0).
b_{ac}	Fracción de tiempo en la que el microondas está encendido, adimensional.
c	Velocidad de la luz, $m \cdot s^{-1}$.
cfu_0	Unidades formadoras de colonias iniciales en el producto, adimensional.
cfu_{fin}	Unidades formadoras de colonias en el producto final, adimensional.
C_p	Calor específico, $J \cdot Kg^{-1}{}^oC^{-1}$. Con subíndices, w (agua), al (alginato), lev (levadura), BB12®.
D	Difusividad efectiva, $m^2 \cdot min^{-1}$. Definidas como D_1, D_2, D_3 para las Fases I, II, III. Diámetro de boquilla (Capítulo 2), m.
D_c	Diámetro del cilindro, m.
D_P	Diámetro característico de la partícula, m.
d_p	Profundidad de penetración, m.
D_{sph}	Diámetro esfera equivalente, m.
d_{wire}	Diámetro del disco de corte, m.
E	Campo eléctrico, $V \cdot m^{-1}$.
E	Eficiencia (Capítulo 7), adimensional.
e_l	Espesor del lecho, m.
f	Frecuencia, s^{-1}.
G	Consumo de energía absorbido por el producto, $kJ \cdot cm^{-3}$.
g	Gravedad , $m \cdot s^{-2}$.

$G_{cal,1}$	Consumo de energía requerido para el calentamiento del aire, kJ/g.
$G_{cal,2}$	Consumo de energía requerido para el calentamiento de las placas, kJ/g.
GE_{Lyo}	Consumo eléctrico para el proceso de liofilización, kJ/g.
GE_{mw}	Consumo eléctrico para el proceso de microondas, kJ/g.
GE_{sd}	Consumo eléctrico para el proceso de spray drying, kJ/g.
G_{max}	Consumo máximo generado por las microondas, $kJ \cdot cm^{-3}$.
G_{mw}	Consumo de energía eléctrica del generador microondas, $kJ \cdot cm^{-3}$.
G_{phc}	Consumo de energía requerido para la sublimación, kJ/g.
G_{pump}	Consumo de energía requerido por la bomba, kJ/g.
G_{sr}	Consumo de energía requerido para el sistema de refrigeración, kJ/g.
h	Coeficiente de convección, $W \cdot m^{-2} \cdot {}^{o}C^{-1}$, altura de la partícula (Capítulo 4), m.
k	Conductividad térmica,$W \cdot m \cdot {}^{o}C^{-1}$. Con subíndices: w (agua), al (alginato), lev (levadura), BB12®.
k_G	Coeficiente externo de transferencia de masa, Kg/ atm m^2s
L	Altura de lecho, m. Longitud del equipo de secado en la dirección de flujo del sólido (Capítulo 2), m.
M	Humedad total (g H_2O/g sólido seco).
M_{av}	Humedad media cápsula (g H_2O/g sólido seco).
$M_{av,t}$	Humedad total media a cada instante (g H_2O/g sólido seco).
M_0	Humedad inicial (g H_2O/g sólido seco).
$\dot{m}$	Flujo del sólido a secar, kg/s.
m_{aD}	masa de aire en el equipo de secado, kg.
m_D	Masa de sólido en el equipo de secado, kg.
M_e	Humedad en el equilibrio (g H_2O/g sólido seco).
m_{fin}	Masa final del experimento de secado, kg.
m_o	Masa inicial, kg.

M_s	Humedad en la superficie o de Shivhare (g H_2O/g sólido seco).
m_{solid}	Masa de sólido seco del producto a secar, kg.
M_t	Humedad a cada instante, (g H_2O/g sólido seco).
m_t	Masa a cada instante, kg.
m_w	Masa de agua del producto a secar, kg.
N	Número de células encapsuladas viables, adimensional.
n	Frecuencia de rotaciones, s^{-1}.
N_0	Número de células libres previa encapsulación, adimensional.
P	Potencia absorbida, $J \cdot min^{-1}$.
P_0	Potencia absorbida en la superficie del material, $J \cdot min^{-1}$.
P_{atm}	Presión atmosférica, atm.
PM_{H_2O}	Peso molecular del agua, kg/mol
$P_{w,\infty}$	Presión de vapor a en el medio, atm.
$P_{w,s}$, P_s	Presión de vapor del material y presión de vapor de saturación, atm.
P_μ	Potencia de microonda incidente, W.
Q_{abs}	Calor absorbida de microondas, $J \cdot min^{-1} \cdot m^{-3}$.
Q_{air}	Caudal de aire, L/min.
Q_h	Potencia de dispositivo calefactor, W.
Q_{vap}	Calor necesario para la vaporización del agua, $J \cdot kg^{-1}$.
R	Radio inicial de la partícula, m.
r	Radio de la partícula contraída, m.
$r_{A,}$	Velocidad de secado referido a la interfase aire-sólido, m/s.
r_e	Radio de la partícula en el equilibrio o secado final, m.
Re_{mf}	Reynolds de mínima fluidización, adimensional.
S	Sección transversal del secadero , $m^{2.}$
t	Tiempo, min.

T	Temperatura del producto a secar (Capítulo2),ºC.
T	Temperatura, ºC.
T_0	Temperatura inicial de la muestra, ºC.
T_a	Temperatura del aire, ºC.
T_{air}	Temperatura media del aire (Capítulo 2), ºC.
T_f	Temperatura del film en lecho de partículas, ºC.
T_f^*	Temperatura del film objetivo, ºC.
T_{in}	Temperatura de entrada del aire, ºC.
T_{in}^*	Temperatura de entrada del aire objetivo, ºC.
t_{on}	Tiempo de encendido de las microondas, min.
T_{out}	Temperatura de salida del aire, ºC.
T_s	Temperatura de la superficie experimental, ºC.
T_s^*	Temperatura máxima de la superficie objetivo, ºC.
t_{total}	Tiempo de duración del proceso real, min.
u_{mf}	Velocidad mínima de fluidización, $m \cdot s^{-1}$.
u_{fkuid}	Velocidad del fluido en la operación de extrusión, m/s.
u_{wire}	Velocidad de corte del disco, m/s.
V_p	Volumen de partícula, m^3.
v_r	Velocidad de contracción, $m \cdot s^{-1}$. Definiendo v_{r1}, v_{r2}, v_{r3} para las Fases I, II y III.
V_s	Fracción volumétrica de la fase sólida, adimensional.
V_w	Fracción volumétrica de la fase liquida, adimensional.
W_{ds}	Fracción de sólido seco, adimensional.
X	Fracción de humedad en base húmeda (g H_2O/g masa total).
X_0	Fracción de humedad en base húmeda inicial (g H_2O/g masa total).
X_e	Fracción de humedad en base húmeda en el equilibrio (g H_2O/g masa total).

Y	Humedad en base húmeda para la corriente de aire, kg H_20/kg

Símbolos griegos

α	Ángulo de inclinación, rad (Capítulo 2).
β	Coeficiente relativo a la ecuación de Shivhare , min^{-1}.
ΔP	Caída de presión en el lecho.
ΔV	Potencia del campo electric, W.
ϕ	Esfericidad, adimensional
$\eta_{cal,1}$, $\eta_{cal,2}$	Rendimiento del sistema de calefacción, Con subíndice 1 para el aire y 2 para la placa de liofilización, adimensional.
η_{pump}, η_{mw} , η_{sr}	Rendimiento del sistema de calefacción, Con subíndice pump para la bomba, mw para el microondas y sr para el sistema de refrigeración, adimensional.
λ_{sub}	Calor latente de sublimación, kJ/kg.
μ	Viscosidad, kg/m s
q	carga eléctrica de los iones, C.
ω	velocidad angular, rad/s
ε	Porosidad, adimensional.
ε'	Constante dieléctrica relativa, adimensional. Con subíndices: w, agua ,al(alginato); ty (tilosa), lev (levadura), prob (probiótico).
ε''	Factor de pérdidas dieléctricas relativo, adimensional . Con subíndices: w, agua ,al(alginato); ty (tilosa), lev (levadura), prob (probiótico).
ε''_d	Factor de pérdidas dieléctricas relativo a la rotación dipolar, adimensional.
ε''_σ	Factor de pérdidas dieléctricas relativo la conductividad iónica, adimensional.
ε_0	Permitividad eléctrica vacío, $F \cdot m^{-1}$.
ε_{mf}	Porosidad de mínima fluidización, adimensional.
ε_r	Permitividad relativa, adimensional.

λ	Longitud de onda, m.
λ_0	Longitud de onda en el vacío, m.
ρ	Densidad material, $kg \cdot m^{-3}$ con subíndices: Con subíndices: w, agua ,al(alginato); ty (tilosa), lev (levadura), prob (probiótico).
ρ_{ap}	Densidad aparente del material

Capítulo 10

BIBLIOGRAFÍA

10 BIBLIOGRAFÍA

Abbasi Souraki, B.,Mowla, D. 2008. Experimental and theoretical investigation of drying behaviour of garlic in an inert medium fluidized bed assisted by microwave. *J. Food Eng.,* 88, 438-449.

Abdelwahed, W., Degobert, G., Stainmesse, S., Fessi, H. 2006. Freeze-drying of nanoparticles: Formulation, process and storage considerations. *Adv. Drug Deliv. Rev.,* 58, 1688-1713.

Abonyi, B.I., Feng, H., Tang, J., Edwards, C.G., Chew, B.P., Mattinson, D.S., Fellman, J.K. 2002. Quality retention in strawberry and carrot purees dried with Refractance Window™ system. *J. Food Sci.,* 67, 1051-1056.

Adams, G.D. and Irons, L.I. 1993. Some implications of structural collapse during freeze drying using Erwinia caratovora l-sparaginase as a model. . *J Chem Biotechnol,* 58, 71-76.

Al-Harahsheh, M., Al-Muhtaseb, A.H., Magee, T.R.A. 2009. Microwave drying kinetics of tomato pomace: Effect of osmotic dehydration. *Chemical Engineering and Processing: Process Intensification,* 48, 524-531.

Ali, S.S., Kasoju, N., Luthra, A., Singh, A., Sharanabasava, H., Sahu, A., Bora, U. 2008. Indian medicinal herbs as sources of antioxidants. *Food Res. Int.,* 41, 1-15.

Alibas, I. 2007. Microwave, air and combined microwave–air-drying parameters of pumpkin slices. *LWT - Food Science and Technology*, 40, 1445-1451.

Andrés, A., Bilbao, C., Fito, P. 2004. Drying kinetics of apple cylinders under combined hot air-microwave dehydration. *J. Food Eng.,* 63, 71-78.

Annunziata, A.,Vecchio, R. 2011. Functional foods development in the European market: A consumer perspective. *Journal of Functional Foods,* 3, 223-228.

Aronsson, K.,Rönner, U. 2001. Influence of pH, water activity and temperature on the inactivation of Escherichia coli and Saccharomyces cerevisiae by pulsed electric fields. *Innovative Food Science & Emerging Technologies,* 2, 105-112.

Asami, D.K., Hong, Y.-., Barrett, D.M., Mitchell, A.E. 2003. Comparison of the total phenolic and ascorbic acid content of freeze-dried and air-dried marionberry, strawberry, and corn grown using conventional, organic, and sustainable agricultural practices. *J. Agric. Food Chem.,* 51, 1237-1241.

Ashwell, M., 2004. Conceptos sobre Alimentos Funcionales. ILSI Europe. ISBN 1-57881-157-0, 48.

Askari, G.R., Emam-Djomeh, Z., Mousavi, S.M. 2008. Investigation of the effects of microwave treatment on the optical properties of apple slices during drying. *Drying Technol,* 26, 1362-1368.

Askari, G.R., Emam-Djomeh, Z., Mousavi, S.M. 2009. An investigation of the effects of drying methods and conditions on drying characteristics and quality attributes of agricultural products during hot air and hot air/microwave-assisted dehydration. *Drying Technol,* 27, 831-841.

Bala, B.K.,Janjai, S. 2013. Solar drying of agricultural products. *Stewart Postharvest Review,* 9.

Bala, B.K.,Mondol, M.R.A. 2001. Experimental investigation on solar drying of fish using solar tunnel dryer. *Drying Technol,* 19, 427-436.

Bala, B.K.,Woods, J.L. 1994. Simulation of the indirect natural convection solar drying of rough rice. *Solar Energy,* 53, 259-266.

Barbosa-Cánovas, G.V.andJuliano, P., 2005. Compression and Compaction Characteristics of Selected Food Powders. Advances in Food and Nutrition Research 49, 233-307.

Basu, S., Shivhare, U.S., Mujumdar, A.S. 2006. Models for sorption isotherms for foods: A review. *Drying Technol,* 24, 917-930.

Berezc, L.e.a., 1999. Combined microwave-convective drying of saccharomyces cerevisiae based yeast. Acta Alimentaria 28, 223-233.

Bergman,T.L.,Incropera,F.P.,Lavine,A.S., 2011. Fundamentals of Heat and Mass Transfer. John Wiley and Sons, Hoboken,NJ.

Beristain, I., Bustinduy, A., 2005. El Envejecimiento De La Población Vasca: Sus Consecuencias Económicas Y Sociales.Estudios De Economía 17. Servicio Central de Publicaciones del Gobierno Vasco.

Beuchat, L.R. 1981. Microbial stability as affected by water activity. *Cereal Foods World,* 26(7), 345-349.

Borgogna, M., Bellich, B., Zorzin, L., Lapasin, R., Cesàro, A. 2010. Food microencapsulation of bioactive compounds: Rheological and thermal characterisation of non-conventional gelling system. *Food Chem.,* 122, 416-423.

Boudhrioua, N., Giampaoli, P., Bonazzi, C. 2003. Changes in aromatic components of banana during ripening and air-drying. *LWT - Food Science and Technology,* 36, 633-642.

Bouraoui, M., Richard, P., Durance, T. 1994. Microwave and convective drying of potato slices. *J. Food Process Eng.,* 17, 353-363.

Brockmann, M.C., 1973. Intermediate Moisture Foods. In: Van Arsdel,W.B., Copley, M.J., Morgan, A.I. (Ed.), Food Dehydration. The AVI Publishing Co., Westport.

Broeckx, G., Vandenheuvel, D., Claes, I.J.J., Lebeer, S., Kiekens, F. 2016. Drying techniques of probiotic bacteria as an important step towards the development of novel pharmabiotics. *Int. J. Pharm.,* 505, 303-318.

Burgain, J., Gaiani, C., Linder, M., Scher, J. 2011. Encapsulation of probiotic living cells: From laboratory scale to industrial applications. *J. Food Eng.,* 104, 467-483.

Calvo, M., 1991. Aditivos Alimentarios.Propiedades, Aplicaciones Y Efectos Sobre La Salud. Mira editores, Zaragoza.

Cámara,M., Pérez, M.L., López,R., Martí,N., Saura,D., Micol, V., 2011. Nutrición y Salud. In: ASOZUMOS, Asociación Española de Fabricantes de Zumos (Ed.), El Libro Del Zumo. , pp. 117-140.

Capela, P., Hay, T.K.C., Shah, N.P. 2006. Effect of cryoprotectants, prebiotics and microencapsulation on survival of probiotic organisms in yoghurt and freeze-dried yoghurt. *Food Res. Int.,* 39, 203-211.

Cárcel, J.A., García-Pérez, J.V., Riera, E., Mulet, A. 2007. Influence of high-intensity ultrasound on drying kinetics of persimmon. *Drying Technol,* 25, 185-193.

Chamchong, M., Datta, A.K. 1999. Thawing of foods in a microwave oven: I. Effect of power levels and power cycling. *J Microwave Power Electromagn Energy*, 34, 9-21.

Champagne, C.P., Gardner, N.J., Roy, D. 2005. Challenges in the addition of probiotic cultures to foods. *Crit. Rev. Food Sci. Nutr.,* 45, 61-84.

Chan, E.W.C., Lim, Y.Y., Wong, S.K., Lim, K.K., Tan, S.P., Lianto, F.S., Yong, M.Y. 2009. Effects of different drying methods on the antioxidant properties of leaves and tea of ginger species. *Food Chem.,* 113, 166-172.

Chan, T.V.C.T., Reader, H.C., 2000. Understanding Microwave Heating Cavities. Artech House Publishers.

Chandramouli, V., Kailasapathy, K., Peiris, P., Jones, M. 2004. An improved method of microencapsulation and its evaluation to protect Lactobacillus spp. in simulated gastric conditions. *J. Microbiol. Methods,* 56, 27-35.

Chang, C.-., Lin, H.., Chang, C.., Liu, Y., 2006. Comparisons on the antioxidant properties of fresh, freeze-dried and hot-air-dried tomatoes. *J. Food Eng.,* 77, 478-485.

Chatelet, C., Damour, O., Domard, A. 2001. Influence of the degree of acetylation on some biological properties of chitosan films. *Biomaterials,* 22, 261-268.

Chávarri, M., Marañón, I., Ares, R., Ibáñez, F.C., Marzo, F., Villarán, M.d.C. 2010. Microencapsulation of a probiotic and prebiotic in alginate-chitosan capsules improves survival in simulated gastro-intestinal conditions. *Int. J. Food Microbiol.,* 142, 185-189.

Chávarri, M., Marañón, I., Ares, R., Ibáñez, F.C., Marzo, F., Villarán, M.d.C. 2010b. Microencapsulation of a probiotic and prebiotic in alginate-chitosan capsules improves survival in simulated gastro-intestinal conditions. *Int. J. Food Microbiol.,* 142, 185-189.

Chávarri, M., Marañón, I., Villarán, M.C., 2012. Encapsulation Technology to Protect Probiotic Bacteria. In: Rigobelo, E.C. (Ed.), Probiotics. InTech, pp. 501-540.

Chávez, B.E., Ledeboer, A.M. 2007. Drying of probiotics: Optimization of formulation and process to enhance storage survival. *Drying Technol,* 25, 1193-1201.

Chegini, G.R., Ghobadian, B. 2005. Effect of spray-drying conditions on physical properties of orange juice powder. *Drying Technol,* 23, 657-668.

Connors, K.A. 1988. The Karl Fischer titration of water. *Drug Development and Industrial Pharmacy,* 14, 1891-1903.

Cook, M.T., Tzortzis, G., Charalampopoulos, D., Khutoryanskiy, V.V. 2012. Microencapsulation of probiotics for gastrointestinal delivery. *J. Controlled Release,* 162, 56-67.

Crank, J.,Gupta, R.S. 1975. Isotherm Migration Method in two dimensions. *Int. J. Heat Mass Transfer,* 18, 1101-1107.

Cruchet, S., Furnes, R., Maruy, A., Hebel, E., Palacios, J., Medina, F., Ramirez, N., Orsi, M., Rondon, L., Sdepanian, V., Xóchihua, L., Ybarra, M., Zablah, R.A. 2015. The Use of Probiotics in Pediatric Gastroenterology: A Review of the Literature and Recommendations by Latin-American Experts. *Pediatric Drugs,* 17, 199-216.

De Vos, P., Faas, M.M., Spasojevic, M., Sikkema, J. 2010. Encapsulation for preservation of functionality and targeted delivery of bioactive food components. *Int. Dairy J.,* 20, 292-302.

Devakate, R.V., Patil, V.V., Waje, S.S., Thorat, B.N. 2009. Purification and drying of bromelain. *Separation and Purification Technology,* 64, 259-264.

Díaz-Maroto, M.C., González Viñas, M.A., Cabezudo, M.D. 2003. Evaluation of the effect of drying on aroma of parsley by free choice profiling. *European Food Research and Technology,* 216, 227-232.

Doymaz, I. 2007. The kinetics of forced convective air-drying of pumpkin slices. *J. Food Eng.,* 79, 243-248.

Dumitriu, S.,Chornet, E. 1998. Inclusion and release of proteins from polysaccharide-based polyion complexes. *Adv. Drug Deliv. Rev.,* 31, 223-246.

El-Aouar, A.A., Azoubel, P.M., Barbosa Jr., J.L., Murr, F.E.X. 2006. Influence of the osmotic agent on the osmotic dehydration of papaya (Carica papaya L.). *J. Food Eng.,* 75, 267-274.

Fang, Y.-., Yang, S., Wu, G. 2002. Free radicals, antioxidants, and nutrition. *Nutrition,* 18, 872-879.

Feng, H. 2002. Analysis of microwave assisted fluidized-bed drying of particulate product with a simplified heat and mass transfer model. *Int. Commun. Heat Mass Transfer,* 29, 1021-1028.

Feng, H.,Tang, J. 1998. Microwave finish drying of diced apples in a spouted bed. *J. Food Sci.,* 63, 679-683.

Foerst, P.,Kulozik, U. 2012. Modelling the Dynamic Inactivation of the Probiotic Bacterium L. Paracasei ssp. Paracasei During a Low-Temperature Drying Process Based on Stationary Data in Concentrated Systems. *Food and Bioprocess Technology,* 5, 2419-2427.

Fonseca, F., Béal, C., Corrieu, G. 2000. Method of quantifying the loss of acidification activity of lactic acid starters during freezing and frozen storage. *J. Diary Res.,* 67, 83-90.

Fowler, A.,Toner, M. 2005. Cryo-injury and biopreservation. *Ann. N. Y. Acad. Sci.,* 1066, 119-135.

Franks, F. 1998. Freeze-drying of bioproducts: Putting principles into practice. *European Journal of Pharmaceutics and Biopharmaceutics,* 45, 221-229.

Freitas, S., Merkle, H.P., Gander, B. 2005. Microencapsulation by solvent extraction/evaporation: Reviewing the state of the art of microsphere preparation process technology. *J. Controlled Release,* 102, 313-332.

Frost& Sullivan, 2012. Strategic Analysis of the Global Natural Food Ingredients Market. Growth Oportunities Emerge in the Natural Antioxidants, Antimicrobials, Colors anf Flavor Segments.

Frost& Sullivan, 2013. Analysis of the Probiotics and Enzymes Market. The Increase in the number of Scientific and Clinical Trials to Validate Benefits are Expected to boost Growth.

Funebo, T., Ahrné, L., Prothon, F., Kidman, S., Langton, M., Skjöldebrand, C. 2002. Microwave and convective dehydration of ethanol treated and frozen apple - Physical properties and drying kinetics. *International Journal of Food Science and Technology,* 37, 603-614.

Funebo, T.,Ohlsson, T. 1998. Microwave-assisted air dehydration of apple and mushroom. *J. Food Eng.,* 38, 353-367.

Gardiner, G.E., O'Sullivan, E., Kelly, J., Auty, M.A.E., Fitzgerald, G.F., Collins, J.K., Ross, R.P., Stanton, C. 2000. Comparative survival rates of human-derived probiotic Lactobacillus paracasei and L. salivarius strains during heat treatment and spray drying. *Appl. Environ. Microbiol.,* 66, 2605-2612.

Geldart, D. 1973. Types of gas fluidization. *Powder Technol,* 7, 285-292.

Geldart, D.,Abrahamsen, A.R. 1978. Homogeneous fluidization of fine powders using various gases and pressures. *Powder Technol,* 19, 133-136.

Ghanem, N., Mihoubi, D., Kechaou, N., Mihoubi, N.B. 2012. Microwave dehydration of three citrus peel cultivars: Effect on water and oil retention capacities, color, shrinkage and total phenols content. *Industrial Crops and Products,* 40, 167-177.

Gharsallaoui, A., Roudaut, G., Chambin, O., Voilley, A., Saurel, R. 2007. Applications of spray-drying in microencapsulation of food ingredients: An overview. *Food Res. Int.,* 40, 1107-1121.

Gibbs, B.F., Kermasha, S., Alli, I., Mulligan, C.N. 1999. Encapsulation in the food industry: A review. *Int. J. Food Sci. Nutr.,* 50, 213-224.

Gibson, G.R.,Roberfroid, M.B. 1995. Dietary modulation of the human colonic microbiota: Introducing the concept of prebiotics. *J. Nutr.,* 125, 1401-1412.

Gohel, M.C., Parikh, R.K., Nagori, S.A., Gandhi, A.V., Shroff, M.S., Patel, P.K., Gandhi, C.S., Patel, V.P., Bhagat, N.Y., Poptani, S.D., Kharadi, S.R., Pandya, R.B., Patel, T.C. 2009. Spray drying: A review. *Pharmaceutical Reviews,* 7.

Gouin, S. 2004. Microencapsulation: Industrial appraisal of existing technologies and trends. *Trends in Food Science and Technology,* 15, 330-347.

Goula, A.M.,Adamopoulos, K.G. 2005. Stability of lycopene during spray drying of tomato pulp. *LWT - Food Science and Technology,* 38, 479-487.

Goula, A.M.,Adamopoulos, K.G. 2008. Effect of maltodextrin addition during spray drying of tomato pulp in dehumidified air: I. Drying kinetics and product recovery. *Drying Technol,* 26, 714-725.

Guan, D., Cheng, M., Wang, Y., Tang, J. 2004. Dielectric Properties of Mashed Potatoes Relevant to Microwave and Radio-frequency Pasteurization and Sterilization Processes. *J. Food Sci.,* 69, FEP30-FEP37.

Gulati, T., Zhu, H., Datta, A.K., Huang, K. 2015. Microwave drying of spheres: Coupled electromagnetics-multiphase transport modeling with experimentation. Part II: Model validation and simulation results. *Food Bioprod. Process.,* 96, 326-337.

Hämäläinen, M., Nieminen, R., Vuorela, P., Heinonen, M., Moilanen, E. 2007. Anti-inflammatory effects of flavonoids: Genistein, kaempferol, quercetin, and daidzein inhibit STAT-1 and NF-κB activations, whereas flavone, isorhamnetin, naringenin, and pelargonidin inhibit only NF-κB activation along with their inhibitory effect on

iNOS expression and NO production in activated macrophages. *Mediators Inflamm.,* 2007.

Hartmann, R.,Meisel, H. 2007. Food-derived peptides with biological activity: from research to food applications. *Curr. Opin. Biotechnol.,* 18, 163-169.

Hawlader, M.N.A., Uddin, M.S., Ho, J.C., Teng, A.B.W. 1991. Drying characteristics of tomatoes. *J. Food Eng.,* 14, 259-268.

Heidebach, T., Först, P., Kulozik, U. 2012. Microencapsulation of Probiotic Cells for Food Applications. *Crit. Rev. Food Sci. Nutr.,* 52, 291-311.

Heredia, A., Barrera, C., Andrés, A. 2007. Drying of cherry tomato by a combination of different dehydration techniques. Comparison of kinetics and other related properties. *J. Food Eng.,* 80, 111-118.

Holscher, H.D., Czerkies, L.A., Cekola, P., Litov, R., Benbow, M., Santema, S., Alexander, D.D., Perez, V., Sun, S., Saavedra, J.M., Tappenden, K.A. 2012. Bifidobacterium lactis Bb12 enhances intestinal antibody response in formula-fed infants: A randomized, double-blind, controlled trial. *J. Parenter. Enteral Nutr.,* 36, 106S-117S.

Iaconelli, C., Lemetais, G., Kechaou, N., Chain, F., Bermúdez-Humarán, L.G., Langella, P., Gervais, P., Beney, L. 2015. Drying process strongly affects probiotics viability and functionalities. *J. Biotechnol.,* 214, 17-26.

Icier, F.,Ilicali, C. 2005. The use of tylose as a food analog in ohmic heating studies. *J. Food Eng.,* 69, 67-77.

Ingham, J., Dunn, I.J., Heinzle, E., Prenosil, J.E., Snape, J.B., 2007. Chemical Engineering Dynamics: An Introduction to Modelling and Computer Simulation: Third Edition. In: Anonymous . 1-618.

Innobasque, 2011. Euskadi envejece: Innobasque en el ámbito del envejecimiento activo y saludable.

Jalali, M., Abedi, D., Varshosaz, J., Najjarzadeh, M., Mirlohi, M., Tavakoli, N. 2012. Stability evaluation of freeze-dried Lactobacillus paracasei subsp. tolerance and Lactobacillus delbrueckii subsp. bulgaricus in oral capsules. *Research in Pharmaceutical Sciences,* 7, 31-36.

Jameela, S.R.,Jayakrishnan, A. 1995. Glutaraldehyde cross-linked chitosan microspheres as a long acting biodegradable drug delivery vehicle: studies on the in vitro release of mitoxantrone and in vivo degradation of microspheres in rat muscle. *Biomaterials,* 16, 769-775.

Jangam, S.V. 2011. An overview of recent developments and some R&D challenges related to drying of foods. *Drying Technol,* 29, 1343-1357.

Jayamanne, V.S.,Adams, M.R. 2006. Determination of survival, identity and stress resistance of probiotic bifidobacteria in bio-yoghurts. *Lett. Appl. Microbiol.,* 42, 189-194.

Jia, L.W., Raisul Islam, M., Mujumdar, A.S. 2003. A simulation study on convection and microwave drying of different food products. *Drying Technol,* 21, 1549-1574.

Jiokap Nono, Y., Giroux, F., Cuq, B., Raoult-Wack, A.. 2001. Study of the parameters of control and checking of dewatering and impregnation soaking process using an automatic experimental system; Application to treatment of "Golden" apples. *J. Food Eng.,* 50, 203-210.

John, R.P., Tyagi, R.D., Brar, S.K., Surampalli, R.Y., Prévost, D. 2011. Bio-encapsulation of microbial cells for targeted agricultural delivery. *Crit. Rev. Biotechnol.,* 31, 211-226.

Jones, P.J.,Jew, S. 2007. Functional food development: concept to reality. *Trends in Food Science and Technology,* 18, 387-390.

Jota, X., 2013. Hágase la luz y la luz se hizo…onda electromagnética (II). Https://Xabierjota. Wordpress. Com/2013/02/13/Hagase-La-Luz-Y-La-Luz-Se-Hizo-Onda-Electromagnetica-Ii/ 2016, 1.

Kailasapathy, K. 2002. Microencapsulation of probiotic bacteria: Technology and potential applications. *Curr. Issues Intestinal Microbiol.,* 3, 39-48.

Khraisheh, M.A.M., Cooper, T.J.R., Magee, T.R.A. 1997. Shrinkage characteristics of potatos dehydrated under combined microwave and convective air conditions. *Drying Technol,* 15, 1003-1022.

Kim, H.S., Kamara, B.J., Good, I.C., Enders Jr., G.L. 1988. Method for the preparation of stabile microencapsulated lactic acid bacteria. *J. Ind. Microbiol.,* 3, 253-257.

Kleerebezem, M.andVaughan, E.E., 2009. Probiotic and gut lactobacilli and bifidobacteria: Molecular approaches to study diversity and activity. Annual Review of Microbiology 63, 269-290.

Knutson, K.M., Marth, E.H., Wagner,M.K. 1987. Microwave heating of foods. *Lebensm-Wiss. U-Technol.,* 20, 101-110.

Konstantinov, S.R., Smidt, H., De Vos, W.M., Bruijns, S.C.M., Singh, S.K., Valence, F., Molle, D., Lortal, S., Altermann, E., Klaenhammer, T.R., Van Kooyk, Y. 2008. S layer protein A of Lactobacillus acidophilus NCFM regulates immature dendritic cell and T cell functions. *Proc. Natl. Acad. Sci. U. S. A.,* 105, 19474-19479.

Kotilainen, L., Rajalahti, R., Ragasa, C., Pehu, E.., 2006. Health enhancing foods : opportunities for strengthening developing countries. ; no. 30. Washington, DC: World Bank. . Agriculture and Rural Development Discussion Paper 30.

Krasaekoopt, W., Bhandari, B., Deeth, H. 2003. Evaluation of encapsulation techniques of probiotics for yoghurt. *Int. Dairy J.*, 13, 3-13.

Krasaekoopt, W., Bhandari, B., Deeth, H. 2004. The influence of coating materials on some properties of alginate beads and survivability of microencapsulated probiotic bacteria. *Int. Dairy J.*, 14, 737-743.

Krokida, M.K., Kiranoudis, C.T., Maroulis, Z.B., Marinos-Kouris, D. 2000. Drying related properties of apple. *Drying Technol,* 18, 1251-1267.

Kunii, D., Levenspiel, O., 1991. CHAPTER 1 - Introduction. In: Kunii, D., Levenspiel, O. (Eds.)Fluidization Engineering (Second Edition). Butterworth-Heinemann, Boston, pp. 1-13.

Lam,T., Strickly, R.G. and Visor, G.C. 2004. An unexpected pH effect on stability of moexipril lyophilized powder. *Pharm Res,* 6, 971-975.

Leatherhead Food Reserch, Market Report::Future Directions for the Global Functional Foods Market. https://www.leatherheadfood.com/functional-foods.

Ledward, D.A. 1987. Water activity: Theory and applications to food. *Meat Sci.*, 21, 157-158.

Leva, M., 1959. Fluidization. McGraw-Hill, New York.

Levenspiel, O., 2014. Flow through Packed Beds, in Engineering Flow and Heat Exchange. Springer, New York.

Lew, A., Krutzik, P.O., Hart, M.E., Chamberlin, A.R. 2002. Increasing rates of reaction: microwave-assisted organic synthesis for combinatorial chemistry. *J. Comb. Chem.*, 4, 95-105.

Li,H., Ramaswamy,H.S., 2008. Microwave drying. In: Hui,Y.H., Clary,C.Farid,M.M., Fasina,O.O.,Noormhorm,A., Welti-Chanes,J. (Ed.), Food Drying Science and Technology:Microbiology Chemistry, Applications. DEStech Publications, Inc., USA, pp. 127-156.

Liapis, A.I., Pikal, M.J., Bruttini, R. 1996. Research and development needs and opportunities in freeze drying. *Drying Technol*, 14, 1265-1300.

Liberman, H.A., Lachman, L. and Schwartz, B.J., 1989. Pharmaceutical Dosage Form: Parenterals. Marcel Dekker publisher.

Lide, D.R., 2005. Handbook of Chemistry and Physics. CRC Press, New York.

Lin, T.M., D. Durance, T., Scaman, C.H. 1998. Characterization of vacuum microwave, air and freeze dried carrot slices. *Food Res. Int.*, 31, 111-117.

Linders, L.J.M., Wolkers, W.F., Hoekstra, F.A., Van 'T Riet, K. 1997. Effect of Added Carbohydrates on Membrane Phase Behavior and Survival of Dried Lactobacillus plantarum. *Cryobiology,* 35, 31-40.

Llave, Y., Mori, K., Kambayashi, D., Fukuoka, M., Sakai, N. 2015. Dielectric properties and model food application of tylose water pastes during microwave thawing and heating. *J. Food Eng.,*.

Lu, Y., Turley, A., Dong, X., Wu, C. 2011. Reduction of Salmonella enterica on grape tomatoes using microwave heating. *Int. J. Food Microbiol.,* 145, 349-352.

Mackenzie, A.P. 1998. A study on impact of the sodium chloride concentration on the lyophilized formulation. . , 36-49.

Manojlovic, V., Nedovic, V.A., Kailasapathy, K., Zuidam, N.J., 2010. Encapsulation of probiotics for use in food products. In: Anonymous , pp. 269-302.

Martín, M.J., Lara-Villoslada, F., Ruiz, M.A., Morales, M.E. 2015. Microencapsulation of bacteria: A review of different technologies and their impact on the probiotic effects. *Innovative Food Science & Emerging Technologies,* 27, 15-25.

Martínez, S., López, M., González-Raurich, M., Alvarez, A.B. 2005. The effects of ripening stage and processing systems on vitamin C content in sweet peppers (Capsicum annuum L.). *Int. J. Food Sci. Nutr.,* 56, 45-51.

Martinsen, A., Skjak-Braek, G., Smidsrod, O. 1989. Alginate as immobilization material: I. Correlation between chemical and physical properties of alginate gel beads. *Biotechnol. Bioeng.,* 33, 79-89.

Maskan, M. 2000. Microwave/air and microwave finish drying of banana. *J. Food Eng.,* 44, 71-78.

Maskan, M. 2001. Drying, shrinkage and rehydration characteristics of kiwifruits during hot air and microwave drying. *J. Food Eng.,* 48, 177-182.

Masters, K., 1985. Changing face of spray drying. Institution of Chemical Engineers Symposium Series, 331-333.

Mcclements, D.J., Decker, E.A., Park, Y., Weiss, J. 2009. Structural design principles for delivery of bioactive components in nutraceuticals and functional foods. *Crit. Rev. Food Sci. Nutr.,* 49, 577-606.

Meda, V., Orsat, V., Raghavan, V., 2005. 4 - Microwave heating and the dielectric properties of foods. In: Schubert, H., , Regier, M. (Eds.)The Microwave Processing of Foods. Woodhead Publishing, pp. 61-75.

Menrad, K. 2003. Market and marketing of functional food in Europe. *J. Food Eng.,* 56, 181-188.

Metaxas,A.C.,Meredith,R.J.,1983.Industrial Microwave Heating. Peter Peregrinus, London.

Ming, L.C., Rahim, R.A., Wan, H.Y., Ariff, A.B. 2009. FormulatIon of protectIve agents for Improvement of LactobacIllus salIvarIus I 24 survIval rate subjected to freeze dryIng for productIon of lIve cells In powderIzed form. *Food and Bioprocess Technology,* 2, 431-436.

Miura, N., Yagihara, S., Mashimo, S. 2003. Microwave Dielectric Properties of Solid and Liquid Foods Investigated by Time-domain Reflectometry. *J. Food Sci.,* 68, 1396-1403.

Mokarram, R.R., Mortazavi, S.A., Najafi, M.B.H., Shahidi, F. 2009. The influence of multi stage alginate coating on survivability of potential probiotic bacteria in simulated gastric and intestinal juice. *Food Res. Int.,* 42, 1040-1045.

Morgan, C.A., Herman, N., White, P.A., Vesey, G. 2006. Preservation of micro-organisms by drying; A review. *J. Microbiol. Methods*, 66, 183-193.

Motevali, A., Minaei, S., Khoshtaghaza, M.H., Amirnejat, H. 2011. Comparison of energy consumption and specific energy requirements of different methods for drying mushroom slices. *Energy,* 36, 6433-6441.

Mudgett, R.E. 1989. Microwave food processing:scientific status summary. *Food Technol.,* 42(1), 117-126.

Mudgett, R.E., 1995. Electrical properties of foods. In: Rao,M.A., Rizci, S.S.H. (Ed.), Engineering Properties of Foods. Macel Dekker Inc., New York, pp. 389-455.

Mujumdar, A.S., 2007. Handbook of Industrial Drying. Taylor and Francis, Philadelphia.

Mulet, A., Sanjuán, N., Bon, J., Simal, S. 1999. Drying model for highly porous hemispherical bodies. *European Food Research and Technology,* 210, 80-83.

Muratore, G., Rizzo, V., Licciardello, F., Maccarone, E. 2008. Partial dehydration of cherry tomato at different temperature, and nutritional quality of the products. *Food Chem.,* 111, 887-891.

Nail, S.L.a.G.,G.A., 1992. Freeze Drying: Principles and Practice. Marcel Dekker publisher, New York.

Neema,S., Washkuhn, R.J.and Brendel, R.J. 1997. Injectable products. *PDA J Pharm Sci Technol,* 51, 166-171.

Nihant, N., Grandfils, C., Jérôme, R., Teyssié, P. 1995. Microencapsulation by coacervation of poly(lactide-co-glycolide) IV. Effect of the processing parameters on coacervation and encapsulation. *J. Controlled Release,* 35, 117-125.

Nogueira, J.N., Sobrinho, J.S., Vencosvsky, R., Fonseca, H. 1978. Retention of ascorbic acid and beta-carotene in freeze-dried red guava pulp (Psidium guayava L.) during storage. *Arch. Latinoam. Nutr.,* 28, 363-377.

Novoa, I., Rey, L., López, A., Gutiérrez, A., Mayo, O. 2004. Development of lyophilization processes for large scale production of pharmaceutical products. *American Pharmaceutical Review,* 7, 46-52.

Oakley, D.E. 1997. Produce uniform particles by spray drying. *Chem. Eng. Prog.,* 93, 48-54.

Ochoa, M.R., Kesseler, A.G., Pirone, B.N., Márquez, C.A., De Michelis, A. 2002. Shrinkage During Convective Drying of Whole Rose Hip (Rosa Rubiginosa L.) Fruits. *LWT - Food Science and Technology,* 35, 400-406.

Okos, M.R., Narsimhan, G., Singh, R.K., Weitnauer, A.C., 1992. Food Dehydration. In Handbook of Food Engineering. In: Heldman, D.R., Lund, D.B. (Eds.)Marcel Dekker, New York, pp. 437-562.

Oliveira, A.C., Moretti, T.S., Boschini, C., Baliero, J.C., Freitas, O., Favaro-Trindade, C.S. 2007a. Stability of microencapsulated B. lactis (BI 01) and L. acidophilus (LAC 4) by complex coacervation followed by spray drying. *J. Microencapsul.,* 24, 673-681.

Oliveira, A.C., Moretti, T.S., Boschini, C., Baliero, J.C.C., Freitas, L.A.P., Freitas, O., Favaro-Trindade, C.S. 2007b. Microencapsulation of B. lactis (BI 01) and L. acidophilus (LAC 4) by complex coacervation followed by spouted-bed drying. *Drying Technol,* 25, 1687-1693.

Orsat, V., Yang, W., Changrue, V., Raghavan, G.S.V. 2007. Microwave-assisted drying of biomaterials. *Food Bioprod. Process.,* 85, 255-263.

Otero, M.C., Espeche, M.C., Nader-Macías, M.E. 2007. Optimization of the freeze-drying media and survival throughout storage of freeze-dried Lactobacillus gasseri and Lactobacillus delbrueckii subsp. delbrueckii for veterinarian probiotic applications. *Process Biochemistry,* 42, 1406-1411.

Ou, B., Hampsch-Woodill, M., Prior, R.L. 2001. Development and validation of an improved oxygen radical absorbance capacity assay using fluorescein as the fluorescent probe. *J. Agric. Food Chem.,* 49, 4619-4626.

Özbek, B.,Dadali, G. 2007. Thin-layer drying characteristics and modelling of mint leaves undergoing microwave treatment. *J. Food Eng.,* 83, 541-549.

Padivitage, N.L.T., Smuts, J.P., Armstrong, D.W., 2014. Chapter 11 - Water determination. In: Riley, C.M.R.W.R.R.R. (Ed.), Specification of Drug Substances and Products. Elsevier, Oxford, pp. 223-241.

Pakowski, Z. and Mujumdar, A.S., 2006. Basic Process Calculations and Simulations in Drying. In: Mujumdar, A.S. (Ed.), Handbook of Industrial Drying. CRC press, Taylor & Francis group, New York, pp. 54-79.

Park, J.K.,Chang, H.N. 2000. Microencapsulation of microbial cells. *Biotechnol. Adv.*, 18, 303-319.

Pata, J., Cárský, M., Hartman, M., Veselý, V. 1988. Minimum fluidization velocities of wet coal particles. *Industrial and Engineering Chemistry Research*, 27, 1493-1496.

Perdana, J., Bereschenko, L., Fox, M.B., Kuperus, J.H., Kleerebezem, M., Boom, R.M., Schutyser, M.A.I. 2013. Dehydration and thermal inactivation of Lactobacillus plantarum WCFS1: Comparing single droplet drying to spray and freeze drying. *Food Res. Int.*, 54, 1351-1359.

Pereira, N.R., Marsaioli Jr., A., Ahrné, L.M. 2007. Effect of microwave power, air velocity and temperature on the final drying of osmotically dehydrated bananas. *J. Food Eng.*, 81, 79-87.

Pereira, N.R., Marsaioli Jr., A., Ahrné, L.M. 2007. Effect of microwave power, air velocity and temperature on the final drying of osmotically dehydrated bananas. *J. Food Eng.*, 81, 79-87.

Pereira, R.N.,Vicente, A.A. 2010. Environmental impact of novel thermal and non-thermal technologies in food processing. *Food Res. Int.*, 43, 1936-1943.

Peyre, F., Datta, A., Seyler, C. 1997. Influence of the Dielectric Property on Microwave Oven Heating Patterns: Application to Food Materials. *J Microwave Power Electromagn Energy*, 32, 3-15.

Phisut, N. 2012. Spray drying technique of fruit juice powder: Some factors influencing the properties of product. *International Food Research Journal*, 19, 1297-1306.

Pikal, M.J., Roy, M.L., Shah, S. 1984. Mass and heat transfer in vial freeze-drying of pharmaceuticals: Role of the vial. *J. Pharm. Sci.*, 73, 1224-1237.

Piyasena, P., Dussault, C., Koutchma, T., Ramaswamy, H.S., Awuah, G.B. 2003. Radio Frequency Heating of Foods: Principles, Applications and Related Properties - A Review. *Crit. Rev. Food Sci. Nutr.*, 43, 587-606.

Prior, R.L., Cao, G., Martin, A., Sofic, E., McEwen, J., O'Brien, C., Lischner, N., Ehlenfeldt, M., Kalt, W., Krewer, G., Mainland, C.M. 1998. Antioxidant Capacity as Influenced by Total Phenolic and Anthocyanin Content, Maturity, and Variety of Vaccinium Species. *J. Agric. Food Chem.*, 46, 2686-2693.

Pruesse, U.a.V., K.D., 2004. The JetCutter Technology. In: Nodovic, N.a.W.,R. (Ed.), Fundamentals of Cell Immobilisation Biotechnology. Kluwer Academic Publishers, Dordrecht, The Netherlands, pp. 295-309.

Prüße, U., Dalluhn, J., Breford, J., Vorlop, K.-. 2000. Production of spherical beads by JetCutting. *Chemical Engineering and Technology,* 23, 1105-1110.

Quek, S.Y., Chok, N.K., Swedlund, P. 2007. The physicochemical properties of spray-dried watermelon powders. *Chemical Engineering and Processing: Process Intensification,* 46, 386-392.

Rajkumar, P., Kulanthaisami, S., Raghavan, G.S.V., Gariépy, Y., Orsat, V. 2007. Drying kinetics of tomato slices in vacuum assisted solar and open sun drying methods. *Drying Technol,* 25, 1349-1357.

Rambhatla, S.,Pikal, M.J. 2003. Heat and mass transfer scale-up issues during freeze-drying, I: Atypical radiation and the edge vial effect. *AAPS PharmSciTech,* 4.

Ramos-Clamont, G., Hernández-González, L.E., Fernández-Michel, S.G., Froto-Madariaga, M.L., Vázquez-Moreno L. 2012. Stratrgies to improve the survival of probiotic in ice cream. *Biotecnia,* XV, 31-38.

Raoult-Wack, A.L. 1994. Recent advances in the osmotic dehydration of foods. *Trends in Food Science and Technology,* 5, 255-260.

Ratti, C. 2001. Hot air and freeze-drying of high-value foods: A review. *J. Food Eng.,* 49, 311-319.

Ratti, C., 2013. Freeze drying for food powder production. In: Anonymous , pp. 57-84.

Regier, M., Mayer-Miebach, E., Behsnilian, D., Neff, E., Schuchmann, H.P. 2005. Influences of drying and storage of lycopene-rich carrots on the carotenoid content. *Drying Technol,* 23, 989-998.

Rendolph, S., Saclier, M., Peczalski, R., and Andrieu, J. 2005. Effect of ultrasonically induced nucleation on ice crystals size and shape during freezing in vials. . *Chem. Eng. Sci.,* 65-88.

Riveros, B., Ferrer, J., Bórquez, R. 2009. Spray drying of a vaginal probiotic strain of lactobacillus. *Drying Technol,* 27, 123-132.

Rokka, S.,Rantamäki, P. 2010. Protecting probiotic bacteria by microencapsulation: Challenges for industrial applications. *European Food Research and Technology,* 231, 1-12.

Roopa, B.S.,Bhattacharya, S. 2008. Alginate gels: I. Characterization of textural attributes. *J. Food Eng.,* 85, 123-131.

Ross, R.P., Desmond, C., Fitzgerald, G.F., Stanton, C. 2005. Overcoming the technological hurdles in the development of probiotic foods. *J. Appl. Microbiol.,* 98, 1410-1417.

Ryynänen, S. 1995. The electromagnetic properties of food materials: A review of the basic principles. *J. Food Eng.,* 26, 409-429.

Sablani, S.S. 2006. Drying of fruits and vegetables: Retention of nutritional/functional quality. *Drying Technol,* 24, 123-135.

Sacilik, K., Keskin, R., Elicin, A.K. 2006. Mathematical modelling of solar tunnel drying of thin layer organic tomato. *J. Food Eng.,* 73, 231-238.

Sagar, V.R.,Suresh Kumar, P. 2010. Recent advances in drying and dehydration of fruits and vegetables: A review. *Journal of Food Science and Technology,* 47, 15-26.

Sanders, M.E. 2008. Probiotics: Definition, sources, selection, and uses. *Clinical Infectious Diseases,* 46, S58-S61.

Santivarangkna, C., Kulozik, U., Foerst, P. 2007. Alternative drying processes for the industrial preservation of lactic acid starter cultures. *Biotechnol. Prog.,* 23, 302-315.

Santos, P.H.S.,Silva, M.A. 2008. Retention of vitamin C in drying processes of fruits and vegetables - A review. *Drying Technol,* 26, 1421-1437.

Scaman, C.H., Durance, T.D., Drummond, L., Sun, D., 2014. Chapter 23 - Combined Microwave Vacuum Drying. In: Sun, D. (Ed.), Emerging Technologies for Food Processing (Second Edition). Academic Press, San Diego, pp. 427-445.

Schiffmann, R. 1986. Food product development for microwave processing. *Food Technology (USA),*.

Schuck, P. 2002. Spray drying of dairy products: State of the art. *Lait,* 82, 375-382.

Sharma, G.P.,Prasad, S. 2001. Drying of garlic (Allium sativum) cloves by microwave-hot air combination. *J. Food Eng.,* 50, 99-105.

Shi, J., Maguer, M.L., Kakuda, Y., Liptay, A., Niekamp, F. 1999. Lycopene degradation and isomerization in tomato dehydration. *Food Res. Int.,* 32, 15-21.

Shivhare, U.S., Raghavan, G.S.V., Bosisio, R.G. 1994. Modelling the Drying Kinetics of Maize in a Microwave Environment. *J. Agric. Eng. Res.,* 57, 199-205.

Shofian, N.M., Hamid, A.A., Osman, A., Saari, N., Anwar, F., Dek, M.S.P., Hairuddin, M.R. 2011. Effect of freeze-drying on the antioxidant compounds and antioxidant activity of selected tropical fruits. *International Journal of Molecular Sciences,* 12, 4678-4692.

Simpson, P.J., Stanton, C., Fitzgerald, G.F., Ross, R.P. 2005. Intrinsic tolerance of Bifidobacterium species to heat and oxygen and survival following spray drying and storage. *J. Appl. Microbiol.,* 99, 493-501.

Siró, I., Kápolna, E., Kápolna, B., Lugasi, A. 2008. Functional food. Product development, marketing and consumer acceptance—A review. *Appetite,* 51, 456-467.

Skják-Bræk, G., Smidsrød, O., Larsen, B. 1986. Tailoring of alginates by enzymatic modification in vitro. *Int. J. Biol. Macromol.,* 8, 330-336.

Smidsrød, O.,Skjåk-Bræk, G. 1990. Alginate as immobilization matrix for cells. *Trends Biotechnol.,* 8, 71-78.

Smidsrod,O.,Haug, A.,Lian,B., 1972. Properties of poly(1,4-heuronates) in the gel state.I. Evaluation of a method for the determination of stiffness. Acta Chemica Scandinavica 26(1), 71-78.

Spence, J.T. 2006. Challenges related to the composition of functional foods. *Journal of Food Composition and Analysis,* 19, Supplement, S4-S6.

Stogryn, A., 1971. Equations for Calculating the Dielectric Constant of Saline Water. IEEE Trans.Microw.Theory Tech.,MTT 19, 733-736.

Strain, J.J., Benzie, I.F.F., 1999. Diet and antioxidant defence. In: Sadler, M.J., Strain, J.J., Caballero, B. (Ed.), Encyclopedia of Human Nutrition. Academic Press., London, UK.

Summa, C., McCourt, J., Cämmerer, B., Fiala, A., Probst, M., Kun, S., Anklam, E., Wagner, K.-. 2008. Radical scavenging activity, anti-bacterial and mutagenic effects of Cocoa bean Maillard Reaction products with degree of roasting. *Molecular Nutrition and Food Research,* 52, 342-351.

Swarbrick, J., Searles, J.A., Andrieu, J., 2004. Freezing and Annealing Phenomena in Lyophilization. Marcel Dekker, New York.

Talwalkar, A.,Kailasapathy, K. 2003. Metabolic and Biochemical Responses of Probiotic Bacteria to Oxygen. *J. Dairy Sci.,* 86, 2537-2546.

Tang, J., Wang, Z., Huang, L. 1999. Recent progress of spray drying in China. *Drying Technol,* 17, 1747-1757.

Tang, M., 2005. Dielectric properties of foods. In: Regier,M., Schubert,H (Ed.), The Microwave Processing of Foods. Woodhead publishing Limited/CRC press, London/USA.

Tang,J.,Feng,H.,Lau,M., 2002. Microwave Heating in Food Processing. In:Yang,X.H., Tang,J..(Eds),Advanced in Bioprocess Engineering.World Scientific, Hackensack,NJ.

Teixeira, P., Castro, H., Mohácsi-Farkas, C., Kirby, R. 1997. Identification of sites of injury in Lactobacillus bulgaricus during heat stress. *J. Appl. Microbiol.,* 83, 219-226.

Teixeira, P.C., Castro, M.H., Kirby, R.M. 1995. Death kinetics of Lactobacillus bulgaricus in a spray drying process. *J. Food Protection,* 58, 934-936.

Therdthai, N.,Zhou, W. 2009. Characterization of microwave vacuum drying and hot air drying of mint leaves (Mentha cordifolia Opiz ex Fresen). *J. Food Eng.*, 91, 482-489.

To, B.C.S.,Etzel, M.R. 1997. Spray drying, freeze drying, or freezing of three different lactic acid bacteria species. *J. Food Sci.*, 62, 576-578+585.

Tonon, R.V., Brabet, C., Hubinger, M.D. 2008. Influence of process conditions on the physicochemical properties of açai (Euterpe oleraceae Mart.) powder produced by spray drying. *J. Food Eng.*, 88, 411-418.

Toor, R.K.,Savage, G.P. 2006. Changes in major antioxidant components of tomatoes during post-harvest storage. *Food Chem.*, 99, 724-727.

Torringa, E., Esveld, E., Scheewe, I., Van Den Berg, R., Bartels, P. 2001. Osmotic dehydration as a pre-treatment before combined microwave-hot-air drying of mushrooms. *J. Food Eng.*, 49, 185-191.

Trump, J.G., In:von Hippel,A.R.(Ed.), Dielectric and Waves. Dielectric Materials and their Aplications. Wiley, New York.

Tsamo, C.V.P., Bilame, A.-., Ndjouenkeu, R. 2006. Air drying behaviour of fresh and osmotically dehydrated onion slices (allium cepa) and tomato fruits (lycopersicon esculentum). *Int. J. Food Prop.*, 9, 877-888.

Tsvetkov, T.,Brankova, R. 1983. Viability of micrococci and lactobacilli upon freezing and freeze-drying in the presence of different cryoprotectants. *Cryobiology*, 20, 318-323.

Tulasidas, T.N., Ratti, C., Raghavan, G.S.V. 1997. Modelling of microwave drying of grapes. *Can. Agric. Eng.*, 39, 57-67.

Turner, I.W.,Jolly, P.G. 1991. Combined microwave and convective'drying of a porous material. *Drying Technol*, 9, 1209-1269.

Unadi, A., Fuller, R.J., Macmillan, R.H. 2002. Strategies for drying tomatoes in a tunnel dehydrator. *Drying Technol*, 20, 1407-1425.

Van Baarlen, P., Troost, F.J., Van Hemert, S., Van Der Meer, C., De Vos, W.M., De Groot, P.J., Hooiveld, G.J.E.J., Brummer, R.-.M., Kleerebezem, M. 2009. Differential NF-κB pathways induction by Lactobacillus plantarum in the duodenum of healthy humans correlating with immune tolerance. *Proc. Natl. Acad. Sci. U. S. A.*, 106, 2371-2376.

Van de Guchte, M., Serror, P., Chervaux, C., Smokvina, T., Ehrlich, S.D., Maguin, E. 2002. Stress responses in lactic acid bacteria. *Antonie Van Leeuwenhoek Int. J. Gen. Mol. Microbiol.*, 82, 187-216.

Vega-Mercado, H., Marcela Góngora-Nieto, M., Barbosa-Cánovas, G.V. 2001. Advances in dehydration of foods. *J. Food Eng.*, 49, 271-289.

Venkatesh, M.S.,Raghavan, G.S.V. 2004. An Overview of Microwave Processing and Dielectric Properties of Agri-food Materials. *Biosystems Engineering,* 88, 1-18.

Vesterlund, S., Salminen, K., Salminen, S. 2012. Water activity in dry foods containing live probiotic bacteria should be carefully considered: A case study with Lactobacillus rhamnosus GG in flaxseed. *Int. J. Food Microbiol.,* 157, 319-321

Viernstein,H., Raffalt,J., Polheim,D., 2005. Stabilization of probiotic microorgamisms. In: Nedovic,V., Willaert,R. (Ed.), Application of Cell Inmobilisation Biotechnology. Springer, Dordrecht, The Netherlands, pp. 439-455.

Viernstein,H., Raffalt,J., Polheim,D., 2005. Stabilization of probiotic microorgamisms. In: Nedovic,V., Willaert,R. (Ed.), Application of Cell Inmobilisation Biotechnology. Springer, Dordrecht, The Netherlands, pp. 439-455.

Wang, Y.-., Yu, R.-., Chou, C.-. 2004. Viability of lactic acid bacteria and bifidobacteria in fermented soymilk after drying, subsequent rehydration and storage. *Int. J. Food Microbiol.*, 93, 209-217.

Weinbreck, F., Bodnár, I., Marco, M.L. 2010. Can encapsulation lengthen the shelf-life of probiotic bacteria in dry products? *Int. J. Food Microbiol.*, 136, 364-367.

Wen, C.Y.,Yu, Y.H. 1966. A generalized method for predicting the minimum fluidization velocity. *AIChE J.*, 12, 610-612.

Witrowa-Rajchert, D.,Rzaca, M. 2009. Effect of drying method on the microstructure and physical properties of dried apples. *Drying Technol,* 27, 903-909.

Zainol, M.M., Abdul-Hamid, A., Bakar, F.A., Dek, S.P. 2009. Effect of different drying methods on the degradation of selected flavonoids in Centella asiatica. *International Food Research Journal,* 16, 531-537.

Zamora, L.M., Carretero, C., Parés, D. 2006. Comparative survival rates of lactic acid bacteria isolated from blood, following spray-drying and freeze-drying. *Food Sci. Technol. Int.,* 12, 77-84.

Zanoni, B., Peri, C., Nani, R., Lavelli, V. 1998. Oxidative heat damage of tomato halves as affected by drying. *Food Res. Int.,* 31, 395-401.

Zayed, G.,Roos, Y.H. 2004. Influence of trehalose and moisture content on survival of Lactobacillus salivarius subjected to freeze-drying and storage. *Process Biochemistry,* 39, 1081-1086.

Zhang, M., Tang, J., Mujumdar, A.S., Wang, S. 2006. Trends in microwave-related drying of fruits and vegetables. *Trends Food Sci. Technol.,* 17, 524-534.

Zhao, G.,Zhang, G. 2005. Effect of protective agents, freezing temperature, rehydration media on viability of malolactic bacteria subjected to freeze-drying. *J. Appl. Microbiol.*, 99, 333-338.

Zhou, Y., Martins, E., Groboillot, A., Champagne, C.P., Neufeld, R.J. 1998. Spectrophotometric quantification of lactic bacteria in alginate and control of cell release with chitosan coating. *J. Appl. Microbiol.,* 84, 342-348.

Capítulo 11

ANEXOS

11 ANEXOS

11.1 Anexo A. Proceso de secado con microondas en lecho fluidizado

A.1.Programa para el balance de materia para la consideración de la contracción de las partículas de alginato-tilosa

TITLE 'Balance de material para capsulas en microondas'

SELECT
plotintegrate
ERRLIM=0.08

COORDINATES cartesian3 {se trabaja en 3D }

VARIABLES
Humc(1)
Xm=MOVE(x)
Ym=MOVE(y)
Zm=MOVE(z)
Vx
Vy
Vz

DEFINITIONS
{masa de sólido seco en gramos}
mss=0.034
M=table("Esp8experimental.txt"){Datos experimentales de masa; masa de sólido seco en gramos}
{Altura del sistema}
z1=0
z2=0.008
{Datos necesarios para el BM, Constantes balance de materia}
Humin=5.77{Humedad inicial}
Humeq=0.204{Humedad en el equilibrio}
Hums0=5.77{Humedad inicial}
Humpri=4.51
Beta=0.12 {min^{-1}, Coeficiente de Shivhare}
diffus0=1E5
diffus1=8.3e-8 {m^2/min, Difusividad en la Fase I}
diffus2=7e-8 {m^2/min; Difusividad en la Fase II}
diffus3=9.8e-8 {m^2/min; Difusividad en la Fase III}

diffus= IF t<10 then diffus0 else if t>10 and t<20 then diffus1 else if t>20 and t<45 then diffus2 else diffus3{Condición para que la diffusion cambie con el tiempo}

Hums1=Hums0-((Humin-Humpri)*t/10)
Hums2=Humeq+((Humpri-Humeq)*exp(-Beta*(t-10))) {Shivhare, 1994}

```
Hums= IF t<10  then Hums1 else Hums2 {Gainazaleko hezetasun edukiaren baldintza denboran zehar}
{Para calcular el valor global o medio del contenido de agua en base seca (Humav), se realiza la integral triple}
Humav=INTEGRAL(Humc)/INTEGRAL(1)

{Constantes a tener en cuenta para la contracción}
c = 0.0025 {valor inicial del radio, m}
r = sqrt(x^2+y^2)
Vz0 = -4*3.61E-11*t^3+3*1.44E-8*t^2-2*2.04E-6*t+1.21E-4 {Velocidad de contracción de axial}
Vr0 = -4*2.7E-11*t^3+3*1.02E-08*t^2-2*1.34E-06*t+7.23E-5 {Velocidad de contracción radial}

{Densidad del sólido}
j=IF t<20 then z2 else if t >20 and t<45 then 0.0063 else 0.0055 {Condición de cambio de la altura y radio según la fase }
V=(j-Vz0*t)*PI*r^2 !(k-Vr0*t)^2
ro=mss/V

LAGRANGIAN EQUATIONS {Se definen las ecuaciones diferenciales del sistema}
Humc: DIV(Diffus*ro*GRAD(Humc))-ro*dt(Humc)-Humc*dt(ro)=0
Xm:  dt(Xm)=Vx
Ym:  dt(Ym)=Vy
Zm:  dt(Zm)=Vz
Vx:  DIV(GRAD(Vx))=0
Vy:  DIV(GRAD(Vy))=0
Vz:  DIV(GRAD(Vz))=0

EXTRUSION
z=-z2/2,z2/2 {altura}

INITIAL VALUES
Humc=Humin
Vx=-Vr0*x/c
Vy=-Vr0*y/c
Vz = Vz0*z/z2

BOUNDARIES {Definición del dominio; condiciones de contorno}

surface 1
value(Humc)=Hums
velocity(Zm) = -Vz0/2   value(Vz) =-Vz0/2

surface 2
value(Humc)=Hums
velocity(Zm) = Vz0/2   value(Vz) =Vz0/2

REGION 1      {Para cada region del material}
START(0,c)
```

```
value(Humc)=Hums
velocity(xm) = -Vr0*x/r  value(Vx) = -Vr0*x/r
velocity(ym) = -Vr0*y/r  value(Vy) = -Vr0*y/r
arc(center=0,0)angle=360

TIME 0  BY 0.5 TO 150
MONITORS        {Como el problema es dependiente del tiempo es necesario establecer
los límites del tiempo y los intervalos}
for t=0 by 1 to 10 by 10 to endtime
contour(Vx) on y=0
contour(Vy) on x=0
contour(Vz) on x=0

grid (y,z) on x=0
grid (x,y) on z=0
contour(humc) on x=0
contour(humc) on z=0

HISTORIES {Gráficos de los datos requeridos}
HISTORY (M, Humav, Hums) as 'humedad centro ec & humedad media & humedad
superficie'export format "#t#r#i"
HISTORY (Humc) at (0,0,0) as 'humedad centro simulación' export format "#t#r#i"
HISTORY (Hums)  as 'humedad superficie'export format "#t#r#i"

END
```

A.2.Programa para el balance de energía de las partículas de alginato-tilosa

```
TITLE 'Balance de energía capsulas en microondas'     {Título del programa}
SELECT
ngrid=1
plotintegrate

COORDINATES cartesian3  { Se trabaja en 3D }

VARIABLES       { Se definen todas las variables del sistema }
Temp(threshold=111)          {Variable Temperatura, ºC}

DEFINITIONS {Se da valor a todas las constants y se establecen no diferenciales para relacionar variables}
T0 =20 { T,ºC muestra inicial}
{Factores}
w=0.10 {Fracción de vaporización}
a=0
Tsp1=2.5
Tsp2=22.5
Tsp=if t <=40 then Tsp1 else Tsp2
h= 9000 {Coeficiente de convección; J/minºC.m^2}
rad=(x^2+y^2)^0.5
Et1=57 { Campo eléctrico}
{f=1/ABS(Temp-TsP)}
{aire}
Temp_media_aire=table("temp_aire_2.txt")!if t<=40 then 0 else if t>40 and t<=62.22 then 0 else 25
{humedad}
mss=14.995{masa de sólido seco, g}
MI=((-0.0999*t^2-0.9011*t+100.5)-mss)/mss{kg agua/kg s.s}
MII=((171.94*t^(-0.446))-mss)/mss
M=If t<15 then MI else MII
M02=3.50
z1=0
z2
fre= 1.470e11{Frecuencia, min^-1}
Eo=8.854E-12 {Permitividad en el vacío ;F/m}
L=  0.008            {altura ,m}
landa0=12.2e-2       {Longitud de onda, m}
Einicial=50 {Campo eléctrico inicial, V/m}
Et=40

Erad= IF T<20  and temp < 12.5 then Et1 else if T>=20 AND T<= 36 AND  Temp<12.5 THEN  Et1 ELSE 0


Ez= IF T<20 and temp <12.5  then Et else if T>=20 AND T<=36 AND temp <12.5 THEN Et  ELSE 0
```

b=IF T<20 and temp<12.5 then 1 else if T>=20 AND T<=36 AND Temp<12.5 THEN 1 ELSE 0

{Propiedades del agua }
Qvap=2257e3 {Calor latente de vaporización del agua; J/kg]}
D=0.005
denw=1000
Cpw=4180 {Capacidad calorífica; J/min.kg.K}
kw=48 {Conductividad térmica; J/min.m.K}
M0=5.67{Humedad inicial}
{Propiedades dieléctricas del agua}
Ectew=0.004*Temp^2-0.5212*Temp+75.241
Eperdw=0.0001*Temp^2+1.6001*Temp+22.241

{Propiedades del alginato}
dalg=1010
kalg=50.22
Cpalg=4120
Valg=0.5
Ectealg=6
Eperdalg=1.5

{Propiedades de la tilosa }
dty=961
kty=78
Cpty=2090
Ectety=6
Eperdty=1.5
Vty=5

{Propiedades del sólido }
dsol=Vty*dty+Valg*dalg
ksol=Vty*kty+Valg*kalg
Cps=Vty*Cpty+Valg*Cpalg
Ectes=Vty*Ectety+Valg*Ectealg
Eperds=Vty*Eperdty+Valg*Eperdalg

{Fracciones volumétricas}
Vw=dsol*M/(denw+dsol*M0)
Vsol=denw/(denw+dsol*M0)

{Factores que van cambiando con el tiempo}
dmix=denw*Vw+dsol*Vsol
Cpmix=Cpw*Vw+Cps*Vsol
Ecte=Ectew*Vw+Ectes*Vsol
Eperd=Eperdw*Vw+Eperds*Vsol
k=Vw*kw+Vsol*ksol
dp=0.0152
Qabs1=2*PI*fre*Eo*Eperd*Erad^2*(exp(-1*((R-rad)/dp))+exp(-1*((R+rad)/dp)))
Qabs2=2*PI*fre*Eo*Eperd*Ez^2*((exp(-z)/dp)+exp(-1*((L-z))/dp))

```
DM=dt(m)

B_int= Tintegral (val (B,0.0025,0.005,0.004))

B_acumulado= IF T>0.1 and T<=36 then B_int/t else 0

EQUATIONS {Ecuaciones diferenciales}
!Variaciones de la Energía por unidad de tiempo y de volumen
Temp: DIV(k*GRAD(Temp))+Qabs1+Qabs2-dmix*Cpmix*dt(Temp)=0
{Etbasico: dt(Etbasico)-dt(M)*(Einicial/M02)=0}
{M: DIV(Deff*GRAD(M))-dt(M)=0}

EXTRUSION
z=z1,z2 {Piezaren altuera}

INITIAL VALUES
Temp=  T0

BOUNDARIES      {Dominio}
surface 1  natural
(Temp)=-(h*(Temp-Temp_media_aire)-Qvap*dsol*dt(M)*0.11882*0.00802*w)/k
{natural(M)=-(Kw*(M-Maire)/Deff)}
surface 2  natural
(Temp)=-(h*(Temp-Temp_media_aire)-Qvap*dsol*dt(M)*0.11882*0.00802*w)/k
{natural(M)=-(Kw*(M-Maire)/Deff)
REGION 1      {Para cada region del material}
z2=0.008
START(0,0.0025)
natural
(Temp)=-(h*(Temp-Temp_media_aire)-Qvap*dsol*dt(M)*0.7636*0.00125*w)/k
arc(center=0.0025,0.0025)angle=360

TIME 0  BY 5 TO 180  {Intervalos de tiempo establecidos}
MONITORS        {Muestra el progreso del sistema}
for cycle=1
grid (y,z) on x=(0.0025)   {Dibujo red plano}
grid (x,y) on z=(0)
report ( integral (b)) as "integral"

HISTORIES{Representación de los datos más característicos}
HISTORY (Temp) at (0.0025,0.005,0.004) as ' temperatura superficie particula'{Exceleko datu eta grafikoak}export format "#t#r#i"
HISTORY (DM) at(0.0025,0.005,0.004) as 'humedad superficie'export format "#t#r#i"
HISTORY (temp_media_aire)
HISTORY (b_acumulado) as 'tiempo encendido'export format "#t#r#i"
END
```

11.2 Anexo B. Secado de microorganismos encapsulados

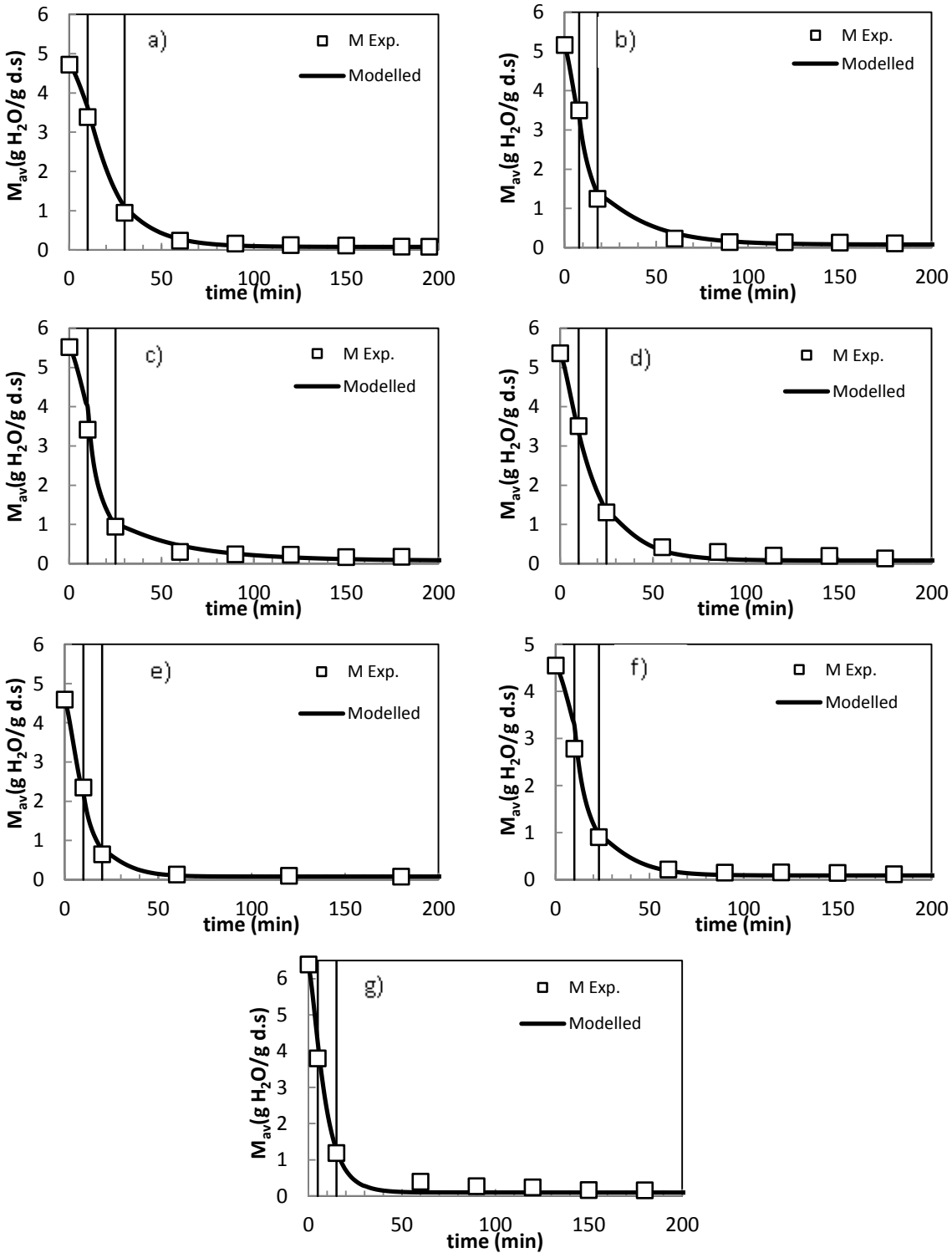

Figura B1. Cinéticas de secado de los Experimentos 2, 3, 4, 5, 6, 7 y 8, se representa la humedad media tanto experimetal como modelada.

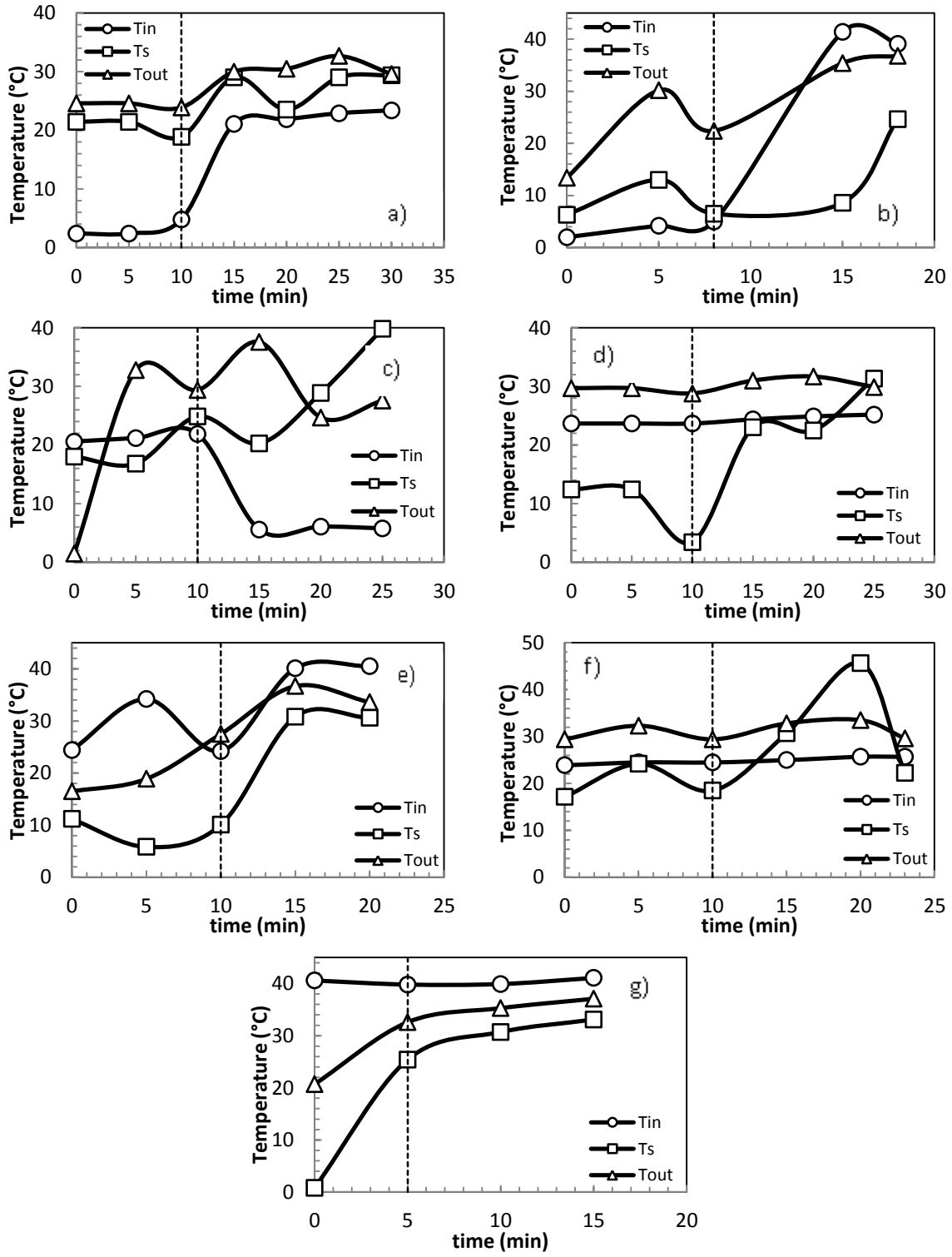

Figura B2. Temperaturas de entrada, salida y de la superficie del producto para los Experimentos 2, 3, 4, 5 ,6 ,7 y 8.

B.1.Programa para el balance de materia sin la consideración de la contracción de las microcapsulas de levadura

```
TITLE 'Balance de materia para capsulas en microondas'     {Título del programa}

SELECT
plotintegrate
ERRLIM=0.02

COORDINATES cartesian3 {Se trabaja en 3D }

VARIABLES       {Se definen todas las variables del sistema}
Hum {Humedad total (g H2O/g sólido seco).}

DEFINITIONS     {Se da valor a todas las constantes y se establecen ecuaciones no diferenciales para relacionar variables}
M=table("Esp1repexperimental esfera_M.txt") {Datos experimentales de masa; masa sol seco en gramos}
Zsphere = sqrt(max(0.001125^2-x^2-y^2,0))  {altura del sistema}
 z1=-max(zsphere,0); z2
{Datos necesarios para el BM simulación; Constantes balance materia}
Humin=4.7619 {Humedad inicial}
Humeq=0.0301 {Humedad en el equilibrio}
Beta=0.060{Coeficiente relativo a la ecuación de Shivhare, min-1}
Hums=Humeq+((Humin-Humeq)*exp(-Beta*T)) {Ecuacion de Shivhare, 1994}
diffus1=3.2e-8 {Difusividad en la fase I, m^2/min}
diffus2=4.8e-8 {Difusividad en la fase II, m^2/min}
diffus3=1e-8 {Difusividad en la fase III, m^2/min}

diffus= IF t<20 then diffus1 else  if t >20 and t<35 then diffus2 else diffus3 {Condición para que la difusión cambie con el tiempo}
{Para calcular el valor global o medio del contenido de agua en base seca (Humav) se hará una integral triple}
Humav=INTEGRAL (Hum)/INTEGRAL (1)

EQUATIONS {Se definen todas las ecuaciones diferenciales del sistema}
Hum: DIV (Diffus*GRAD(Hum))-dt(Hum)=0  {Variaciones de la energía por unidad de tiempo y de volumen}

EXTRUSION
z=z1, z2 {Altura de la pieza}
INITIAL VALUES {Condición inicial; la Humedad sea igual a la humedad inicial}
Hum=Humin

BOUNDARIES {Definición del dominio; condiciones de contorno}
surface 1
value(Hum)=Hums
surface 2
value(Hum)=Hums
```

```
REGION 1      {Para cada región del material}
z2=max(Zsphere,0)
START(0.001125,0)
value(Hum)=Hums
arc(center=0,0)angle=360

TIME 0  BY 5 TO 275  {Como el problema es  dependiente del tiempo es necesario establecer los límites del tiempo y los intervalos }
MONITORS        {Muestra el progreso del sistema}
for cycle=1
grid (y,z) on x=(0.000225)   {Dibujo red plano}
grid (x,y) on z=(0)

HISTORIES {Gráficos de los datos requeridos}
HISTORY (M, Humav,Hums) as 'humedad centro ec & humedad media'export format "#t#r#i"
HISTORY (Hum) at (0,0,0) as 'humedad centro simulación' export format "#t#r#i"
HISTORY (Hums)  as 'humedad superficie'export format "#t#r#i"
END
```

B.2.Programa para el balance de materia con la consideración de la contracción de las microcapsulas de levadura

```
TITLE 'Balance de materia con contracción'     {Titulo del programa}

SELECT
plotintegrate
ERRLIM=0.02

COORDINATES cartesian3 {Se trabaja en 3D}

VARIABLES       {Todas las variables del sistema se encuentran determinadas}
Humc(1)
Xm=MOVE(x)
Ym=MOVE(y)
Zm=MOVE(z)
Vx
Vy
Vz
DEFINITIONS {Todas las constantes o variables no lineales}
mss=1.0351e-9{ g, masa del solido seco de una particular esférica}
M=table("Exp1_experimental.txt") { contenido de humedad; tabla con los diferentes valores de humedad}
rad=0.001125 {Radio de la partícula}
Zsphere = sqrt(max(rad^2-x^2-y^2,0)) {Representación de la cápsula esférica}
z1=-max(zsphere,0)
z2=max(zsphere,0)
{Datos necesarios para la simulación del balance de materia}
Humin=4.7619 {Humedad inicial}
Humeq=0.0301 {Humedad en el equilibrio}
Beta=0.06 {Coeficiente definido por la ecuación de Shivhare, min-1}
diffus1=2e-8 {Difusividad en la fase I, m^2/min}
diffus2=3e-8 {Difusividad en la fase II, m^2/min}
diffus3=5e-9 {Difusividad en la fase III, m^2/min}
Hums= Humeq+((Humin-Humeq)*exp(-Beta*t)) {Humedad de la superficie de acuerdo a la ecuación de Shivhare (1994)}
diffus= IF t<20 then diffus1 else if t>20 and t<35 then diffus2 else diffus3 {Periodos de cambio de las difusividades durante el tiempo, variando en función del experimento}
{Para calcular el valor de la humedad global en base seca, Humav, se resuelve una integral triple}
Humav=INTEGRAL(Humc)/INTEGRAL(1)

{Constantes que tienen en cuenta la consideración de los cambios de volumen}
Vr0= IF t<20  then 1.7117E-5 else if t >20 and t<35 then 9.1033E-6 else 3.5552E-7
c = 0.001125 {Valor inicial del radio, m}
ro=mss/INTEGRAL(1) {Densidad del solido seco}
{ECUACIONES DE LAGRANGIAN, todas las ecuaciones diferenciales del Sistema se encuentran definidas}
EQUATIONS
```

```
Humc: DIV(Diffus*ro*GRAD(Humc))-ro*dt(Humc)-Humc*dt(ro)=0
Xm:  dt(Xm)=Vx
Ym:  dt(Ym)=Vy
Zm:  dt(Zm)=Vz
Vx:  DIV(GRAD(Vx))=0
Vy:  DIV(GRAD(Vy))=0
Vz:  DIV(GRAD(Vz))=0

EXTRUSION
z=z1,z2 {Dimensión de la pieza}

INITIAL VALUES  {Condiciones iniciales}
Humc=Humin
Vx=-Vr0*x/c
Vy=-Vr0*y/c
Vz =-Vr0*z/c

BOUNDARIES      {Definición del dominio, condiciones de contorno}
surface 1
value(Humc)=Hums
value(Vx) = -Vr0*x/r
value(Vy) = -Vr0*y/r
value(Vz) = -Vr0*z/r
surface 2
value(Humc)=Hums
value(Vx) = -Vr0*x/r
value(Vy) = -Vr0*y/r
value(Vz) = -Vr0*z/r

REGION 1      {Para cada región del material}
START(0,c)
value(Humc)=Hums
value(Vx) = -Vr0*x/r
value(Vy) = -Vr0*y/r
value(Vz) = -Vr0*z/r
arc(center=0,0)angle=360

TIME 0  BY 0.5 TO 275  { Como el problema depende del tiempo debe limitarse los
valores y los intervalos de tiempo establecidos }

MONITORS        {Muestra el progreso del sistema a lo largo de la contracción}
for t=0 by 1 to 10 by 10 to endtime
contour(humc) on x=0  frame(-rad,-rad,2*rad,2*rad)  {Dibujo red plano}
contour(humc) on z=0  frame(-rad,-rad,2*rad,2*rad)

HISTORIES {Graficos más representativos}
HISTORY (M, Humav) as 'humedad centro ec & humedad media'export format "#t#r#i"
HISTORY (Humc) at (0,0,0) as 'humedad centro simulación' export format "#t#r#i"
HISTORY (Hums)  as 'humedad superficie'export format "#t#r#i"END
```

11.3 Anexo C. Aplicación del proceso NFMD al secado de material probiótico

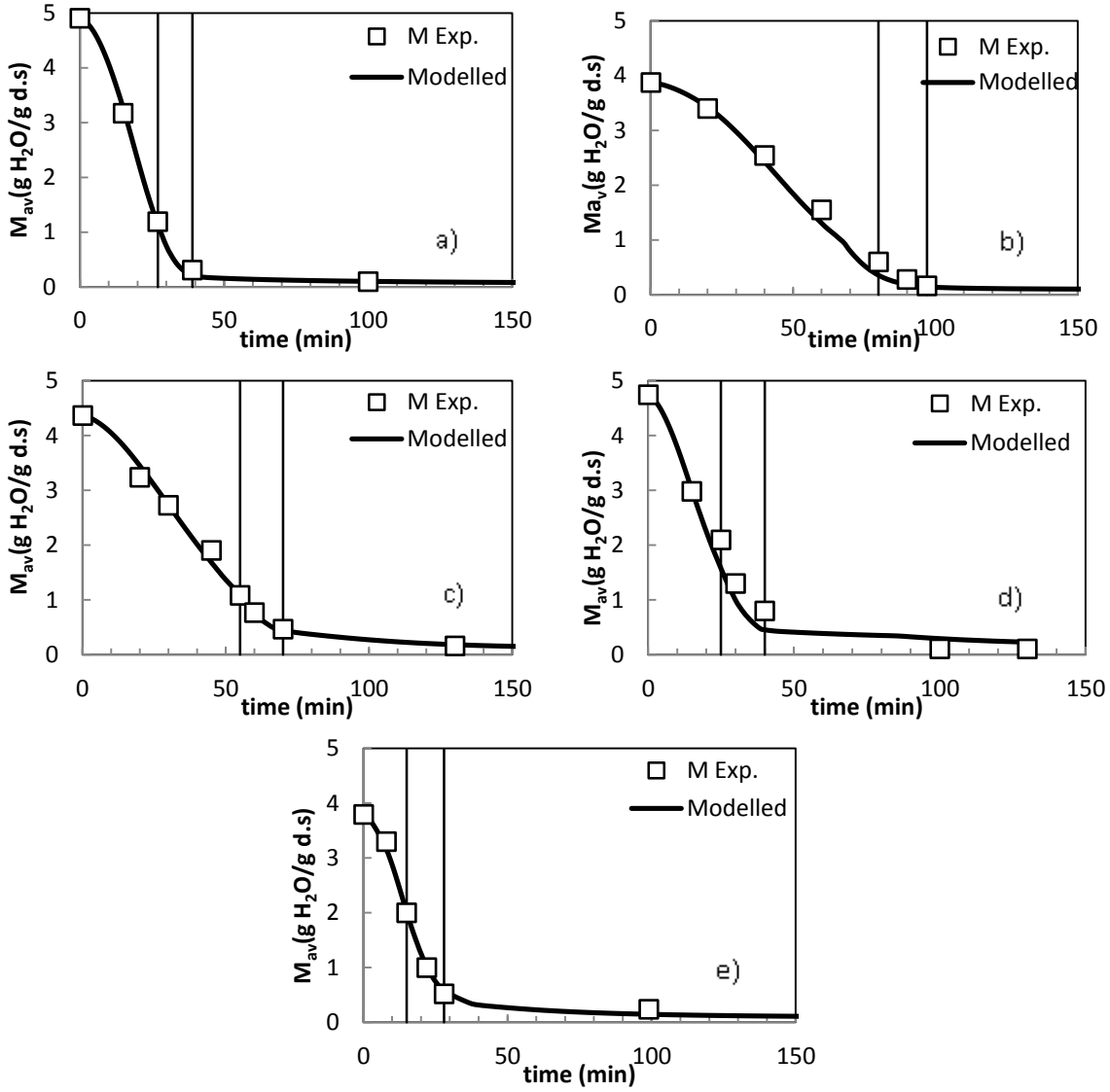

Figura C1. Cinéticas de secado de los Experimentos 1, 2, 3 4 y 5, se representa la humedad media tanto experimetal como modelada.

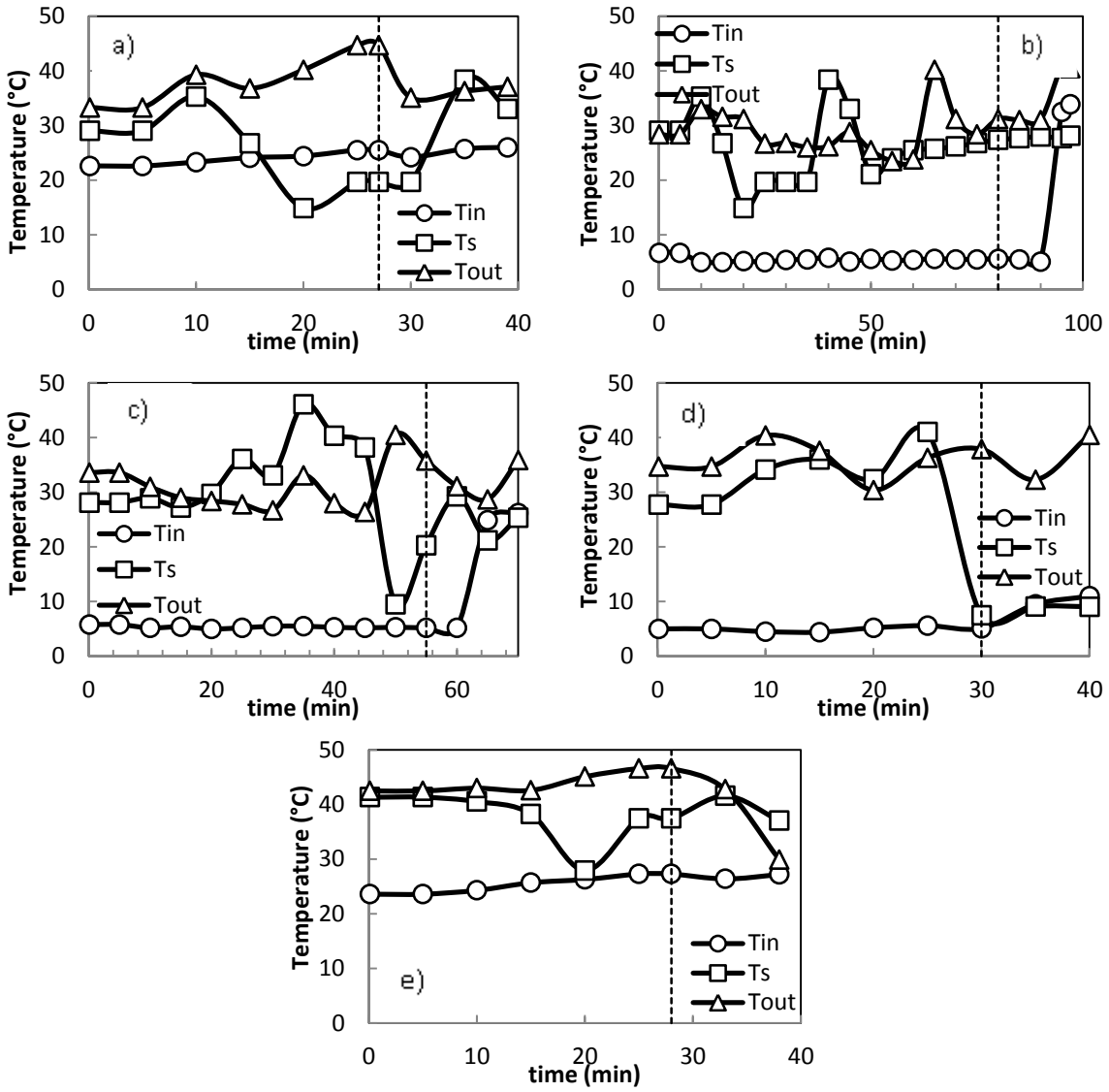

Figura C2. Temperaturas de entrada, salida y de la superficie del producto para todo los experimentos realizados con material probiótico

.

C.1.Programa para el balance de energía de material probiótico BB12®

```
TITLE 'Balance de energía capsulas en microondas'     {Título del programa}

SELECT
plotintegrate
ERRLIM=0.02

COORDINATES cartesian3 {Se trabaja en 3D }

VARIABLES       {Se definen todas las variables del sistema}
Temp  (threshold=50)          { Variable Temperatura, ˚C }

DEFINITIONS {Se da valor a todas las constantes y se establecen ecuaciones no diferenciales para relacionar variables}
T0 =20 {T (˚C) inicial muestra}
{Factores}
w1=1{Fracción de vaporización, definida para la fase I}
w2=1 {Fracción de vaporización, definida para la fase II}
w3=1 {Fracción de vaporización, definida para la fase III}

h1=10000{Coeficiente de transferencia de calor, definido para la fase I, J/min˚C.m2; (PARAMETRO DE AJUSTE)}
h2=7000{Coeficiente de transferencia de calor, definido para la fase II, J/min˚C.m2; (PARAMETRO DE AJUSTE)}
h3=7000{Coeficiente de transferencia de calor, definido para la fase III, J/min˚C.m2; (PARAMETRO DE AJUSTE)}

rad=(x^2+y^2+z^2)^0.5{definición del radio de una esfera}
Et1=1750 {El parámetro del campo eléctrico es un parámetro ajustable, V/m}
R=0.001125 {Radio de la partícula}

{Tablas datos experimentales}
Temp_media_aire=table("temp_aire_media_esfera_modificado.txt")
Temp_superficie_experi=table("Ts_experimental_modificado.txt")
M=table("M_average_esfera.txt") {Tabla con los valores obtenido previamente con el Flexpde™ para el balance de materia}

{Geometría esférica}
Zsphere = sqrt(max(0.001125^2-x^2-y^2,0))
z1=-max(zsphere,0)
z2
{Constantes características de procesos que emplean microondas}
fre= 1.470e11 {Frecuencia, min-1}
Eo=8.854E-12 {Permisividad en el vacío, F/m}
landa0=12.2e-2  {Longitud de onda de la microonda, m}
{Restricciones}
Exyz=IF  T<=39   and  (val  (temp,0,0,0.001125))<=(Temp_superficie_experi)  then  Et1 ELSE 0
```

h= IF T<=27 then h1 else IF T>27 and T<=39 THEN h2 else h3
w= IF T<=27 then w1 else IF T>27 and T<=39 THEN w2 else w3
b=IF T<=39 and (val (temp,0,0,0.001125))<=(Temp_superficie_experi) then 1 ELSE 0

{Propiedades agua}
Qvap=2257e3 {Calor latente de vaporización del agua, J/kg]
denw=1000 {densiad del agua, kg/m3}
Cpw=4180 {Capacidad calorífica, J/kg.K}
kw=48 {Conductividad térmica, J/min mºC}
M0=4.9045 {Humedad inicial del producto encapsulado}
Ectew=0.004*Temp_superficie_experi^2-0.5212*Temp_superficie_experi+75.241
Eperdw=0.0001*Temp_superficie_experi^2+1.6001*Temp_superficie_experi+22.241

{Propiedades alginato}
dalg=1010{Densidad kg/m3}
kalg=50.22 {Conductividad térmica , J/min m.˚C }
Cpalg=4120 {Capacidad calorífica, J/kg.˚C}
Valg=0.03 {Fracción de volumen de alginato, calculado a partir de la masa de las densidades}
Ectealg=6 {Constate dieléctrica, adimensional}
Eperdalg=1.5 {Factor de perdidas, adimensional}

{Propiedades probioticos}
dprob=1042.864{densidad, kg/m3}
kprob=32.394{Conductividad térmica, J/min m K}
Cpprob=3980 {capacidad calorífica, J/kg.K}
Ecteprob=67.5 {Constate dieléctrica, adimensional}
Eperdprob=13.2 {Factor de perdidas, adimensional}
Vprob=0.97 {Fracción de probotico}

{Propiedades del sólido}
dsol=Vprob*dprob+Valg*dalg
ksol=Vprob*kprob+Valg*kalg
Cps=Vprob*Cpprob+Valg*Cpalg
Ectes=Vprob*Ecteprob+Valg*Ectealg
Eperds=Vprob*Eperdprob+Valg*Eperdalg

{Fracciones volumétricas}
Vw=dsol*M/(denw+dsol*M0)
Vsol=denw/(denw+dsol*M0)

{Propiedades dependientes del grado humedad y tiempo}
dmix=denw*Vw+dsol*Vsol
Cpmix=Cpw*Vw+Cps*Vsol
Ecte=Ectew*Vw+Ectes*Vsol
Eperd=Eperdw*Vw+Eperds*Vsol
k=Vw*kw+Vsol*ksol

{Profundidad de penetración, m}
dp=(landa0/((2*Ecte)^0.5*2*PI))*(((1+((Eperd/Ecte)^2))^0.5-1)^(-0.5))

```
{Calor generado por microondas}
Qabs=2*PI*fre*Eo*Eperd*Exyz^2*(exp(-1*((R-rad)/dp))+exp(-1*((R+rad)/dp)))

{Fracción encendido/ apagado}
B_int= Tintegral (val (B,0,0,0.001125))
B_acumulado= IF T>0.01 and T<=39 then B_int/t else 0
Q_int= Tintegral (val (Qabs,0,0,0.001125))
Qabs_acumulado= IF T>0.01 and T<=39 then Q_int/t else 0
{Calor convectivo, de evaporación y de absorción por superficie (2R/6)}
Qconvectivo=-h*((val (temp,0,0,0.001125))-Temp_media_aire)
Qevaporacion=Qvap*dsol*(dt(M))*((2*R)/6)*w
Qabs_superficie=Qabs*(2*R/6)

EQUATIONS {Se definen todas las ecuaciones diferenciales del sistema}
Temp: DIV(k*GRAD(Temp))+Qabs-dmix*Cpmix*dt(Temp)=0

EXTRUSION
z=z1,z2 {Dimensión del pieza}

INITIAL VALUES
Temp= T0

BOUNDARIES    {Definición del dominio, Condiciones de contorno}
surface 1
natural(Temp)=-h*(Temp_superficie_experi-
Temp_media_aire)+Qvap*dsol*(dt(M))*((2*R)/6)*w
surface 2
natural(Temp)=-h*(Temp_superficie_experi-
Temp_media_aire)+Qvap*dsol*(dt(M))*((2*R)/6)*w

REGION 1      {Para cada región del material }
z2=max(Zsphere,0);START(0.001125,0)
natural  (Temp)=-h*(Temp_superficie_experiTemp_media_aire)+Qvap*dsol*(dt(M))*((2*R)/6)*w
arc(center=0,0)angle=360

TIME 0 BY 0.1 TO 39 {Como el problema es dependiente del tiempo hay que establecer
los límites del tiempo y los intervalos}

MONITORS        {Muestra el progreso del sistema}
for cycle=1
grid (y,z) on x=(0)   {Dibujo red plano}
contour(temp) on z=0
report ( integral (b)) as "integral"
HISTORIES {Representación de los datos más característicos}
HISTORY  (Temp,Temp_superficie_experi,Temp_media_aire)  at  (0,0,0.001125)  as  '
temperatura superficie particula'{Gráficas y datos que después pasamos a excel, en este
caso en punto central de la pieza}export format "#t#r#i"
HISTORY (b_acumulado) as 'tiempo encendido'export format "#t#r#i"
HISTORY (Qabs) as 'calor absorbido'export format "#t#r#i"
END
```